Hyaluronan and CD44 Control of Cell Fate.

Emma Louise Woods

School of Medicine

Cardiff University

Thesis submitted for the degree of Philosophiae Doctor

2016

DECLARATION

This work has not previously been accepted in substance for any degree and is not concurrently submitted in candidature for any degree.

Signed…… (candidate) Date ……

STATEMENT 1

This thesis is being submitted in partial fulfilment of the requirements for the degree of ……(insert MCh, MD, MPhil, PhD etc., as appropriate)

Signed…… (candidate) Date ……

STATEMENT 2

This thesis is the result of my own independent work/investigation, except where otherwise stated.

Other sources are acknowledged by explicit references.

Signed…… (candidate) Date ……

STATEMENT 3

I hereby give consent for my thesis, if accepted, to be available for photocopying and for inter-library loan, and for the title and summary to be made available to outside organisations.

Signed…… (candidate) Date ……

STATEMENT 4: PREVIOUSLY APPROVED BAR ON ACCESS

I hereby give consent for my thesis, if accepted, to be available for photocopying and for inter-library loans **after expiry of a bar on access previously approved by the Graduate Development Committee.**

Signed…… (candidate) Date ……

Dedication

To my closest family members -I dedicate this thesis to you all for your support, encouragement and continued belief in me. Thank You

Acknowledgements

First and foremost I would like to say a special thank you to my supervisors Dr. Robert (Bob) Steadman and Dr. Timothy Bowen. To Bob for his consistent help, guidance, encouragement and patience (of a saint) he has shown me over these PhD year. His advice and extensive knowledge has always been freely available, as has his wit and understanding, and for this I am truly grateful. I would also like to thank Tim for always being available to offer advice with his extensive knowledge, whenever I required it and supporting me at difficult times throughout my PhD.

Fortunately, I was extremely privileged to have undertaken my PhD in a group of not only brilliant and inspiring scientists both past and present, but also a group of kind and hysterically humorous individuals who have made my PhD years so enjoyable. I would like to thank Professor Aled Phillips, Professor Donald Fraser and Dr. Soma Meran for all the support over the years and for inspirational ideas when I had none. I owe a special thank you to Dr. Adam Midgely and Dr. John Martin (the matrix crew) for all their help throughout the years. They were both always available to help and support me and offer their extensive knowledge. At times of despair (of which there were many) they both offered possible solutions and consistent ideas, I have learnt so much from these truly talented scientists. To Melisa Anton Lopez (my fellow PhD student sufferer), Dr. Kate Rogers (Simpson), Dr Lucy Newbury, Jordanna Dally, Jennifer Holmes, Dr. Robert Jenkins, Dr. Chantal Colman, Dr. Usman Khalid, and the rest of the office crew, I would like to say a massive thank you for always listening to my dramas and helping me sort through any problems that I had, usually on a daily basis. A massive thank you to Kim Abberley and Cheryl Ward who were always available to help and continuously had time to scan my abundant amount of Western Blots.

Of course it would not have been possible to carry out this PhD without the Funding from Cardiff University School of Medicine and for this is am extremely grateful. I have enjoyed meeting people from this inspirational academic institute and it has been a great privilage to be a part of it.

Finally, I would like to give the largest thank you to my family Gareth Bastin, Charlie Reid, Sheila Woods (Mum), Robert Woods (Dad) Rachel Jones, Kate and Callum Mitchell. I dedicate this thesis to all of you for all your support, for listening to my constant moaning and complaining, for believing in me and encouraging me to continue, when I wanted to quit. You are truly the best family. Thank you.

Publications

J. Martin, A. Midgley, S. Meran, E.Woods, T, Bowen, A. O. Phillips* and R. Steadman*. Tumour necrosis factor-stimulated gene (TSG) 6-mediated Interactions with the Inter–alpha-Inhibitor Heavy Chain 5 facilitate TGFβ_1-dependent Fibroblast to Myofibroblast Differentiation. J. Biol. Chem. (2016) DOI: Pii:M115.670521[Epub Ahead of Print].

Presentations

E. Woods, A. Midgley, T. Bowen, R. Steadman. HA and CD44 control of Cell Fate: Implications in Chronic Kidney Disease. Annual Life Sciences Postgraduate Research Day, Cardiff, UK, 2014 (Poster).

E. Woods, A. Midgley, T. Bowen, R. Steadman. HA and CD44 control of Cell Fate: Implications in Chronic Kidney Disease. Annual Meeting of Cardiff Institute of Tissue Engineering and Repair (CITER), Carmarthenshire, UK 2014.

E. Woods, A. Midgley, T. Bowen, R. Steadman. HA and CD44 control of Cell Fate: Implications in Chronic Kidney Disease. Annual Meeting of Infection and Immunity (I&I) Cardiff, UK 2014 (Poster).

E.Woods, T. Bowen, R.Steadman. The Role of CD44 Variants in Fibroblast Differentiation and Monocyte Binding. South West RNA Meeting, Bath, UK 2015

Contents

Glossary of Abbreviations

AP1	Activating Protein 1
ALK	Activin-like kinase receptor
αSMA	A smooth muscle actin
APP	Amyloid precursor protein
Asn	Asparagine
bFGF	Basic fibroblast growth factor
BM	Basement membrane
BMP	Bone morphogenic protein
BSA	Bovine serum albumin
BSG	Basigin
CAMKII	Calmodulin kinase II
CAV-1	Caveolin-1
CD147	Cluster of differentiation one four seven
CD44	Cluster of differentiation forty four
CF	Cystic fibrosis
CKD	Chronic kidney disease
CREB	cAMP response element binding protein
CS	Chondroitin sulphate
CTGF	Connective tissue growth factor
DMEM/F12	Dulbeccos Modified Eagle Medium and nutrient mixture F-12 Ham's medium
DS	Dermatan sulphate
ECM	Extracellular matrix
EDA-FN	EDA-fibronectin
EEA-1	Early endosomal antigen 1
EGF	Epidermal growth factor
EGFR	Epidermal growth factor receptor
EGR-2	Early growth response-two
EMMPRIN	Extracellular matrix metalloproteinase inducer
EMT	Epithelial to mesenchymal transition
ER	Endoplasmic reticulum
ERK	Extracellular regulated kinase
ERM	Ezrin, radixin and moesin
ESE	Exonic splicing enhancers
ESI	Exonic splicing inhibitors
FACIT	Fibril associated collagens with interrupted triple helices
FAK	Focal adhesion kinase
FBS	Foetal bovine serum
FERM	Four point one ezrin, radixin, moesin
FGF	Fibroblast growth factor

FN	Fibronection
FRET	Florescence resonance emission transfer
ICC	Immunocytochemistry
IdoA	Iduronic acid
GAG	Glycosaminoglycan
GalN	D-galactosamine
GLcN	D-glucosamine
GlcA	D-glucuronic acid
HA	Hyaluronan
HAS	Hyaluronan synthase
HBV	Hepatitis B virus
HC	Heavy chains
HG	High glycosylation
HGF	Hepatocyte growth factor
HIV	Human immunodeficient virus
HLF	Human lung fibroblasts
HMW	High molecular weight
hnRNPs	Heterogeneous nuclear ribonucleoproteins
HRP	Horse radish peroxidase
HS	Heparan sulfate
HYAL	Hyaluronidase
IαI	Inter α trypsin inhibitor
ICAM-1	Intercellular adhesion molecule -1
ICD	Intracellular Domain
ICE	IL-1 β converting enzyme
IgSF	Immunoglobulin superfamily
IL-1α	Interleukin -1 α
IL-1β	Interleukin - 1 β
IL-1R	Interleukin 1 receptor
IL-1R AcP	Interleukin 1 receptor associated protein
INF -γ	Interferon gamma - γ
IRAP	Interleukin receptor antagonist protein
ILDFbs	Interstitial lung disease fibroblasts
ISE	Intronic splicing enhancers
ISI	Intronic splicing inhibitors
JNK	Jun N terminal kinase
LAP	Latent associated protein
LG	Low glycosylation
LMW	Low molecular weight
LYVE-1	Lymphatic vessel endothelial hyaluronan receptor 1
MAPK	Mitogen-activated protein kinases
MMP	Matrix metalloproteinases
mRNA	Messenger ribonucleic acid

MSC	Mesenchymal stem cells
MW	Molecular weight
NFκB	Nuclear factor kappa B
NSAID	Non-steroidal anti-inflammatory drugs
PBS	Phosphate buffer saline
PαI	Pre-α-trypsin inhibitor
PCI	Protease cocktail inhibitor
PCR	Polymerase chain reaction
PDGF	Platelet derived growth factor
PIC	Protease inhibitor cocktail
PKC	Protein kinase C
PMSF	Phenylmethylsofonyl floride
PPI	Peptidyl propyl cis-trans isomers
qPCR	Quantitative polymerase chain reaction
RA	Rheumatoid arthritis
RASF	Rheumatoid arthritis synovial fibroblasts
RHAMM	Receptor for hyaluronan - mediated motility
RIPA	Radio immunoprecipitation assay
RNA	Ribonucleic acid
RNase	Ribonucleases
rRNA	Ribosomal ribonucleic acid
RQ	Relative quantification
RT	Reverse transcription
SAP	Stress-activated protein
s.e.m.	Standard Error of Mean
siRNACD44	siRNA targeting CD44
siRNACD147	siRNA targeting CD147
SMI	Schistosoma mansoni infectious
Sp1	Specific protein 1
SR	Splicing regulators
T3	Triiodothyronine
TACE	TNF-α converting enzyme
TCSF	Tumour cell derived collagenase stimulatory factor
TIE	TGF-β1 inhibitory element
TGF-β1	Transforming growth factor-β 1
TGFSF	Transforming growth factor superfamily
TIMP	Tissue inhibitors of matrix metalloproteinases
TNF-α	Tumour necrosis factor-α
TSG-6	Tumour necrosis factor stimulated gene-6
VEGF	Vascular endothelium growth factor

Thesis Summary

Fibrosis can be charactorised as abberent wound healing resulting from an increased presence of α-smooth muscle actin (αSMA)-rich, myofibroblasts and a continued influx of immune cell mediators. The pro-fibrotic and pro-inflammatory cytokines TGF-β1 and IL-1β, respectivley, have been implicated in fibrotic progression by activating hyaluronan (HA)/CD44-mediated pathways. CD44, the principal HA receptor, exists as multiple spliced variants which mediate multiple celluar functions through their association with HA. The aim of this Thesis was to investigate the expression and interactions of CD44 variants asociated with fibroblast activation induced by TGF-β1 or IL-1β.

Multiple forms of CD44 spliced variants were identified in fibroblasts. Stimulation with TGF-β1 decreased the expression of all variants, whereas IL-1β-increased global CD44 expression. CD44s was the variant identified as essential for both TGF-β1 induction of myofibroblasts and IL-1β-induced monocyte binding to fibroblasts.

CD147 is a matrix metaloproteinase (MMP) inducer that mediates receptor interactions within the plasma mebrane; and contributes to ECM re-arrangment in response to various stimuli. CD147-medaited-αSMA incorporation into F-actin stress fibres that were essential for the myofibroblast contractile phenotype. It associated with CD44s and the EDA-Fibronectin-associated integrin, α4β7, suggesting that through receptor interaction it mediated the mechanotransduction properties required for differentiation. Decreased expression of CD147 prevented intracellular activativation of ERK1/2, an essential kinase involved in mechanotransdction.

These data suggest that CD44s regulates both a fibrotic and inflammatory response by fibroblasts through two separate mechanistic pathways. It also implicates CD44s in mechanotransduction, via its association with CD147. In conclusion, both CD44s and CD147 are essential mediators of fibrosis and further research into downstream mediators could lead to potential therapeutic targets to combat fibrotic progression.

Chapter 1 - General Introduction

1.1. - Wound Healing

Wound healing can be defined as a highly orchestrated process involving the simultaneous collaboration of multiple cell types in wound closure, resulting in the formation of scar tissue. The process requires the finely balanced activation of resident and systemic cells, the extracellular matrix (ECM) and wound healing mediators, such as cytokines and growth factors. Any alteration in surrounding environment conditions can result in dysregulated wound healing. The wound healing process is best described in dermal tissue, but a similar process is observed in other tissues types, including vital organs. Under optimal conditions, healthy wound healing occurs in four overlapping stages: homeostasis, inflammation, proliferation and remodelling (reviewed by Steed 1997). ***Figure 1.1.*** is an adapted schematic overview of these wound healing stages.

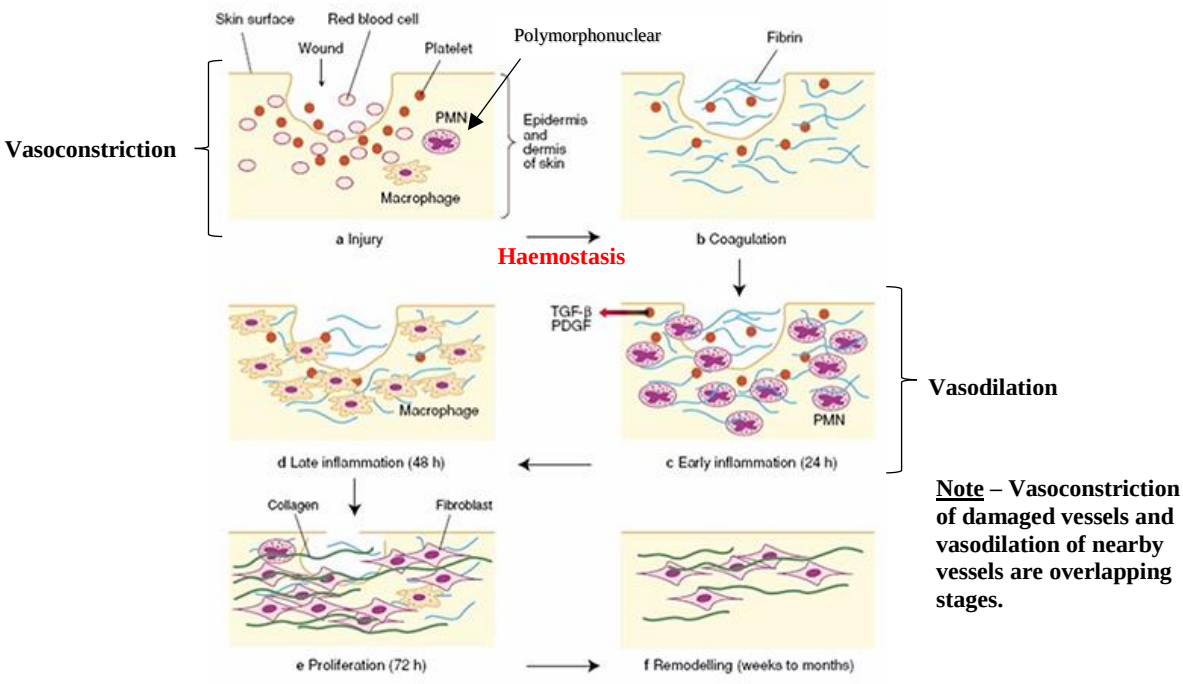

Figure 1.1. Wound Healing

The overlapping stages of wound healing include haemostasis which generally occurs between **a)** initial injury and **b)** coagulation. Damaged vessels undergo vasoconstriction to limit blood loss at the same time that nearby vessels undergo vasodilation to allow for the influx of initial mediators including neutrophils, platelets and plasma proteins. Panels **c)** and **d)** represent the overlapping stages of early and late inflammatory response, respectively. The influx of fibroblasts into the wound area is essential for the later stages of wound healing **e)** proliferation and finally **f)** the long term remodelling stage. Times given for each stage are approximate. Adapted from Beanes et al. (2003).

1.1.1.-Haemostasis

On initial tissue damage a rapid response results, this limits blood loss and maintains homeostasis. Damage to the cells of the endothelium releases vasoactive amines and lipid mediators, including prostaglandins and thromboxanes, triggering damaged blood vessels within the wound region to undergo vasoconstriction and reduce local haemorrhaging (Wu et al. 1988). Endothelial cells and platelets activate the coagulation cascade, this results in thrombin cleaving soluble fibrinogen to form insoluble fibrin, which together with collagen, thrombin and fibronectin form an insoluble clot (Li et al. 2007). Along with preventing further blood loss, the clot acts as a scaffold for platelets and cells migrating into the wound area to release growth factors and cytokines into the surrounding region (Baum and Arpey 2005).

1.1.2. - Inflammation

Overlapping the late stage of coagulation is the early stage of inflammation. Resident mast cells release histamines and other vasoactivators, indirectly activating an increased production of prostaglandins. These activate blood vessels within the wound to undergo vasodilation and become leaky, allowing rapid influx of passing immune cells to the site (Urb and Sheppard 2012). It should be noted that vasoconstriction of damaged blood vessels and vasodilation of other blood vessels within the wound region may happen simultaneously. Platelets release a cascade of cytokines including interleukin 1β (IL-1β), platelet derived growth factor (PDGF), transforming growth factor - β1 (TGF-β_1) and tumour necrosis factor - α TNF-α (Barrientos et al. 2008). These cytokines, along with products produced from pathogens that have entered the wound area, activate an initial immune response from passing neutrophils, monocytes and other leukocytes.

First to migrate to the site are neutrophils. These polymorphonuclear cells destroy bacteria that have entered via the wound using antimicrobial peptides, reactive oxygen species

and proteolytic enzymes. They also engulf bacteria and any debris from dead cells by phagocytosis, before undergoing apoptosis (Wilgus et al. 2013). Monocytes that have migrated to the wound site differentiate into macrophages, which engulf wound debris, pathogens and any apoptotic neutrophils at the injury site. Macrophages release further chemo-attractants and growth factors in the wound area. These include PDGF, fibroblast growth factor (FGF-2), TGF-β_1, vascular endothelium growth factor (VEGF); and hepatocyte growth factor (HGF), together with a host of pro-inflammatory cytokines such as IL-1β, IL-1α and TNF-α. TGF-β_1 released by macrophages stimulates nearby fibroblasts and circulating fibrocytes to migrate to the wound using the fibril scaffold for adherence (Janis and Harrison 2014).

1.1.3.-Proliferation

The proliferation stage encompasses multiple overlapping wound healing phases including epithelialisation, angiogenesis, granulation tissue formation and collagen deposition. In this stage, epithelial cells at the edge of the wound are stimulated by inflammatory cytokines including IL-1 and TNF-α released by macrophages, platelets and fibroblasts, to undergo rapid proliferation to form a protective barrier. Vascular endothelial cells also undergo increased proliferation in response to VEGF, FGF and PDGF and form new capillaries from pre-existing vessels, thereby re-oxygenating the region.

Fibroblasts are continuously activated to migrate into the region by growth factors, such as PDGF, TGF-β_1 and connective tissue growth factor (CTGF); and by the interaction of cell surface integrins with fibronectin (Repesh et al. 1982; Barrientos et al. 2008). The migration of cells into the region is regulated by increased expression of matrix metalloproteinases (MMPs), e.g. MMP 1, 2 and 3, which modify the ECM and any cell debris that may prevent migration. This increased MMP secretion results from the activation of TGF-β_1 (reviewed by Baum and Arpey 2005).

Fibroblast activation by PDGF, Epidermal Growth Factor (EGF) and TGF-β_1, induces a rapid proliferative response. Further, stimulation by PDGF and other mediators activates fibroblasts to lay down a provisional matrix of collagen III, fibronectin and glycosaminoglycans (GAGs) (Pierce et al. 1992). Resident fibroblasts undergo less proliferation than migrating fibroblasts and following stimulation by macrophage-secreted TGF-β_1, they are activated to undergo differentiation to myofibroblasts, cells with a contractile phenotype that contribute to wound closure. TGF-β_1 activates myofibroblasts to increase collagen I synthesis and inhibit MMP activity, via upregulated expression of tissue inhibitors of metalloproteinases (TIMPs) (reviewed in Goldman 2004). This complex stage of wound healing results in a provisional scar known as granulation tissue, which is re-organised within the remodelling stage.

1.1.4. –Remodelling

The provisional weaker scar formed from granulation tissue contains a higher percentage of collagen III than the original tissue. In the remodelling phase, which can continue for up to a year after initial damage, fibroblasts replace collagen III in the tissue and replace it with collagen I. Further, the remodelled collagen has more structure than the original granulation tissue giving it more strength. However, the new scar tissue only retains 80% of the original strength of the tissue, prior to injury (Janis and Harrison 2014).

1.2 - Fibrosis Overview

Fibrosis is a pathological condition that can affect multiple tissue types including vital organs such as the liver, kidneys and lungs (Veeraraghavan et al. 2001; Bataller and Brenner 2005; Liu 2006). There are many underlying conditions that can lead to fibrosis. For example, chronic kidney disease (CKD), a progressive fibrotic disease, maybe initiated by various inflammatory, metabolic, obstructive or systemic disorders, (reviewed by Meran and Steadman

2011). Regardless of the origin of fibrosis, the result is an accumulation of scar tissue that eventually leads to tissue damage and the loss of organ function. In healthy wound healing, each phase is mediated by multiple growth factors and cytokines. However, under fibrotic conditions, aberrant expression of these mediators by surrounding cells leads to a non-resolving wound healing response.

1.2.1. – Fibrosis as Dysregulated Wound Healing

Under the normal wound healing conditions described above, the immune response is acute and leads to the rapid activation of the innate immune system to eliminate pathogens and initiate resolution. Fibrotic wound responses are often associated with chronic inflammation that continues for an extended period of time. This leads to aberrant tissue repair and a failure of scar resolution. As the inflammatory response continues, normally tightly regulated growth factors and cytokines continue to be released and activate surrounding cells to respond accordingly. Since inflammatory mediators are implicated in fibrotic progression, treatments commonly used for fibrotic diseases are anti-inflammatories, such as corticosteroids and non-steroidal anti-inflammatory drugs (NSAIDs). Both are often used for the treatment of many inflammatory diseases that eventually lead to fibrosis, including the genetic disease cystic fibrosis (CF) and the autoimmune disease rheumatoid arthritis (RA) (Young et al. 2007; Konstan et al. 2010). Current treatments have proved inadequate in combating fibrotic progression, leading to the theory that the immune response is separate from fibrogenesis (Yu et al. 2009). However, it is conceivable that immune response prevention has no effect on fibrotic progression, since the aberrant cycle has already begun and fibrotic cells are continuously expressing fibrotic mediators. Therefore, anti-inflammatory treatments may combat some but not all immune response-related problems.

Wynn (2004) suggests that a more specific treatment may be required, that targets fibrotic mediators. A given example is the indirect activation of TGF-β_1 by interleukin 13 (IL-13), which has previously been identified to activate MMP 9, a known activator of pro-fibrotic cytokine, TGF-β_1 (Lee et al. 2001). Inhibiting these two cytokines in inflammatory disease may prevent further fibrotic progression and targeting these fibrotic mediators indirectly by the administration of interferon gamma (IFN –γ) and/or IL-12, may have a more inhibitory in effect than current treatments (Wynn, 2004). Both of these cytokines have previously been identified to decrease the expression of TGF-β_1 and IL-13 in *Schistosoma mansoni* infection (SMI). This disease is transmitted from flatworms found in fresh water e.g. Uganda; and the accumulation of parasitic eggs in the liver leads to periportal fibrosis (fibrosis that accumulates around the hepatic portal vein) in a large percentage of affected people (Wynn et al. 1995). However, in a study by Booth et al. (2004), it was found that patients with high blood levels of IFN-γ and IL-12 had a decreased risk of fibrosis from this infectious disease; and suggested that direct administration of these cytokines may decrease the percentage of patients with a fibrotic response.

The increased presence of myofibroblasts is a marker for fibrotic progression. The contractile phenotype of the myofibroblast is the result of increased expression of α-smooth muscle actin (αSMA), which is incorporated into the F-actin cytoskeleton of these cells (Gabbiani et al. 1971; Clement et al. 2005). In healthy wound healing, myofibroblasts lay down ECM and their contractile phenotype facilitates resolution, following which these cells undergo apoptosis.

In fibrotic tissue, myofibroblasts are continually present and constantly stimulated by growth factors and mediators to synthesise and lay down excessive interstitial ECM. This ECM accumulation leads to damage to the surrounding tissue and eventual loss of function (reviewed in Gabbiani 2003). It is widely accepted that TGF-β_1 is responsible for fibroblast to

myofibroblast differentiation and is, therefore, a major contributor to fibrotic progression (Desmouliere et al. 1993). Furthermore, TGF-β_1 is a powerful chemo-attractant for fibroblasts and is, therefore, responsible for their excessive infiltration into damaged regions. Under inflammatory conditions, local immune cells, including macrophages secrete TGF-β_1 (Wynn 2008). Furthermore, removing exogenous TGF-β_1 does not inhibit the myofibroblast phenotype, due to an autocrine feedback loop that is mediated by hyaluronan; a major ECM component (Webber et al. 2009c). The origins of myofibroblasts of fibrosis are controversial, although it is generally agreed that they differentiate from resident or migrating fibroblasts. However, a number of studies have associated increased expression of myofibroblasts with epithelial to mesenchymal transition (EMT), resulting from a fibrotic environment (Iwano et al. 2002).

MMPs are regulators of ECM turnover that are vital for final wound resolution. They have multiple, sometimes contradictory roles, including activating immune regulators, stimulating and inhibiting myofibroblasts; and re-organising the ECM. MMPs comprise a large family of over 20 endopeptidases, with a pro-domain and zinc active site; and they are released in a latent form (Ra and Parks 2007).

There are four known tissue inhibitors of matrix metalloproteinases (TIMPs 1-4) that inhibit MMP activity by preventing ECM turnover; and limiting fibrotic progression. However, in a study by Yoshiji et al. (2000) transgenic mice that overexpressed TIMP1 were subjected to spontaneously-induced, hepatic fibrosis in a carbon tetrachloride (CCl_4) model. The study found that transgenic mice overexpressing TIMP1 had a seven-fold increase in fibrosis compared, to control mice. There was a marked increase in fibrotic markers including collagen I, IV and αSMA in TIMP1 transgenic mice; and decreased expression of the active form of MMP2. It was speculated that this imbalance contributed to fibrotic progression by the lack of

ECM degradation that resulted from decreased activity of MMP2 and its continuous inhibition by increased levels of TIMP1.

TIMP3 inhibits not only MMP, but also TNF-α converting enzyme (TACE) (Baker et al. 2002). In TIMP3 $^{-/-}$ mice models subjected to unilateral ureteral obstruction (UUO), the expression of TNF-α decreased, as did interstitial fibrosis, while inhibition of MMPs and mice that had a combined TIMP3$^{-/-}$ TNF-α$^{-/-}$ knockout had reduced inflammation and fibrosis (Kassiri et al. 2009). Consistent with this study, the induction of lung fibrosis in TIMP3$^{-/-}$ mice lengthened the immune response and the influx of neutrophils, indicating that TIMP3 regulates the immune resolution (Gill et al. 2010). Interestingly, TNF-α induces TGF-β_1 production in lung fibroblasts through the activation of the Extracellular Regulated Kinase (ERK) pathway. Therefore, increased expression of TNF-α, due to decreased TIMP levels, may ultimately contribute to the overall aberrant response observed in fibrosis (Sullivan et al. 2005).

Similar to TIMP expression, the presence of several MMPs in fibrotic models initiates both pro- fibrotic and anti -fibrotic responses. An anti-fibrotic role for MMP2 was determined has been observed in a study showing exacerbated fibrosis in MMP2$^{-/-}$ mice that were subjected to two different models of liver fibrosis (Onozuka et al. 2011). Furthermore, TIMP1, TGF-β_1 and PDGF all showed increased expression in MMP2 deficient mice in the fibrotic CCl_4 model. Therefore, MMP 2 seems to have a regulatory anti-fibrotic role and deletion of its expression leads to upregulation of fibrotic mediators. MMP 3, also known as stromelysin 1, activates latent TGF-β_1 and has been shown to be pro-fibrotic and upregulated in human idiopathic pulmonary fibrosis (Giannandrea and Parks 2014). Furthermore, a recombinant form of MMP-3 introduced into the lungs of rats induced fibrosis; and MMP 3 deficient mice were protected from bleomycin-induced pulmonary fibrosis (Yamashita et al. 2011).

In conclusion, tight regulation of ECM production and degradation together with immune response and mediators is vital for conclusive wound resolution; and any deviation from this regulation can result in fibrotic disease.

1.3. – Cells involved in Fibrosis

1.3.1. – The Fibroblast

Fibroblasts are a mesenchymal cell type that display a thin spindle like morphology. They play a key role in maintaining healthy ECM turnover and the structural integrity of renal interstitial connective tissue, synthesising many proteolytic enzymes and growth factors. Fibroblasts are a principal cell type involved in restoring ECM homeostasis following tissue damage, moving rapidly to the site of injury where they proliferate rapidly and initiate a wound healing response (Janis and Harrison 2014). There is no definitive cell marker of fibroblasts. While these mesenchymal cells have been identified by vimentin expression, this intermediate filament is not exclusive to fibroblasts, making them difficult to identify conclusively (Eriksson et al. 2009).

While the fibroblast is ubiquitous to many tissues, these cells display a large degree of heterogeneity and tissue specificity. Early studies by Castor et al. (1962) identified that fibroblasts extracted from various anatomical sites including dermis, mesothelial and articular tissue had different proliferation rates and ECM production. Furthermore, activation of fibroblasts is tissue specific. For example, Smith et al. (1989) identified that thyroid hormone triiodothyronine (T3) and synthetic glucocorticoid dexamethasone inhibited dermal fibroblast synthesis of hyaluronan (HA), a major ECM component, but in retro-ocular fibroblasts, neither hormone affected HA synthesis. Therefore, the same stimuli can have a different response in fibroblasts that are present in different tissue types. Fibroblast populations can also vary at the

same anatomical site in injured tissue with the presence of non-contractile fibroblasts, contractile myofibroblasts and an intermediate proto-myofibroblast population being commonly observed (Tomasek et al. 2002b).

The origin of fibroblasts is controversial and their abundance is tissue specific. For example, resident fibroblasts are often abundant in connective tissues and when the tissue is injured these resident fibroblasts are stimulated to proliferate rapidly and secrete cytokines to surrounding regions; making these fibroblasts the principal wound healing population. However, in the renal cortex under homeostasis, fibroblasts are comparatively sparse. Therefore, following kidney damage, the origin of interstitial fibroblasts involved is not fully understood (Meran and Steadman 2011). There are several potential sources for these cells. First, numerous studies report that local epithelial cells undergo dedifferentiation to fibroblasts in a process described as EMT (Zavadil and Böttinger 2005). Epithelial cells become depolarised and lose their tight cell junctions, due to the loss of adherence proteins, including ZO1 and cadherin. The commonly expressed epithelial integrin α6β4 is lost and replaced by the mesenchymal integrin, α5β1. These transformations lead to altered actin organisation and the release of MMPs that mediate the digestion of the basement membrane and permit cellular migration. Evidence describing this process has mainly been identified *in vitro* and multiple cytokines have been suggested to mediate the process. Most research, however, has focussed on and implicated TGF-β_1 as a major contributor to EMT. Research *in vivo*, however, is limited due to the lack of specific markers, although alternative models have been successfully utilised. For example, Kim et al. (2006) successfully overexpressed β-galactosidase in lung epithelial cells. Using a pulmonary fibrotic mouse model that over-expressed TGF-β_1, they identified cells that exhibited mesenchymal markers and were positive for β-galactosidase, indicating EMT had taken place.

Other studies have reported that a source of bone marrow stem cells known as fibrocytes, that circulate through the blood; are a major source of fibroblasts found at sites of tissue damage. These precursor cells are present in peripheral blood and express markers for hematopoietic cells, leukocytes and fibroblast products, including collagen I, III and fibronectin (McAnulty 2007). They do not, however, express markers for monocytes/macrophages or neutrophils. Fibrocytes have also been reported to differentiate from $CD14^+$ mononuclear cells that enter the wound area with inflammatory cells (Abe et al. 2001). Furthermore, it has been shown *in vitro* that this activation is dependent on T-cells and the pro-fibrotic cytokine TGF-β_1 (Abe et al. 2001). The importance of these fibrocytes can be demonstrated by a study that identified a higher percentage of fibrocytes present in severely burned patients compared to control groups, using collagen I as a marker of identification. Further, the increased fibrocytes presence correlated with increased TGF-β_1 (Bretscher et al. 2002). These studies highlight the importance of these stem cells in the maintenance of tissue integrity at the site of injury; and may explain the presence of fibroblasts in tissues that have a normally sparse fibroblast population. However, the correlation of their presence with increased TGF-β_1 may also indicate that they have a role in fibrotic progression. The local mesenchymal stem cells that reside in all postnatal tissues has been proposed as a further source of fibroblast-like cells (Meirelles et al. 2006).

Multiple cytokines/growth factors influence fibroblast behaviour at the site of injury. It is well understood that growth factors, including PDGF, FGF and heparan binding-EGF (HB-EGF), mediate the increases in fibroblast proliferation and increased fibroblast production of ECM. Cytokines, including TGF-β_1 and members of the interleukin family upregulate fibroblast production of VEGF an important mediator of angiogenesis. Fibroblasts also mediate MMP production in the surrounding region, a process known to be vital for ECM degradation and re-organisation; and for cellular movement (Asano-Kato et al. 2005).

The characteristic fibroblastic spindle morphology results from a cytoskeleton that is situated close to the peripheral edge of the cell membrane. It is well-documented that activated fibroblasts undergo a multistage differentiation process ***(Figure 1.2[A])*** that alters this cytoskeletal arrangement and results in differentiation to become a myofibroblast.

1.3.2. – The Myofibroblast

Myofibroblasts are terminally differentiated fibroblasts, that have an increased ability to synthesise ECM components. The principal marker for the presence of myofibroblasts in tissues is αSMA, which becomes incorporated into the F-actin cytoskeleton, giving these cells a contractile phenotype similar to that observed in a smooth muscle cell (Gabbiani et al. 1971). As a result, myofibroblasts exhibit a similar morphology to smooth muscle cells with a flattened, irregular shape, an increased cell-ECM association and advanced gap junction formation. Furthermore, the cytoskeleton is rearranged and is seen not only around the peripheral regions of the cell membrane, as in fibroblasts, but is present throughout the cortical regions of the cytoplasm (Sandbo and Dulin 2011). Under healthy wound healing conditions, myofibroblasts participate in tissue repair by replacing the damaged ECM and closing the wound site by virtue of their contractile properties. Conversely, myofibroblasts are not usually present in healthy tissue. Under fibrotic conditions, this increased ECM production and contractile phenotype leads to damage to parenchymal tissue and eventual loss of tissue function, hence this cell type is the principal mediator of fibrotic progression.

The cytokine, TGF-β1, is widely documented as the principal mediator of fibroblast to myofibroblast differentiation. The proto-myofibroblast represents an intermediate cell phenotype between fibroblast and myofibroblasts ***(Figure 1.2[A])***. Under normal conditions, fibroblasts have very limited actin-associated cell–cell or cell-ECM contact (Tomasek et al. 2002b). However, in damaged tissue, normally quiescent fibroblasts acquire a migratory

phenotype, in order to re-populate and repair the damaged area. The proto-myofibroblast can be described as an activated fibroblast that results from changes in the mechanical properties and organisation of the ECM. A combination of these ECM alterations and activation by TGF-β_1 results in quiescent fibroblasts acquiring the more contractile phenotype typical of a proto-myofibroblast. However, proto-myofibroblasts differ from myofibroblasts, as they do not express αSMA. Instead of αSMA incorporation into the cytoplasmic filaments, proto-myofibroblasts have cytoplasmic β and γ actin; and consequently generate less contractile force than myofibroblasts (Tomasek et al. 2002b; Hinz et al. 2007).

The ECM component, fibronectin, functions in the contractile phenotype of myofibroblasts. In particular, ED-A fibronectin is required to generate the mechanical tension required for differentiation to occur. Increased ED-A fibronectin production is necessary for differentiation and this precedes the presence of αSMA at the site of injury, while the elimination of ED-A prevents differentiation (Serini et al. 1998).

This increased mechanical tension in the ECM environment, along with TGF-β_1 activation, leads to alterations in cell–ECM interactions and the formation of mature focal adhesions. Focal adhesions are complexes formed from integrin and integrin-associated proteins, such as focal adhesion kinases; and actin-associated proteins, like ezrin, radixin and moesin (ERM) (Geiger et al. 2001). The formation of mature focal adhesion complexes leads to a re-arrangement of the actin cytoskeleton, which becomes distributed throughout the peripheral and cortical regions of the myofibroblast. How αSMA is incorporated into the F-actin cytoskeleton is not entirely understood, however, it has been identified that the αSMA NH_2 terminal peptide sequence, ACEED, is vital for the contractile phenotype of the myofibroblast (Hinz et al. 2002). The incorporation of αSMA into actin fibres and the increase in intracellular and extracellular tension contribute to the formation of supermature focal adhesions, formed from αSMA, tenascin, ED-A fibronectin and α5β1 integrin. The increased

presence of αSMA incorporation results in further stress fibre formation and is central to the formation of supermature focal adhesion formation, but also increases the contractile properties of the myofibroblast (Hinz et al. 2003).

Similar to the fibroblast, the origin of increased myofibroblast numbers in fibrotic tissue is controversial. Multiple cytokines and growth factors have been implicated in fibrotic progression and one generally accepted source of myofibroblasts is activation of resident fibroblasts by TGF-β_1 ***(Figure 1.2. [B])***. However, circulating bone marrow-derived fibrocytes, EMT and activation of resident mesenchymal stem cells (MSCs), have all been implicated in the increased myofibroblast presence (McAnulty 2007) ***(Figure 1.2. [B])***. However, as both fibroblasts and myofibroblasts have an increased presence in fibrotic tissue, it is not well established if other cell types first transform to fibroblasts and are then TGF-β_1-activated to proto-myofibroblasts and then myofibroblasts, or if the transformation to myofibroblast is direct. Alternatively, fibrocytes, epithelial and stem cells may transform directly to proto-myofibroblasts, leading to the continuous presence of this intermediate cell type within the damaged tissue. In a recent study of the fibroblasts/myofibroblasts presence in heart tissue by Driesen et al. (2014), it was found that proto-myofibroblasts were able to undergo a dedifferentiation process into fibroblasts, as well as differentiate into myofibroblasts. However, myofibroblasts did not undergo dedifferentiation and therefore, were terminally differentiated. It is, therefore, conceivable that the continuous presence of proto-myofibroblasts may account for both the fibroblast and myofibroblast populations found in tissue under fibrotic conditions.

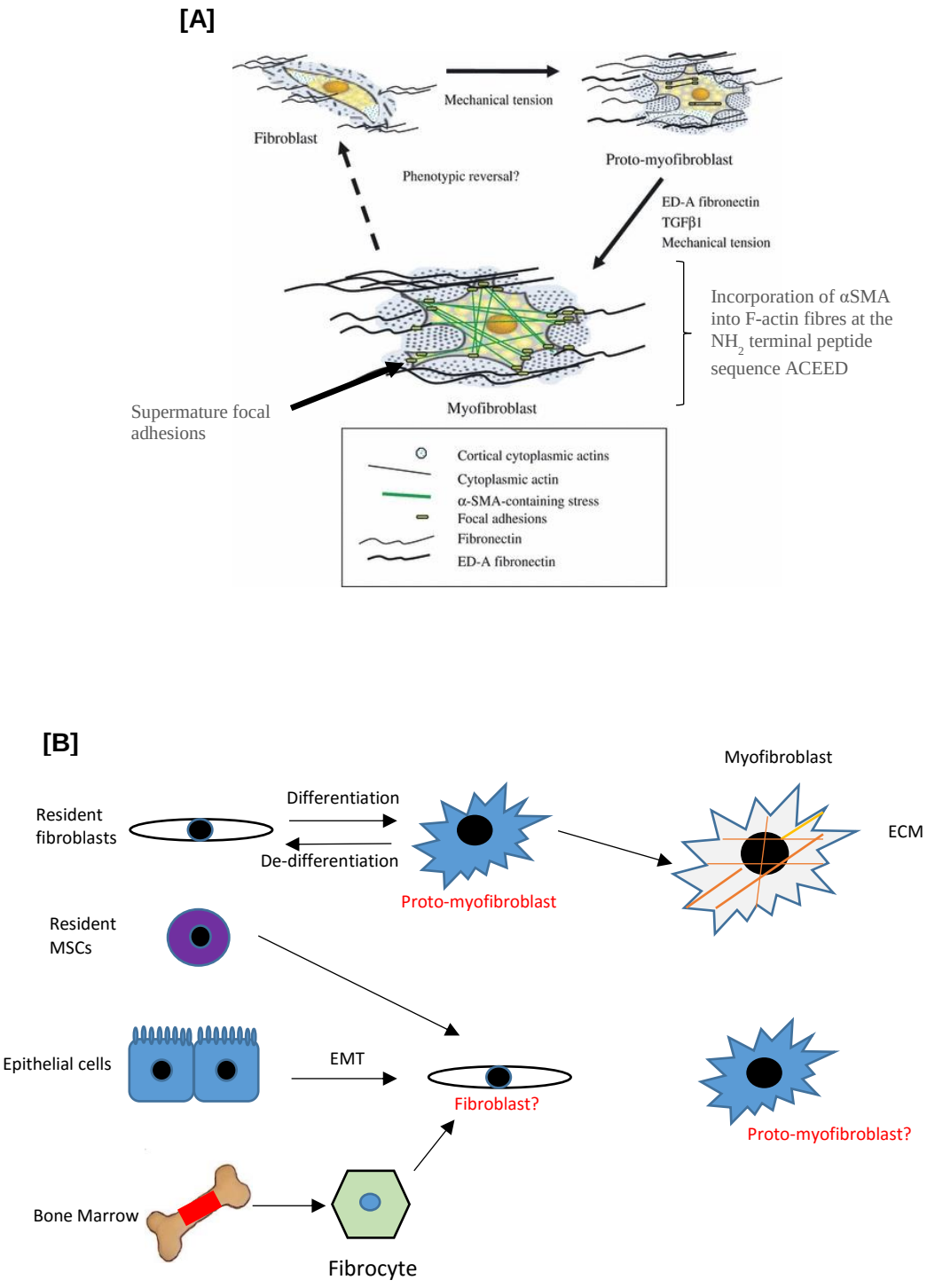

Figure 1.2 – Myofibroblast Differentiation and Epithelial to Mesenchymal Transition

[A] Schematic adapted from (Tomasek et al. 2002) illustrates the differentiation process of fibroblasts to myofibroblasts (via the intermediate stage of a proto-myofibroblast) and the altered protein expression at each stage. Schematic ***[B]*** is an illustration of the potential origins of fibroblasts and myofibroblasts in wound healing and fibrosis.

1.4 - Extracellular Matrix (ECM)

1.4.1. – Collagens

Collagen family proteins represent the most abundant component of the ECM. Collagens exist in the interstitial regions of all parenchymal tissues and contribute to the fibril back bone of the ECM, providing structure and strength. All collagens are formed from three polypeptide α-chains that form a right-handed triple helix. In the ECM, collagens exist in a range of sizes, have different functions and their expression varies between tissue types. Collagens all have repeating proline-rich tripeptide domains, Gly-X-Y, involved in forming the triple helix. Currently, 26 collagens have been identified and can be characterised as fibril forming collagens (the most abundant group, making up 90% of the ECM), fibril associated collagens with interrupted triple helix (FACIT), network forming collagens, anchoring fibrils, transmembrane collagens and basement membrane collagens (Gelse et al. 2003).

Collagen biosynthesis is regulated by 42 genes, some of which have complicated intron-exon patterns which contributes to the production of multiple mRNA transcripts. Most knowledge of collagen synthesis is focused on the formation of fibril collagens, such as collagen I. Collagen mRNA transcripts link with ribosomal subunits, where an initial procollagen helix is formed from the N-terminus to the C-terminus, assisted by enzymes peptidyl propyl cis-trans isomerase (PPI) and other collagen specific mediators (Lang et al. 1987). Collagen also undergoes posttranslational modifications, including hydroxylation at proline and lysine motifs, which thermally stabilize the helix and maintain the structure (Cohen-Solal et al. 1986). Procollagens are packaged into vesicles in the Golgi and secreted into the ECM, where the C-propeptides and N-propeptides are cleaved by procollagen proteases and collagen fibrils are "self assembled" (Prockop et al. 1998).

The function of collagen in the ECM is not limited to structural maintenance. It is vital for cell integrity and cell adhesion; and binds, stores and regulates essential growth factors. For example, it has been shown to mediate TGF-β_1 activity by its association with the proteoglycan decorin (Yamaguchi et al. 1990). It is well understood that collagen has a major role in the wound healing process. However, dysregulated collagen production by resident myofibroblasts is also associated with fibrotic progression. This can be seen in an early study by Zhang et al. (1994) in a bleomycin-induced pulmonary fibrosis mouse model, in which an increase in procollagen I was observed in fibrotic regions within the lung, together with an associated abundance of myofibroblasts. The importance of collagen in regulating and maintaining a balanced matrix environment was shown in a study by Zeisberg et al. (2001). This group's research shows that collagen IV, an important component of basement membranes, is essential for the integrity and function of mouse kidney proximal tubular epithelial cells; and that damage to the basement membrane or inhibition of collagen IV expression results in increased production of TGF-β_1 and facilitates EMT. Furthermore, epithelial cells cultivated on collagen IV maintained the epithelial phenotype. Conversely, epithelial cells cultivated on collagen I began to spontaneously transdifferentiate into a mesenchymal cell type, hence, showing the importance of a balanced collagen expression within the ECM and its contribution toward fibrotic progression.

1.4.2.-Fibronectin

Fibronectin (FN) is an adhesive protein found within blood and the ECM with a molecular weight of ~500kDa. In humans it exists in 2 forms, a soluble form that is found in blood plasma and an insoluble form that is deposited in the ECM. It is formed from an 8 kb mRNA and has two subunits ranging from ~230 kDa to ~270 kDa, that are linked by a disulphide bond to form a dimer, and composed of repeating protein units, known as type I, type II and type III. Proteins type I and II stabilise the folding of fibronectin by virtue of two intramolecular disulphide

bonds. In humans, there are 20 known isoforms of fibronectin that result from alternative splicing in 3 regions. These are EIIIA, EIIIB and a third at region IIICS that is also known as the V region (Singh et al. 2010). In the ECM, fibronectin forms from soluble to insoluble mature fibril bundles that are cell associated and form a network between adjacent cells. This development of insoluble matrix FN was first discovered by McKeown-Longo and Mosher (1983). It was later determined that multiple regions on the fibrinogen dimer were required to initiate fibril formation. These include a 70kDa N-terminal domain that also extends through a collagen/gelatin binding domain; and the association of cell integrins such as α5β1, with the RGD (Arg-Gly-Asp) domain (McKeown Longo and Mosher 1985; Singh et al. 2010).

The interaction between fibronectin and cells via integrins has a role in regulating cell functions, including cell adhesion, migration and differentiation (Serini et al. 1998; Urbich et al. 2002). An example of this is the interaction between integrin α4β7, which associates with EDA-fibronectin, a spliced isoform of cellular fibronectin that includes the alternatively spliced domain A. The association mediates the differentiation of fibroblasts to myofibroblasts by altering the tension of stress fibres and incorporation of contractile αSMA (Kohan et al. 2010). Fibronectin also contains binding sites via which it interacts with other ECM components. These include a collagen/gelatin binding domain and two or more heparin binding domains that mediate the interaction between fibronectin and glycosaminoglycans (Singh et al. 2010).

1.4.3. - Proteoglycans and Glycosaminoglycans

Proteoglycans are a large family of molecules that have a central protein core covalently bound to highly anionic glycosaminoglycan (GAG) side chains. The GAGs are the most common heteropolysaccharides in the body and are formed from repeating disaccharide units. Each disaccharide unit consists of either the hexosamine D-glucosamine (GLcN) or D-galactosamine (GalN) in combination with an uronic acid. These are either D-glucuronic acid (GlcA) or L-

iduronic acid (IdoA). The most abundantly expressed GAGs include chondroitin sulphate (CS), dermatan sulphate (DS), heparan sulphate (HS) and heparin, which are essential in maintaining the structure and function of various tissue types (reviewed by Kjellen and Lindahl 1991). The number of GAG chains added onto the core protein can vary between one to more than one hundred; and they are usually attached via a tetrasaccharide bridge that contains a single glucuronic acid, two galactose residues and a xylose residue (GLAc-Glu-Glu-Xyl). This sequence binds to a serine or threonine residue within the protein core to form an O-glycosylic bond, although some GAGs, for example keratan sulphate, can form an N-glycosylic bond. The variability of these proteoglycans results from a large range of protein cores and the arrangement of GAG chains, for example attachment sites usage may vary from cell to cell.

Proteoglycans have multiple functions and their negative charge may influence these functions. The anionic charge derives from the addition of sulphate and hydroxyl groups on to the GAG chain and results in regulation of the functional properties of proteoglycans. The negative charge creates an osmotic potential and water travels into the surrounding area giving a hydrated matrix environment that maintains the required conditions for optimum cell interactions (Hardingham and Bayliss 1990) . Furthermore, proteoglycans in the ECM provide low viscosity, increased lubrication and compressive strength, making them important in synovial joints (Beasley 2012). They also provide a ridged structure that allows for cell attachment, interaction and migration (Wight et al. 1992). There are four main classes of proteoglycans: interstitial proteoglycans, basement membrane proteoglycans, membrane bound proteoglycans and granule secretory proteoglycans (of which the major one is serglycin). All proteoglycans are placed into groups dependent on function, their distribution in tissue types and core protein homology (Kjellen and Lindahl 1991).

A different form of GAG is hyaluronan (HA). This ubiquitously expressed GAG exists alone as repeating nonsulphated disaccharide units that are not bound to a protein core.

1.5. – Hyaluronan: An Overview

HA is a linear polysaccharide formed from repeating disaccharide units of D-glucuronic acid and *N*-acetyl-D –glucosamine ***(Figure 1.3.)***. The saccharide units are linked by alternate β1-4 and β1-3 glucuronic bond units (Weissmann and Meyer 1954). First discovered in 1934 in the vitreous of the bovine eye by Meyer and Palmer (1934), HA has since been recognised as a ubiquitously expressed ECM component that is widely abundant in connective tissues, including the ocular vitreous, heart valves, skin, synovial joints, neural and skeletal tissue. It is also present in much smaller quantities in soft organ tissues, such as the lungs, kidneys and the brain, although there is minimal expression of HA within the liver matrix (Fraser et al. 1997).

The structure of HA regulates the osmotic potential of the interstitial matrix and maintains a continuous hydrated environment and lubrication of joints (Swann et al. 1974). It interacts with other ECM components to form strong structural bonds that maintain the stability of the matrix environment (Fraser et al. 1997). Along with maintaining homeostasis, HA regulates cell-cell and cell-ECM associations, as well as cell proliferation, differentiation and migration through its association with cell surface receptors, principally CD44 and RHAMM (Evanko et al. 1999; Webber et al. 2009a). The dysregulation of HA metabolism, catabolism, ECM distribution and alterations in HA function have a major role in pathology; and have been associated with pathological conditions including multiple cancer types, cardiovascular, neurological, inflammatory and fibrotic diseases (Itano 2008; Jiang et al. 2011; Albeiroti et al. 2015; Sherman et al. 2015).

1.5.1. - HA Biosynthesis

Unlike other GAGs that are commonly synthesised in the Golgi apparatus, uniquely HA is synthesised within the inner plasma membrane. HA is synthesised by membrane-bound enzymes known as hyaluronan synthases (HASs), that may be classified into class I and class

II. Class I includes eukaryotic HASs, which use UDP-N-acetyl-D-glucosamine and UDP-α-D-glucuronate as substrates for HA synthesis (Weigel and DeAngelis 2007). There are three isoforms of HASs in vertebrates known as HAS1, HAS2 and HAS3, each transcribed from discrete autosomal loci on different chromosomes (Spicer and McDonald 1998).

The synthesis of HA by HAS enzymes is mediated by the addition of each new sugar onto the reducing (UDP) end of the previously added sugar. This allows for the addition of the next sugar, via the loss of the covalently bonded UDP residue. The non-reducing end is extended and elongated into the peri-cellular space as shown in ***(Figure 1.3 [B])*** (Bodevin-Authelet et al. 2005). HA accumulates and forms a peri-cellular matrix or coat around the exterior of many cell types (Clarris and Fraser 1968).

In a study by Itano et al. (1999), the enzymatic functions of the three HAS isoforms were observed in cells transfected with HAS1, 2 or 3 overexpression vectors. Following transfection, these workers observed that cells overexpressing HAS1 had a much smaller HA peri-cellular coats, compared to cells overexpressing HAS2 or 3. It was also found that the HAS isoforms synthesised HA of different molecular weights. HAS3 synthesised the lowest molecular weight HA of ~1 x 10^5 – 1 x 10^6 Da. HAS 1 and 2 synthesised HA with a larger mass ranging between ~2 x 10^5 – 2 x 10^6 Da, HAS2 synthesised the largest molecular weight HA with a mass at the higher end of the given range. Furthermore, they found the synthesis rate and stability of HA produced varied between isoforms, suggesting they all have different properties. Successive subsequent studies have shown different cellular responses are HA size-dependent and that induction of HAS gene expression varies between cell types (Craig et al. 2009; Campo et al. 2010). In summary, current evidence suggests that the properties and functions of each HAS protein may depend on the cellular context in which its corresponding gene is expressed.

1.5.2. HA Assembly and Hyaladerins

Considering the simplicity of its structure, HA exhibits considerable functional diversity. Following synthesis and release by the cell, HA undergoes re-organisation and assembly by interstitial hyaldherins, contributing significantly to its functional diversity. Many hyaldherins belong to the link domain family and bind to HA using this link region. These include HA receptor, CD44, which mediates multiple HA functions including migration, ECM re-arrangement and differentiation. The HA receptor know as lymphatic vessel endothelial hyaluronan receptor 1 (LYVE-1), also has a link domain that has been associated with HA degradation in lymphatic vessels (reviewed in Day and Prestwich 2002).

Tumour necrosis factor stimulated gene 6 (TSG-6) contains a single link domain and is widely documented to be involved in the formation of HA peri-cellular matrices. For example, TSG-6 expression is upregulated following TGF-β_1 stimulation in myofibroblasts, and is important in the formation of the HA peri-cellular coat that maintains cellular phenotype (Simpson et al. 2009). Further, in kidney proximal tubular cells from line HK2, that can be activated to undergo EMT using TGF-β1 stimulation *in vitro*, silencing TSG-6 mRNA prevented formation of HA cables (Bommaya et al. 2011). These HA cables are commonly associated with the immune response and bind leukocytes to HA in a process that is CD44-dependent (de la Motte et al. 1999; Selbi et al. 2006). Other ECM components with link binding domains include the proteoglycans, aggrecan, versican and neurocan. The association of these proteoglycans with HA through the link domain forms stabilizing complexes that are important in maintaining the structural integrity of tissues (Day and Prestwich 2002).

Not all hyaldherins that mediate HA assembly contain a link domain. Members of the Inter α trypsin Inhibitor family (IαI) are non-link domain hyaldherins, comprised of a light chain and a varied arrangement of six heavy chains (HCs). The light proteoglycan chain is

formed of a chondroitin4-sulphate chain linked to the core protein, bikunin. Bikunin is widely documented as a protease inhibitor, due to the presence of two Kunitz type protease inhibitor domains (Xu et al. 1998). The bikunin domain is often associated with either one or two HCs. For example, in pre-α-trypsin inhibitor (PαI), only HC3 is associated with bikunin, while in IαI, bikunin is associated with HC1 and HC2. These linkages take place via an ester bond formed between the carboxyl end of the HCs and the chondroitin4-sulphate chain (Enghild et al. 1999). One key HC function is the stabilisation of HA matrices. For example, IαI is essential for ovulation, due to its covalent bonding and stabilizing of the HA-rich, ECM. TSG-6 has been widely documented to be required for the transfer of HCs from IαI onto HA, thereby facilitating the formation of HA matrices indirectly, as well as directly through its link domain (Colón et al. 2009).

Another commonly described non-link domain hyaldherin is the receptor for hyaluronan - mediated motility (RHAMM), that mediates cellular migration and proliferation via its association with HA (Akiyama et al. 2001; Nedvetzki et al. 2004). The precise mechanisms of hyaldherin-HA association are presently under intensive study. However, it is well established that these molecules are highly important in maintaining homeostasis; and that aberrant expression alters HA assembly and function and can result in disease.

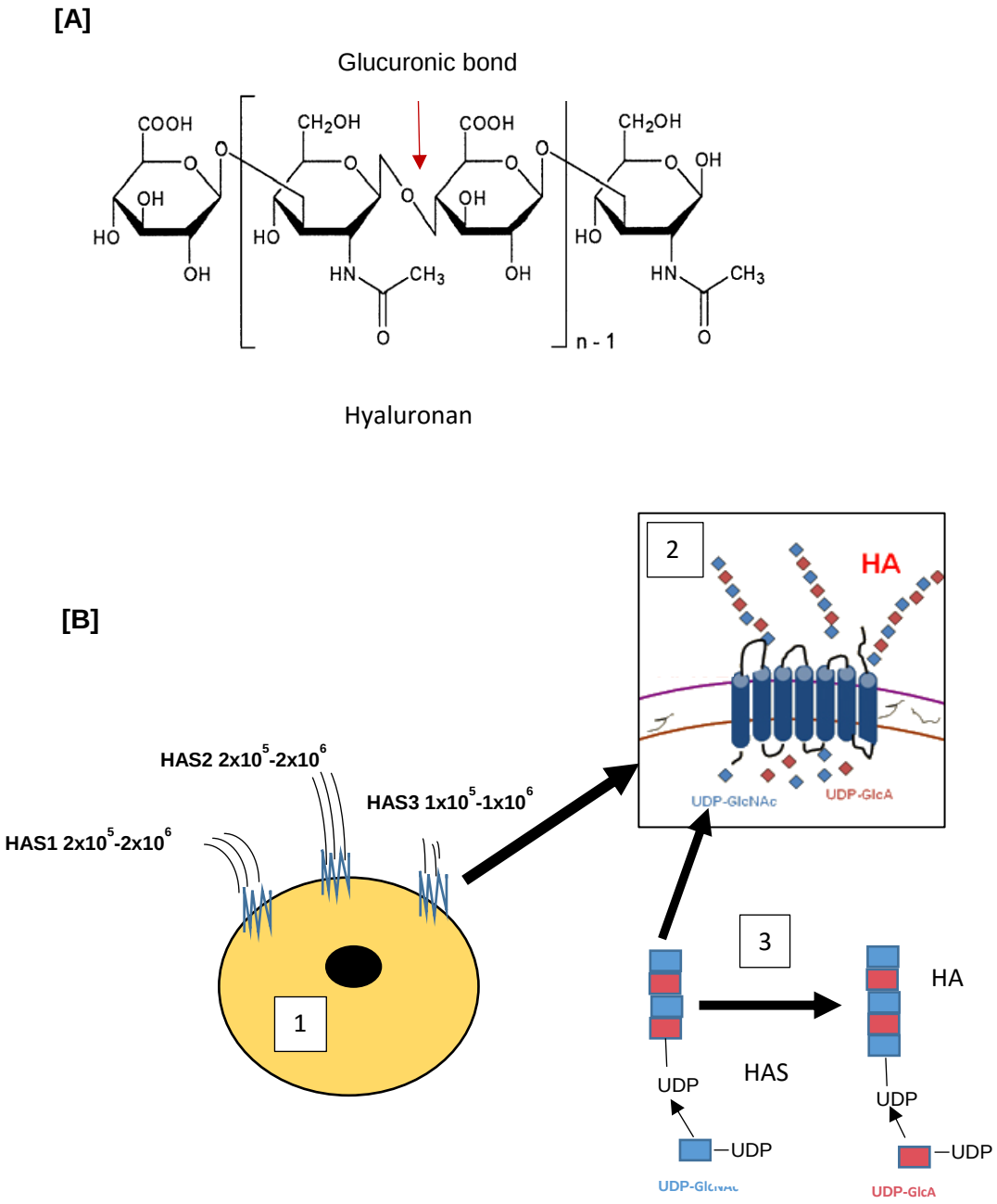

Figure 1.3. Hyaluronan Synthesis and Structure

[A] Chemical structure of linear HA polysaccharide formed from repeating disaccharide units. Each disaccharide unit is comprised of D-glucuronic acid and *N*-acetyl-D –glucosamine, linked by alternating β1-4 and β1-3 glucuronic bond units (red arrow). Adapted from (http://morebrainpoints.blogspot.co.uk/2013/10/naked-mole-rats-cure-for-cancer.html). **[B]** Synthesis of HA in the plasma membrane. (1) Position of HA synthesis in the plasma membrane and variable lengths of HA synthesis by HAS 1, 2 and 3. (2) Class 1 eukaryote HAS with six transmembrane domains. (3) Addition of saccharide units UDP-GLcNAc and UDP-GlcA at the reducing UDP end of the HA chain by HAS enzymes. HA elongates into extracellular regions at the non-reducing end of the molecule. (1) Adapted from Stridh et al. (2012). (2) and (3) adapted from Dr. Paul H. Weigel http://www.glycoforum.gr.jp/science/hyaluronan/HA06a/HA06aE.html#III.

1.5.3. - HA Degradation

HA production and degradation is a rapid and continuous process. However, the half-life of HA varies between tissue types. Hyaluronidases (HYALs) are a family of enzymes that are encoded by six HYAL-like sequences at two discrete autosomal loci. Three HYAL enzymes are principally involved in HA degradation in somatic tissue: HYAL1, HYAL2 and HYAL3. HYAL1-3 are all located in a cluster at 3p21.3. Three further HYAL-like sequences, clustered at 7q31.3, are known as HYAL4, SPAM1 and a HYALP1; and respectively encode proteins HYAL4, sperm protein PH-20 and a pseudogene (a gene that is transcribed, but not translated). However, the latter three genes are not relevant in somatic tissue and will not be discussed any further in this text (Itano et al. 1999; Csoka et al. 2001).

HYAL1, also known as plasma hyaluronidase, is found in abundance in multiple tissue types and is expressed as a 57 kDa protein. It is an active acid lysosomal enzyme that can degrade HA of any size, usually into tetrasaccharides (Afify et al. 1993). HYAL2 is also an acid active enzyme that functions optimally in an acidic environment, is attached to the plasma membrane by a glycophospatidylinositol (GPI) anchor (Rai et al. 2001); and specifically cleaves high molecular weight HA into 20 kDa fragments. The HA receptor CD44 is essential to HA degradation by HYAL1 and 2 (Harada and Takahashi 2007). Using cells that stably overexpressed HYAL1, 2 and 3, simultaneously, with the overexpression of the HA receptor CD44, it was essential that HA was internalised by CD44 to allow lysosomally-located HYAL1 to catabolise HA (Harada and Takahashi 2007). Blocking CD44 activity using antibodies prevented HYAL1 function and HA degradation into tetrasaccharides (Harada and Takahashi 2007).

Furthermore, HYAL2 catabolism of HA at the plasma membrane was also shown to be CD44-dependent, consistent with previous research by (Bourguignon et al. 2004), that

observed that CD44 co-localisation with HYAL2 at the plasma membrane was essential for HA catabolism by HYAL2. Interestingly, this study found that the CD44/HYAL2 complex was increased in caveolae microdomains, due to optimal environmental pH. HYAL3 was not involved in HA breakdown in the overexpression model.

It has previously been suggested that these two enzymes work together in the degradation of HA (Csoka et al. 2001). These authors suggest that HYAL2 breaks down large exogenous HA into 20 kDa fragments and that these smaller fragment are then internalised and further catabolised by HYAL1 enzymes within lysosomes. However, the aforementioned study by Harada and Takahashi (2007), showed that HYAL1 and HYAL2 have the ability to degrade HA independently of each other. ***(Figure 1.4)*** is a schematic that shows the generally accepted model of internalisation and degradation of HA.

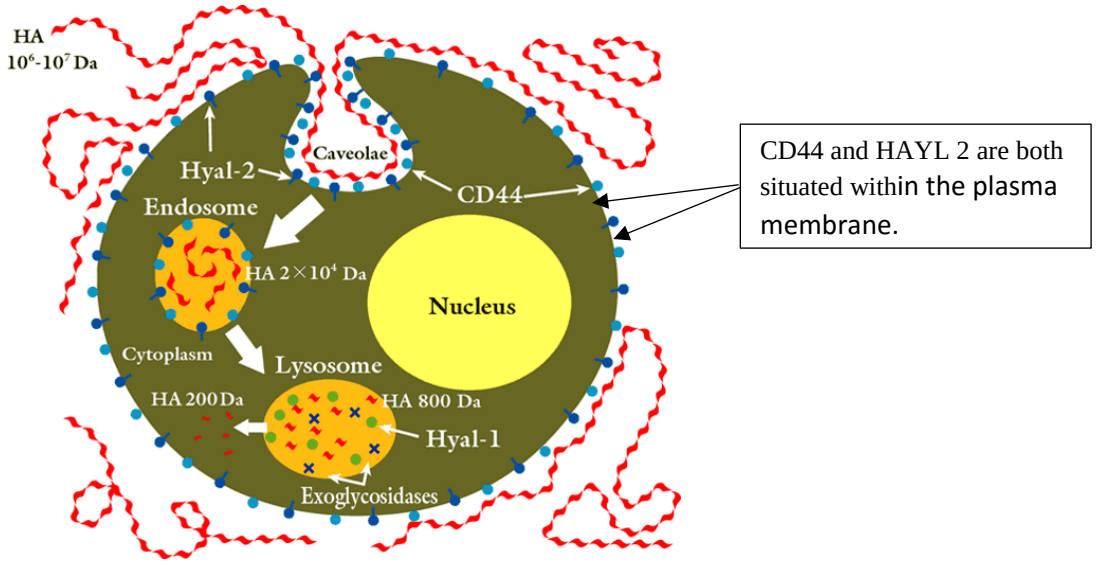

Figure 1.4. HA Internalisation and Degradation

Internalisation of HA via CD44 located in caveolae raft regions. Following internalisation into endosomes, large linear HA is broken down into approximately 20 kDa fragments by HYAL2. Fusion of endosomes with lysosomes containing HYAL1 leads to further breakdown of HA. Adapted from Dr. Robert Stern http://www.glycoforum.gr.jp/science/hyaluronan/HA15a/HA15aE.html.

1.5.4. - HA Involvement in Fibrosis

Increased HA expression and correlation with progression of fibrosis has been observed in many tissue types, leading to the suggestion that HA is a marker for fibrotic progression (Halfon et al. 2005). HA accumulation has been associated with inflammatory response induction, since upregulated HA synthesis has been observed in inflammatory diseases, such as asthma and inflammatory bowel disease (de la Motte 2011; Liang et al. 2011). However, different molecular weights of HA regulate both anti-inflammatory and pro-inflammatory immune responses. For example, in a study by Nakamura et al. (2004), using T-cell induced liver injury in mice, injection with high molecular weight HA (HMW-HA) of ~900 kDa, a significant reduction in expression of pro-inflammatory cytokines was seen, including, TNF-α and IFN-γ; indicating an anti-inflammatory role for HMW-HA. Conversely, HMW-HA that has been depolymerised to fragmented or low molecular weight HA (LMW-HA) elicits a pro-inflammatory response in inflammatory diseases, such as rheumatoid arthritis (RA). It is not understood how LMW-HA mediates this pro-inflammatory response. However, it is known that LMW-HA can mediate intracellular signalling through multiple receptors, including CD44 (Termeer et al. 2002; Wolny et al. 2010; Kouvidi et al. 2011).

HA molecules also cross-link to form cables between adjacent cells that facilitate leukocyte binding. This cross linking is achieved by the HCs of IαI and pre-α inhibitor (PαI) being covalently linked to HA, a process known to be facilitated by the hyaldherin, TSG-6. It has been proposed by Day and de la Motte (2005), that cables act as an anti-inflammatory mediator by binding leukocytes and preventing the activation of receptors on resident cells, thereby preventing the release of pro-inflammatory cytokines. It is thought that CD44 receptors on the plasma membrane of leukocytes form clusters and internalise a proportion of the HA cables to facilitate binding. Furthermore, it has been shown that the HA peri-cellular coat can mediate the activation of resident cells by leukocytes. For example, it was previously

determined by Selbi et al. (2004), that HA cables were formed between unstimulated, adjacent cells proximal tubular cells. In addition, monocytes were shown to bind to the cables via CD44. The association of the monocytes with the HA cables prevented the association and subsequent activation of the cells by monocytes.

In a later study, it was reported that removal of HA from the cell surface lead to increased association of monocytes with the intracellular adhesion molecule 1 (ICAM-1). This increased association resulted in upregulation of TGF-β_1 promoter activity that was ICAM-1 dependent (Zhang et al. 2004). Moreover, TGF-β_1 has previously been shown to activate epithelial to mesenchymal transition in these cells. Therefore, the HA cables seem to play a role in preventing and limiting an inflammatory and fibrotic response (Zhang et al. 2004).

As well as indirectly mediating fibrotic progression through a dysregulated immune response, HA contributes directly to a pro-fibrotic response. Under fibrotic conditions, HA oligomers have been shown to interact with RHAMM and mediate fibrosis via increasing inflammation, migration and angiogenesis. Using a HA oligomer targeting HA/RHAMM association, Tolg et al. (2012) found that preventing HA binding to RHAMM significantly decreased the presence of fibroblasts within rat wounds. Furthermore, they suggested that the reduction in cell migration results from interference with the required RHAMM association with focal adhesion kinases. A previous study by Webber et al. (2009b), found that association of HA with principal receptor CD44 is central to the formation of a peri-cellular coat. Moreover, this HA peri-cellular coat was essential for both differentiation and maintaining the myofibroblast phenotype. The host laboratory has previously identified the importance of the HA/CD44 interaction in both inflammatory and fibrotic regulation (Meran et al. 2008a; Simpson et al. 2009; Midgley et al. 2013). Two cytokines that are known to mediate CD44/HA regulation of pro-fibrotic and pro-inflammatory responses are TGF-β_1 and IL-1β, respectively.

1.6. – Transforming Growth Factor–β (TGF-β) and Fibrosis

1.6.1. - Transforming Growth Factor-beta (TGF-β)

There are three isoforms of TGF-β known as TGF-β_1, β_2 and β_3. These multifunctional cytokines are members of the transforming growth factor super family (TGFSF). All three isoforms are transcribed from different genes and play roles in embryogenesis, cellular regulation and progression of diseases, including cancer, heart disease and fibrosis (Lawrence 1996).

TGF-β is secreted ubiquitously by multiple parenchymal cell types and infiltrating leukocytes in a latent form that is biologically inert. Latent TGF-β is secreted as a large protein with a range of 390-412 amino acids in length. To become activated, it is cleaved to produce a pro-region known as a latency-associated protein (LAP) and active mature TGF-β. The LAP can be released or re-organised to allow for exposure of the TGF-β receptor binding site. There are multiple proteases reported to cleave latent TGF-β including plasmin, thrombospondin-1 and MMP-2 and -9 (Yu and Stamenkovic 2000; Robertson et al. 2015). Furthermore, environmental changes including pH and increased temperature can release the LAP association from the active region. TGF-β_1 is the most studied member of the isoforms and it is widely acknowledged that it is a major mediator of wound healing and fibrosis.

1.6.2. -Transforming Growth Factor-β1 (TGF-β1)

TGF-β_1 is encoded by the TGF-β_1 gene at 19q13. The three subtypes of TGF-βR (TGF Receptor) are known as types I, II and III. TGF-β1 signalling requires both type I and type II receptors. TGF-βRIII (also known as betaglycan) is a proteoglycan with approximately 10 kDa of N-linked glycan chains, together with chondroitin sulphate and/or a heparan sulphate chains. Betaglycan exists in both soluble and plasma membrane-bound forms, both of which bind members of the TGF-β superfamily and other ligands, including basic fibroblast growth factor

(bFGF) (Andres et al. 1989; 1992). The membrane bound form does not have an active intracellular signalling domain, but forms dimers with both TGF-βRII and TGF-βRI (Henis et al. 1994; Zhang et al. 2010). In this way both soluble and membrane bound TGF-βIII forms act as accessory proteins, providing a reservoir of ligands that can present or restrict TGF-β superfamily member association with TGF-βRI and II (Andres et al. 1989; Zhang et al. 2010). Initially, TGF-β_1 interacts with TGF-βRII prior to interaction with TGF-βRI, the phosphorylation of a threonine residue in a glycine/serine domain in TGF-βRI by TGF-βRII results in intracellular signalling. In the absence of TGF-βRII, there is no signal from TGF-βRI, indicating the importance of this complex formation (Feng and Derynck 1996).

The type I receptor that is associated with TGF-β_1 signalling has been identified as an activin-like kinase receptor (ALK-5). Activation of this receptor following TGF-β_1 binding activates the downstream SMAD pathway, resulting in the translocation of SMAD proteins to the nucleus where they form complexes and mediate gene regulation. In mammals, SMAD2 and 3 are TGF-β/activin receptor dependent, the other SMADs are bone morphogenic protein (BMP)-dependent.

BMP cytokines also represent a subfamily of the TGF-β superfamily. TGF-β_1 induced SMAD regulation has previously been shown to be anti-proliferative, and therefore has a tumour suppressive role (Seoane 2006). By contrast, TGF-β_1 induction of ERK1/2 has a role in EMT, contributing to tumour progression (Xie et al. 2004), and TGF-β_1:receptor interactions are therefore cell specific. Similarly, stimulation of dermal fibroblasts with TGF-β_1 results in increased cellular proliferation, but oral fibroblasts stimulated with TGF-β_1 have an anti-proliferative response (Meran et al. 2008b).

TGF-β_1 has also been associated with cellular regulation of the ECM, integrin expression and increased production of protease regulators; and thus acts as a major mediator

of cell-ECM contact. TGF-β_1 activation increases fibroblast expression of fibronectin, collagen I and HA, all of which are important in cell differentiation, migration and adhesion (Streuli et al. 1993). However, not only fibroblasts are activated by TGF-β_1 to produce ECM components. For example, TGF-β_1 activation of SMAD2 and 3 through TGF-βRI in corneal endothelial cells increased their production of laminin and fibronectin (Usui et al. 1998).

Regulation of cellular TGF-β_1 expression is also commonly mediated by ECM components. For example, in an early study by Streuli et al. (1993), the basement membrane (BM) was determined to be important in regulating cellular TGF-β_1 expression. In the absence of the BM, TGF-β_1 promoter activity increased significantly. Furthermore, when epithelial cells were in contact with a BM that was either endogenously synthesised or added exogenously, the activity of the promoter significantly decreased.

TGF-β_1 also regulates cellular synthesis of proteases, including MMPs, and therefore indirectly modulates ECM arrangement and turnover. For example, TGF-βR complexes activate downstream SMAD and co-SMADs, these transcription factors have been shown to target the TGF-β1 inhibitory element (TIE) within the promotor regions of MMP 1 and MMP 3, thereby, regulating their expression. Furthermore, MMP gene expression varies depending on the cell type and location (Brinckerhoff and Matrisian 2002; Burrage et al. 2006). Therefore, TGF-β_1 expression and the ECM work synergistically to maintain a tightly regulated cellular environment and disruption of this homeostasis may result in disease.

1.6.3. – TGF-β_1 Induced HA/CD44 in Fibrosis

Under normal conditions in damaged tissue, TGF-β_1 mediates a healing response by activating phenotypic transition of resident fibroblasts to myofibroblasts. Early studies determined that TGF-β_1 stimulation of fibroblasts resulted in altered morphology, resulting from increased αSMA expression and subsequent increase in contractile force (Serini and

Gabbiani 1999; Vaughan et al. 2000). Multiple studies have shown a distinct change in fibroblast morphology, following TGF-β_1 stimulation, from a thin spindle-like morphology to the three dimensional polygon structure; typical of myofibroblasts. Furthermore, F-actin re-arrangement also alters in myofibroblasts and actin bundles show an increased thickness resulting from αSMA incorporation (Desmoulière et al. 1993; Hinz et al. 2001; Tomasek et al. 2002a; Evans et al. 2003b). Interestingly, removal of TGF-β_1 does not reverse this morphology, indicating that the differentiation process is stable and non-reversible (Evans et al. 2003a; Webber et al. 2009b). The morphological change is associated not only with upregulated αSMA expression, but also an increased presence of ECM components, including collagen I, II, III and fibronectin (Ignotz and Massague 1986; Varga et al. 1987; Evans et al. 2003b). It has long been determined that TGF-β_1 interaction with its receptor, ALK5, activates the phosphorylation of downstream SMAD proteins (Heldin et al. 1997; Goumans et al. 2002). Interestingly, the overexpression of SMAD3 in fibroblasts induces terminal differentiation in a TGF-β_1-independent manner. However, overexpression of SMAD2 does not activate a differential change, suggesting that SMAD3 activation regulates cell morphology (Evans et al. 2003b).

An important feature of the myofibroblast's role in fibrotic progression is its excessive production of ECM components (Hinz 2007). In fibrotic tissue, collagen is the major ECM component laid down by myofibroblasts and can be used as a further marker of fibrotic progression (Rosenberg et al. 2004; Fontana et al. 2008). In order for fibroblasts to increase collagen production independent of TGF-β_1, the over expression of SMAD2, SMAD3 and Co-SMAD4 was required. Furthermore, silencing any of these SMADs individually prevented differentiation, highlighting the importance of this complex in gene transcription associated with myofibroblast differentiation (Evans et al. 2003b).

The association of increased HA expression in scar tissue with fibrotic progression is well-documented. TGF-β_1 stimulation increases HA metabolism, leading to an accumulation of both intracellular and extracellular HA and the formation of a peri-cellular coat (Eddy 1996; Jenkins et al. 2004). Terminally differentiated myofibroblasts exhibit a HA peri-cellular coat assembled from crosslinking of linear HA (Webber et al. 2009a). HA is tethered by hyaldherins, such as HC from IαI and PαI, which are localised by association with TSG-6 (Selbi et al. 2006). TSG-6 gene expression is elevated following TGF-β_1 stimulation. Interestingly, inhibition of TGF-β_1 receptor, ALK5, decreased TSG-6 expression; and in recent unpublished data it was determined that the transcriptional expression of TSG-6 was also SMAD3-dependent.

In dermal fibroblasts, peri-cellular coat assembly is central to the maintenance of the myofibroblast phenotype. By contrast, the rapid, non-scarring healing of the oral mucosal membrane results from a fibroblast population with different myofibroblastic differentiation properties. Comparison of non-scarring oral fibroblasts with scar forming dermal fibroblasts reveals different transcriptional expression of HAS isoforms. HAS1 is not expressed in oral fibroblasts and HAS2 expression decreases in the presence of TGF-β_1. By contrast, scar-forming dermal fibroblasts express HAS1 and HAS2 and expression of both increases in TGF-β1-induced myofibroblasts (Meran et al. 2007).

HAS2 siRNA silencing and depleting the cytoplasmic pool of UDP-glucuronic using 4MU, prevents myofibroblast differentiation in dermal fibroblasts, but TGF-β_1 phosphorylation of the SMAD pathway is not affected (Webber et al. 2009c). Therefore, the formation of the HA peri-cellular coat is essential for myofibroblast differentiation. The lack of a HA peri-cellular coat prevents TGF-β_1- induced myofibroblast differentiation in oral fibroblasts, therefore, the synthesis and arrangement of the peri-cellular coat is central to the differentiation process (Webber et al. 2009c). HA accumulation occurs simultaneously with

the secretion of HYAL1 and 2, but the expression of both these HA degrading enzymes is decreased in myofibroblasts. A subsequent decrease in HA degradation might also favour accumulation of HA in fibrotic disease (Jenkins et al. 2004).

Increased dermal fibroblast proliferation is also thought to be central to scar formation and hence, fibrotic progression. Analysis of proliferation in dermal and oral fibroblasts stimulated with TGF-β_1 has shown an anti-proliferative response in oral fibroblasts, compared to increased proliferation in dermal fibroblasts (Meran et al. 2008b) Although both cell types are activated by TGF-β_1 through the SMAD pathway, but different expression patterns of the genes encoding HA-associated proteins, including aggrecan and versican were observed (Meran et al. 2008b).

The interaction between HA and receptor CD44 is central to both fibroblast differentiation and proliferation; and this HA/CD44 interaction is TGF-β_1-dependent. Co-localisation of CD44 with epidermal growth factor receptor (EGFR) is also central to both fibroblast proliferation and differentiation. In oral fibroblasts, the involvement of CD44 is not required for an anti-proliferative response, but in dermal fibroblasts, the upregulation of HA is associated with the increased interaction of CD44 and EGFR; and HA mediates the co-localisation between the two receptors. Furthermore, the overexpression of HAS2 in oral fibroblasts can reverse the anti-proliferative response and drive proliferation.

A similar response can be observed in aged dermal fibroblasts. These cells have impaired differentiation properties resulting from decreased HAS2 expression, limited HA peri-cellular coat assembly and downregulation of TSG-6. There is also a failure of HA to associate with CD44 and a decreased expression of EGFR, preventing the CD44/EGFR association essential for αSMA induction. This inability to undergo differentiation may contribute to non-healing wounds, which are commonly associated with age or disease.

However, overexpression of HAS2 alone is not enough to restore the myofibroblast phenotype observed in young dermal fibroblasts. Simultaneous overexpression of EGFR with HAS2 is required to recover the differentiation properties of aged fibroblasts to myofibroblasts (Simpson et al. 2009; 2010).

The association of HA-mediated CD44/EGFR results in the phosphorylation of EGFR and subsequent downstream activation of ERK1/2. The activation of ERK1/2 happens in a biphasic manner, with early and late phase activations. The proliferative response is associated with the late activation of ERK1/2 and is TGF-β_1/HA/CD44/EGFR dependent. It is not observed in oral cells that exhibit an anti-proliferative response, due to limited HA synthesis (Meran et al. 2011a). A similar HA/CD44/EGFR response has been observed in fibroblast-myofibroblast differentiation; and TGF-β_1 induction of this complex formation activates downstream ERK1/2 followed by calmodulin kinase II (caMKII), which is phosphorylated in a similar biphasic pattern as upstream ERK1/2 (Midgley et al. 2013). Recent work has shown that EGFR is present within caveolin lipid raft regions in both fibroblasts and myofibroblasts. Conversely, CD44 is more mobile in fibroblasts and is present inside and outside lipid raft regions (Midgley et al. 2013). However, the motility of CD44 throughout the plasma membrane is significantly decreased in myofibroblasts, resulting from its association with EGFR within lipid raft regions. Dysregulation of HAS2, CD44 or EGFR expression results in loss of downstream ERK1/2 and CAMK-II phosphorylation; and subsequently a loss of αSMA induction (Midgley et al. 2013). Therefore, it has previously been determined that the pro-fibrotic cytokine, TGF-β_1 mediates fibrosis through the continuous activation of the SMAD2/3 and co-SMAD4 pathway simultaneously, with the HA/CD44/EGFR pathway, both of which are required for differentiation (***Figure 1.3)*** and proliferation of resident fibroblasts.

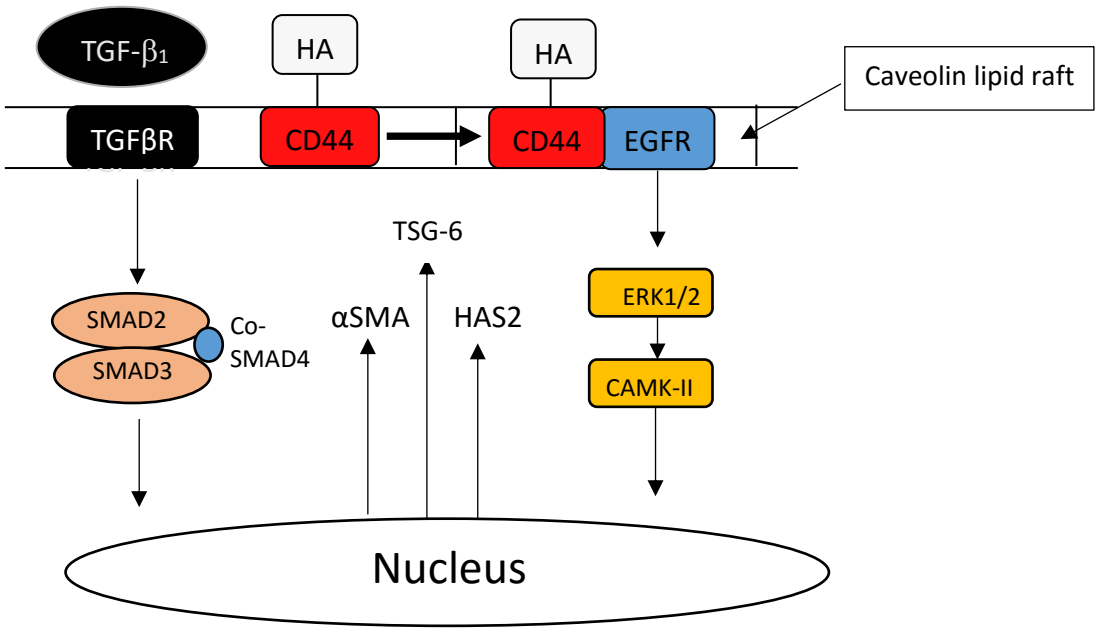

Figure 1.5. TGF-β1 mediated fibroblast –myofibroblast differentiation. I

Interaction of TGF-β1 with TGF-βR activates the downstream SMAD pathway. Simultaneously, HA modulates the movement of CD44 through the plasma membrane where it co-localises with EGFR and becomes locked into caveolae lipid rafts. This co-localisation results in EGFR phosphorylation and the subsequent downstream activation of ERK1/2 and CAMK-II, both of which are essential for increased production of αSMA, HAS2 and TSG-6. The upregulation of HAS2 increases HA synthesis, and HA is rearranged on the cell surface to form a peri-cellular coat. The coat is formed from crosslinking of HA to hyaldherins such as HCs from IαI and PαI, which is facilitated by TSG-6. The HA coat maintains the myofibroblast phenotype, and αSMA becomes incorporated into the F-actin cytoskeleton to give the myofibroblast its contractile phenotype.

1.7 – Interleukin-1 β (IL-1β) and Fibrosis

1.7.1. – Interleukin-1

IL-1 was purified several times and given multiple names, including endogenous pyrogen, lymphocyte activating factor and thymocyte proliferating factor. In 1979, it was given the uniform name of IL-1(Aarden et al. 1980). Two forms of the three identified members of the IL-1 family are agonistic while one is antagonistic. All have been identified as sharing approximately 20-25% amino acid sequence homology (Burger et al. 2006; Brocker et al. 2010). Respectively, these are IL-1α and IL-1β; and a receptor antagonist known as interleukin receptor antagonist protein (IRAP) also abbreviated to (IL-1Ra) (Stylianou and Saklatvala 1998).

There are two identified receptors to IL-1 proteins known as IL-1R1, an 80 kDa protein that has a long cytoplasmic tail; and IL-1R2, a 60 kDa protein that has a short cytoplasmic tail (Wesche et al. 1997; Arend et al. 1998). Interaction of IL-1 proteins with IL-1R2 does not activate a signalling pathway and, therefore, IL-1RII is often referred to as a decoy receptor. The activation of both IL-1α and IL-1β occurs via association with the IL-R1 and its association with an IL-1 receptor associated protein (IL-1R AcP); and this complex is required for intracellular signalling (Dinarello 1991; Arend 2002). The IL1-Ra isoform also associates with the IL-1R1, but fails to activate intracellular signalling and acts as a regulator of IL-1 signalling (Arend et al. 1998).

IL-1α and IL-1β are produced mainly by inflammatory cells, including monocytes and macrophages. However, they are also commonly secreted by fibroblasts, endothelial and epidermal cells (Dinarello 1988). Both isoforms are synthesised as 31 kDa pro-IL1 and cleaved into their 17 kDa active form (Krumm et al. 2014). IL-1β is cleaved in the plasma membrane by a protease named IL-1β converting enzyme (ICE) and is secreted in its active mature form (Thornberry et al. 1992). IL-1β is largely involved in inflammatory responses, and has also been widely accepted to have a major role in wound healing and fibrosis (Arend 2002).

1.7.2. – IL-1β and Inflammation

IL-1β is a potent inflammatory mediator that has an increased expression in disease tissue. The promoter region of the IL-1β gene contains a typical TATA region along with binding sites for NFκB, Activating Protein 1 (AP1), cAMP response element binding protein (CREB), NF-IL6 and novel nuclear factor NF-βA. Stimuli that induce pathways that regulate the transcription of pro-IL-1β mRNA include IL-1β itself, TNF-α and toll like receptor ligands, such as lipopolysaccharides (found on gram-negative pathogens), that activate the toll like receptor pathway. IL-1β induces several genes via the activation of intracellular signalling pathways,

including the activation of NF-κB (biding sites for which are often found within promoter regions of inflammation-associated genes), AP1 and mitogen activated kinase (MAPK) p42 and p44, i.e. the ERK1/2 pathway (Liacini et al. 2002)

Increased IL-1β expression has been observed in the synovial fluid of arthritic joints, the skin of patients that suffer from fibromyalgia, as well as ulcerative colitis and neurodegenerative diseases (Gan et al. 2002; Salemi et al. 2003; Granet et al. 2004; Koprich et al. 2008). This increased expression results in further activation of other inflammatory mediators and cytokines that results in a further influx of inflammatory cells. In acute tissue damage, IL-1β activates IL-6, a potent inflammatory mediator. However, in *IL-1β*$^{-/-}$ mice, the acute phase response usually observed in local tissue damage is prevented, as there is no activation of IL-6 (Fantuzzi and Dinarello 1996). In degenerative disease, there is increased expression of MMPs that contributes to degradation of local tissue. In tendonopathy, increased expression of IL-1β correlates with the increased expression of MMP-13 (collagenase-3), an MMP that has been linked to osteoarthritis, rheumatoid arthritis and peridontal disease; and silencing IL-1β mRNA expression decreases expression of MMP-13 (Sun et al. 2008). Blocking signalling pathways of transcription factors NF-κβ, AP-1 and mitogenic kinase proteins prevented the upregulation of MMP-1, MMP-8 and MMP-13, all of which have been implicated in arthritic progression (Sun et al. 2008). Furthermore, IL-1 stimulation increased phosphorylation of kinase pathways, including P38, ERK1/2 and JNK, upregulated MMP expression, which is known to contribute towards cartilage degeneration in arthritis (Liacini et al. 2002).

In wound healing, the initial response by pro-inflammatory cytokines contributes towards the regulation and activation of other wound healing mediators. When this response is continuous, it leads to multiple dysregulated wound healing. For example, diabetes is often associated with non-healing wounds, due to dysregulation of wound healing mediators. The

induction of IL-1β under hyperglycemic conditions has previously been identified in some cell types, including macrophages (Lachmandas et al. 2015). Analysis of IL-1β expression in diabetic non-healing wounds by Mirza et al. (2013), found that macrophages exhibit a pro-inflammatory response inhibited by IL-1β. Inhibiting the IL-1β pathway in diabetic mice resulted in an increase in wound healing associated with a change in resident macrophage phenotype (Mirza et al. 2013).

Increased expression of IL-1β has also been associated with fibrotic progression. In a study by Kolb et al. (2001), the effects of increased IL-1β expression were analysed using an adenovirus that transiently overexpressed IL-1β in rat lungs. In response to overexpression of IL-1β, there was increased expression of pro-fibrotic cytokines, PDGF and TGF-β_1, as well as an upregulated expression of pro-inflammatory cytokines, IL-6 and TNF-α. All of these mediators have previously been determined to have increased expression in fibrotic progression. Furthermore, the increase in IL-1β was associated with tissue damage, due to the increase in TGF-β_1, which subsequently lead to the increased myofibroblast numbers and ECM components, fibronectin and collagen. Increased expression of IL-1β, therefore, regulates expression of other fibrotic mediators and matrix production.

A further example of this regulatory role of IL-1β and TGF-β_1 has been described in pancreas fibrosis (Aoki et al. 2006). This group determined that both IL-1β and TGF-β_1 activated each other in an autocrine loop. The activation of TGF-β_1 by IL-1β was associated with ERK1/2 activation, but the activation of IL-1β by TGF-β_1 was associated with SMAD3 activation. The continuous secretion and auto-induction of cytokines mediates an effect on multiple resident cell types. For example, in a study by Campo et al. (2012), the stimulation of rheumatoid arthritis synovial fibroblasts (RASF) with TNF-α increased the expression of HYAL enzymes, oxidative species, CD44 and multiple immune response mediators, including IL-1β. These workers concluded that increased expression of HYAL enzymes resulted in

continuous HA degradation and the formation of HA oligomers. The association of these HA oligomers with CD44 stimulated transcription factor NF-κB, which increased the expression of many pro-inflammatory mediators. This association of HA with CD44 has previously been shown to activate NF-κB through protein kinase C (PKC) (Fitzgerald et al. 2000). NF-κB then upregulates further fibrotic mediators, including IL-6, TNF-α, TGF-β_1, IL-1β; and matrix degrading MMPs (Tak and Firestein 2001; Liacini et al. 2002).

1.7.3. - IL-1β Induction of HA/CD44 Mediated Monocyte Binding

The association of HA and CD44 has previously been described to be important in TGF-β_1-induced, fibroblast to myofibroblast differentiation. The association of HA/CD44 also has a role in maintaining a monocyte/macrophage presence at the site of injury by an association with fibroblasts. Macrophages are a principle mediator of wound healing, they not only engulf bacteria and debris at the site of injury, but also release cytokines and growth factors into the damaged region (Laskin et al. 2011) . These cytokines activate resident cells to mediate wound closure. Comparatively few macrophages at this site originate from resident tissue, the rest are derived from blood borne monocytes that then differentiate to mature macrophages (Martin and Leibovich 2005). The consistent presence of monocyte/macrophages results in increased proliferation, migration and differentiation of resident cells that are associated with fibrotic progression (Lech and Anders 2013; Xue et al. 2015).

IL-1β is a principal cytokine released by monocytes/macrophages that induces the expression of TGF-β_1 by fibroblasts and surrounding cells; and thereby activates fibroblast differentiation to myofibroblasts via HA/CD44 association. Therefore, IL-1β can indirectly act in a pro-fibrotic way. However, IL-1β stimulation has also been shown to have a direct effect in fibrosis by its continued association with resident monocytes (Meran et al. 2013). This

process is also mediated by HA interactions with CD44. Similar to TGF-β_1 induction of peri-cellular coat formation seen in myofibroblasts, the activation of fibroblasts by IL-1β results in the formation of a HA coat, which is also synthesised by HAS2. However, by contrast with TGF-β_1 induction, the HA forms a spiked matrix characterised by cell membrane protrusions (Meran et al. 2013). The association of HA with CD44 is essential for this coat assembly. However, unlike the TGF-β_1-induced peri-cellular coat observed in myofibroblasts, the IL-1β induced coat does not require TSG-6 activity, suggesting that other hyladherins are involved in maintaining the coat structure (Meran et al. 2013).

Meran et al. (2013) also concluded that the IL-1β-dependent HA spikes on protrusions of the plasma membrane were ICAM-1 dependent; and the association of ICAM-1/CD44 was essential for monocyte binding. ICAM-1 is a transmembrane receptor that stabilises cell-cell interactions and it has previously been shown that its association with HA activates intracellular signalling of NF-κβ and AP-1 (Oertli et al. 1998). Furthermore, as ICAM-1 is an adhesion receptor, it is often associated with facilitating leukocyte migration. Therefore, its ability to bind resident cells is essential for the movement of leukocytes into an inflamed region, but also for intracellular activation and response (Walpola et al. 1995).

Similar to the observed CD44 and HAS2 upregulation, both ICAM-1 mRNA and surface protein expression are induced by IL-1β stimulation (Ledebur and Parks 1995; van der Velden et al. 1998). In unstimulated fibroblasts, ICAM-1 and CD44 are diffuse throughout the membrane. However, after stimulation with IL-1β, both ICAM-1 and CD44 co-localise within the HA-rich membrane protrusions. Unlike TGF-β_1-induced myofibroblasts that result from the co-localisation of CD44 with EGFR in lipid raft regions, the co-localisation of CD44 with ICAM-1 is lipid raft independent and the association happens outside of raft regions, within the membrane (Meran et al. 2013).

Inhibiting the expression of HAS2 or CD44 and preventing or degrading the HA coat decreased the ability of IL-1β-induced fibroblasts to bind monocytes. Therefore, CD44/HA association is essential for this cellular function (Meran et al. 2013). Co-localisation of CD44 with ICAM-1 also activated downstream ERK1/2 ***(Figure 1.4 [A&B])***. Silencing CD44 expression prevented intracellular phosphorylation of ERK1/2, highlighting the importance of CD44 in modulating intracellular signalling (Meran et al. 2013). Since CD44 is associated with the cytoskeleton, the activation of ERK1/2 may be an important signal in the modulation of the cell membrane protrusions.

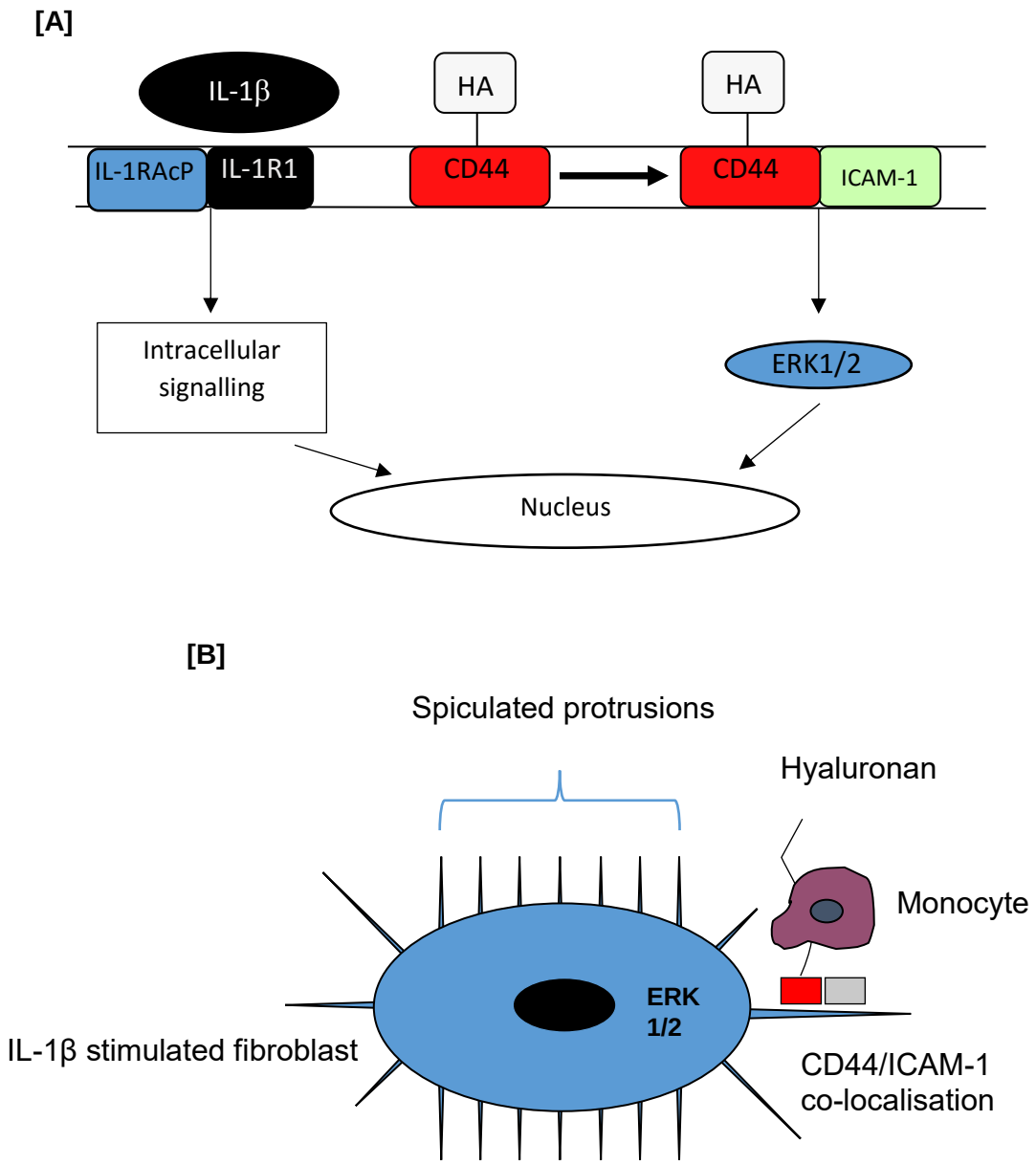

Figure 1.6. Activation of HA spiculated protrusions by IL-1β promotes monocyte binding

[A] IL-1β activation of fibroblast monocyte binding by HA/CD44/ICAM-1 mediated spiculated protrusions. Formation of a complex of IL-1β, IL-1R1 and IL-1RAcP activates intracellular signalling. At the same time, CD44 moves through the membrane and associates with ICAM-1 resulting in the activation of downstream ERK1/2 and the subsequent formation of the HA spiculated protrusions involved in monocyte binding. **[B]** IL-1β stimulated fibroblast, the location on the plasma membrane of CD44/ICAM-1 and the binding of monocytes to spiculated HA.

1.8. -CD44 Regulation of Fibrosis

The CD44 transmembrane receptor exists in multiple isoforms that have marked variability in function (Ponta et al. 2003). Dysregulation of CD44 splice variants has been implicated in multiple diseases, including many cancers. As described in this chapter, the association of

CD44 with HA is central to the TGF-β_1-induced, fibroblast to myofibroblast differentiation, and to IL-1β- induced monocyte binding. However, the CD44 splice variants involved in these HA mediated functions, or if multiple spliced variants are required for the maintenance of the myofibroblast phenotype or the regulation of monocyte binding, is not known. Furthermore, CD44 associates with other receptors in various cell types and induces multiple functional properties in various cells, via its association with HA (Wielenga et al. 2000; Wang and Bourguignon 2006). One such receptor is the MMP inducer, EMMPRIN/CD147, which has previously been shown to associate with CD44 and EGFR in breast cancer cells. This association leads to an increase in invadapodia on breast cancer cells in a CD44/HA-dependent manner (Grass et al. 2013). Furthermore, this CD147/CD44/EGFR association activates downstream ERK1/2 in a similar mechanism that is observed in fibroblast–myofibroblast differentiation and IL-1β induced monocyte binding. Investigation of a role for CD147 in fibroblast activation will be one of the aims of this Thesis. A more detailed description of CD147 is given in Chapter 5.

The work in this Thesis aims to identify which CD44 spliced isoforms are expressed and involved in TGF-β_1-induced, fibroblast-myofibroblast differentiation and IL-1β-induced monocyte binding. Furthermore, interaction of CD147 with CD44 and the role of this interaction in mediating these differentiation or monocyte binding responses was also investigated.

1.9 –Specific Aims

The principal aims are to:-

- Investigate the effects of TGF-β1 and IL-1β on CD44 spliced variant expression.
- Determine the involvement of CD44 variants in myofibroblast differentiation and inflammatory cell interactions.
- Elucidated the role of CD147 in fibroblast differentiation and monocyte binding.

Chapter 2 - Methods

2.1 – Materials

All materials were purchased from Sigma-Aldrich (Poole, UK), GIBCO/Thermo-Fisher Scientific (Roskilde, Denmark) or Life Technologies (Paisley, UK), unless otherwise stated.

2.2 – Cell Culture

2.2.1 – Primary Cells

All experiments were carried out using primary Human Lung Fibroblasts (HLFs) (no. AG02262 Coriell Institute for Medical Research, NJ, USA) within a passage range of 6-10. Fibroblasts were cultured in Dulbeccos Modified Eagle Medium and Nutrient Mixture F-12 Ham's Medium (DMEM/F12, 1:1 ratio), was supplemented with 2mM L-glutamine, 100units/ml penicillin, 100μg/ml streptomycin, 10% foetal bovine serum (FBS, Biological Industries Ltd., Cumbernauld, UK). Cells were incubated at 37°C in 5% CO_2. Fresh growth medium was added to cells every 3-4 days until cells had grown to confluent monolayers. Cells were growth arrested in serum-free medium for 48h, prior to all experiments. This allowed for cell cycles to synchronise.

2.2.2. – U937 Cell Line

The U397 (human histiocytic lymphoma cell line) was purchased from ATCC (Manassas,VA). U937 cells were cultured in RPMI-1640 medium, supplemented with 2mM L-glutamine, 100units/ml penicillin, 100 μg/ml streptomycin, 10% FBS. Cells were incubated at 37°C in 5% CO_2, until the cells reached a high cell density.

2.2.3. - Cellular Sub-Culture

Fibroblast were grown to confluent monolayers in 75cm^2 tissue culture flasks. Cells were then treated with a phosphate buffer saline solution (PBS), containing 0.05% w/v trypsin, 0.53mM EDTA and incubated at 37°C for 1-2 minutes, until cells became detached from the flask. An equal volume of FBS was then used to neutralise the trypsin and the cell suspension was

centrifuged for 5 min at 1500rpm, at room temperature. The subsequent pellet was suspended in 50 ml of DMEM/F12 containing 10% FBS. To continue culture expansion, the cell suspension was split with a 1:3 ratio into sterile 75cm^2 tissue culture flasks.

U937 cells were grown to a high density in 75cm^2 tissue culture flasks. To expand the culture, the cell suspension was diluted 1in 10, using fresh RPMI medium containing 10% FBS, before being placed into a sterile 72 cm^2 tissue culture flask. Any remaining unused cells were cryogenically frozen and stored, as described in section 2.2.6.

2.2.4. - Cell Stimulation

Following a 48 h growth arrest period, fibroblasts were incubated in serum–free DMEM/F12 containing either TGF-β_1 (10ng/ml) or IL-1β (1ng/ml) (R&D Systems, Abingdon, UK). Unstimulated control fibroblast were incubated in fresh serum-free medium at the time of stimulation, unless otherwise stated. Individual experimental conditions are described in each subsequent results chapter.

2.2.5. – Cell Storage and Retrieval

Cells that we not required for subsequent experiments were cryogenically stored. Briefly, following subculture, cells were centrifuged to form a pellet. The pellets of fibroblasts or U937 cultures were taken from a 75cm^2 flask and re-suspended in 1 ml of a solution containing 10% dimethyl sulphoxide (DMSO), 30% FBS and 60% DMEM or RPMI, respectively. 1 ml of solution was then transferred to a cryogenic vial (Thermo-Fisher Scientific) and stored at 80°C for 24 h. Cells were stored long-term in liquid nitrogen at -196°C.

2.2.6 – Cell Counting

Cells were counted using a Beckman Coulter Particle Count and Size Analyzer. For each cell count, 20 µl of cell suspension was added to 20 ml of Coulter® Isioton® II Diluent. Each cell count gave an average of two separate counts. This was repeated three times. An average of

these three counts was then calculated and the cell quantity calculated using the following equation.

Average cell count x2000 = cell/ml

2.3 -Alamar Blue Assay

Alamar Blue is a redox indicator that incorporates a fluorometeric growth indicator. Cellular metabolism is monitored by a colour change that occurs when the environment is reduced (red colour) from its oxidative state (blue colour). The increase in reduction is correlated to the metabolic efficiency of the cells in their environment. To assess experimental conditions on the cell viability, fibroblasts were seeded into 6-well culture plates. At the experimental endpoint the medium was removed from each well and replaced with 1 ml of fresh serum-free medium, containing 10% v/v Alamar blue (Invitrogen/Thermo-Fisher Scientific). A negative control containing just medium and 10% Alamar blue was placed in an empty well. Samples were then incubated for 1 h at 37°C, 5% CO_2. 100µl of conditioned medium from each well (i.e. each sample) was then placed into a Microfluor® 96-well plate (Thermo-Fisher Scientific). Detection was performed using fluorescent spectroscopy (Fluostar Optima Spectrometer), with wavelengths of 540nm excitation and 590nm emission. The fluorescent values of the control sample (containing only medium and Alamar blue) were subtracted from each sample to give a final arbitrary fluorescent unit.

2.4. – Reverse Transcription Polymerase Chain Reaction (RT-PCR)

2.4.1.-RNA Isolation

To analyse gene expression, total RNA was extracted following each experiment according to TRIzol® manufacturers' protocol (Ambion; Life Technologies). Briefly, cells were lysed using 1 ml of Trizol® per well of a 6-well tissue culture plate. To extract cells from smaller well plates, the volumes were scaled down accordingly. The subsequent supernatant was then

transferred into a 1.5 ml micro-centrifugation tube. Samples were then left at room temperature (RT) for 5 min to allow for dissociation of any nucleoprotein complexes. 200 µl of chloroform was added to each sample and thoroughly vortexed, before being left at room temperature for 5 min. The samples were then centrifuged at 12,000rpm for 15 min at 4ºC. Following centrifugation, the sample separated into three distinct phases a lower red phenol phase, a white interphase and a top aqueous phase. The aqueous phase containing RNA only was carefully pipetted into a freshly labelled Eppendorf. 500 µl of isopropyl alcohol was added to each sample and vortexed. Following an incubation period of 15 min at room temperature, samples were centrifuged at 12,000rpm for 10 min at 4ºC. The subsequent pellet was then washed with 75% ethanol before being vortexed and re- centrifuged at 7500rpm 4ºC for 5 min. This wash step was repeated twice more. The ethanol was removed and the pellet was air dried for 10 min. 16 µl of RNase-Free Water was added to solubilise the pellet. Purified RNA samples were quantified (ng/µl), using a Nanodrop 3300 (Thermo Scientific). The volume required for 1 µg of sample was quantified using the following equation:

1 / (Total RNA ng/µl) /1000

2.4.2. -Reverse Transcription Polymerase Chain Reaction (RT-PCR)

Reverse transcription (RT) of purified RNA samples was carried out using the random primer method. All stages throughout the RT procedure were carried out on ice. Briefly, 1 µg of RNA (made up to a final volume of 10 µl with RNase-free, deionised H_2O), was placed into a RT-PCR reaction tube with 10 µl of the following reaction mixture: 10X random primers (2.0 µl), 25X 100mM deoxynucleotide triphosphates - dNTPs (0.8 µl), Multiscribe^{TM} reverse transcriptase (1.0 µl), RNase inhibitor (1.0 µl), 10X RT buffer (2.0 µl) and nuclease free dH_2O (3.2 µl). A negative control consisting of 10 µl of RNase-free, deionised H_2O only and 10 µl of the reaction mix was carried out for each experiment. All reagents used were from a high

capacity cDNA Reverse Transcription Kit (Life Technologies). Reverse transcription was carried out using a (PTC-225, Peltier Thermal Cycler, Bio-Rad Laboratories, Berkely USA). Cycle conditions were as follows: 25°C for 10 min, to allow the random primers to anneal to the RNA. This was followed immediately by an extension stage of 37°C for 120 min, in order to allow reverse transcriptase to attach the free dNTPs. A final dissociation stage of 85°C for 5 min was used to separate the template strand from the final cDNA strand and denature the reverse transcriptase. Following RT, the cDNA was diluted with 60 µl of RNase-free de-ionised H_2O and stored at -20ºC until further use.

2.5. - Real Time - Quantitative Polymerase Chain Reaction (RT-qPCR)

2.5.1 -Taqman Gene Expression qPCR

Following RT-PCR, samples were analysed using qPCR. Each reaction had final volumes of 20 µl, consisting of 4 µl of cDNA, 10µl of Taqman Fast Universal PCR master mix (x2 No AmpErase® UNG; Applied Biosystems), 5 µl nuclease-free dH_2O and 1 µl of a Taqman gene expression primer and probe (Applied Biosystems, see ***Table 2.1.***) A negative control containing RNase-free de-ionised H_2O in place of the cDNA, was carried out for each experiment. An rRNA 18S target was used as an endogenous control and amplified simultaneously with the gene target to be used as a reference gene. Expression analysis was carried out using the ViiA-7 Real Time PCR System (Applied Biosystems).

Primer target	*Primer Identity Number*
TNFA1P6 (TSG6) (Applied Biosystems)	Hs0113602_m1
TGF-β_1 (Applied Biosytems)	Hs0017127_m1
PTPRC (CD45) (Applied Biosystems)	HS00236304
αSMA (ACTA2) (Applied Biosystems)	HS_00426835_gl
18s Ribosomal RNA (Applied Biosystems)	Catalog. No. 4319413E

Table 2.1. Primer targets and identity number for Taqman gene expression assay

2.5.2. -Power SYBR Green qPCR

Following RT-PCR, samples were analysed using qPCR. Each reaction had final volume of 20 µl, consisting of 4 µl of cDNA, 10 µl of Power SYBR Green PCR Master Mix (Applied Biosystems), 4.8 µl of RNase-free dH_2O and 0.6 µl of 10µM custom-designed forward, primer and 0.6µl of 10µM custom-designed, reverse primer. All custom-designed primer sequences are given in ***(Table 2.2.)***. RNase-free dH_2O was used in the place of the cDNA for a negative control for each experiment. GAPDH was used as an endogenous control and amplified simultaneously with the gene target. Expression analysis was carried out using the ViiA-7 Real Time PCR System.

2.5.3. -Relative Quantification

Relative quantification was calculated using the comparative CT method. The CT value (the threshold cycle where the amplification is in the linear range of the amplification curve) of the standard endogenous control reference gene was subtracted from the CT value of the target gene in order to obtain a delta CT (dCT) value. The mean dCT was then calculated for control experiments. The relative quantification (RQ) for the experimental target genes was then calculated using the mean of the control experiments with the following equation.

2^- (dCT(Experimental Target) - dCT(Mean Control Group))

2.7. - Small Interfering RNA (siRNA)

Transient transfection was carried out using either custom designed siRNA that targeted specific CD44 variants or a specific siRNA to CD147. For siRNA targeted regions of CD44, see methods section in Chapter 4. Fibroblasts were grown to 50-60% confluence in 6-well plates in DMEM/F12 containing 10% v/v FBS, before growth arrest in serum-free DMEM/F12 for 24 h. Two solution were made for transfection, the first contained 100µl per sample of OPTIMEM transfection medium and the specific target siRNA (33nm; final concentration.). The second contained 100µl of OPTIMEM transfection medium and Lipofectamine 2000 (1:50 dilution; Invitrogen). The two solutions were incubated at room temperature for 45 min, combined and mixed thoroughly. 800µl of OPTIMEM transfection media was added to the solution for each sample, this gave a final transfection solution volume of 1 ml per well. The cells were incubated in 5% CO_2 at 37ºC for 6 h. 1 ml of fresh DMEM/F12 containing 20% v/v FBS was then added to each well and samples were incubated for a further 24 h. Following transfection, the medium was removed and fresh serum-free DMEM/F12 was added 1 ml/well to growth arrest cells for 48 h, prior to experimentation. A negative control scrambled siRNA I.D. AM4613 (Ambion) was carried out simultaneously for all transfection experiments (a nonsense sequence, bearing no resemblance to known human mRNA sequence).

Target	*Primer sequence*
CD44s	**Forward** 5'-GCTACCAGAGACCAAGAC-3' **Reverse** 5'-GCTCCACCTTCTTGACTCCC-'3
CD44v2	**Forward** 5'-CCTGCTACCACTTTGATGAGC-'3 **Reverse** 5'-GTGTCTTGGTCTCCAGCCAT-'3
CD44v3	**Forward** 5' -TGCTACCAGTACGTCTTCAAAT-'3 **Rever**se 5'-GTGTCTTGGTCTCTGGTGCT-'3
CD44v4	**Forward** 5'-CTGCTACCATTTCAACCACACC-'3 **Reverse** 5'-TGGTCTCAGTCATCCTTGTGG -'3
CD44v5	**Forward** 5'-CAGAATCCCTGCTACCAATGT-'3 **Reverse** 5'-TCTTGGTCTCTTGTGCTTGTAGA-'3
CD44v6	**Forward** 5'-TGCTACCATCCAGGCAACTC-'3 **Reverse** 5'-GGAATGTGTCTTGGTCTCCAGC-'3
CD44v7	**Forward** 5'-GAATCCCTGCTACCACAGCCTC- '3 **Reverse** 5'-TCTCCCATCCTTCTTCCTGCTT-'3
CD44v8	**Forward** 5'-ATGTGTCTTGGTCTGGCGTT-'3 **Reverse** 5'-TCCCTGCTACCAATATGGACTC-'3
CD44v9	**Forward** 5'-CAGAATCCCTGCTACCAAGC-'3 **Reverse** 5'-ACTGGGGTGGAATGTGTCTT-'3
CD44v10	**Forward** 5'-TCCCTGCTACCAATAGGAATGA-'3 **Reverse** 5'-TAAGGAACGATTGACATTAGAGTTG-'3
CD147	**Forward** 5'- CAGAGTGAAGGCTGTAAGTCG-'3 **Reverse** 5'-TCGGAGGAACTCACGAAGAA-'3
GAPDH	**Forward** 5'-CCTCTGATTCAACAGCGACAG-'3 **Reverse** 5'-TGTCATACCAGGAAATGAGCTTGA-'3
EDA-Fibronectin (EDA-FN)	**Forward** 5'GCTCAGAATCCAAGCGGAGA'3 **Reverse** 5'-CCAGTCCTTTAGGGCGATCA-'3

Table 2.2. - Custom designed primer sequences used for Sybr Green qPCR analysis

2.6. - Touch-Down Conventional PCR (TD-PCR)

To determine the expression of larger CD44 variants, touch-down conventional polymerase chain reaction (TD-PCR) was used, to prevent unselected hybridisation. Following RNA extraction and reverse transcription (described in section 2.4) the resulting cDNA was amplified using custom-designed primers, to amplify CD44 variants (***Table 2.3.)***, according to the Phusion® DNA Polymerase Kit protocol (Bio-RAD Laboratories). Briefly, 2µl of cDNA was added to a solution containing, 1 µl of dNTPs (10mM), 2.5 µl of each 10mM primer (forward and reverse), 10 µl of Phusion® buffer and 0.5 µl of DNA polymerase to an appropriate PCR tube. RNase-free dH_2O was added to each sample to give a final volume of 50 µl. Samples were amplified using an ATC-225, Peltier Thermal Cycler. The calculated melting temperature (Tm) +10ºC was used as the initial starting annealing temperature, the temperature was then decreased by 1ºC for each additional cycle for the first 10 cycles. The temperature then remained consistent for the remaining 22 cycles. Each PCR reaction was run for a total of 32 cycles. Following amplification, the samples were mixed with a gel loading dye (Qiagen, Manchester, UK) and pipetted into wells of a 1% agarose gel, containing ethidium bromide. Flatbed electrophoresis was used to separate DNA amplicons. Gels were submerged in 1X Tris-acetate buffer solution containing ethidium bromide. Electrophoresis was run at 90V for 1 h. Bands were visualised and extracted from the gel using an Ultra Violet (UV) trans-illuminator. DNA was isolated from the extracted bands using a QIAquick Gel Extraction Kit (Qiagen) and quantified using a Nanodrop 3300 (Thermo-Fisher Scientific). Product were confirmed by using 5ng/µl for DNA sequencing (BioCore Sequencing, Central Biotechnology Services, Cardiff University, UK).

Target	*Primer sequence*
Common forward primer	5'TCAATGCTTCAGCTCCACCT'3
CD44S Reverse	5'CAAAGCCAAGGCCAAGAGGGATGC'3
CD44v2 Reverse	5'CAGCCATTTGTGTTGTTGTGTGAA'3
CD44v3 Reverse	5'CCTTCATCATCATCATCAATGCCTGATCC'3
CD44v4 Reverse	5'TTTGAATGGCTTGGGTTCCACTGG'3
CD44v5 Reverse	5'GCTTGTAGAATGTGGGGTCTCTTC'3
CD44v6 Reverse	5'GAATGGGAGTCTTCTTTGGGTGTT'3
CD44v7 Reverse	5'CCATCCTTCTTCCTGCTTGATGAC'3
CD44v8 Reverse	5'GTCATTGAAAGAGGTCCTGTCCTG'3
CD44v9 Reverse	5'TGTCAGAGTAGAAGTT'3
CD44v10 Reverse	5'TGGAATCTCCAACAGTAACTGCAGT'3

Table 2.3. Primer targets and sequences used for touch-down PCR analysis.

2.7. - Lipid Raft Analysis

Caveolae raft analysis was performed using a Caveolae/Raft Isolation Kit (Sigma - Aldrich), in order to determine the localisation of membrane proteins in fibroblasts or myofibroblasts. Briefly, fibroblasts were grown to approximately 80% confluence in DMEM containing 10% v/v FBS at 37ºC and 5% CO_2 in 6-well plates. Cells were then growth arrested in serum-free DMEM/F12 for 48 h. Cells were incubated in serum -free DMEM/F12 containing TGF-β_1 (10ng/ml) or serum-free DMEM/F12 alone (control samples) for 72 h. Cells were lysed in 1ml of ice cold lysis buffer containing 1% v/v Triton X- 100 and 1% v/v of protease inhibitor cocktail (PIC). Cells were harvested using a cell scraper and incubated on ice for ~30 min, before transfer into a pre-cooled 2ml Eppendorf. Lysed samples were centrifuged at 450rpm for 5 min at 4ºC and the supernatant was discarded. The cell pellet was carefully washed twice in ice-cold PBS, before re-suspension in 1ml of lysis buffer, containing 1% Triton–X100 and 1% PIC. Samples were stored at -80ºC until use.

2.7.1. - Preparation of Density Gradient

The density gradient consisting of 5 layers was created using OptiPrep Medium (Sigma-Aldrich). These were (starting from the lowest layer) 35%, 30%, 25%, 20% and 0% and made up to 1ml with lysis buffer. All stages were carried out on ice. 1 ml of the pre-prepared 35% OptiPrep solution was added to a pre-cooled ultracentrifugation tube. 1ml of each subsequent gradient layer was carefully pipetted onto the previous layer, until the final top gradient layer of 0% OptiPrep lysis buffer was level with the top of the tube. Samples were then centrifuged at 200,000 x *g* for 14 h at 4ºC, using a Optima-Max ultracentrifuge (Beckman Coulter). Fractions were then carefully collected into 500µl aliquots. Each fraction was placed into a pre-chilled pre-labelled Eppendorf. The fractions were labelled 1-9, in accordance with their removal from the ultracentrifugation tube. To precipitate the protein from each fraction, samples were treated with 10% trichloroacetic acid (TCA) and left for 30 min on ice. Samples were the centrifuged at 12,000rpm for 10 min, until a pellet was formed. The subsequent pellet was washed in 50:50 ethanol/ether and the resulting protein from each fraction was then analysed by Western blot.

2.8. - Protein Analysis

5.8.1. – Immunocytochemistry

Immunocytochemistry (ICC) was used to analyse αSMA stress fibre formation and the co-localisation of CD147 with CD44, EGFR and the integrin α4β7. All ICC experiments were carried out in 8-well Permanox chamber slides (Nunc; Thermo-Fisher Scientific) On completion of each experiment, cells were fixed using 200 µl of a 4% paraformaldehyde solution for 10 min and then washed using PBS. For intracellular analysis, cells were treated with 0.1% (v/v) Triton X-100 and left for 5 min at room temperature. Analysis of membrane receptors did not require Triton X-100 treatment. The cells were then washed three times with

200 µl per well of 0.1% (w/v) Bovine Serum Albumin (BSA)/PBS and left for 5 min on a STR6 platform shaker (Stuart scientific, UK). This wash stage was repeated twice more. Samples were blocked using 200µl of 1% (w/v) BSA/PBS per well for 30 min, to prevent unspecific binding. Samples were then washed and treated with 200µl of the appropriate primary antibody (***Table 2.4),*** overnight at 4ºC. Following a further wash stage, samples were treated with a secondary antibody conjugated to a fluorescent tag (***Table 2.5.),*** for 1 h at room temperature. Samples were washed and the chamber wells were removed. Samples were left to air dry and slides were then mounted using Vector Shield mounting media for fluorescence containing a DAPI nuclear stain (Vector Laboratories Inc. Birlingane. UK). Samples were visualised and examined under UV-light, using a Leica Dialux 20 Fluorescent Microscope (Leica Microscope UK Ltd, Milton Keynes, UK). For F-actin and lipid raft visualisation, a phalloidin conjugate Alexa Fluor® 555 (Sigma-Aldrich) and Cholera toxin B subunit conjugated with Alexa Fluor® 548 (Invitrogen) were used ***(Table 2.4)***.

Antibody	***Type and Host***	***Dilution***
Anti-EGFR(528) Merck Millipore	Monoclonal –Mouse	1:25
Anti-CD44(A020) Merck Millipore	Monoclonal – Rat	1:100
Anit-CD147 BD Pharminogen	Polyclonal –Mouse	1:50
Anti-α-SMA (Sigma)	Monoclonal –Mouse	1:100
Phalloidin – Conjugate Alexa Fluor 555 (Sigma)	N/A	1:100
Cholera –Toxin subunit B-conjugate Alex Fluor 548 (Invitrogen)	N/A	1:100

Figure 2.4 - Primary antibodies and dilutions used for ICC analysis.

Antibody	Type and Host	Dilution
Anti-mouse-IgG AlexaFlour 488 (FITC)	Polyclonal -Goat	1:500
Anti - Rat-IgG AlexaFlour 555 (TRITC)	Polyclonal -Goat	1:500

Figure 2.5. - Secondary antibodies and dilutions used for ICC analysis.

5.8.2. - Protein Extraction

All experiments that required protein analysis were carried out in 6-well cell culture plates. Cell were dissociated from the plate using a cell scraper, before being pipetted into a 1.5 ml, pre-chilled, pre-labelled, Eppendorff tube. Samples were centrifuged at 8,000rpm at 4ºC for 10 min, until a pellet was formed. The supernatant was then discarded and the remaining pellet was treated with 200µl of lysis buffer (pH 7.4) (±0.1), containing 10 µl of (100mM) sodium orthovanadate (Na_3VO_4), 10µl of (200mM) phenylmethylsofonyl floride (PMSF) 200mM and 10µl of protease cocktail inhibitor. All reagents were included in a Radio Immunoprecipitation Assay (RIPA) Kit (Santa Cruz, Biotechnology, U.S.A.). Samples were vortexed for 1 min and then re-centrifuged at 8,000 rpm at 4ºC, for 10 minutes. The subsequent supernatant was transferred into a fresh Eppendorff. Samples were stored at -80ºC until further analysis.

5.8.3. - Protein Quantification

All extracted protein was quantified using Bradford Assay method (Bio-Rad Laboratories Inc.). Samples were diluted 5µl to 125µl Bradford Assay. Quantification was performed using absorbance spectroscopy (Fluostar Optima Spectrometer), with wavelengths of 620nm excitation and 590nm emission. A standard of BSA serial dilution was used as a reference for sample concentrations.

5.8.4. - Co-Immunoprecipitation (Co-IP)

Following protein extraction, Co-Immunoprecipitation (Co-IP) was carried out using MagnaBind Goat anti-Mouse IgG magnetic beads or Pierce Protein G Magnetic Beads (Thermo-Fisher Scientific), depending on analysis. Briefly, beads were washed 3 times in PBS before use. 10 µg of primary antibody ***(Table 2.6)***, was added to 200µl of beads and incubated at 4°C for 2 h. The beads/antibody complex were then washed with PBS to remove any unattached antibody. 5 µg of sample was then added to the beads/antibody complex and samples left on a roller overnight. Samples were further washed 3 times with PBS, proceeded by a single wash with a 1% (v/v) Nonidet P40 detergent solution (Sigma-a

Aldrich). The beads were then transferred to a fresh pre-labelled Eppendorff tubes. Beads were dissociated from the antibody sample complex by boiling for 5 min at 95°C, under reducing conditions. The beads were then removed using a magnetic holder and co-precipitated proteins were identified using SDS-PAGE/Western Blot analysis.

5.8.5. -SDS-PAGE/Western Blot Analysis

Following protein extraction and quantification, protein separation and identification was performed by SDS-PAGE/Western blot, using a BioRad Mini Protein II apparatus (Bio-Rad Laboratories). 30 µg of sample was boiled at 95°C for 5 min with an equal volume of reducing buffer (pre-prepared and containing 0.8ml glycerol, 1.6ml 10% (w/v) SDS, 0.4ml β-Mercaptoethanol and 0.05% Bromophenol Blue). The total volume of sample/reducing buffer was loaded into the wells of a 7.5% polyacrylamide gel. Each experiment was carried out alongside 10 µl of a ColourPlus^{TM} Prestained Protein Ladder, Broad Range (New England Biolabs, UK). To separate the proteins, electrophoresis was carried out at 100V for 20 min followed by 150V for 40 min under reducing conditions. Following electrophoresis, samples were transferred at 100V for 1 h onto a nitrocellulose membrane (GE Healthcare, UK). In

order to prevent non-specific binding, the nitrocellulose membrane was blocked with 5% (w/v) skimmed milk in 0.5% (v/v) Tween/PBS for 1 h. The membrane was then washed in 0.1% (v/v) Tween/PBS three times for 5 min. The primary antibody of interest (***Table 2.6***.) was diluted in 0.1% (v/v) Tween/PBS, containing 1% (w/v) BSA and incubated with the membrane at 4°C, overnight. The membrane was then washed before the addition of the secondary antibody, conjugated to horseradish peroxidase (HRP) ***(Table 2.7)*** diluted in 0.1%(v/v) Tween/PBS containing 1% (w/v) BSA. Following a further wash step the Enhanced Chemoluminecense (ECL) method was used to visualise the samples. Briefly, the membrane was treated with ECL reagent (GE Healthcare) and left to react for 1 min. HyperFilm X-ray film (GE Healthcare) was then placed onto the membrane and left to expose for a pre-determined time. The film was developed using a Curix-60 developer (AGFA Healthcare, Greenville SC, USA).

Antibody	***Type and Host***	***Dilution***
Anti-Phospho-p44/p42(ERK1/2) (T202/Y204) (Cell Signalling Technology)	Monoclonal-Mouse	1:1000
Anti-CD44(A020) (Merck Millipore)	Monoclonal – Rat	1:500
Anit-CD147 (BD Pharminogen)	Polyclonal -Mouse	1:2000
Anti-Caveolin-1 (Sigma-Aldrich)	Polyclonal -Rabbit	1:1000
Anti-EEA-1 (BD Biosciences)	Monoclonal-Mouse	1:1000
Anti-GAPDH (SantaCruz)	Monoclonal-Mouse	1:5000
Anti-ICAM-1 (SantaCruz)	Monoclonal-Mouse	1:1000

Table 2.6 – Primary antibodies used for Western Blot analysis

Antibody	*Type and Host*	*Dilution*
Anti-mouse-IgG (HRP)	Polyclonal –Goat	1:5000
Anti-Rabbit-IgG (HRP)	Polyclonal -Goat	1:5000
Anti - Rat-IgG (HRP)	Polyclonal –Goat	1:5000

Table 2.7. – Secondary antibodies used for Western Blot analysis

2.9. -Collagen Gel Analysis

Collagen type I (5mg/ml) sourced from rat tails (Gibco) was diluted to 4mg/ml. Briefly, 8ml of collagen was added to (1ml) 10xPBS, (0.20ml) 1M NaOH, and 0.8ml (dH_2O). The subsequent solution was then slowly mixed to achieve the optimal pH 7.0. The gel was pipetted into 6-well plates and incubated at 37°C for 40 min, until the gel was firm. The gels were then washed using culture medium before fibroblasts were seeded and left to adhere in DMEM/F12 containing 10% FBS. Following a 24 h growth period, fibroblasts were then growth arrested in serum-free medium for 48 h, before being transfected with siRNA targeting CD147 or a scrambled negative control. Following a 48 h growth arrest period, cells were stimulated with TGF-β_1 (10ng/µl). Control (non-stimulated) fibroblast cultures were used as experimental controls (0h). Subsequent time points were 72 h and 144 h. Gel contraction was measured using Image J processing program (National Institutes of Health, Bethesda, Maryland, USA).

2.10. - Statistical Analysis

Data is displayed as ± s.d. (Standard deviation) or ± s.e.m. (Standard error of mean) dependent on the number of experimental repeats. Statistical analysis was carried out using the one way ANOVA of variance followed by the unpaired student's *t* test. Graph Pad (version 6) was used for each graphical analysis. *P=<0.05 was considered significant.

Chapter 3- The Effects of Transforming Growth Factor- β ($TGF\text{-}\beta_1$) and Interleukin -1 β (IL-1β) on CD44 Spliced Variant Expression

3.1 - Introduction

3.1.1. CD44

CD44 is a transmembrane glycoprotein that regulates cell adhesion, migration, proliferation, differentiation and signalling (Kosaki et al. 1999; Legg et al. 2002; Ito et al. 2004; Meran et al. 2011b; Midgley et al. 2013), through its interaction with hyaluronan. First identified in 1983 in human white blood cells (Gallatin et al. 1983), CD44 is encoded by a single highly conserved gene that is located on chromosome 11 at p13 (Gao et al. 1997). A combination of alternative splicing and posttranscriptional modification leads to multifunctional isoforms (known as CD44 variants), of the protein being expressed with a large molecular weight range of 80-200kDa.

3.1.2. - CD44 Transcription

In humans, nineteen exons encode for CD44 pre-mRNA. The first five exons (1-5) and the last five exons (15-19) are common to all the CD44 variants. The variability of CD44 is the result of alternative splicing of ten exons (6-14) that are situated between these constant regions. ***(Figure 3.1. [A])***. The simplest CD44 variant has only the common exons translated into protein and is known as CD44 standard or CD44s. This is the most abundant of all the CD44 variants and is present in most cell types. Conversely, much less expressed is the largest CD44 variant, this has all the variable exons translated into protein and is known as CD44 (v2-10).

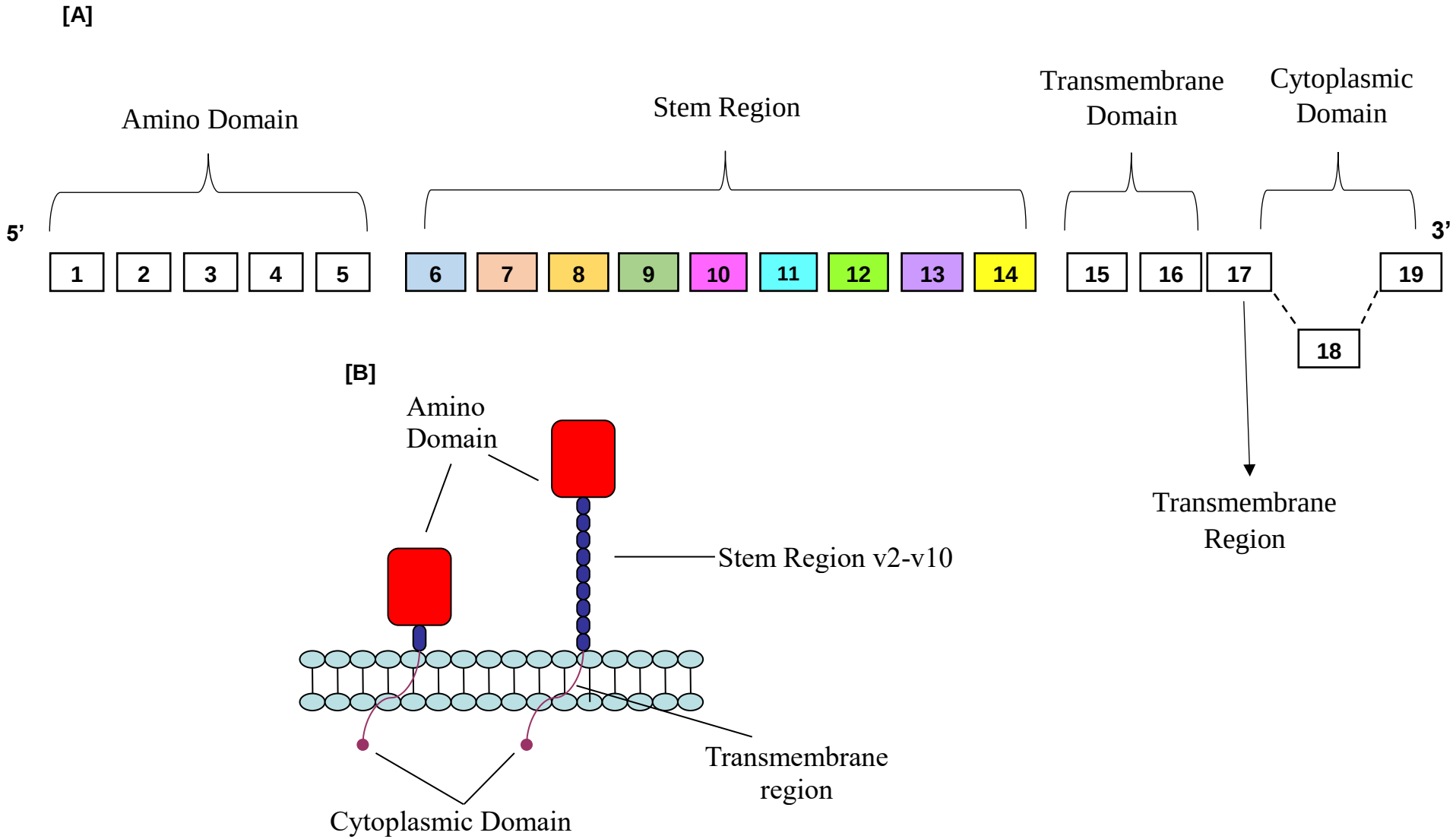

Figure 3.1 – Schematic of CD44 Exon and Protein Structure.

Exon arrangement of CD44 [A], shows the exons that code for the corresponding region of the protein [B]. [A] indicates (exons 1-5) and (15-16) code for the amino domain, (exon 17) codes for the transmembrane region and part of (exon 17) and all of (exon 19) code for the cytoplasmic domain. Exon 18 is not often present and its insertion results in the translation of a stunted cytoplasmic region.

3.1.3. CD44 Protein Structure

All CD44 variants express three domains; an extracellular domain, a transmembrane domain and a cytoplasmic tail region. CD44s contains only these regions and, therefore, is the smallest protein with a molecular mass of 80-95kDa. The CD44 size variation is due to the insertion of a stem region between the extracellular domain and the transmembrane region that results from the translation of exons within the variable region of the gene ***(Figure 3.1[B])***.

3.1.3.1. - The Extracellular Domain

The extracellular domain, also known as the amino terminal domain or the hyaluronan-binding domain, is a globular structure that is encoded by the common exons (1-5 and 15-19) ***(Figure 3.1. [A])***. This domain regulates the interaction of CD44 with the ECM, including its primary ligand hyaluronan. Two known binding domains have been located in the amino terminal of CD44. The first is the *link domain* (amino acids 32-132), which has homology with the cartilage link protein and also contains a hyaluronan-binding motif. The second is the hyaluronan binding site that is situated away from the link domain (amino acids 150-158) (Peach et al. 1993). The amino domain also mediates binding of other ECM proteins, such as collagen, laminin and fibronectin (Wayner and Carter 1987; Faassen et al. 1992; Jalkanen and Jalkanen 1992). In order to maintain the correct folding of both the link domain and the HA binding domain, the amino terminal is folded and stabilised by four highly conserved cysteine residues that form disulphide links; inhibition of these results in an inability of HA to bind to CD44 (Day and Sheehan 2001). A stem region links the amino domain to the transmembrane region in CD44s. In CD44 variants, however, this stem region can be extended by the incorporation of variable spliced exons.

3.1.3.2. - The Stem Region

The variation of CD44 is the combined result of the insertion of spliced variable, exon products into the stem region and specific post-translational modifications within this region. This combination allows for multiple products/variants to be produced from a single gene.

3.1.3.3. - Alternative Splicing

The exact mechanism of alternative splicing is not fully understood; however, it is generally accepted that spliceosomes play a role in determining the final exon expression of mature mRNA. Spliceosomes are large complexes that are composed of five small nuclear ribonucleoproteins (snRNP) U1, U2, U4, U5 and U6 and numerous polypeptides, that modulate the removal of non-coding introns from pre-mRNA by recognising poor consensus sequences within the intron-exon boundary; allowing exons to ligate and form mature mRNA. In a similar process, alternative splicing removes exons using a combination of poor consensus sequence and recognition of splice sites. There are four categories of consensus sequences (known as *cis*-regulatory elements), identified as exonic splicing enhancers (ESEs), exonic splicing inhibitors (ESIs), intronic splicing enhancers (ISEs) and intronic splicing inhibitors (ISIs). These sequences are identified by splicing regulators (SRs), such as SR factors and heterogeneous nuclear ribonucleoproteins (hnRNPs reviewed by Jurica and Moore 2003; Chen and Manley 2009). Splicing regulators are subjected to extensive post-transcriptional modifications and either promote or inhibit splicing through a combinatory effect (Mayeda et al. 1993). Dysregulation of alternative splicing can be the consequence of either a Cis-Acting or a *Trans*-Acting mutation. A *Cis*-Acting mutation is either an acquired or inherited mutation of splice sites, or the addition of new splice motifs and defective protein translation. Trans-Acting mutations are associated with defective splicing machinery and regulators (Brinkman 2004).

3.1.3.4. – Post-Transcriptional Modifications of CD44 Variants

The interaction between CD44 and the ECM is highly dependent on modifications in the amino terminal and the stem region. The standard form of CD44 alone has large N-linked and O-linked glycosylations and GAG modifications that increase the molecular mass of the protein from 37kDa to 80-95kDa. The majority of N-glycosylation's are within the amino domain situated close to the link region. However, the O-linked glycosylation and GAG modification sites are situated closer to the carboxyl terminal of the amino domain (Naor et al. 2009). The addition of spliced exons into the stem region in CD44 variants further increases these glycosylation and GAG modifications. For example, CD44 v3 contains the heparan sulphate site which binds to heparin binding proteins (Bennett et al. 1995); and CD44 v6 exhibits a binding site for hepatocyte growth factor (HGF) and vascular endothelial growth factor (VEGF) (Tremmel et al. 2009). HA binding is usually induced after some form of external stimulus that switches CD44 from its inactive to active form. This is thought to be modulated by N-linked glycosylations (Lesley et al. 1995). Whether CD44s or a CD44 spliced variant interacts with HA varies depending on cell type (Stamenkovic et al. 1991; He et al. 1992).

3.1.3.5 - The Transmembrane Domain

The transmembrane domain is encoded by exon 17 ***(Figure 3.1[A])***; and is composed of 23 hydrophobic amino acids and a single cysteine residue. The exact role of the transmembrane region in modulating CD44 binding with ECM ligands is not entirely understood. It is known, however, to play a role in modulating the CD44-HA association in the cell membrane through its cysteine residue (Liu and Sy 1997). Preventing this CD44 clustering using chimera CD4/CD44 molecules has been shown to down regulate the HA-CD44 interaction (Liu and Sy 1997). Furthermore, the transmembrane region has been associated with the interaction with lipid raft regions in the cell membrane (Neame et al. 1995; Perschl et al. 1995). This indicated

that the transmembrane region may also be involved in the ability of CD44 to act as a co-receptor with other transmembrane receptors. As many of these receptor associations happen within lipid raft regions, it indicates that the transmembrane region may play an important role in controlling CD44 interactions and signalling.

3.1.3.6. – CD44 Cytoplasmic Domain Phosphorylation and the Cytoskeleton Interaction.

The cytoplasmic domain is encoded partially by exon 17 and all of exon 19 ***(Figure 3.1 [A])*** of the CD44 gene and is ~70 amino acids in length. It contains a constitutively expressed phosphorylated region at Ser325, which when mutated dysregulates cell migration (Peck and Isacke 1998). Phosphorylation at this site has been shown to be regulated by calmodulin kinase II (CaMKII) and protein kinase C (PKC). The activation of PKC has been shown to play a role in the cytoplasmic domain association with the cytoskeleton, by switching phosphorylation of Ser325 to Ser219. This results in a dissociation of the cytoplasmic tail from ezrin, a component of the cytoskeleton (Legg et al. 2002).

The intracellular partner proteins that modulate the association of CD44 with the cytoskeleton are ankyrin, ERM proteins, ezrin, radixin, and moesin and merlin. Ankyrin is a protein linker that is known to associate with spectrin; a component of the cytoskeleton. The importance of CD44/ankyrin binding has not been fully investigated, but it is known that blocking the ankyrin binding site situated between amino acid 305 and 355 on the cytoplasmic tail prevents the HA/CD44 association within the amino domain (Lokeshwar et al. 1994); indicating it may play an essential role in ligand binding and, therefore, HA-dependent cell adhesion, migration and differentiation. The ERM proteins regulate the linking of F-actin in the cytoskeleton to receptors within the plasma membrane making them essential for cell morphology and multiple cell functions, including cell migration, adhesion and signalling. ERM proteins are a subfamily within the band 4.1 superfamily, that consist of a ~300 amino

acid FERM (four point one ezrin, radixin, moesin) domain at the N-terminus and a F-actin binding site at the C-terminus (Algrain et al. 1993). CD44 interacts with ERM proteins (Tsukita et al. 1994) *in vitro* and *in vivo*, using a binding domain situated between the transmembrane region and the ankyrin binding domain (Yonemura et al. 1998). Furthermore, a similar motif can be found in cytoplasmic regions of other transmembrane proteins, including members of the intercellular adhesion molecule (ICAM) family, (Heiska et al. 1998). Inactive ERM proteins fold together through the interaction of the N-terminal and the C-terminal preventing the interaction of protein sites in a homotypic association or with each other in a heterotypic association (Gary and Bretscher 1993). ERM proteins are activated by binding to the phospholipids in the plasma membrane (Hirao et al. 1996); and phosphorylation has been observed of a conserved threonine residue in the C-terminal by kinases, including, Rho-kinase (Matsui et al. 1998), PKCα (Ng et al. 2001); and PKCθ (Pietromonaco et al. 1998). Finally, merlin, which is an ERM related protein, exhibits similarity to the ERM proteins, however, it does not have an F-actin binding domain in the C-terminus. Moreover, merlin associates with the ERM proteins and both work as a molecular switch. Interestingly, it is the dephosphorylated form of merlin that binds with the CD44 cytoplasmic tail. This in turn prevents the interaction of CD44 with the cytoskeleton, due to the lack of an F-actin binding site. Furthermore, when CD44 associates with hyaluronan, merlin becomes phosphorylated, dissociates and the ERM proteins link CD44 with the cytoskeleton. Therefore, the ERM-merlin complex acts as a mediator of HA-dependent cellular functions (Morrison et al. 2001).

The interaction between the cytoskeleton and the cytoplasmic domain of CD44 variants is not well understood. It is, however, known that the epithelial form of CD44 (CD44v6-10) along with CD44s, does interact with both ERM proteins and ankyrin and that the association of these two region varies in their binding affinity (Lokeshwar et al. 1994; Tsukita et al. 1994).

In a review by Bourguignon et al. (1998), it was suggested that isoforms of CD44 have different affinities with ankyrin/ERM, which may mediate differences in intracellular signalling.

3.1.4. – Alternative Splicing of CD44 Variants in Cell Types

Early investigation of CD44 variant expression in different cell types identified that CD44s was widely distributed in multiple tissues and that the different isoforms of CD44 varied between cells of hematopoietic lineage (Dougherty et al. 1991). Moreover, transfection of a B cell line with both CD44s and epithelial CD44v8-10 altered the adhesion properties of the cell (Stamenkovic et al. 1991), indicating that each variant has a different role. Multiple studies have examined the expression of CD44 variants in normal tissues and found them to be less abundant and have more specific functions, compared to standard CD44. For example, studies using specific CD44 variant antibodies have shown CD44v9 to be expressed in nearly all epithelial cell types. The expression of CD44v6 and v3 has been detected in squamous or glandular epithelium and CD44v4 expression has shown to be limited to epidermis or oesophageal tissue (Terpe et al. 1994; Fonseca et al. 2000). Larger CD44 variants have been detected in keratinocytes, including CD44v2-10, v3-10, v4-10, v6-10 and v8-10; and this expression changed after keratinocytes had terminally differentiated into corneocytes (Hudson et al. 1995).

More recently, due to an extended knowledge of defective splicing at the pre-mRNA level, more studies have focused on the dysregulated expression of CD44 variants in cancer, with the aim of using altered expression as a marker for cancer growth and its progression. In the prognosis of cancer, the upregulation of CD44s has been linked to Non-Hodgkinson lymphoma and has been shown to be a useful marker for prognosis. The upregulation of CD44s correlates with increased HA deposition and enhanced migration and metastasis (Horst et al. 1990). In a review by Bourguignon et al. (1998), CD44v5 was linked to colon rectal

progression, CD44v9 was deemed a positive marker for gastric carcinoma and CD44v7/8 was a marker for cervical cancer progression.

More recent research of CD44 and its role in tumour growth shows that overexpression of CD44s in the metastatic breast cancer cell line, MCF7, induced increased proliferation, migration and invadapodia *in vitro*. This was confirmed *in vivo*, where high levels of CD44s correlated with increased invadapodia and liver metastasis (Ouhtit et al. 2007). The co-expression of CD44v10 with CD44s results in the inability of CD44s to form clusters within the cell membrane. This cluster formation usually enhances the CD44/HA binding affinity. However, CD44v10 interacted with CD44s decreasing CD44s/HA binding affinity. This decrease in binding is thought to initiate metastatic progression (Iida and Bourguignon 1997). Isoforms containing v3 been have found to be associated with breast and head and neck cancer; and are thought to increase the expression of MMPs, known mediators of invadapodia and migration in metastasis. The variant CD44v3,8-10 has a heparin binding domain that was shown to preferentially interact with VEGF and therefore, it is implicated in angiogenesis (Wang et al. 2007).

The research into CD44 variants in cancer is extensive, however, there is limited knowledge about their expression and role in fibrosis. Previous studies in our laboratory have identified that total CD44 is highly expressed in fibroblasts and that this expression is down regulated upon TGF-β_1 stimulation, but upregulated by IL-1β (Meran et al. 2011b; Meran et al. 2013). What is not known is which individual CD44 variants are expressed in fibroblasts or how this expression alters when they are stimulated with these two cytokines.

3.2 -Chapter Aims

The aims of this chapter are:

1) Determine CD44 variant expression in unstimulated fibroblasts.
2) Investigate the effect of TGF-β_1 stimulation on CD44 variant expression.
3) Analyse the effect of IL-1β stimulation on CD44 variant expression.

3.3. – Methods

3.3.1. - Analysis of CD44 Spliced Variants

The transcriptional expression of the CD44 variants was analysed by two methods:

i) Analysis of single variant expression

In order to identify any variants that existed as a distinct single exon between the two common regions, primers were designed to overlap the 3' end of exon 5 with the 5' end of each selected target exon of the variable region ***(Figure 3.2 [A])***. (This was the forward primer. The 3' end of the target was then overlapped with the 5' end of exon 15 as the reverse primer) ***(Figure 3.2 [B]).*** Each exon product has a corresponding variant name, which is outlined in (***Table 3.1).*** Amplified targets were then quantified using QPCR, as previously described in Chapter 2.

ii) Analysis of large transcript variant expression

To investigate the expression of larger spliced variants, a forward primer located between the exon-exon boundary of exons 3 and 4 of the 5' constant region was used (***Figure 3.3. [A]).*** A panel of reverse primers, each specific to a sequence in each of the variable exons (6-14), enabled the identification of variants between the regions v2-v10 ***(Figure 3.3. [B])***. A final reverse primer in exon 17 was located in the transmembrane region and enabled the identification of CD44s.

Primer Design for single exon expression variants

[A]

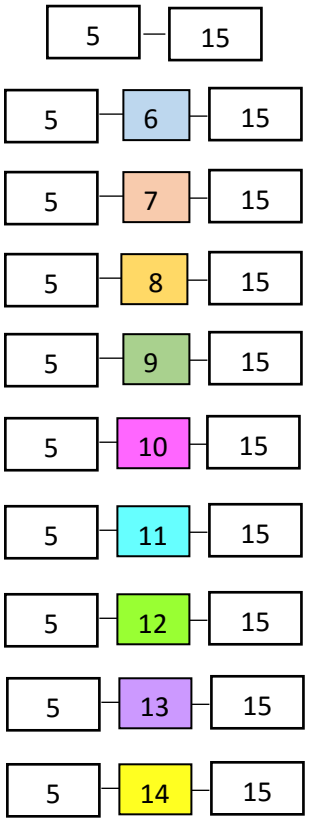

[B]

No Exon	CD44s
Exon 6	v2
Exon 7	v3
Exon 8	v4
Exon 9	v5
Exon 10	v6
Exon 11	v7
Exon 12	v8
Exon 13	v9
Exon 14	v10

Table 3.1 – Corresponding exon expression with variant

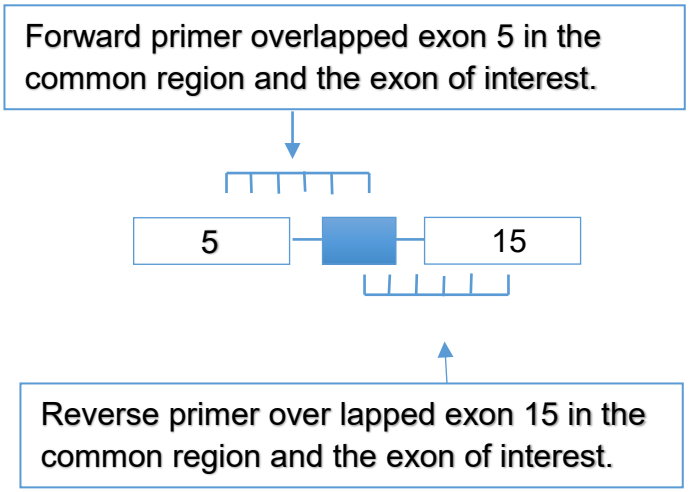

Figure 3.2. - Final Target Sequence and Corresponding Nomenclature of Single CD44 Variants

To enable a more detailed analysis of CD44 expression a preliminary investigation was carried out to examine the expression of single exons between the common regions. Custom primers were designed to target variants that express one of the variable exons (6-14) between the common regions. Final target products are indicated in schematic ***[A]***. The corresponding nomenclature of CD44 variant to exon expressed is indicated in table 3.1 ***[B]***. Primers were designed to span the exon boundary of the common region and the variant of interest. Forward primers overlapped the 3' end of exon 5 in the common region with the 5' end of the exon of interest. Reverse primers overlapped the 5' end of exon 15 with the 3' end of the exon of interest ***[C].***

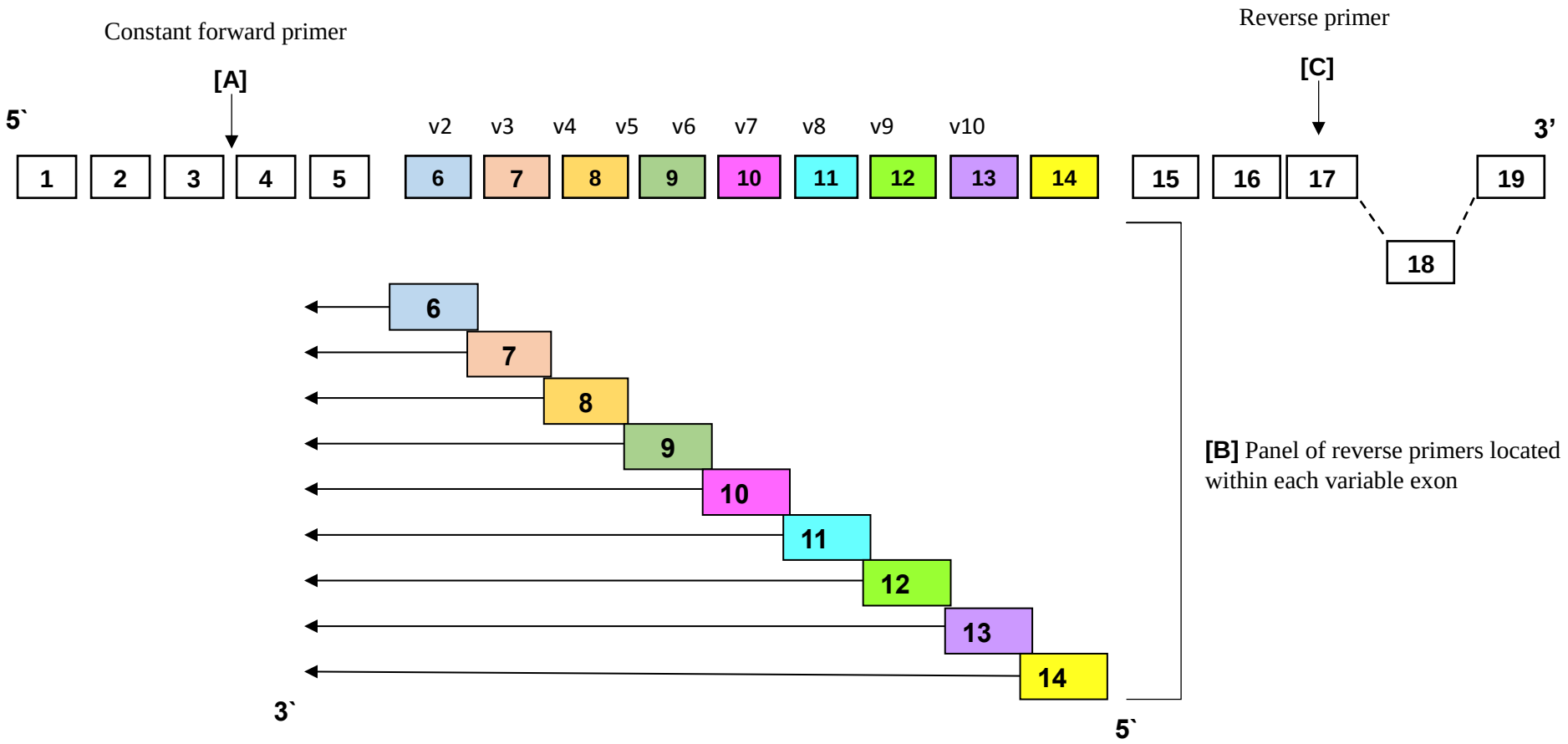

Figure 3.3. - Primer Design for Analysis of Large CD44 Spliced Variants

A common forward primer located in exon 5 was used for all targets ***[A]***. A panel of reverse primers that were located within spliced variant exons (6-14) were used to amplify CD44 spliced variants (v2-v10) ***[B].*** An additional reverse primer was located in exon 17 ***[C]*** was used to identify CD44 standard.

3.4. - Results

3.4.1 – The Expression of Single Exon CD44 Variants in Fibroblasts.

Total CD44 expression has previously been described, using a CD44 primer that targeted multiple exon - exon boundaries within the CD44 variable stem region. This enabled the amplification of multiple isoforms. Using this primer, TGF-β_1 decreased total CD44 expression in fibroblasts over time (Meran et al. 2011b). Conversely, IL-1β stimulation increased total CD44 expression (Meran et al. 2013).

A preliminary analysis of basal CD44 variant expression was carried out to investigate if the CD44 variants containing single exons between the common regions were expressed in fibroblasts. Initial analysis indicated that all the CD44 variants were expressed in fibroblasts with the exception of v5. To estimate how abundant the basal expression of each variant was in fibroblasts, the DCT values were subtracted from the final CT value 40 and analysed (***Figure 3.4.)***. The highest expressed variant was CD44 standard, followed by variants v3, v6 and v10. CD44 variants that were least expressed were v2, v7 and v9. ***Table 3.2*** shows the CT expression range of CD44 variants, which corresponds to these findings.

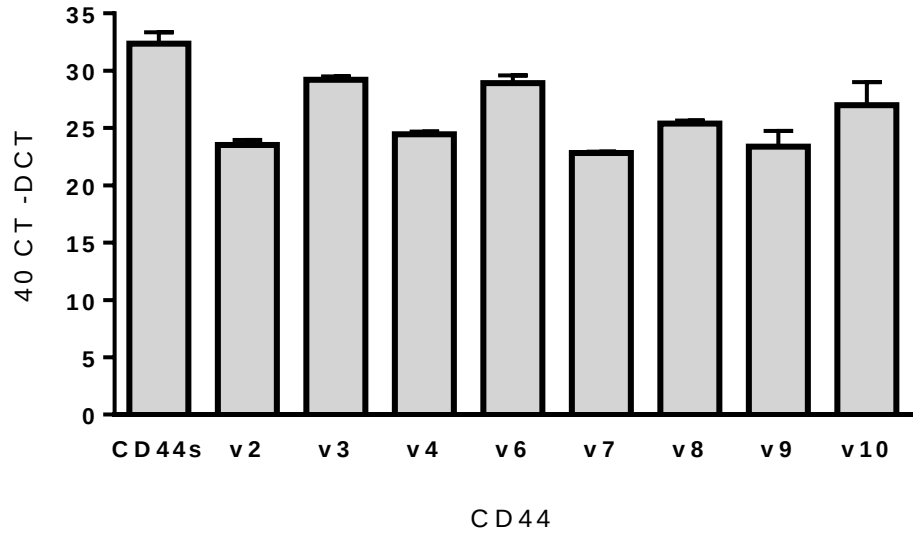

Figure 3.4. – Preliminary Analysis of CD44 Variant Expression in Fibroblasts.

Fibroblasts were grown to confluence and total RNA was extracted. Analysis of fibroblast expression of CD44 variants that had one exon between common regions was done using qPCR and the primer combinations that were previously described in ***Figure 3.2.1.*** Graph shows the DCT expression of variants subtracted from the total CT number (40). Data is shown as ±SD from two separate experiments. l n=2 Sample.

Basal Expression Range (CT values)	Variant
20-25	Standard
25-30	v3<v10 < v6
30-35	v8<v4<v7<v9 <v2

Table 3.2. – CT Expression of CD44 Variants in Basal Fibroblasts

Table shows the different expression of CD44 variant in unstimulated fibroblasts. The total cycle number for qPCR amplification was 40 and all the variants were expressed with in this range with the exception of v5. CD44s was the highest expressed variant in basal fibroblast and amplified within the range of 20-25 CT. All the variants amplified are stated in the table in order of amplification.

3.4.2 – The Effect of TGF-β_1 and IL-1β Stimulation on CD44 Variant Expression.

To investigate how the cytokines TGFβ_1 and IL-1β affected CD44 variant expression, fibroblasts were stimulated with TGF-β_1 (10 ng/ml) or IL-1β (1 ng/ml) over a time course of 0-72 h. Control samples were treated with serum-free medium alone and extracted simultaneously at each time-point. Total RNA was extracted and samples were analysed using

qPCR, described in chapter 2. Analysis of CD44 variants was carried out using the primers previously described ***(Figure 3.3.)***.

Preliminary analysis suggested that TGF-β_1 stimulation of fibroblasts decreased the expression of all CD44 variants. After 12 h of stimulation with TGF-β_1, the expression of CD44 standard, v2, v3, v4, v6, v8, v9 and v10 all decreased, when compared to control fibroblast expression ***(Figure 3.4. [A-E&H-I])***. Expression of CD44 v7 was unchanged, compared to control fibroblasts at all the time-points ***(Figure 3.4. [F])***.

Stimulation of fibroblasts with the pro-inflammatory cytokine IL-1β increased all the variants after 6 h of stimulation, compared to control fibroblasts ***(Figure 3.5. [A-I])***. Interestingly, CD44v10 had the highest increase of 9-fold at the 6 h time point ***(Figure 3.5. [I])***. However, CD44s, the most expressed variant in fibroblasts, increased by only 4-fold *(Figure 3.5. [A])*. CD44v2 increased the least of all the variants by 2-fold at 6 hours ***(Figure 3.5. [B])***. The expression of CD44v7 did not peak until 24 h, therefore, it was the only variant that did not exhibit its highest expression at 6 h ***(Figure 3.5. [F])***. After 72 h, all the variants had an expression equal to or below basal level control fibroblasts, with the exception of CD44 v2 and v7. This preliminary data suggested that there was some variability in the response of CD44 variant expression following IL-1β stimulation.

Using the observations made during this experiment, the time-points used for the subsequent investigations were 72 h for TGF-β_1 stimulation and 6 h for IL-1β induced stimulations.

Figure 3.4. - The Effect of TGF-β_1 Stimulation on CD44 Single Variant Expression

Human lung fibroblasts were grown to 80% confluence in 6-well plates and growth-arrested in serum-free medium for 48h. Cells were stimulated with TGF-β_1 (10ng/ml) or fresh serum-free medium was added to control cells. Cell were extracted at different time-points over 72 h. The extraction time-points were 0 h (this was immediately after stimulation of TGF-β_1 or the addition of fresh serum free medium in control samples) 6, 12, 24, 48; and 72 h. Total RNA was extracted, as described in ***Chapter 2.*** QPCR was used to quantify the expression of a single CD44 exon between the common regions, using primers previously described in section 3.2 and ***(Figure 3.2.1.)*** The relative CT method was used for analysis. Each graph represents the expression of a single CD44 variant over the 72 h time course. Graph compares control sample expression (open bars) against cells stimulated with TGF-β_1 (black bars) at each of the time-points. Comparative exon expression between common regions with co-responding variant names are: ***[A]*** CD44s (no exon), ***[B]*** v2 (exon 6), ***[C]*** v3 (exon 7), ***[D]*** v4 (exon 8), ***[E]*** v6 (exon 10), ***[F]*** v7 (exon 11), ***[G]*** v8 (exon 12), ***[H]*** v9 (exon 13), ***[I]*** v10 (exon 14). Sample were normalised to control samples at each of the respective time point. Data shown is preliminary data, experimental N=1, sample N=3.

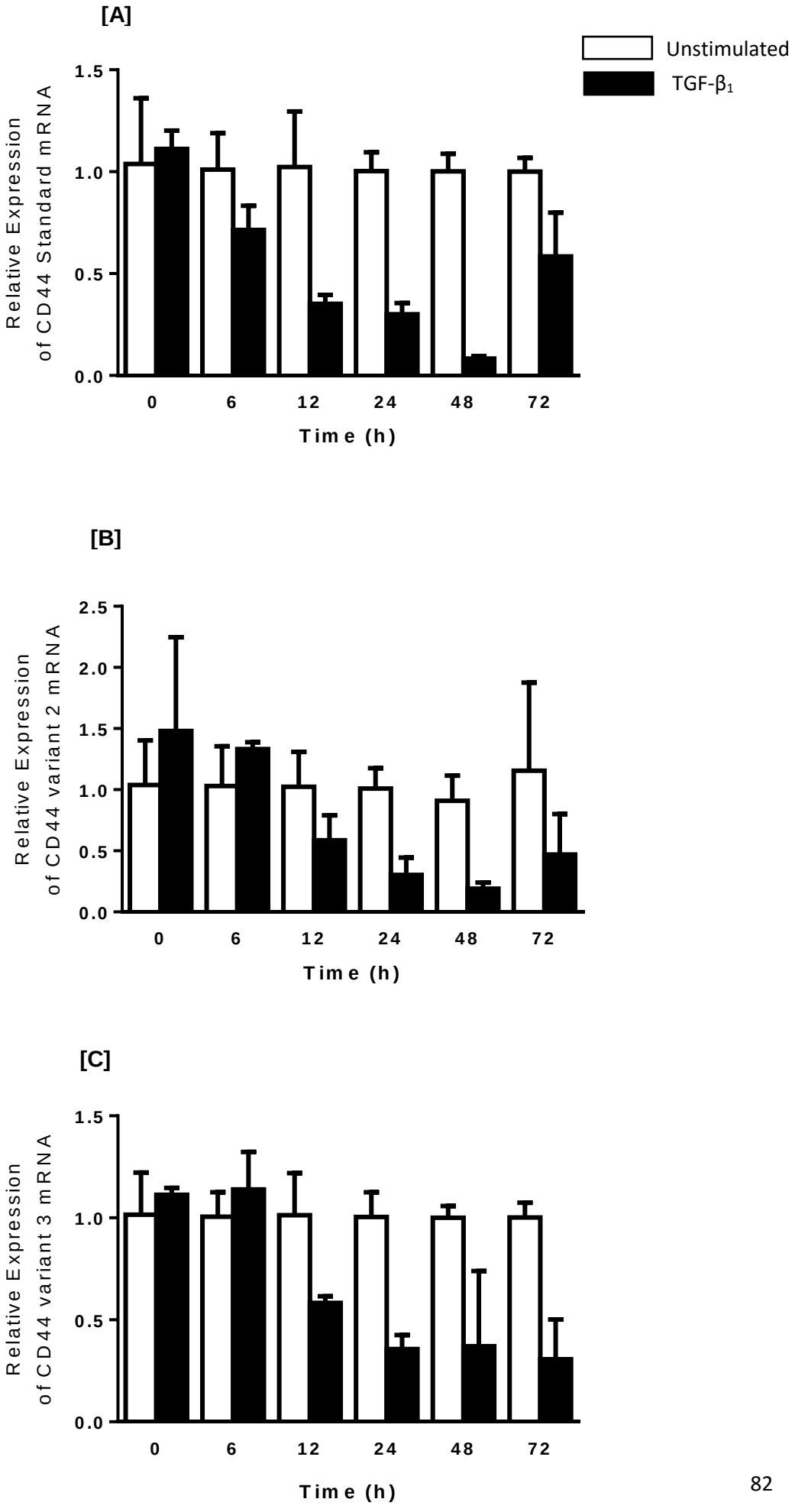
[A]
Unstimulated
TGF-β1
Relative Expression of CD44 Standard mRNA
1.5
1.0
0.5
0.0
0
6
12
24
48
72
Time (h)
[B]
Relative Expression of CD44 variant 2 mRNA
2.5
2.0
1.5
1.0
0.5
0.0
0
6
12
24
48
72
Time (h)
[C]
Relative Expression of CD44 variant 3 mRNA
1.5
1.0
0.5
0.0
0
6
12
24
48
72
Time (h)

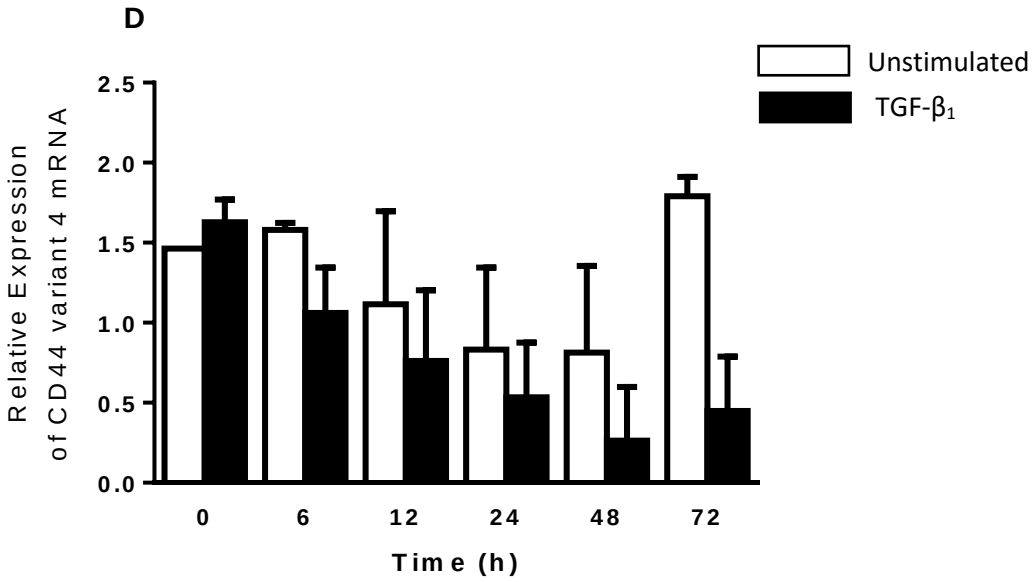
D
Unstimulated
TGF-β1
Relative Expression of CD44 variant 4 mRNA
2.5
2.0
1.5
1.0
0.5
0.0
0
6
12
24
48
72
Time (h)

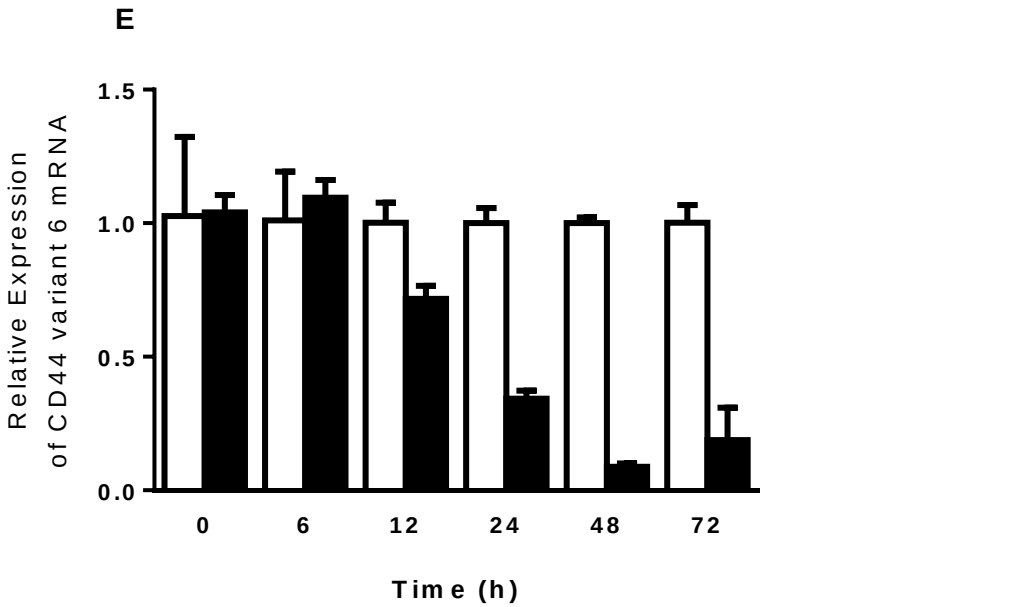
E
Relative Expression of CD44 variant 6 mRNA
1.5
1.0
0.5
0.0
0
6
12
24
48
72
Time (h)

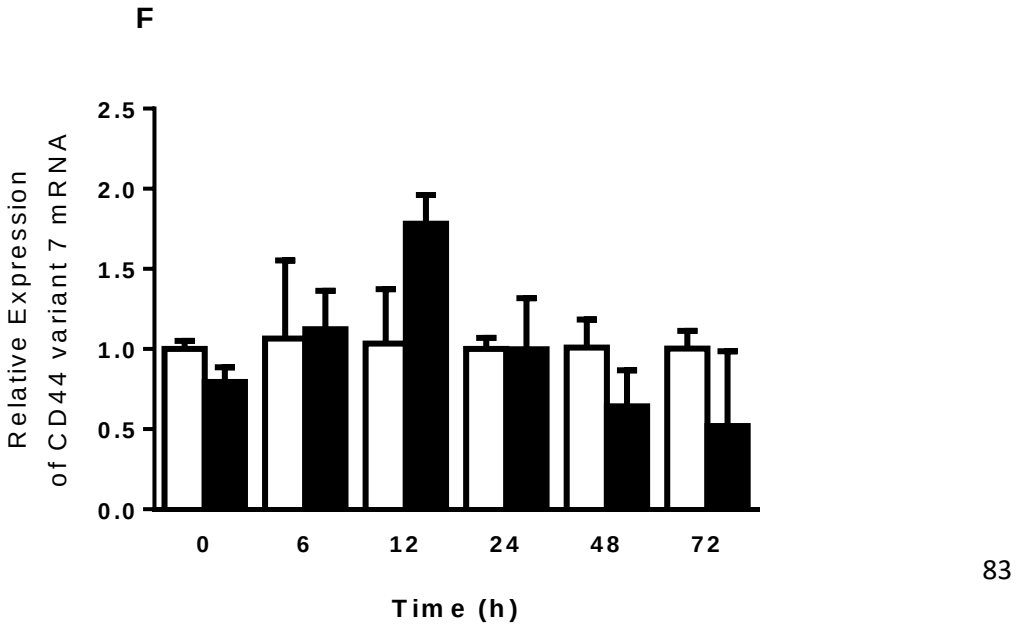
F
Relative Expression of CD44 variant 7 mRNA
2.5
2.0
1.5
1.0
0.5
0.0
0
6
12
24
48
72
Time (h)

G

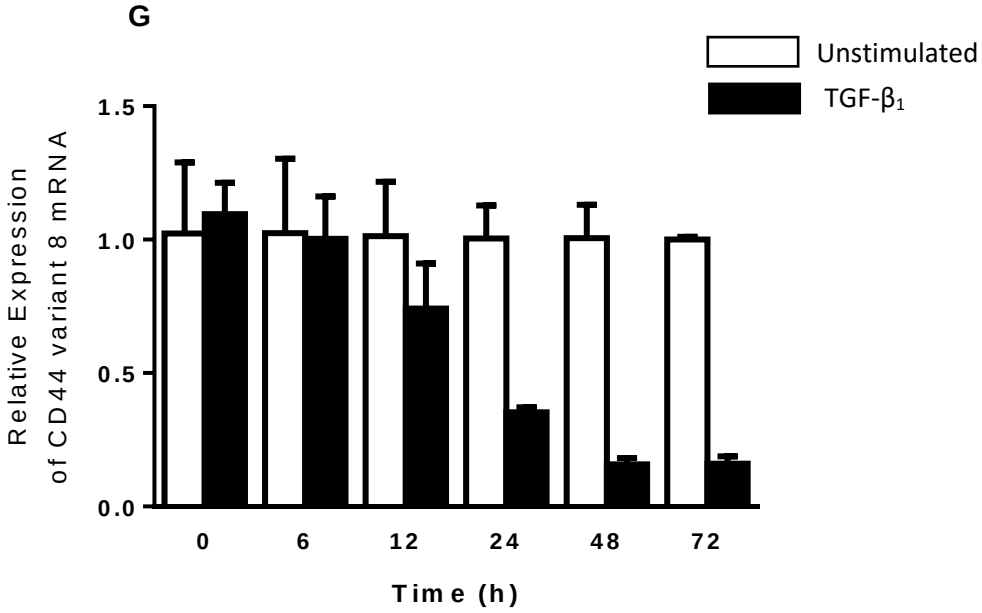
Unstimulated
TGF-β1
Relative Expression of CD44 variant 8 mRNA
1.5
1.0
0.5
0.0
0
6
12
24
48
72
Time (h)

H

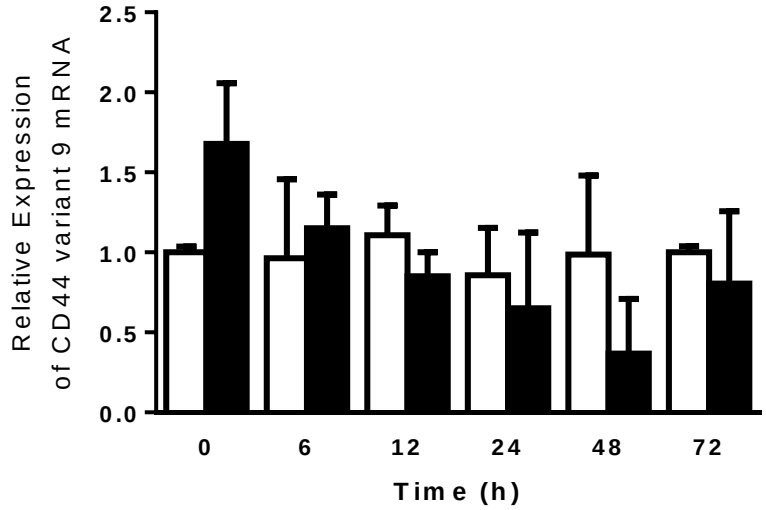
Relative Expression of CD44 variant 9 mRNA
2.5
2.0
1.5
1.0
0.5
0.0
0
6
12
24
48
72
Time (h)

I

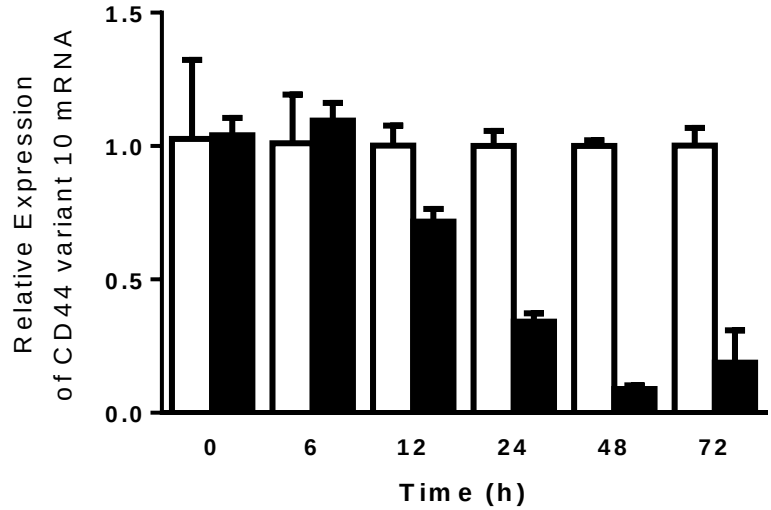
Relative Expression of CD44 variant 10 mRNA
1.5
1.0
0.5
0.0
0
6
12
24
48
72
Time (h)

Figure 3.5. - The Effect of IL-1β Stimulation on CD44 Single Variant Expression

Human lung fibroblasts were grown to 80% confluence in 6-well plates and growth-arrested in serum-free medium for 48h. Cells were stimulated with IL-1β (1ng/ml) or fresh serum-free medium was added to control cells. Cell were extracted at different time points over 72 h. The extraction time points were 0 h (this was immediately after stimulation of IL-1β or the addition of fresh serum-free medium in control samples) 6, 12, 24, 48; and 72 h. Total RNA was extracted, as described in ***Chapter 2.*** QPCR was used to quantify the expression of a single CD44 exon between the common regions, using primers previously described in section 3.2 and ***(Figure 3.2.1).*** The relative CT method was used for analysis. Each graph represents the expression of a single CD44 variant over the 72 h time course. Graph compares control sample expression (open bars) against cells stimulated with IL-1β (black bars) at each of the time-points. Comparative exon expression between common regions with co-responding variant names are:- ***[A]*** CD44s (no exon), ***[B]*** v2 (exon 6), ***[C]*** v3 (exon 7), ***[D]*** v4 (exon 8), ***[E]*** v6 (exon 10), ***[F]*** v7 (exon 11), ***[G]*** v8 (exon 12), ***[H]*** v9 (exon 13), ***[I]*** v10 (exon 14). Sample were normalised to control samples at each of the respective time-point. Data shown is preliminary data, experimental N=1, sample N=2.

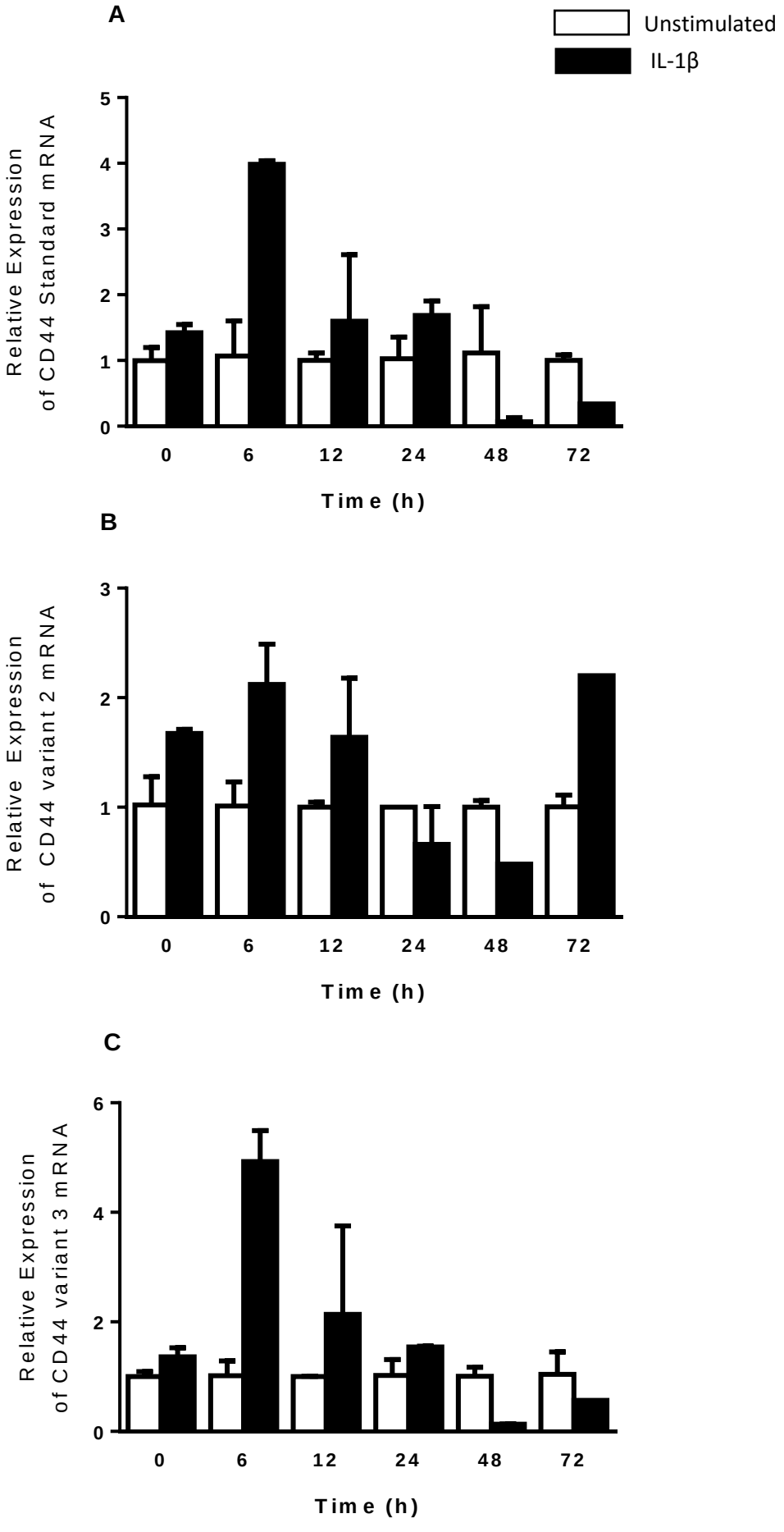
A
Unstimulated
IL-1β
Relative Expression of CD44 Standard mRNA
0
1
2
3
4
5
0
6
12
24
48
72
Time (h)
B
Relative Expression of CD44 variant 2 mRNA
0
1
2
3
0
6
12
24
48
72
Time (h)
C
Relative Expression of CD44 variant 3 mRNA
0
2
4
6
0
6
12
24
48
72
Time (h)

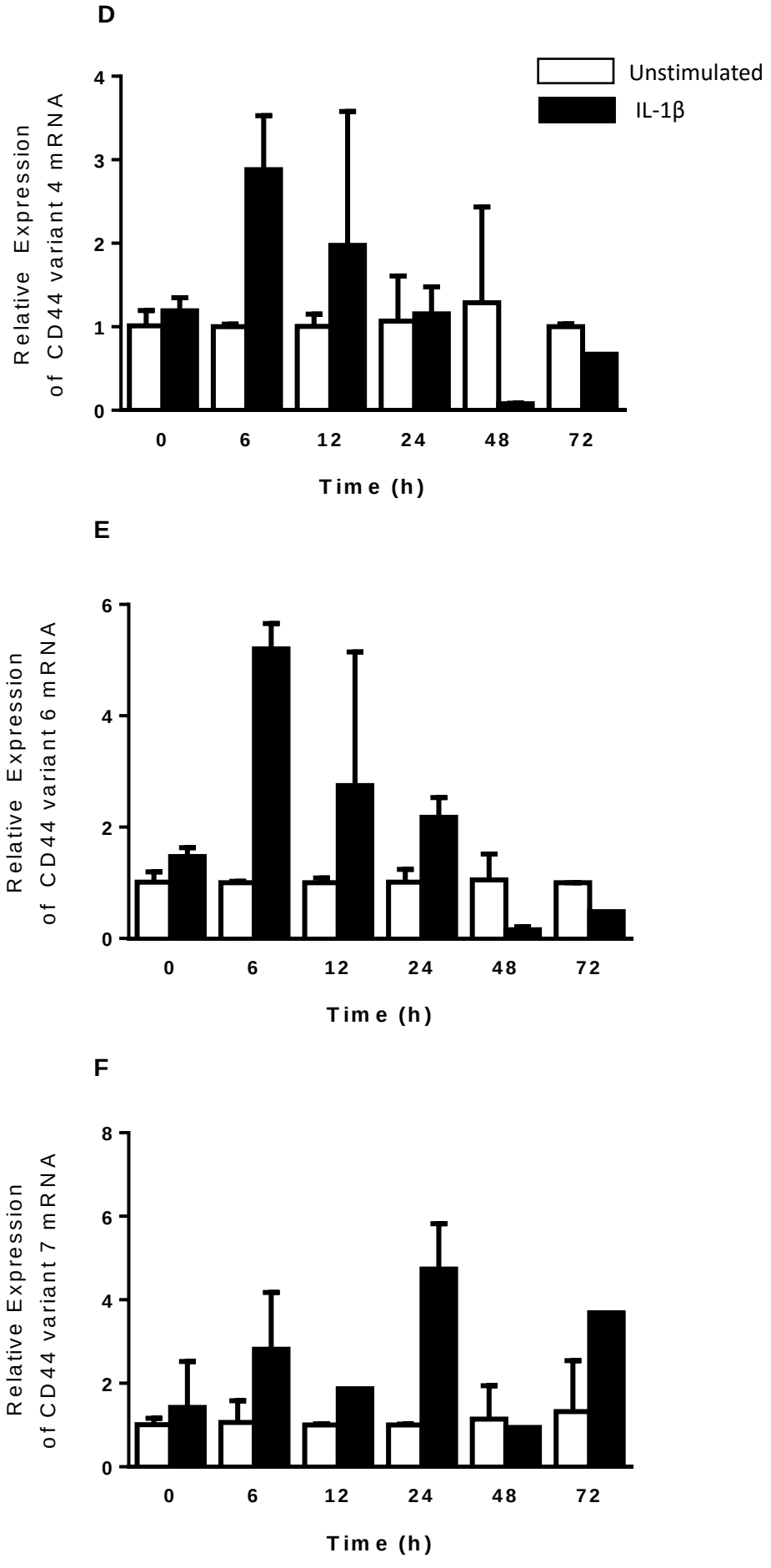
D
Unstimulated
IL-1β
Relative Expression of CD44 variant 4 mRNA
0
1
2
3
4
0
6
12
24
48
72
Time (h)
E
Relative Expression of CD44 variant 6 mRNA
0
2
4
6
0
6
12
24
48
72
Time (h)
F
Relative Expression of CD44 variant 7 mRNA
0
2
4
6
8
0
6
12
24
48
72
Time (h)

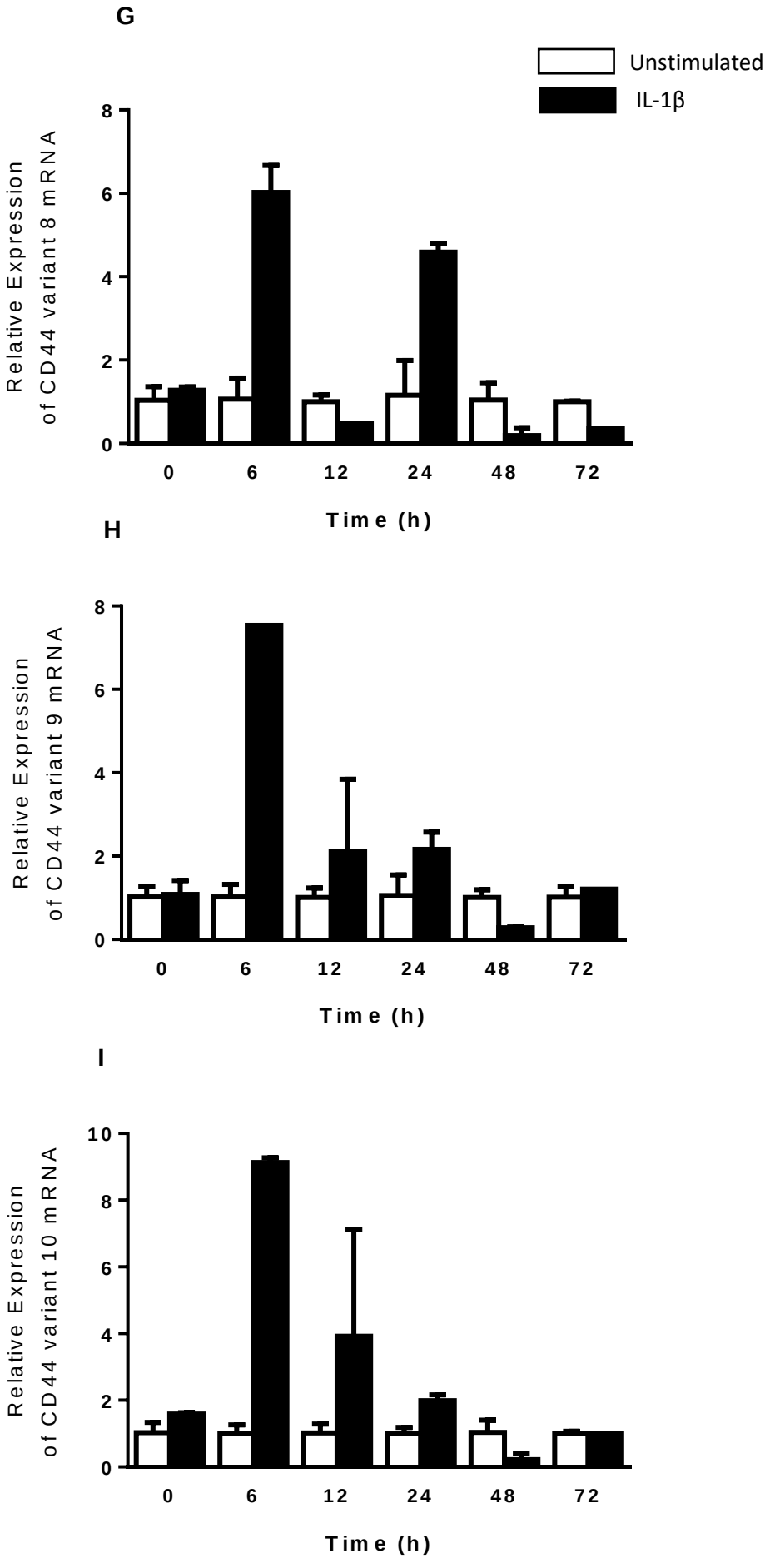
G
Unstimulated
IL-1β
Relative Expression of CD44 variant 8 mRNA
0
2
4
6
8
0
6
12
24
48
72
Time (h)
H
Relative Expression of CD44 variant 9 mRNA
0
2
4
6
8
0
6
12
24
48
72
Time (h)
I
Relative Expression of CD44 variant 10 mRNA
0
2
4
6
8
10
0
6
12
24
48
72
Time (h)

3.4.3. -The Effect of TGF-β_1 and IL-1β on Large CD44 Spliced Variants

To identify CD44 variants that expressed multiple exons between the common regions, a panel of reverse primers and a common forward primer was used as described in ***(Figure 3.3.)***. Fibroblasts were grown to 80% confluence and growth-arrested for 48 h. Fibroblasts were stimulated with TGF-β_1 (10ng/ml) for 72 h or IL-1β (1ng/ml) for 6 h. Control fibroblasts were treated with fresh serum-free medium. A further set of control samples were extracted, prior to treatment directly following growth arrest to assess experimental conditions.

Separate amplification of the constant forward primer ***(Figure 3.3[A])*** with the reverse primer that targeted a region within exon 17 ***(Figure 3.3[C])*** and primers located within exons 6, 7 and 8 figure 3.3***[B]***, all amplified a single product. ***(Figures 3.6 [A-D])*** and ***(Figure 3.7 [A-D])*** bands (1-4) were identified using DNA sequencing as (1) CD44s, (2) CD44v2, (3) CD44v3 and (4) CD44v4. TGF-β_1 stimulation decreased the expression of CD44s (1), CD44v2 (2) and CD44v3 (3) at 72 h compared to control fibroblasts ***(Figure 3.6 [A-C])***. The expression of CD44v4, however, did not alter after stimulation of TGF-β_1, compared to controls ***(Figure 3.6. [D].)*** Stimulation with IL-1β ***(Figure 3.7 [A-D])*** bands (1-4) increased the expression of CD44s (1), CD44v2 (2), CD44v3 (3) and CD44v4 (4), after 6 h.

As previously seen, variant 5 did not amplify and was not affected by either TGF-β_1 or IL-1βstimulation *(data not shown).*

(Figure 3.6 [E-H]) and ***(Figure 3.7 [E-H])*** are the products of reverse primers located within exons 10, 11, 12 and 13. Using these reverse primers with the constant forward primers multiple products were identified, bands (5-11). These were CD44v6 (5), CD44v 6-7 (6), CD44v8 (7), CD44v6-8 (8), CD44v9 (9), CD44 v8-9 (10) and CD44v6-9 (11). Bands 5, 6, 8, 10 & 11 show a sequential base pair increase of approximately one exon in length, respectively. Starting from exon 10/v6 (5), each reverse primer is located in an upstream variant exon. Each

of the sequential variants increased by one exon, indicating that they were all different length amplicons of the same product. The final reverse primer located within exon 14 ***(Figure 3.6 [I])*** and ***(Figure 3.7 [I])***, amplified one band that was determined to be CD44v10 (12). As previously seen with the other variants, all of the amplicons decreased when treated with TGF-β_1 ***(Figure 3.6 [E-I])*** and increased when treated with IL-1β ***(Figure 3.7[E-I]).***

An additional set of primers was used to amplify the largest target. A forward primer that overlapped the 3' of exon 5 in the common region with the 5' end of exon 10/variant 6; and a reverse primer that overlapped the 5' end of exon 15 in the common region and with the 3' end of exon 14 /variant 10. This is a combination of the previously designed primers described in ***(Figure 3.2. [C])***. A large amplicon of approximately 720bp was identified ***(Figure 3.6. [J])*** and ***(Figure 3.7. [J])*** band (13). The amplicon size was larger than the expected product size of 480bp stated in ***(Table 3.5*** and ***Table 3.9).*** This was due to the continued amplification of the product into exon 5 and exon 15 in the common region from the forward and the reverse primers. DNA sequencing of this band identified the amplicon to be CD44v6-10 (see Appendix 1). Consistent with previous results, this largest target had a decreased expression following 72 h stimulation with TGF-β_1 decreased and showed an increase after 6 h IL-1β treatment.

Details of the expected amplicon length, reverse primer used, and identified product are given in ***(Tables 3.2-3.5)*** for TGF-β_1 and ***(Tables 3.6-3.9)*** for IL-1β amplicons.

Figure 3.6. - TGF-β_1 Effects on Large CD44 Spliced Variant Expression

To identify the expression of large variants that contained multiple exons between common regions, fibroblasts were grown to 80% confluence and growth-arrested for 48 h. Cell were then stimulated with TGF-β_1 (10ng/ml) for 72 h. Control fibroblasts were treated with serum-free medium for the same time period as treated fibroblasts. A further control group was extracted at 0 h, prior to the addition of medium. Total ribosomal RNA was extracted and samples were reverse transcribed, as described in Chapter 2. Touch down PCR was used to amplify CD44 variant targets, using the combination of primers described in Figure 3.2.2. cDNA was separated on a 0.5% agarose gel containing ethidium bromide, using electrophoresis at 100v for 90 min. Bands were visualised and extracted under a UV light. DNA was extracted from each gel band using a QIAquick Gel Extraction Kit (Qiagen) and sequenced. Figures ***[A-I]*** show photos of the final gels. Lane 1 are control fibroblasts that have been extracted immediately after the 48 h growth arrest period. Lane 2 is control fibroblasts treated with serum-free medium. Lane 3 is TGF-β_1 stimulated fibroblasts. Both Lanes 2 and 3 were extracted at 72 h.

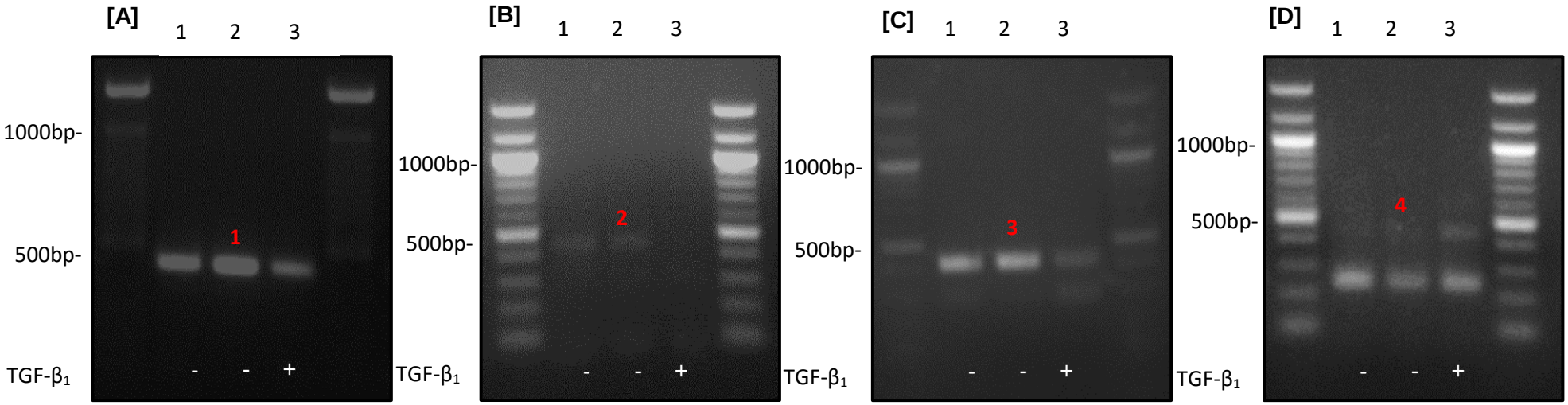

Band Number	*Exon position of Reverse Primer*	*Target Size*	*Identified Product*
1	Exon 17	391bp	CD44 Standard
2	Exon 2	441bp	CD44 v2
3	Exon 3	420bp	CD44v3
4	Exon 4	388bp	CD44v4

Table 3.2. – Shows the reverse primer position, the expected product size and the product identified for each of the bands (1-4).

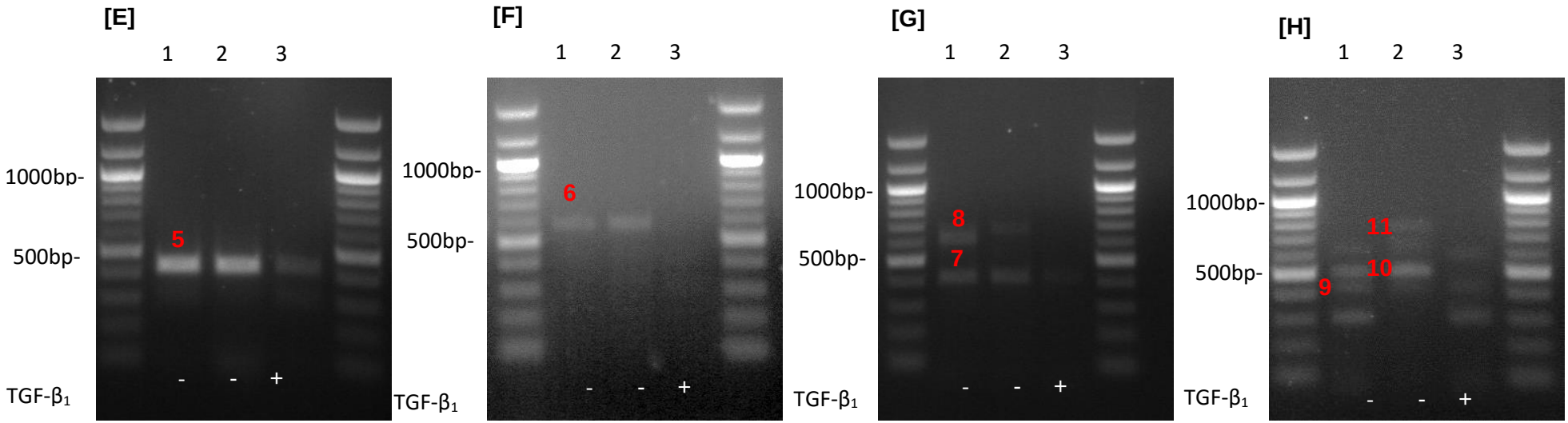

Band Number	*Exon position of Reverse Primer*	*Target Size*	*Identified Product*
5	Exon 6	424bp	CD44v6
6	Exon 7	573bp	CD44 v6-7
7	Exon 8	408bp	CD44v8
8	Exon 8	674bp	CD44v6-8
9	Exon 9	402bp	CD44v9
10	Exon 9	469bp	CD44v8-9
11	Exon 9	757bp	CD44v6-9

Table 3.3. – Shows the reverse primer position, the expected product size and the product identified for each of the bands (5-11).

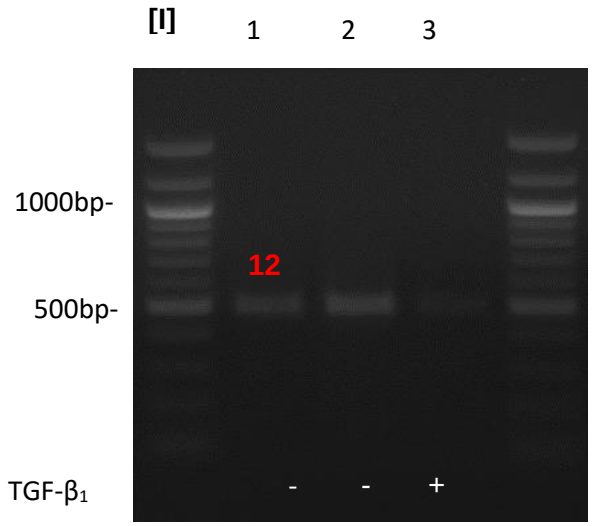

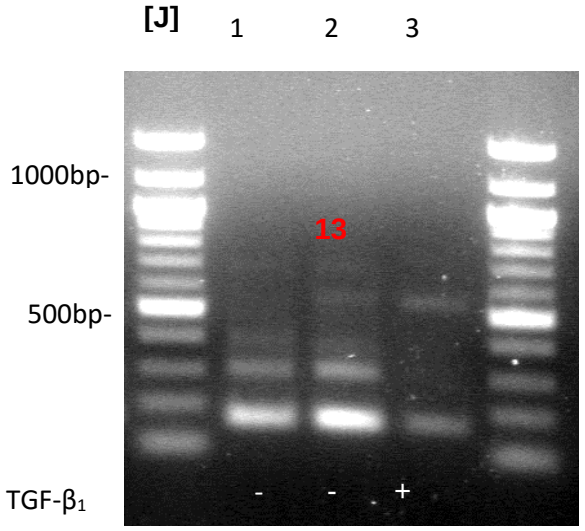

Band Number	*Exon position of Reverse Primer*	*Target Size*	*Identified Product*
12	Exon 14	489	CD44v10

Table 3.4. – Shows the reverse primer position, the expected product size and the product identified for band (12).

Band Number	*Exon position of forward Primer*	*Exon position of reverse primer*	*Target size*	*Identified Product*
13	Exon5/Exon 10 boundary	Exon 15/Exon 14 boundary	720bp	CD44v6-10

Table 3.5. – Shows the reverse primer position, the expected product size and the product identified for band (13).

Figure 3.7. - IL-1β Effects on Large CD44 Spliced Variant Expression

To identify the expression of large variants that contained multiple exons between common regions, fibroblasts were grown to 80% confluence and growth-arrested for 48 h. Cell were then stimulated with IL-1β (1ng/ml) for 6 h. Control fibroblasts were treated with serum-free medium for the same time period as treated fibroblasts. A further control group was extracted at 0 h, prior to the addition of medium. Total ribosomal RNA was extracted and samples were reverse transcribed, as described in Chapter 2. Touch down PCR was used to amplify CD44 variant targets, using the combination of primers described in Figure 3.2.2. cDNA was separated on a 0.5% agarose gel containing ethidium bromide, using electrophoresis at 100v for 90 min. Bands were visualised and extracted under a UV light. DNA was extracted from each gel band using QIAquick Gel Extraction Kit (Qiagen) and sequenced. Figures ***[A-I]*** show photos of the final gels. Lane 1 are control fibroblasts that have been extracted immediately after the 48 h growth arrest period. Lane 2 is control fibroblasts treated with serum-free medium. Lane 3 is IL-1β stimulated fibroblasts. Both Lanes 2 and 3 were extracted at 72 h.

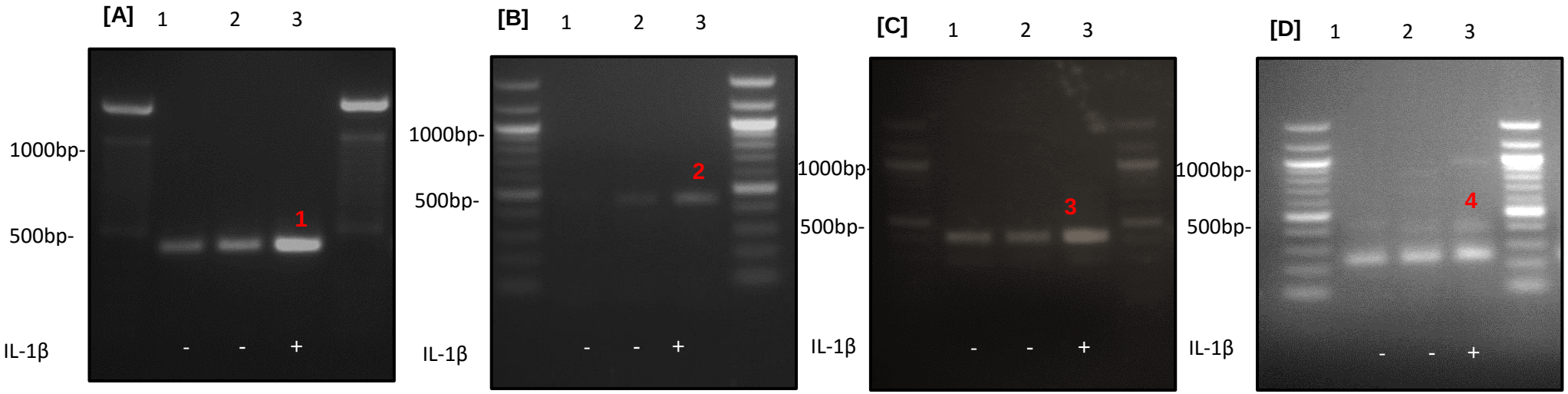

Band Number	Exon position of Reverse Primer	Target Size	Identified Product
1	Exon 17	391bp	CD44 Standard
2	Exon 2	441bp	CD44 v2
3	Exon 3	420bp	CD44v3
4	Exon 4	388bp	CD44v4

Table 3.6. – Shows the reverse primer position, the expected product size and the product identified for each of the bands (1-4).

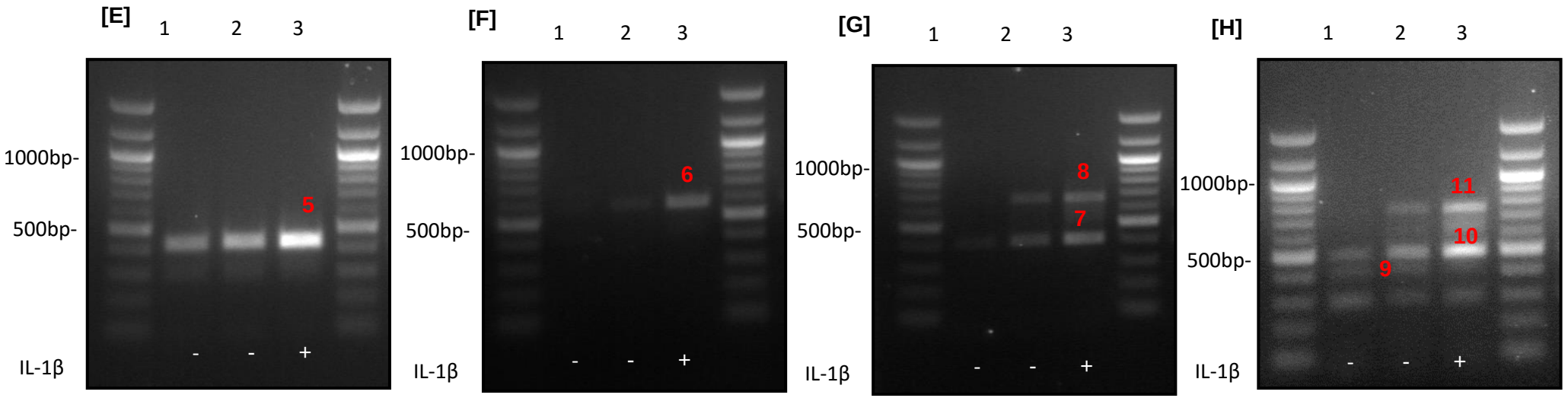

Band Number	Exon position of Reverse Primer	Target Size	Identified Product
5	Exon 6	424bp	CD44v6
6	Exon 7	573bp	CD44 v6-7
7	Exon 8	408bp	CD44v8
8	Exon 8	674bp	CD44v6-8
9	Exon 9	402bp	CD44v9
10	Exon 9	496bp	CD44v8-9
11	Exon 9	757bp	CD44v6-9

Table 3.7. – Shows the reverse primer position, the expected product size and the product identified for each of the bands (5-11).

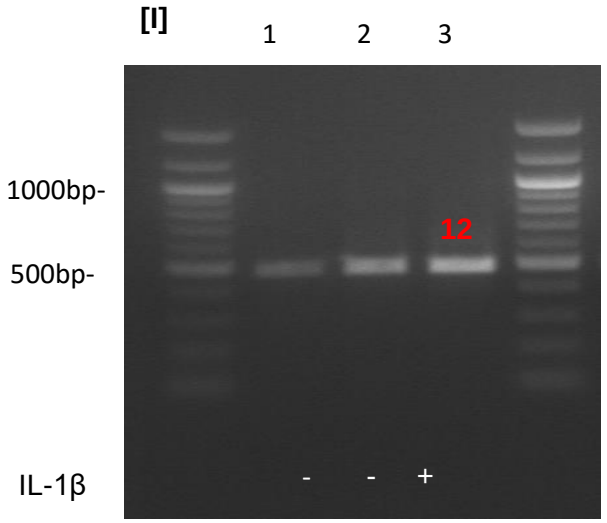

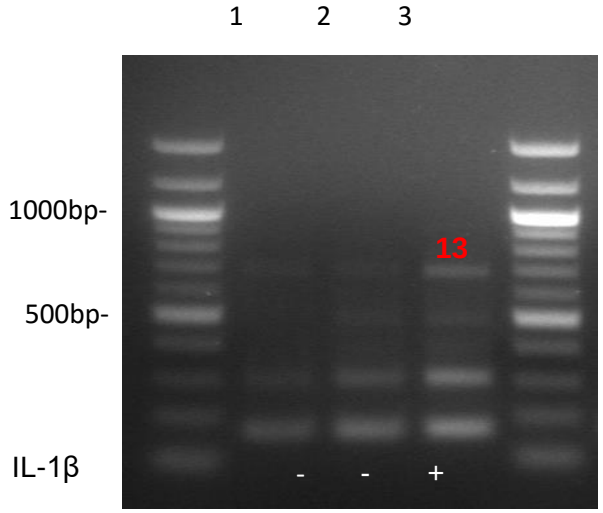

Band Number	*Exon position of Reverse Primer*	*Target Size*	*Identified Product*
12	Exon 14	489bp	CD44v10

Table 3.8 – Shows the reverse primer position, the expected product size and the product identified for band (12).

Band Number	*Exon position of forward Primer*	*Exon position of reverse primer*	*Target size*	*Identified Product*
13	Exon5/Exon 10 boundary	Exon 15/Exon 14 boundary	720bp	CD44v6-10

Table 3.9 – Shows the reverse primer position, the expected product size and the product identified for band (13).

3.5. - Discussion

This chapter aimed to identify which CD44 variants were expressed in fibroblasts and how the cytokines TGF-β_1 and IL-1β, affected their expression. A summary of all the variants identified is given in ***(Figure 3.8)***. A preliminary investigation to examine the expression of CD44 variants that had only one spliced exon between common regions, found that all the CD44 variants from CD44v2 up to CD44v10 were expressed in fibroblasts, with the exception of CD44v5.

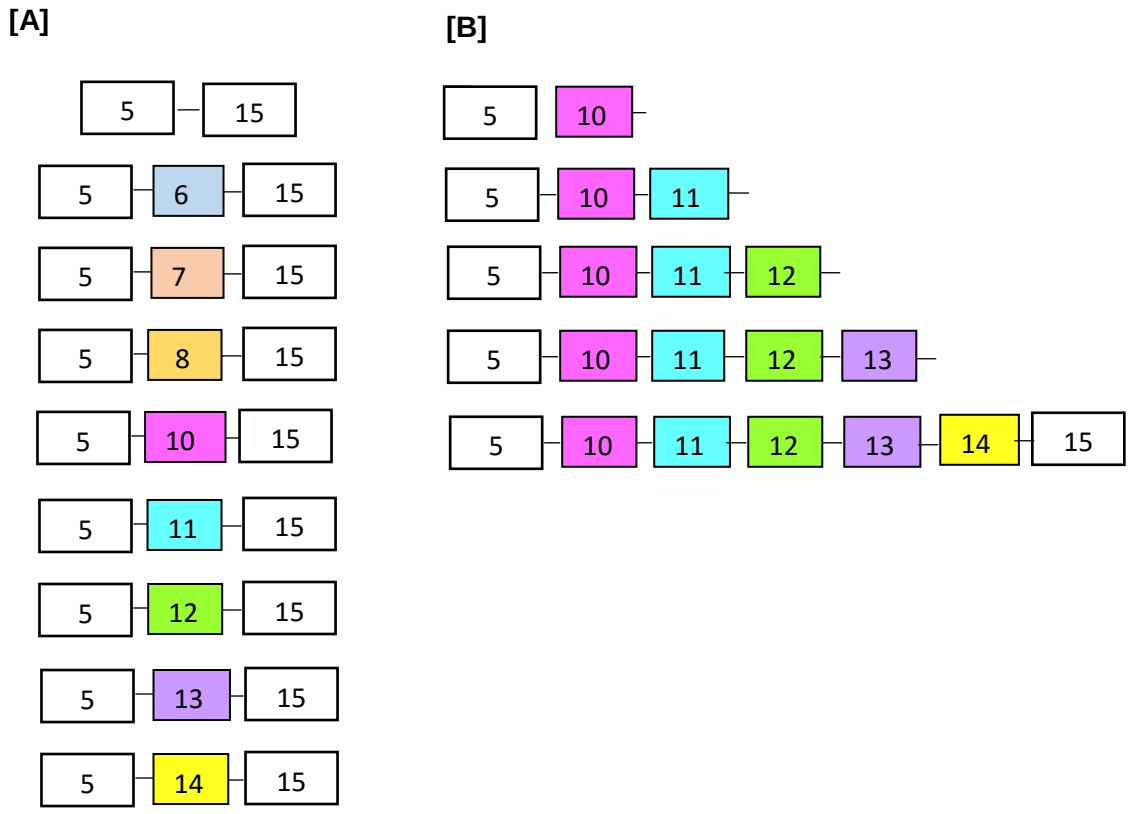

Figure 3.8 – Summary of CD44 variants identified to be expressed in fibroblasts

Diagrams show the CD44 variants identified to be expressed in fibroblasts. Figure [A] shows a summary of the CD44 variants containing only one single exon from the stem region between common regions Identified using qPCR. Figure [B] shows the final identification of the large CD44 spliced CD44v6-10 using Touch down PCR.

Previous research within our group has determined that fibroblast migration, proliferation and differentiation are HA/CD44 dependent (Meran et al. 2011b). The

preliminary data in this chapter indicates that CD44s is the highest expressed variant in lung fibroblasts. It is well documented the CD44s is the most abundant and widely distributed isoform of CD44 and the most commonly associated with HA binding functions (Bourguignon et al. 1998). Therefore, it could be speculated that CD44s may be the principle receptor involved in CD44/HA mediated functions in fibroblasts.

However, this study also suggests that CD44 variants v3, v6 and v10 are highly abundant in fibroblasts ***(Table 3.1.)*** Variants of CD44 all have the same HA binding domains within the extracellular region, but they display a different HA binding affinity. However, the variants CD44v3 v6 and v10 have all been documented to have an increased interaction with HA in cancer progression; and be associated with migration and increased proliferation (Bourguignon et al. 1998; Afify et al. 2009). Fibroblasts are the principle mediator in wound healing. Resident fibroblasts migrate to the damaged region and undergo increased proliferation, preceding differentiation to a myofibroblast. Therefore, the high expression of these isoforms may contribute to increased CD44/HA interactions and facilitate these functions. CD44 variants v2, v4, v7, v8 and v9 were all expressed in fibroblasts, although to a lesser extent ***(Table 3.1.)***. These variants, with the exception of variant 2, have all previously been documented to have an increased expression in cancer cells, indicating that they also can interact with HA (Iczkowski et al. 2003; Zen et al. 2008; Lau et al. 2014).

The pro-fibrotic cytokine, TGF-β_1, is a major contributor to fibrotic progression. Our research has previously shown that TGF-β_1-activated fibroblasts differentiate to myofibroblasts in a HA/CD44/EGFR-dependent manner. The HA/CD44 interaction moves CD44 through the membrane into lipid rafts, where it associates with EGFR. This complex formation initiates an intracellular signalling cascade through ERK1/2 and the differentiation process (Midgley et al. 2013).

The effect of TGF-β_1 on CD44 variant expression in fibrosis is not well researched. It is known that overexpressing CD44v3 inhibited the expression of TGF-BR1 and downstream activation of TGF-β_1 in CD44 knockout/knockin mice. This led to the prevention of tubular damage and increased proliferation of tubular epithelial cells, preventing fibrotic progression in obstructive nephropathy. Furthermore, overexpression of CD44s increased TGF-β_1 expression and fibrotic progression (Rampanelli et al. 2014). In addition, upregulated CD44v6 and v9 have been observed in pulmonary fibrosis, compared to normal lung tissue (Kasper et al. 1995). More recently, our group has shown that total CD44v7/8 expression is significantly decreased in TGF-β_1-induced myofibroblasts, compared to an increased expression observed in fibroblasts stimulated with BMP-7. Further, stimulation of myofibroblasts with BMP-7 has been observed to reverse the fibrotic effect probably by the internalization of HA and prevention of TGF-β_1 induced signalling (Midgley et al. 2015).

To elucidate how TGF-β_1 regulates CD44 variants in differentiating fibroblasts, a preliminary study investigated the expression of CD44 variants containing only one exon between common regions after TGF-β_1 activation. This study is consistent with previous findings in our group and shows that CD44s and all the variant isoforms CD44v2 to v10 had a reduced expression after 72 h (this is the time the cells were deemed to be myofibroblasts), with the exception of CD44v7 which had no variation in expression throughout the time course.

Why CD44 expression in myofibroblasts is attenuated is undetermined. One explanation may be that the HA/CD44 interaction alters in myofibroblasts, compared to fibroblasts. In fibroblasts, CD44 is diffuse throughout the plasma membrane when TGF-β_1 induces differentiation, CD44 is moved into clusters by HA resulting in the formation of a TSG-6/HA/CD44-dependent peri-cellular coat (Webber et al. 2009c; Midgley et al. 2015). This different orientation of CD44 alters the affinity of the HA/CD44 complex, a factor that is known to alter the cellular response (Iida and Bourguignon 1997). As the functions of a

fibroblast are different to a myofibroblasts, it may suggest that this reduction alters signalling pathways that mediate the cell functions.

A continued inflammatory response plays a role in the underlying pathology of fibrotic progression by mediating the influx of healing mediators to the site of injury, including monocytes/macrophages and fibroblasts. The association of fibroblasts with monocytes/macrophages has been previously demonstrated to play a role in fibrogenesis. Recent evidence has implicated the pro-inflammatory cytokine, IL-1β, in the induction of fibroblast-monocyte binding in a HA/CD44-dependent manner. After IL-1β stimulation, fibroblasts form cell membrane protrusions that associate with linear spikes of HA. CD44 is central to this formation and accumulates within the protrusions and associates closely with ICAM-1 mediating monocyte binding (Meran et al. 2013).

IL-1β induced the expression of all the CD44 variants identified in this preliminary study after 6 h. As seen in fibroblasts and myofibroblasts, CD44v5 was not detected. Previously, it has been shown that both TGF-β_1 and IL-1β upregulate CD44v5 in cervical adenocarcinoma (Ibrahim et al. 2006). In this study, both these cytokines failed to stimulate a CD44v5 product. Therefore, it may suggest that this variant is not expressed in fibroblasts or myofibroblasts. CD44v10 had the highest increase of nearly 9-fold, comparative to control fibroblast following IL-1β stimulation. In inflammatory conditions, cell migration plays a pivotal role. CD44v10 has been associated with upregulated cell migration to a similar extent as that seen by CD44s in cancer (Bourguignon et al. 1998). Therefore, the large increase in this variant following stimulation with pro-inflammatory IL-1β may suggest an increased migratory response. Interestingly, CD44v7, v8, and v9, which were deemed to be the least expressed variants in fibroblasts, exhibited a higher fold increase comparative to the more highly expressed variants, CD44s CD44v3 and v6. However, these latter variants already have a high basal expression and therefore, an increase may not be as noticeable. The increase of

CD44 variants in inflammatory disease is well-researched. For example, in rheumatoid arthritis synovial fluid, there is a high expression of CD44 isoforms containing v6 and v9; and v3, v6 and v7 containing isoforms are largely associated with inflammatory bowel disease (Hale et al. 1995; Rosenberg et al. 1995b; Wittig et al. 2000). Moreover, due to the high expression of CD44s on lymphoid cells, it has long been established that upregulation of the standard CD44 plays a role in inflammatory diseases (Jalkanen et al. 1986; Haynes et al. 1991). This study, therefore, presents data in line with previous work that states that CD44 is upregulated under inflammatory conditions.

Larger CD44 spliced variants have mostly been identified in association with cancer. The increased insertion of amino acids into the stem region results in further potential glycosylation. This alters the association of CD44 with ECM components and hence, changes the cell properties. The large variant identified in fibroblasts in this study, CD44v6-10 has been shown to have a lower affinity for HA binding, compared to the standard form of CD44. Furthermore, the upregulation of this variant has been observed to delay lymphoma progression. It does this as it undergoes a significantly higher shedding than CD44s. Moreover, this shed form interacts with CD44s to prevent HA binding mediating HA/CD44s interactions that are associated with cancer progression (Bartolazzi et al. 1995). Therefore, it may be speculated that the decreased expression of CD44v6-10 in myofibroblasts and increased expression in IL-1β-stimulated fibroblasts have a role in regulating CD44/HA interactions in these mechanisms that contribute to the overall function.

This chapter aimed to identify which CD44 variants are expressed in fibroblasts and determine how stimulation with TGF-β_1 and IL-1β affected the overall expression of each variant. The next aim was to determine which of the CD44 variants are involved in the TGFβ_1-induced HA/CD44/EGFR mechanism and the IL-1β-induced HA/CD44/ICAM-1 pathways.

Chapter 4 -The Role of CD44 Variants in Myofibroblast Differentiation and Inflammatory Cell Interactions

4.1-Introduction

The work described in Chapter 3 profiled the expression pattern of cluster of differentiation 44 (CD44) spliced variants in fibroblasts and demonstrated how the stimulation by the pro-fibrotic cytokine, TGF-β_1, or the pro-inflammatory cytokine, Interleukin-1β (IL-1β), affected variant expression. The overall effect of TGF-β_1 was decreased expression of all variants, whereas in contrast, IL-1β increased the expression of all the variants examined.

Previous research has shown the interaction of HA with CD44 to be central to TGF-β_1-induced fibroblast to myofibroblast differentiation, wherein a re-localisation of membrane-associated CD44, resulted in the co-localisation of CD44 with epidermal growth factor receptor (EGFR) in cholesterol-rich lipid raft regions. The CD44/EGFR association was an essential process for downstream Extracellular regulated kinase 1/2 (ERK1/2) activation and upregulation of hyaluronan synthase 2 (HAS2) and αSMA gene transcription in this pathway. This re-localisation of CD44 was dependent on HA and may also orchestrate the formation of the HA peri-cellular coat that maintains the myofibroblast phenotype (Webber et al. 2009a; 2009c; Midgley et al. 2013). Silencing total CD44 expression was previously shown to inhibit the expression of α smooth muscle actin (αSMA) following TGF-β_1 stimulation (Midgley et al. 2013).

A similar role for HA/CD44 has been described in IL-1β-induced monocyte binding. Fibroblasts stimulated with IL-1β formed HA/CD44-modulated cell membrane protrusions. CD44 and intercellular adhesion molecule-1 (ICAM-1) re-distributed through the cell membrane and co-localised within these protrusions, activating downstream ERK1/2 signalling. Using a siRNA to all CD44 mRNAs, fibroblasts failed to form HA protrusions, they lost CD44/ICAM-1 co-localisation, downstream ERK1/2 activation and monocyte binding (Meran et al. 2013).

Although it has been established that CD44 has a critical role in both TGF-β_1 induction of αSMA and IL-1β-induced monocyte binding, which of the CD44 variants mediates the functional outcomes has not yet been investigated. In the previous chapter, there were CD44 variants identified in fibroblasts that had more abundant levels of expression than others. This suggested that these CD44 variants (CD44s, v3, v8, v6 and v10), may have an important role in the regulation of fibroblast function. These variants have previously been reported to bind HA and regulate important cellular functions, excluding CD44v8, which currently has an unknown role (Bourguignon et al. 1998). The role of the larger variant, CD44v6-10, that was identified will also be investigated as this splice variant was previously described to regulate HA interactions (Bartolazzi et al. 1995).

It is hypothesised that there may be one or more specifically highly expressed CD44 variants that have roles central to myofibroblast differentiation, or the induction of pro-inflammatory fibroblasts.

4.2 – Chapter Aims

The objectives of this chapter are:-

1) To determine which of the CD44 variants previously identified, have roles in the HA/CD44 induction of αSMA upregulation, following TGF-β_1 activation.
2) To investigate which CD44 variants have roles in HA/CD44-dependent monocyte binding, following IL-1β stimulation.

4.3 – Methods

4.3.1. – Custom-designed siRNA

Custom-designed, short interfering ribonucleic acids (siRNA), were designed to target specific CD44 variants. The variants found to have the highest expression in fibroblasts were CD44s, v3, v10, v6 and v8 ***(Table 3.2)***. In order to silence CD44 variants v3, v10 and v8, siRNAs were designed to be situated within variant-specific exons ***(Figure 4.1. [A] (1-3))***. The siRNA to silence CD44v6 was designed to overlap the common region exon 5 with exon 10/v6 ***(Figure 4.1. [B](1))***. The siRNA to CD44s targeted the overlap of the exon boundaries, bridging the two common regions; exon 5 and exon 15 ***(Figure 4.1. [C](1)).***

In the previous chapter, the larger CD44 splice variant, CD44v6-v10, was found to be expressed by fibroblasts. To examine the effect of this variant on TGF-β_1-induced, fibroblast to myofibroblast differentiation and IL-1β- induced monocyte binding, multiple custom siRNA were designed to target distinct regions within CD44v6-10. Firstly, a siRNA to CD44v7/8 was designed. This siRNA overlapped the exon 11 and exon 12 boundary, as shown in ***(Figure 4.1. [B](2))***. Furthermore, the siRNAs that were designed to target CD44v6, v8 and v10, also targeted regions within CD44v6-10 ***(Figure 4.1. [B] (1, 3 & 4))***.

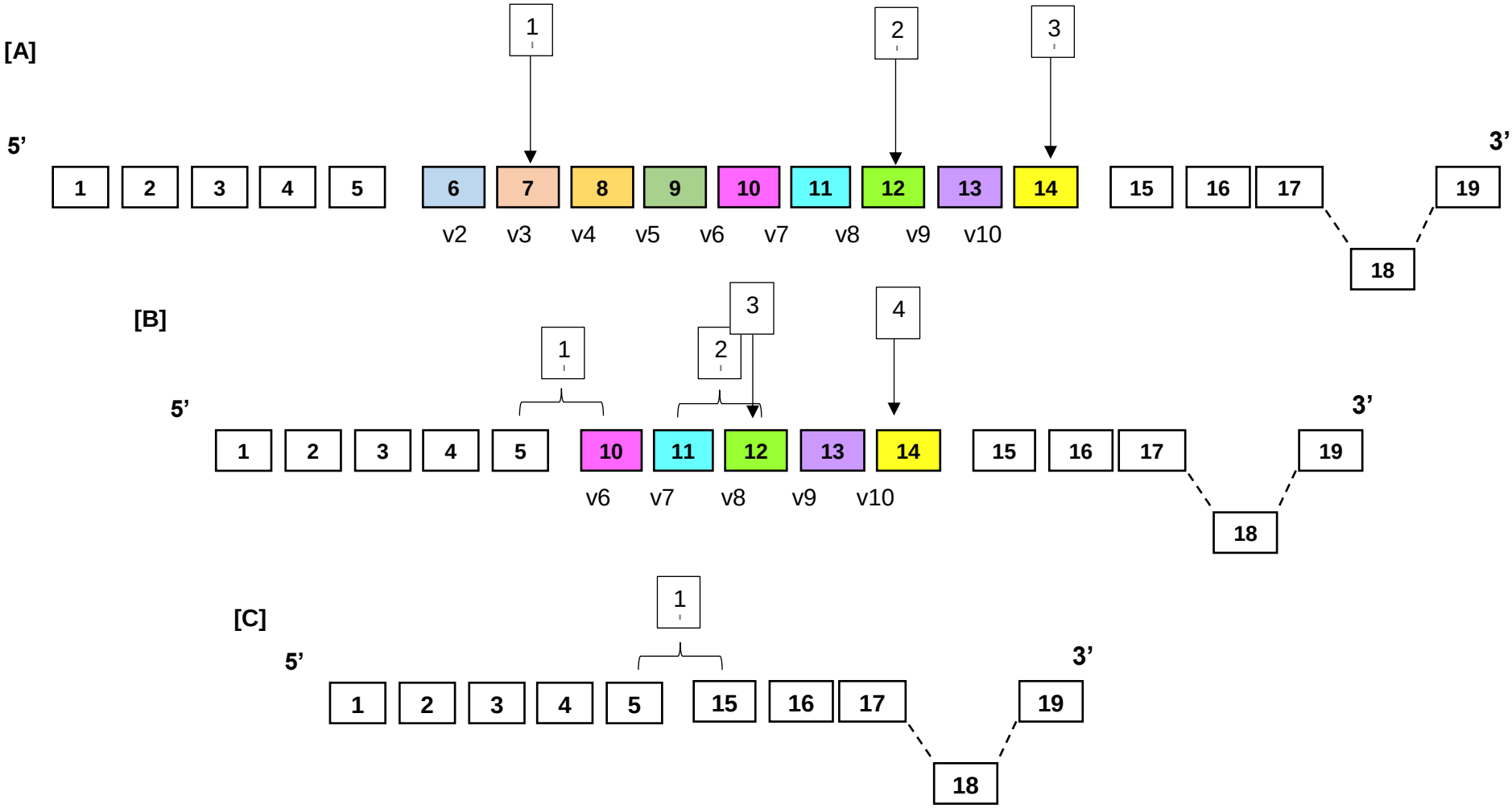

Figure 4.1. – Custom-designed siRNA for CD44v knockdown

Schematic shows target regions of custom-designed siRNA to CD44 variants. ***Figure [A]*** shows the targeted regions of siRNA against **(A1)** CD44 v3, **(A2)** CD44v8; and **(A3)** CD44v10. These primers were designed to target regions within the exons 7, 12 and 14, respectively. To silence the larger variant, CD44v6-10, multiple siRNAs were designed to confirm knockdown ***Figure [B]***.These were a siRNA that overlapped exon 5 within the common region with exon 10/CD44v6 B**(1);** and a siRNA targeted the exon-exon boundaries of exon 11 and 12/ (CD44v7/8)**(B2)**. The siRNA to v8 **(B3)** and v10 **(B4),** also targeted regions in CD44v6-10. The siRNA designed to targeting CD44s targeted overlapped the exon-exon boundary between common region exons; 5&15. **(C1)**.

4.4 – Results

4.4.1 – TGF-β1-Induced Myofibroblast Differentiation

To identify the time-point at which myofibroblast differentiation was complete, fibroblasts were stimulated with TGF-β_1 and αSMA expression was analysed over a time course of 24-72 h, using quantitative polymerase chain reaction (qPCR). ***(Figure 4.2. [A])***, demonstrates the gradual increase of αSMA mRNA expression over 72 h. A significant increase was observed at 72 h. αSMA protein expression was observed at 72 h, using immunocytochemistry (previously described in chapter 2). The change in cell morphology and formation of αSMA stress fibres, a known characteristic of the myofibroblast phenotype was observed and is shown in ***(Figure 4.2. [C]).*** Unstimulated fibroblast controls are shown in ***(Figure 4.2. [B])***, where there is a distinct lack of αSMA and stress fibre formation. These data correspond with previous research in our group that has identified 72 h as a time-point at which myofibroblasts are completely differentiated (Evans et al. 2003b; Webber et al., 2009a). Therefore, all subsequent analysis of myofibroblast induction was performed following 72 h of TGF-β_1 stimulation.

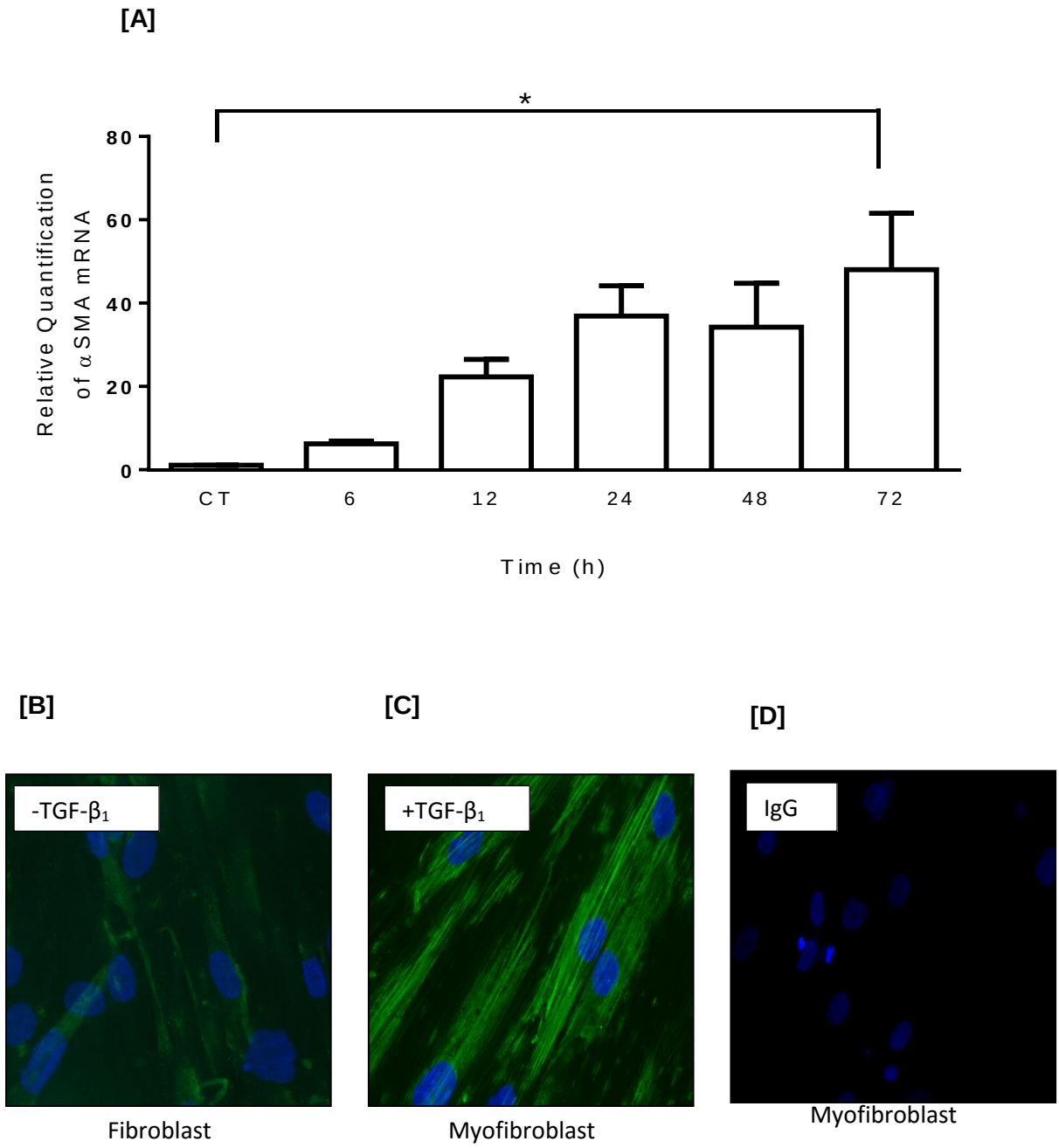

Figure 4.2. – TGF-β1 Induction of α Smooth Muscle Actin.

To determine the time-point of complete differentiation from fibroblast to myofibroblast, the expression of αSMA was analysed over a time course of 72 h, using qPCR ***[A]***. Fibroblasts were grown to 80% confluence, before growth arrest. Cells were treated with TGF-β1 (10ng/ml) or serum-free medium alone (control samples). Data represents the mean of 3 separate experiments ± SEM. Statistical analysis used the one way ANOVA, followed by the Student's unpaired *t*-test. Immunocytochemistry was used to visualise αSMA protein and stress fibre formation, following 72 h of TGF-β1 (10ng/ml) stimulation. Cells were grown to 50% confluence before growth arrest in serum-free medium. Cells were then treated with TGF-β1 (10ng/ml) or with fresh medium for controls for 72 h. Cells were then fixed before being analysed using immunocytochemistry. ***Figure [B]*** is representative of control fibroblast populations that lack αSMA and stress fibres***. Figure [C]*** is representative of TGF-β1 stimulated myofibroblasts. An IgG control was used to show antibody specificity ***Figure [D].*** Samples were visualised using a Lecia Dialux 20 Fluorescent Microscope. Original magnification X 400.

4.4.2. – IL-1β-Induced Monocyte Binding

The ability of fibroblasts to bind monocytes following IL-1β has previously been shown in our laboratory, in a CD44-dependent manner (Meran et al. 2013). In order to assess the role of CD44 variant expression on IL-1β-stimulated monocyte binding, it was necessary to identify a highly sensitive assay for monocyte binding. CD45 is a specific marker of leukocytes. ***Figure 4.2 [A]*** shows qPCR analysis of CD45 expression in unstimulated and IL-1β-stimulated fibroblasts, compared to the expression of CD45 by U937 ($1x10^6$ cells /ml). There was limited detectable expression of CD45 in unstimulated fibroblasts or fibroblasts treated with IL-1β, compared to U937 cells. Therefore, all further experiments assessing monocyte binding were analysed using CD45 as a marker of monocyte numbers.

To identify an optimum time-point for monocyte binding, following growth arrest, fibroblasts were stimulated with IL-1β or serum-free medium alone (control samples), over a 72 h time course. At each of the indicated time-points between 24 and 72 h, U397 cells ($1x10^6$ cells/ml) were added to IL-1β-stimulated and unstimulated (control) fibroblast cultures and incubated for 4 h. Unattached monocytes were removed by washing with PBS; and remaining cells were assessed for mRNA expression using qPCR. ***(Figure 4.3.[B])*** shows a significant increase in monocyte binding, compared to control fibroblasts, with an optimum time of 72 h which was the time point used for all subsequent experiments.

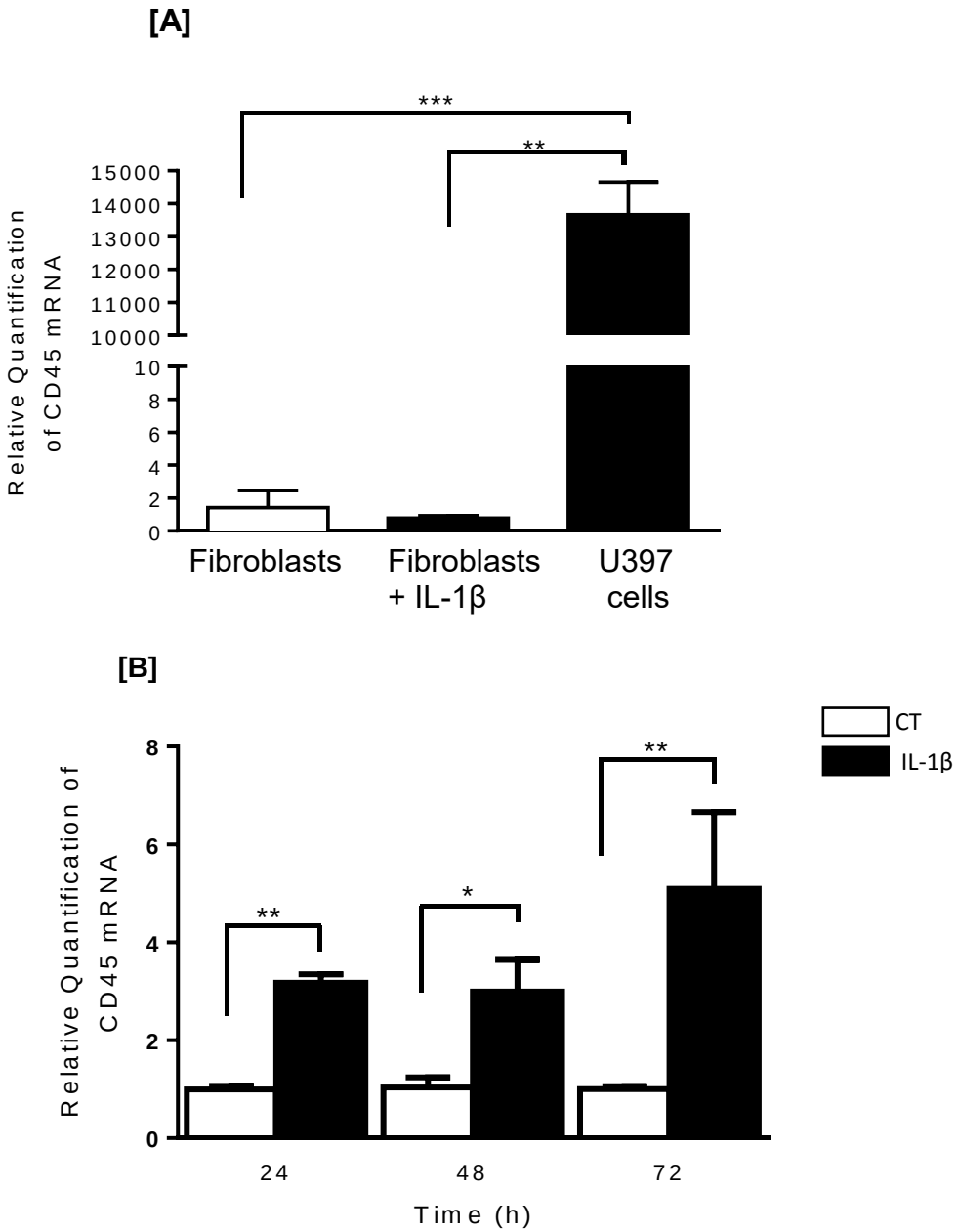

Figure 4.3. – IL-1β Induction of Monocyte Binding

Data ***[A]*** shows the expression of CD45 in 1 µg of total cell cDNA in unstimulated and IL-1β-stimulated fibroblasts, compared to U397 positive control cells. Fibroblasts were grown to 80% confluence and growth-arrested. Cells were incubated in serum-free medium alone (controls) or serum-free medium containing IL-1β (1ng/ml), for a further 72 h. As a positive control, U397 cells ($1x10^6$ cells/ml) were also included. CD45 expression was analysed using qPCR. Figure **[B]** shows the assessment of monocyte–binding over 72 h. Fibroblasts were grown to 80% confluence, prior to growth arrest. Cultures were then treated with serum-free medium alone or serum-free medium containing IL-1β (1ng/ml). At each time point, U397 cells ($1x10^6$cells/ml) were added to the control fibroblasts ***(white bars)*** and IL-1β-stimulated fibroblasts ***(black bars)*** and incubated for 4 h. Unbound monocytes were washed using PBS. CD45 was analysed using qPCR. Statistical analysis was carried out using the ANOVA followed by the Student's unpaired *t*-test. Results are displayed as the mean of three individual experiments ± SEM. *P<0.05, **P<0.01, ***P<0.001.

4.4.3. -CD44 Variant Involvement in αSMA Expression and Monocyte Binding

Using a siRNA that targeted global CD44 expression in fibroblasts, our laboratory has previously shown that CD44 is required for both TGF-β_1-induced fibroblast to myofibroblast differentiation and IL-1β-induced fibroblast to monocyte binding (Webber et al. 2009b; Meran et al. 2013; Midgley et al. 2013). However, it is not understood which of the CD44 variants are involved in these processes.

The efficiency of knockdown by each custom-designed siRNA (***Figure 4.1)*** was assessed (see; ***Figure 4.4. [A&B]***, ***Figure 4.5. [A&B]***, ***Figure 4.6. [A-C]*** and ***Figure 4.7. [A-C]***). All control fibroblasts transfected with the custom-designed siRNA to CD44 had a decreased expression of CD44 targets, when compared to fibroblasts transfected with the negative scrambled control ***(Figure 4.4. [A&B])*** and ***(Figure 4.6. [A-C])***. IL-1β-stimulated fibroblasts, transfected with the custom designed siRNA to CD44, also had knockdown of targeted CD44 variants ***(Figure 4.5. [A&B])*** and ***(Figure 4.7. [A-C])***.

Following knockdown of CD44v3 and v8, αSMA expression and monocyte binding were assessed ***(Figure 4.4[C-D])*** and ***(Figure 4.5[C-D])***. These CD44 variants were both highly expressed in quiescent fibroblasts **(Table 3.2**). It was, therefore, important to investigate the effects of silencing them on both pathways. TGF-β_1 induction of αSMA expression was not affected in samples transfected with siRNA to CD44v3 ***(Figure 4.4 [C])*** or CD44v8 ***[D]),*** when compared to samples transfected with the scrambled siRNA. Fibroblasts stimulated with IL-1β showed no significant difference in monocyte binding between samples transfected with siRNA to CD44v3 ***(Figure 4.5 [C])***, when compared to fibroblasts transfected with scrambled siRNA control. Interestingly, unstimulated control fibroblasts transfected with a siRNA to CD44v8 had a significant increase in monocyte binding, compared to scrambled

controls ***Figure 4.5. [D].*** These data suggest that the fibroblast expression of CD44v8 may have a regulatory role in monocyte binding.

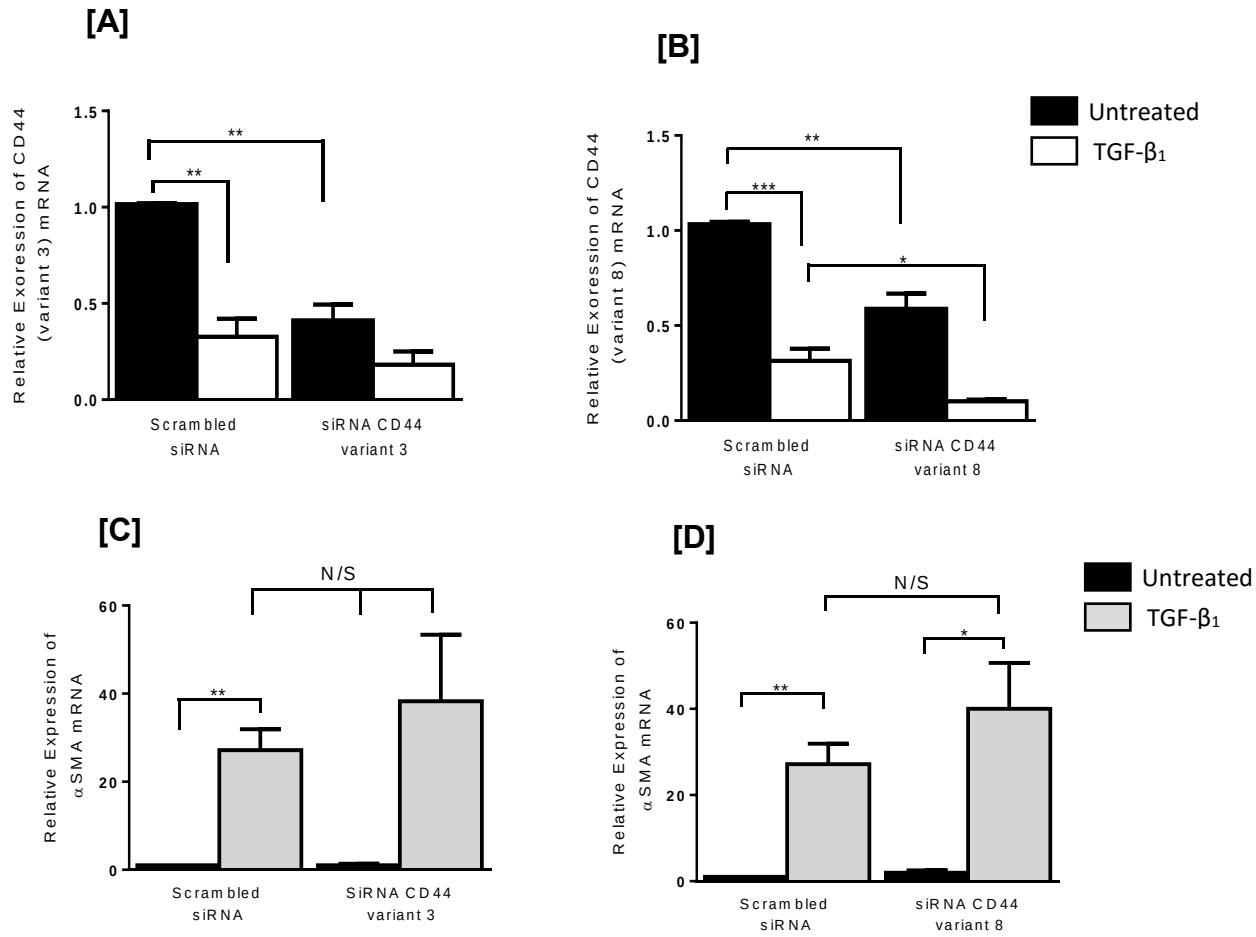

Figure 4.4 – Transfection with siRNA to CD44v3 and v8 had no Effect on αSmooth Muscle Actin Induction in Myofibroblasts.

To investigate the effect of silencing CD44v3 and v8 on αSMA induction in myofibroblasts, fibroblasts were grown to 50-60% confluence. Cells were transfected with either a siRNA to CD44v3, CD44v8 or a negative scrambled siRNA (control samples). Following a growth arrest period, cells were treated with TGF-β_1 (10ng/ml) or serum-free medium alone (control samples) for 72 h. Data ***[A]*** and ***[B]*** show the knockdown of CD44v3 and CD44v8, respectively, at the experimental end-point. Unstimulated control cells ***(black bars)*** were compared to TGF-β_1 (10ng/ml) stimulated cells ***(white bars*)*.** The knockdown of each variant was compared to a negative scrambled control. The expression of αSMA after significant knockdown of CD44v3 and v8 are shown in graphs ***[C]*** and ***[D]***. Data shows the αSMA expression of control unstimulated fibroblasts ***(black* bars)*** against TGF-β_1 (10ng/ml) stimulated cells ***(grey bars)***. Data is displayed as the mean of three separate experiments ± SEM. Statistical analysis was performed using the one way ANOVA, followed by the unpaired Student's *t*-test. N/S= not significant, *P <0.05, **P<0.01, ***P<0.001.

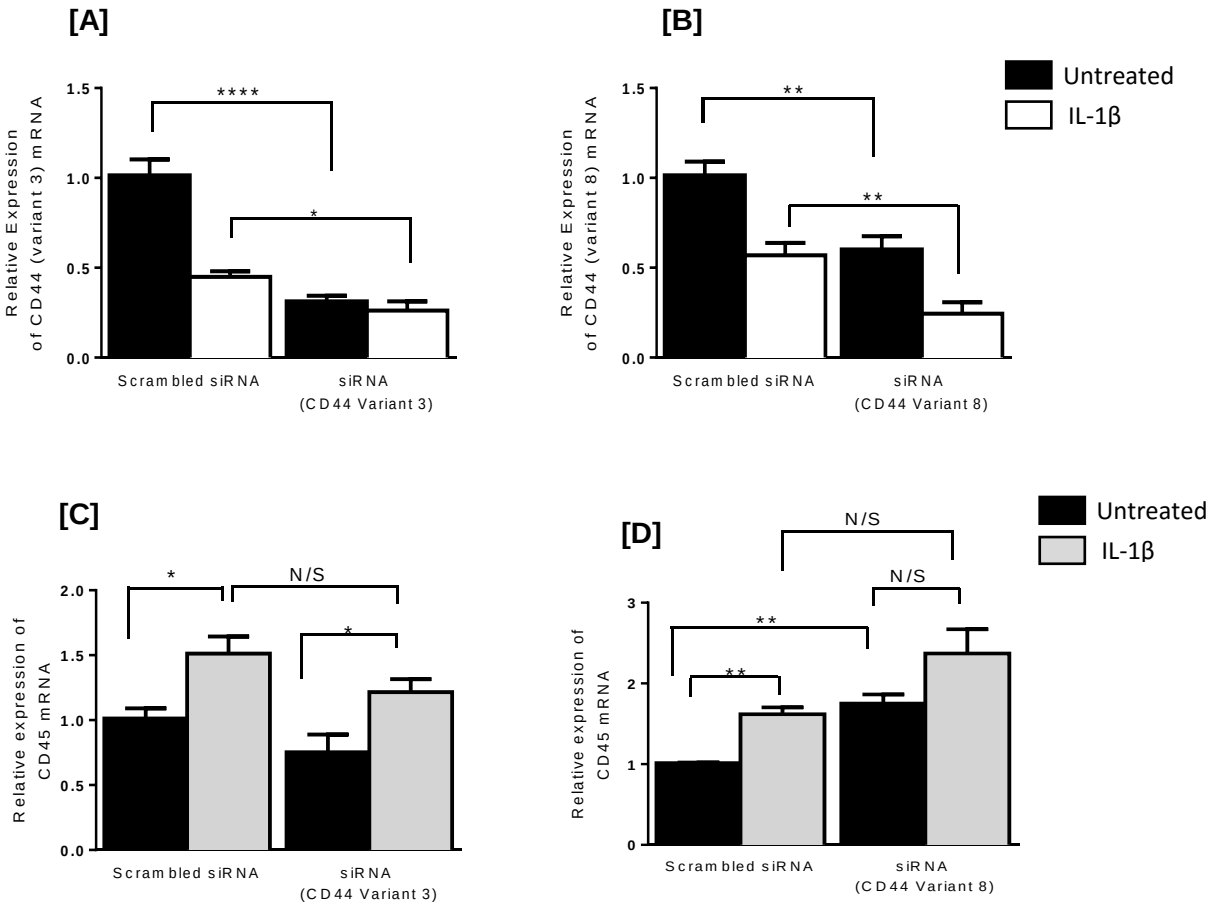

Figure 4.5 – Transfection with siRNA to CD44v3 had no Effect on Monocyte Binding, Although, siRNA to CD44v8 Increased Monocyte Binding in Control Fibroblasts

To investigate the effect of silencing CD44v3 and v8 on IL-1β induction of monocyte binding, fibroblasts were sub-cultured in 6-well plates, until 50-60% confluence. Cells were transfected with either a siRNA to CD44v3, CD44v8 or a negative scrambled siRNA control. Following growth arrest, cells were treated with IL-1β (1ng/ml) or serum-free medium alone (control samples) for 72 h. Data ***[A]*** and ***[B]*** show the knockdown of CD44v3 and CD44v8, respectively, at the experimental end-point. Unstimulated control cells ***(black bars)*** were compared to IL-1β (1ng/ml) stimulated cells ***(white bars*)*.** The knockdown of each variant was compared to a negative scrambled control. The expression of CD45 after significant knockdown of CD44v3 and v8 are shown in graphs ***[C]*** and ***[D]***. Data shows the CD45 expression of control unstimulated fibroblasts ***(black* bars)** against IL-1β (1ng/ml)-stimulated, cells ***(grey bars)***. Data is displayed as the mean of three separate experiments ± SEM. Statistical analysis was performed using the one way ANOVA followed by the unpaired Student's *t*-test. N/S = not significant, *P<0.05, **P<0.01, ***P<0.001, ****P<0.0001.

Previously in Chapter 2, it was determined that CD44v6 and v10 were highly expressed in quiescent fibroblasts. The larger CD44 variant (CD44v6-10) contains the exons that encode smaller variants: CD44 v6, v8 and v10. The siRNA used to target CD44v6, v8 or v10 also silence the mRNA expression of CD44v6-10; ***(***see ***Figure 4.1.)***. However, using siRNAs that are designed to target CD44v6, v8 or v10 gives two possible outcomes to the results:

1) The result is due to siRNAs targeting the single variants CD44v6, v8 and v10.
2) Any observed results are from the siRNA targeting the larger CD44v6-10.

To clarify involvement, a further siRNA was designed to target the exon-exon boundaries of exons 11/12 (also known as CD44v7-8), that would only effect the expression of the larger variant and not CD44v6, v8 or v10.

Following successful knockdown of CD44v6, v7/8 and v10, the effect of silencing these variants on myofibroblast differentiation and monocyte binding were analysed. Preliminary data comparing myofibroblasts transfected with the scrambled siRNA to samples transfected with siRNA to CD44v6 and v10, showed no difference in αSMA expression ***(Figure 4.6. [D&F])***. This indicated that these two variants did not appear to have a role in regulating αSMA. Furthermore, these data suggest that the larger spliced variant CD44v6-10 also has no role in TGF-β_1-induced αSMA, due to collateral knockdown. To confirm this, the effect of siRNAv7/8 on αSMA expression was assessed ***(Figure 4.6[B])***. Comparing cells transfected with siCD44v7/8 to those transfected with the scrambled control, indicated that there was no effect on induction of αSMA. Therefore, this combined preliminary data along with the data from siRNA CD44v8 analysis, where no effect on induction of αSMA was also seen, suggests that CD44v6-10 does not play a role in TGF-β_1 upregulation of αSMA.

Figure 4.7 [A-B] shows the preliminary analysis of siRNA to CD44v6 and v10 and the effects on monocyte binding. Knockdown ***(Figures 4.7. [D])*** CD44v6 and ***(Figure 4.7. [F])***

CD44v10 suggest that these variants, do not have a role in CD44-dependent, monocyte binding. Similarly, these data suggest that the larger variant, CD44v6-v10, also has no role in monocyte binding. Conformational experiments using siRNA against CD44v7/8 ***(Figure 4.7. [E])*** showed there was no difference in CD45 expression, following silencing of CD44v7/8. This preliminary data is in line with the observations made when fibroblasts were transfected with siRNA to v6, v8 and v10. Therefore, using the analysis of these combined data, it may be assumed that the larger CD44v6-10 has no role in CD44-dependent, fibroblast-monocyte binding.

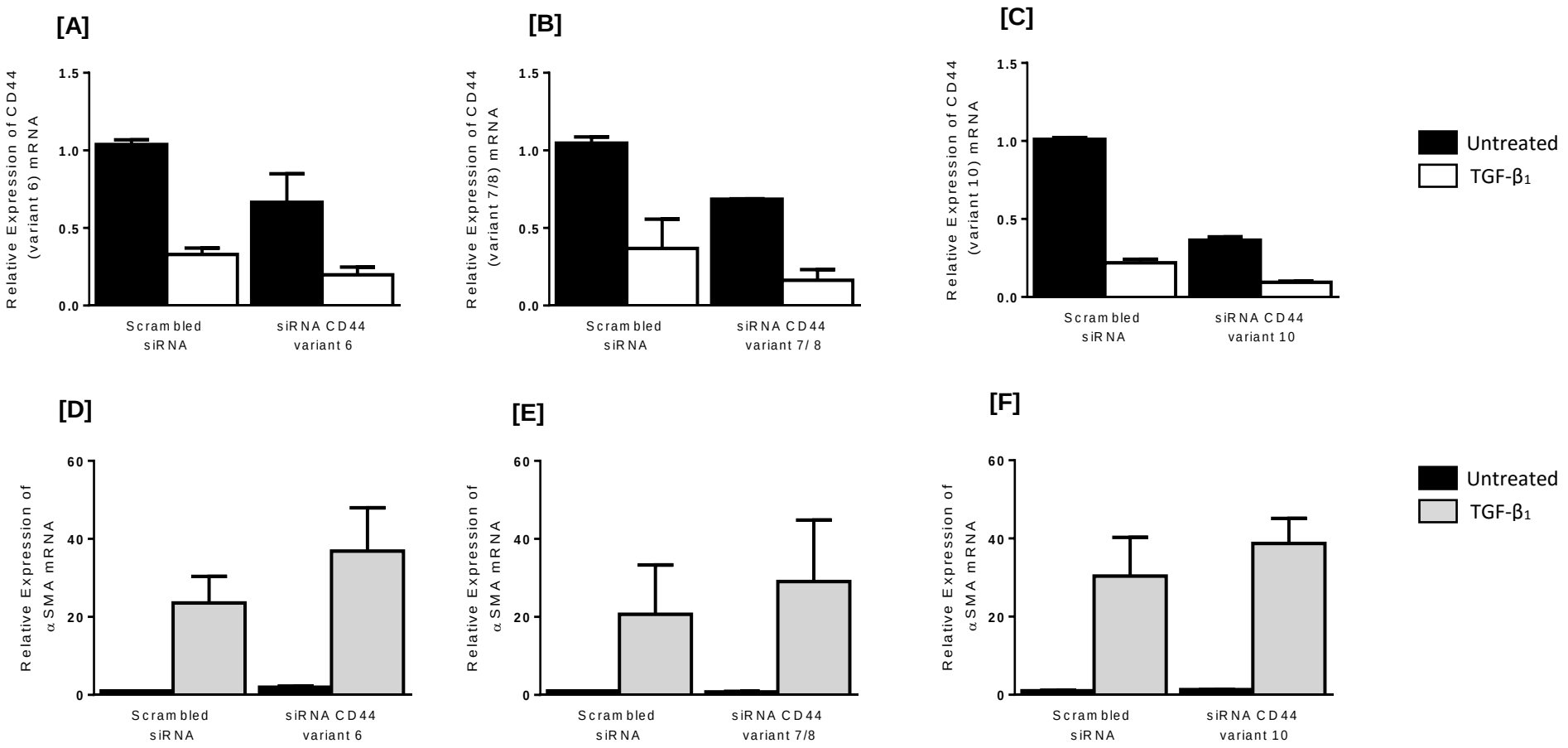

Figure 4.6. – CD44v6, v7/8 and v10 Knockdown Had no Effect on αSmooth Muscle Actin.

Custom-designed siRNA to CD44v6, v7/8 and v10, were used to analyse the effects of silencing CD44v on TGF-β_1- induced αSMA. A negative scrambled siRNA was used in control samples to ensure siRNA specificity. Following growth arrest, cells were treated with TGF-β_1 (10ng/ml) or serum-free medium alone (control samples) for 72 h. mRNA expression was analysed using qPCR. Data **[A-C]** show the knockdown of CD44v6, v7/8 and v10, respectively. TGF-β_1-stimulated cells (white bars) and control cells (black bars). The expression of αSMA after siRNA CD44v6, 7/8 and v10 are shown in graphs **[D-F]**, control unstimulated fibroblasts (black bars) against TGF-β_1 (10ng/ml)-stimulated cells (grey bars). Data is representative of two separate experiments ± S.D.

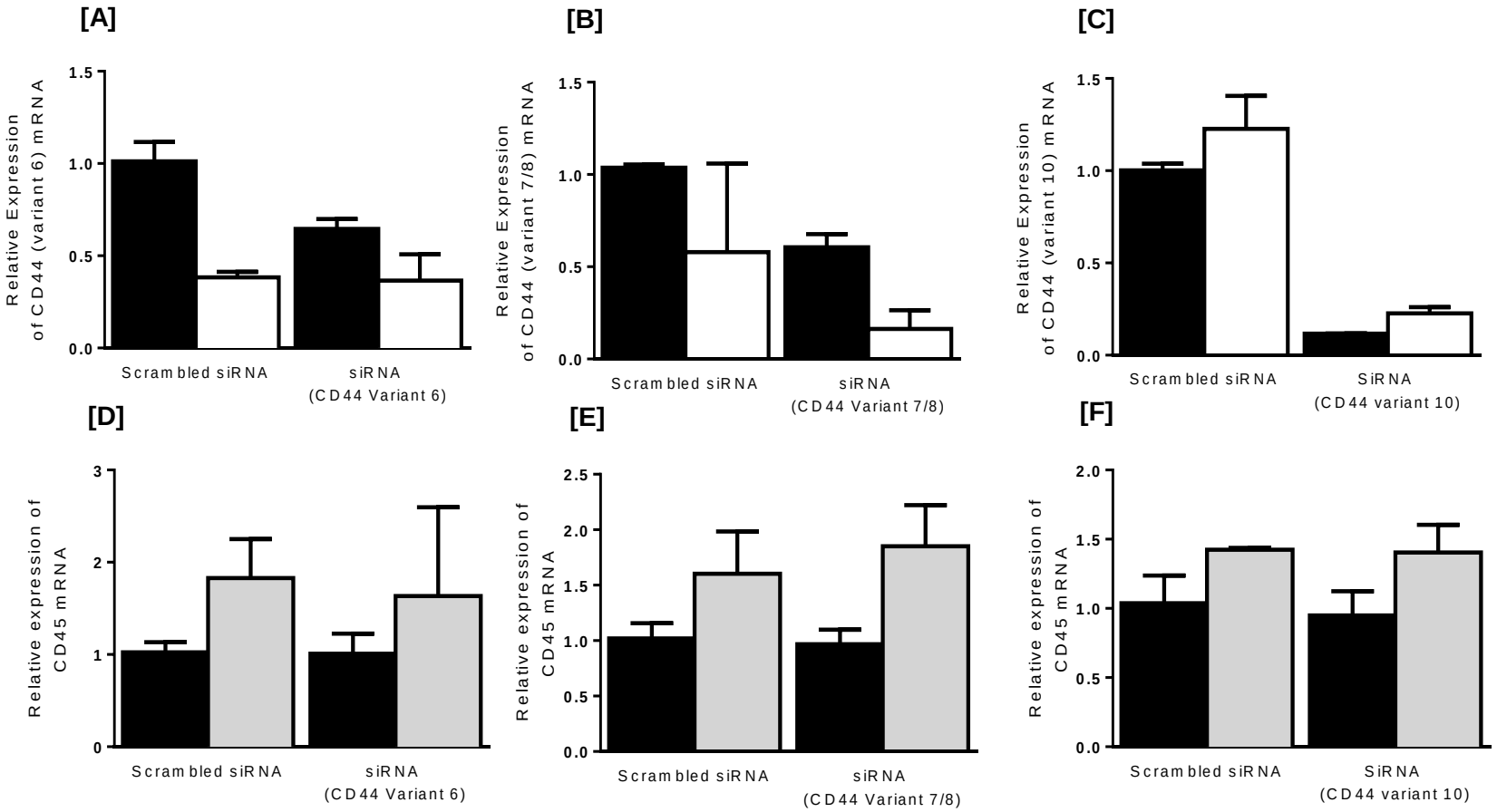

Figure 4.7. – CD44v6, v7/8 and v10 Knockdown Had no Effect on Monocyte Binding.

Custom designed siRNA to CD44v6, v7/8 and v10 were used to analyse the effects of silencing CD44v on IL-1β-induced monocyte binding. A negative scrambled siRNA was used in control samples. Following growth arrest, cells were treated with IL-1β (1ng/ml) or serum-free medium (control samples) for 72 h. Total RNA was extracted and samples were reverse transcribed before analysis by qPCR, as described in chapter 2. Data **[A-C]** show the knockdown of CD44v6, v7/8 and v10, respectively, IL-1β stimulated cells (white bars) and control cells (black bars). The expression of CD45 (the monocyte marker) after siRNA CD44v6, 7/8 and v10, are shown in graphs **[D-F]**. Data shows the CD45 expression of control unstimulated fibroblasts (black bars) against IL-1β (1ng/ml) stimulated cells (grey bars). Data is representative of ±S.D. of two separate experiments.

4.4.4. - Standard CD44 (CD44s) Decreases αSMA Expression in Myofibroblasts and Reduces Fibroblasts Ability to Bind Monocytes

The standard form of CD44, was the highest expressed of all the CD44 variants identified (***Table 3.2)***. Therefore, the effect of siRNA targeting CD44s on αSMA induction and IL-1β-induced monocyte binding was investigated. The mRNA expression of αSMA was assessed in myofibroblasts that had been transfected with a siRNA to CD44s ***(Figure 4.8.)***. There was a significant decrease in αSMA expression in TGF-β_1–stimulated fibroblasts transfected with siRNA against CD44s, compared to TGF-β_1-stimulated fibroblasts that had been transfected with the scrambled siRNA ***(Figure 4.8 [B])***.

The monocyte binding capacity of fibroblasts, following transfection with siRNA to CD44s, was subsequently assessed. Fibroblast cultures that were transfected with scrambled siRNA had an increase in monocyte binding when stimulated with IL-1β, as expected ***(Figure 4.9 [B])***. Transfection of fibroblasts with a siRNA targeting CD44s significantly decreased monocyte binding, compared to fibroblasts transfected with a scrambled siRNA ***(Figure 4.9. [B])***. Together, these results suggest that the standard form of CD44 is the predominant CD44 receptor involved in both IL-1β-induced monocyte binding and TGF-β_1-induced myofibroblast differentiation.

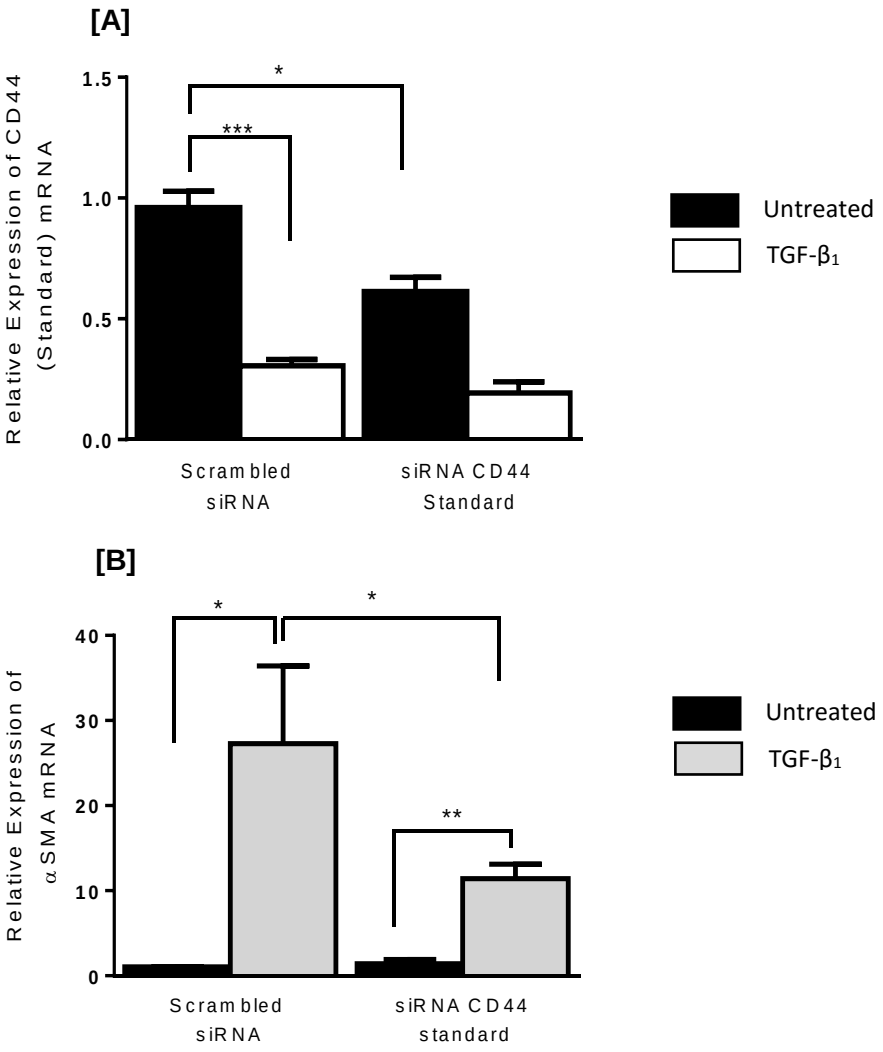

Figure 4.8. – CD44s Knockdown Decreases α Smooth Muscle Actin mRNA Induction by TGF-β_1

Fibroblasts were cultured in 6-well culture plates, to 50-60% confluence. Cells were growth-arrested for 24 h, before transfection with a siRNA to CD44s. To ensure siRNA specificity, control cells were transfected with a negative scrambled siRNA. Cells were growth-arrested for a further 48 h, before being treated with TGF-β_1 (10ng/ml) or serum-free medium alone for 72 h. ***Figure [A]*** demonstrates the knockdown of CD44s in cells stimulated with TGF-β_1 ***(white bars)*** or untreated cells ***(black bars)***). ***Figure [B]*** shows the expression of αSMA in control samples ***(black bars)*** and TGF-β_1-stimulated samples ***(grey bars)***, following transfection with a siRNA to CD44s or a negative scrambled control. Data is displayed as the mean of three separate experiments ± SEM. Statistical analysis was performed using the one way ANOVA followed by unpaired Students *t*-test. Data was deemed *P=<0.05, P***=<0.001.

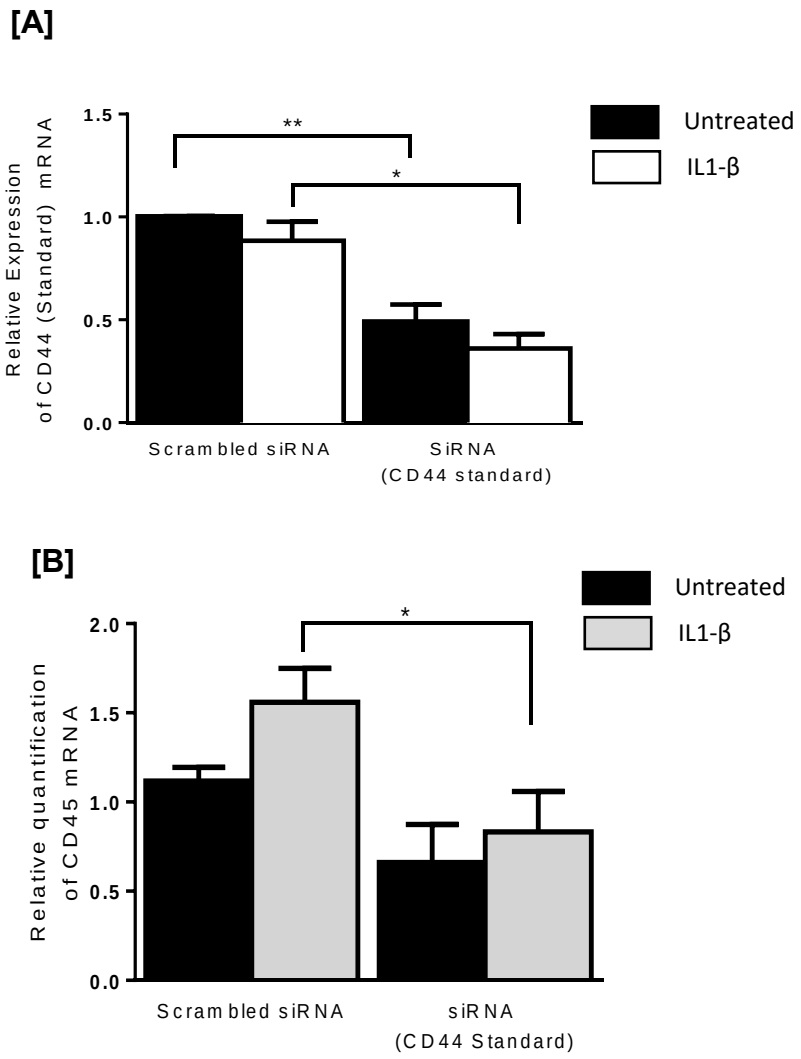

Figure 4.9. – CD44s Knockdown Decreases Fibroblasts- Induced, Monocyte Binding by IL-1β

Fibroblasts were sub-cultured in 6-well plates, until 50-60% confluence. Cells were growth-arrested for 24 h, before transfection with a siRNA to CD44s. To ensure siRNA specificity control cells were transfected with a negative scrambled siRNA. Cells were growth-arrested for a further 48 h before, being treated with IL-1β (1ng/ml) or serum-free medium alone (control samples) for 72 h. Two sample sets were run side by side, the first was used to assess sufficient silencing of CD44s ***Figure [A]*** demonstrates a CD44 siRNA knockdown IL-1β ***(white bars)***; untreated controls ***(black bars)*** as analysed by qPCR***. Figure [B]*** shows the expression of CD45 following a incubation of fibroblasts with monocytes. Data shows unstimulated fibroblasts ***(black bars)*** and IL-1β-stimulated samples ***(grey bars)***. Data is displayed as the mean of three separate experiments ± SEM. Statistical analysis was performed one way ANOVA, followed by unpaired Students *t*-test. *P<0.05, **P0.01.

4.4.5. - CD44s Mediates αSMA Stress Fibres Formation in TGF-β$_1$ - Treated Fibroblasts

Following 72 h stimulation, TGF-β$_1$ induced the expression of αSMA stress fibres in myofibroblasts (***Figure 4.2. [C])***. This supports previous research undertaken in our laboratory (Webber et al. 2009b). To investigate the role CD44s plays in the formation of αSMA stress fibres, cells were transfected with siRNA to CD44s and visualised for αSMA stress fibres using ICC. Observations of untreated control fibroblasts transfected with either a negative scrambled siRNA or a siRNA to CD44, had limited αSMA and no stress fibre formation ***(Figure 4.10 [A&B])***. This was to be expected, as αSMA is known to not be highly expressed in resting fibroblasts (Clayton et al. 1997). ***(Figure 4.10 [C&D])*** shows the effect of the siRNA targeting CD44s, compared to the siRNA scrambled controls, following 72 h of stimulation with TGF-β$_1$. Fibroblasts transfected with the scrambled siRNA had the distinct stress fibre formation typical of differentiation to the myofibroblast phenotype ***(Figure 4.10 [C])***. However, in cells transfected with siRNA to CD44s, the majority of cells visualised maintained the fibroblast phenotype and had limited stress fibre formation ***(Figure 4.10. [D])***. These data correspond with previously observed data in this chapter and confirm the reduced mRNA expression data shown above. Together, these data imply that CD44s has a significant role in the regulation of αSMA stress fibre formation in myofibroblasts.

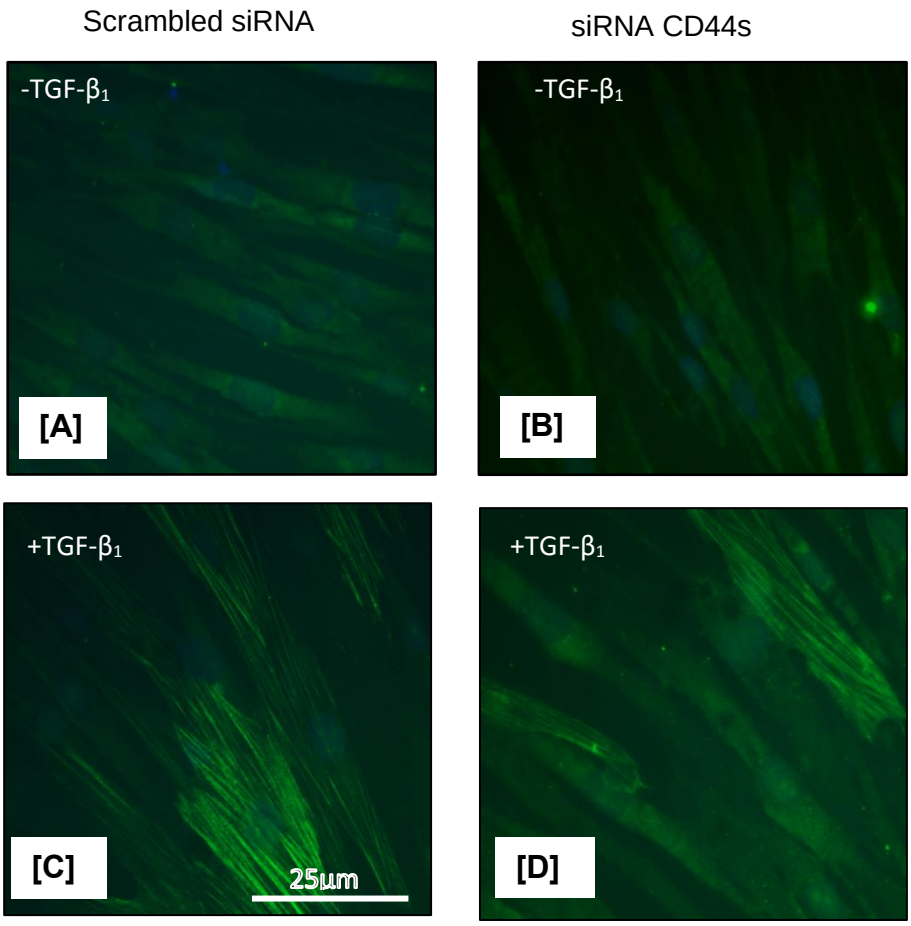

Figure 4.9 Silencing CD44s Prevents Stress Fibre Formation in Myofibroblasts

To assess the role of CD44s in the formation of αSMA stress fibres, fibroblasts were grown to 50% confluence in chamber slide wells. Cells were then transfected with siRNA to CD44s or a siRNA negative scrambled control. Following a growth arrest period of 48 h cells were treated with serum-free medium (controls) or serum free medium containing TGF- β_1 (10ng/ml). Cell cultures were then analysed using ICC. Cells were visualised for αSMA stress fibres by a florescent microscopy. A representative picture was taken of each cell populations under each condition. ***[A&C]*** are cells transfected with scrambled siRNA. Picture ***[A]*** represents unstimulated fibroblasts ***[C]*** represents TGF-β_1 pictures ***[B&D]*** represents cells transfected with siRNA to CD44s, unstimulated fibroblasts ***[B]*** and TGF-β_1 stimulated ***[D].*** Original magnification x 400.

4.4.6. - Silencing CD44s Has No Effect on Other CD44 Spliced Variant Expression.

It has previously been documented that increased proteolytic cleavage of CD44 at the ectodomain and within the intracellular domain, results in increased cellular migration and pro-oncogenic activity (Okamoto et al. 2001). Whilst cleavage at the ecdodomain results in the shedding of CD44 and the formation of soluble CD44, cleavage of the intracellular domain results in the release of intracellular domain fragment (ICD), which can translocate to the nucleus and regulates gene transcription. It has been suggested that ICD translocation upregulates CD44 transcripts as a positive feedback loop (Nagano and Saya 2004). Furthermore, CD44s has been shown to associate with other CD44 variants, changing their interactions and thereby indirectly altering cellular function (Iida and Bourguignon 1997). It was, therefore, important to assess the possibility that CD44s regulates other CD44 spliced variants. Furthermore, the siRNA that targeted CD44s potentially could target other variants. Therefore, there were two main aims to this investigation:-

1. To determine if CD44s resulted in a change of other CD44 variant expression levels.
2. To validate the specificity of the custom designed siRNA targeting CD44s and eliminate the possibility of unwanted targeting of other variants.

Figure 4.11. [A-E] and **Figure 4.12** ***[A-E]*** show the effect of siRNA CD44s on the mRNA expression of the other CD44 variants. This data shows the expression of CD44v3 ***[A]***, v6 ***[B]***, v7/8 ***[C]***, v8 ***[D]*** and v10 ***[E],*** following knockdown of CD44s, compared to scrambled control. The effect of TGF-β_1 and IL-1β stimulation was also analysed. Silencing CD44s had no effect on the expression of any of the CD44 variants under investigation, compared to the scrambled controls. Furthermore, the expression patterns observed were similar to those observed in chapter 3. This preliminary data indicated that silencing CD44s did not affect transcription of

the other CD44 variants or altered their expression following TGF-β_1 or IL-1β stimulation. Furthermore, this data demonstrated the specificity of the siRNA designed to target CD44s.

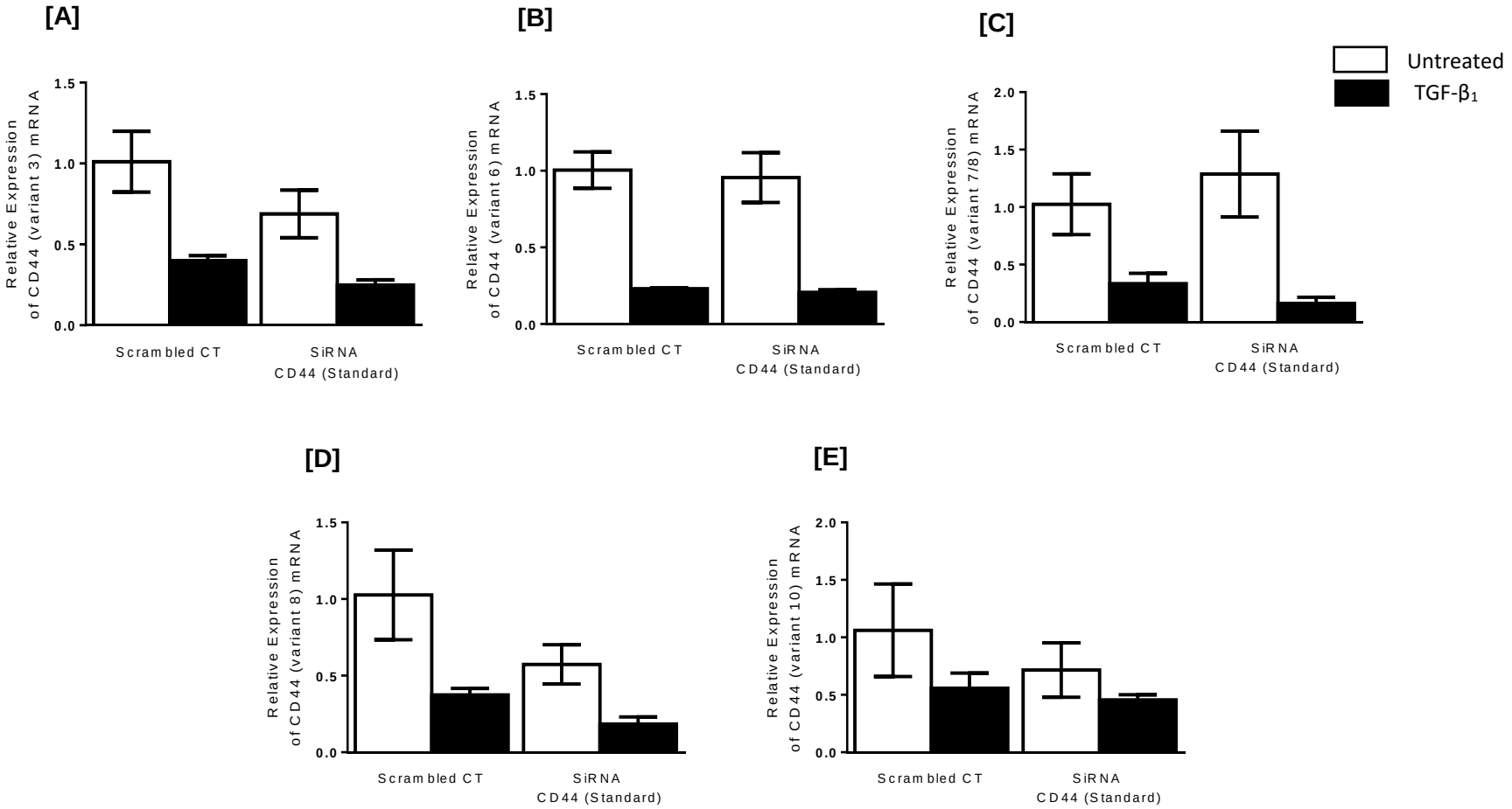

Figure 4.11 – Silencing CD44s had no Effect on other CD44 Spliced Variants in Fibroblasts or Myofibroblasts

To assess the effects of silencing CD44s on CD44 spliced variant transcription, fibroblasts were grown to 50-60% confluence. Cells were transfected with either a scrambled control siRNA (Scrambled CT) or siRNA targeting CD44s (siRNA CD44 standard). Following growth arrest cells were treated with TGF-β_1 (10ng/ml) or serum free medium alone (control fibroblasts). The mRNA expression of CD44v3 ***[A]***, v6 ***[B]***, v7/8 ***[C]***, v8***[D]*** and v10 ***[E]*** in fibroblasts ***(white bars)*** and TGF-β. treated fibroblasts ***(black bars)***, following siRNA to CD44s. Data is representative of one experiment (sample N=3) and data is displayed as ±S.D.

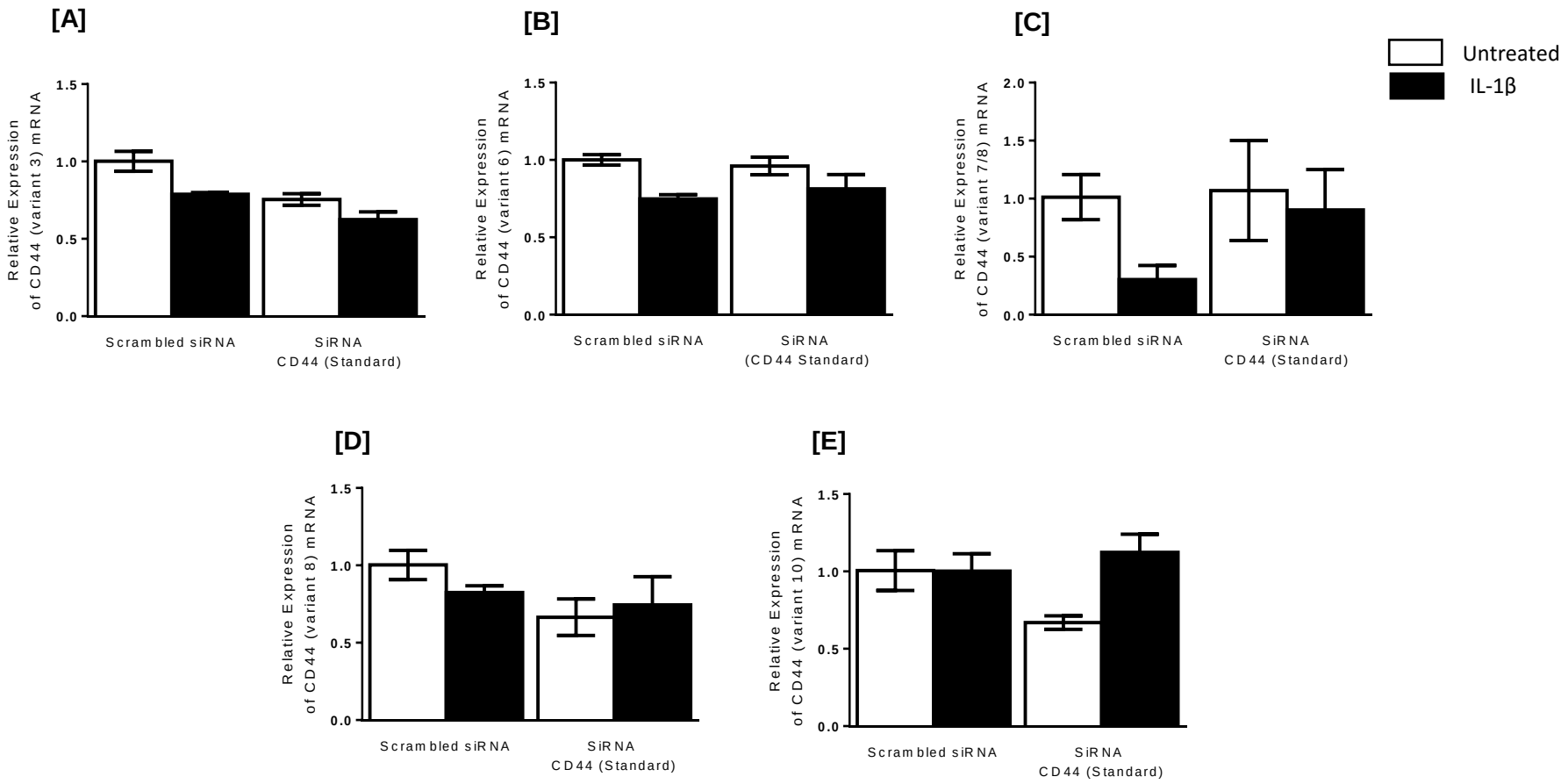

Figure 4.12 – Silencing CD44s Had no Effect on Other CD44 Spliced Variants Expression in Control Fibroblasts or IL-1β-Stimulated Fibroblasts

To assess the effects of CD44s on the ability of CD44 spliced variant transcription, fibroblasts were grown until 50-60% confluence. Cells were transfected with either a scrambled negative control (scrambled CT) or siRNA targeting CD44s (siRNA CD44 standard). Following growth arrest, cells were treated with IL-1β (1ng/ml) or serum-free medium alone (control fibroblasts). Figures show the mRNA expression of CD44v3 ***[A]***, v6 ***[B]***, v7/8 ***[C]***, v8***[D]*** and v10 ***[E]*** by fibroblasts ***(white bars)*** and IL-1β-induced fibroblasts ***(black bars),*** following transfection with siRNA to CD44s samples were analysed using qPCR. Samples transfected with siRNA to CD44s were compared to samples transfected with a negative scrambled control. Data is representative of one experiment with a sample N=3. Data is displayed as ±S.D.

4.5. – Discussion

In the previous chapter, the effects of TGF-β_1 and IL-1β stimulation on the expression of CD44 variants were investigated. This chapter aimed to investigate which of the CD44 variants were involved in the TGF-β_1-induced, HA/CD44 dependent upregulation of αSMA in myofibroblasts and the IL-1β-induced, HA/CD44 dependent monocyte binding. Using a process of elimination, the CD44 variants with the highest expression were silenced using a panel of custom-designed siRNAs ***(Figure 4.3.)*** The results show that the standard form of CD44 (CD44s) is essential for the upregulation of αSMA and the maintenance of the myofibroblast phenotype. Furthermore, CD44s was also found to be the principal mediator for fibroblast-monocyte binding, following IL-1β induction.

The important role of CD44 in fibrosis has been demonstrated in previous research (Rouschop et al. 2004). Mice deficient in CD44 (*Cd44*$^{-/-}$) underwent unilateral ureter obstruction (UUO), resulting in a marked decrease in collagen and αSMA expression. This was suggested to be the result of a downregulation of TGF-β_1 and a decreased myofibroblast presence. The mechanism of fibroblast to myofibroblast differentiation is well-defined and the role of CD44 in this process is also well understood. TGF-β_1 stimulation activates the re-localisation of CD44 in the cell membrane, resulting in CD44 clusters within cholesterol-rich lipid rafts. In these lipid raft regions, CD44 associates with EGFR and results in downstream activation of extracellular signalling receptor kinase 1/2 (ERK1/2) and calmodulin kinase II (CaMKII) (Midgley et al. 2013). In turn, HAS2 and αSMA expression is upregulated and both are also fundamental to the myofibroblast phenotype. The movement of CD44 is modulated by hyaluronan (HA) and is essential for HA-rich, peri-cellular coat formation and for maintenance of the myofibroblast phenotype.

The presence of immune cells within the pro-fibrotic environment is central to the initiation of fibrotic progression, due to a constant release of cytokines into the immediate region. This leads to a continuous influx of fibrotic mediators and an aberrant wound healing response. Stimulation of fibroblasts with the pro-inflammatory cytokine, IL-1β, mediates a change in the cell membrane, which forms protrusions. HA mediates the movement of CD44 into these protrusions, where CD44 co-localises with ICAM-1. This HA/CD44/ICAM-1 complex activates intracellular signalling ERK1/2 (Meran et al. 2013). Silencing total CD44 expression in IL-1β-stimulated fibroblasts decreased their ability to bind monocytes (Meran et al. 2013). Unlike TGF-β_1 activation, however, HA does not form a peri-cellular coat, instead it is arranged in spiked formations on the cell membrane protrusions. These are the areas shown to bind monocytes. To elucidate which of the CD44 variants mediated the TGF-β_1 and IL-1β responses, custom siRNAs were designed to target CD44s and variants, v3, v6, v8, v10 and v6-10.

Silencing CD44v3 had no effect on TGF-β_1 induced αSMA mRNA expression ***Figure 4.4 [C]*** or IL-1β-induced monocyte binding ***Figure 4.5[C]***, suggesting that CD44v3 was not involved in activation of αSMA expression or monocyte adhesion. CD44v3 is well-described and identified to contain a heparan sulfate (HS) binding domain, known to favour association with heparin binding proteins, such as bone morphogenetic protein (BMP-7) and hepatocyte growth factor (HGF). These growth factors are well-documented for their ability to counterbalance the effects of pro-fibrotic cytokine, TGF-β_1 (Zeisberg et al. 2003; Narmada et al. 2013; Midgley et al. 2015). Overexpression of CD44v3 in transgenic mice subjected to UUO, propagated an increase in bone morphogenic protein-7 (BMP-7) and a decrease in TGF-β_1 (Rampanelli et al. 2014). Therefore, CD44v3 was suggested to have an anti-fibrotic role. An upregulation of CD44v3 in inflammatory diseases, such as ulcerative colitis (Rosenberg et al. 1995b), along with the identified binding of HS motifs to act as an adhesion ligands in cell-cell

associations, suggested that CD44v3 may have a role in fibroblast–monocyte binding. However, here it was found that silencing this variant had no effect on IL1-β-induced monocyte binding. One explanation for this is that HS motifs are abundant, diverse and cell specific and known to be associated with different cell-cell recognition patterns (Coombe et al. 1994). Furthermore, HS is a polyanionic molecule that can be altered depending on cell type, resulting in cell-specific function (Parish 2006). HS is a GAG exhibiting different consensus sequences that mediate interactions within the ECM. Different consensus sequences have been reported to alter binding affinity (Hileman et al. 1998). Therefore, a possible suggestion for CD44v3 not being involved in monocyte binding may be due to HS modifications that prevent its association with HA.

Most of the current research has found the CD44v8 encoding exon to be present in large/multiple exon isoforms, with multiple exons between common regions, e.g. within the epithelial form, CD44v8-10 (Bourguignon and Iida 1994). In the previous chapter, it was identified that CD44v8 containing solely v8/exon12 was expressed in fibroblasts, however, it was not as highly expressed as some of the other identified variants. Silencing CD44v8 did not prevent the expression of αSMA, following TGF-β_1 stimulation ***(Figure4.4 [D])***. Although, interestingly silencing CD44v8 significantly increased fibroblast-monocyte binding in control samples, compared to scrambled controls ***(Figure 4.6 [D])***. A further increase in monocyte binding was observed in fibroblasts stimulated with IL-1β, compared to scrambled controls. These data suggest that CD44 variants containing v8/exon 12 may have a negative regulatory role on monocyte binding. However, the analysis of the only larger variant identified in this study containing v8/exon 12 (CD44v6-10), did not suggest that this variant played a role in monocyte to fibroblast binding. Therefore, CD44v8 may have an independent role from the larger CD44 isoform, which also contain the v8 segment of the variable domain. Research in our laboratory has also identified CD44v7/8 expression in fibroblasts (Midgley et al. 2013).

However, siRNA to v7/8 did not show any effect on monocyte binding in control or IL-1β-stimulated fibroblasts, eliminating its involvement and further confirming that CD44v6-10 was not involved. Why silencing CD44v8 increased monocyte binding and not TGF-β_1 induced αSMA expression is not understood and would need to be further investigated.

In this study, transfection of fibroblasts with siRNA to CD44v6 or v10 had no effect on the induction of αSMA by TGF-β_1 or IL-1β-induced monocyte binding, respectively. CD44v6 is one of the most studied CD44 variants, due to its association with c-Met, the receptor for HGF. In some inflammatory diseases CD44v6 has an increased expression (Rosenberg et al. 1995a). However, there is limited evidence that it co-localises with either EGFR or ICAM-1. In a study by Ghatak et al. (2014), it was found that interstitial lung disease fibroblasts (ILDFbs) had a persistently upregulation of CD44v6 and c-Met, which promoted sustained auto-induction of TGF-β_1 and increased collagen I and αSMA expression. Furthermore, the increased expression of TGF-β_1 supressed HGF expression by ILDFbs. Interestingly, the addition of exogenous HGF suppressed the TGF-β_1 fibrotic effects and reversed the fibrotic process. Therefore, it could be assumed that silencing CD44v6 would attenuate its interaction with c-Met and decreasing the fibrotic role of CD44v6/c-MET and decrease fibrotic progression. However, this study demonstrated that silencing v6 had no effect on αSMA upregulation, suggesting that the anti-fibrotic effects of CD44v6/c-Met association may be dependent on signalling pathways distinct from the TGF-β_1-mediated HA/CD44/EGFR pathway. An essential role of CD44v6 has previously been defined. CD44v6 was required for the activation of the c-Met/HGF complex and cytoskeletal association with ezrin. This suggests that in fibroblasts, the CD44v6/c-Met/HGF complex is associated with cytoskeletal re-organisation instead, of αSMA upregulation or monocyte binding.

CD44v10 is commonly described as having modifications, such as the addition of N-/O-linked glycosylation containing unique chondroitin sulphate (CS) motifs. Moreover, this

variant has a specific binding sequence, B[X_7]B, which modulates interactions with other chondroitin sulfate and serine-glycine motifs (Hayes et al. 2002). This motif also allows for the association with other CD44 receptors and mediation of cell-cell adhesion properties. However, the overexpression of v10 in breast cancer cells decreased CD44 cluster formation and it is speculated that the increased presence of CS reduced the CD44/HA binding affinity, due to lack of cluster formation, leading to limited cellular adhesion and contributing towards cancer metastasis (Iida and Bourguignon 1997; Bourguignon et al. 1998). This was confirmed in a more recent study by Ruffell et al. (2011), which demonstrated that the presence of CS motifs correlated inversely with CD44/HA binding by mouse bone marrow macrophages. This was demonstrated by the addition of various inflammatory mediators that altered CS expression. For example, tumour necrosis factor-α (TNFα) limited the presence of CS motifs and increased CD44/HA binding affinity. Conversely, interleukin-4 (IL-4) stimulation increased CS motifs and decreased CD44/HA affinity. Previously, it was demonstrated that CD44 was re-localised in the membrane and formed clusters when stimulated with TGF-β_1 or IL-1β in a HA-dependent manner; suggesting that the HA/CD44 binding affinity was increased (Meran et al. 2013). That different stimuli modulate the HA/CD44v10 binding affinity by the addition of CS motifs may have suggested that these stimuli both limit the HA binding affinity, by reduced presence of posttranslational CS motifs. However, the results in this study demonstrated that using a siRNA targeting CD44v10 did not affect fibroblast αSMA expression or monocyte binding.

The involvement of the larger variant CD44v6-10 in differentiation or monocyte binding was assessed previously, using individual siRNAs targeting CD44v6, v8 and v10. The effects of silencing these variants had no effect on αSMA expression or monocyte binding. A siRNA targeting CD44v7/8 confirmed these data, leading to the conclusion that the larger CD44v6-10 isoform had no role in these two activation pathways. That CD44v7/8 was not

involved in these pathways is in line with previous research in our laboratory, which has shown that CD44v7/8 had an anti-fibrotic role when induced by BMP-7; and was able to reverse fibrotic progression that resulted from TGF-β_1 through the internalization of HA (Midgley et al. 2015).

Silencing CD44s significantly decreased the expression of αSMA mRNA and the formation of αSMA stress fibres. It is not understood why this standard form of CD44 controls αSMA expression. However, it had previously been determined in chapter 3, that CD44s had the highest expression of all CD44 variants in fibroblasts, suggesting it may be responsible for multiple gene regulations. For example, it was previously demonstrated that CD44s was responsible for the upregulation of matrix metalloproteinase-9 (MMP-9), resulting from intracellular proteolytic cleavage of the cytoplasmic tail by the enzyme presinillin (γ-secretase); and nuclear translocation of the signal peptide (PDZ) (Miletti-González et al. 2012). This cleavage of intramembranous CD44 results in a CD44 intracellular domain (ICD) fragment, that translocate to the nucleus and activates MMP-9 expression. It has previously been reported that CD44 acts as a docking site for MMP-9 and MMP-2, both known to activate pro-TGF-β_1 into its active form (Yu and Stamenkovic 2000). Furthermore, past research demonstrated that autocrine induction of TGF-β_1 was important for maintaining the myofibroblast phenotype. It was shown that preventing the expression of SMAD2/3 (the downstream signalling pathway of TGF-β_1), reduced TGF-β_1-induced αSMA expression in myofibroblasts (Webber et al. 2009a). Therefore, decreasing CD44s in this study may have decreased the ICD formation leading to decreased MMP-9 expression and limited activation of TGF-β_1; leading to reduced αSMA induction.

Furthermore, maintenance of the myofibroblast phenotype is dependent on the formation of the HA peri-cellular coat that is anchored into position by CD44. This HA/CD44 association mediates the movement of CD44 through the membrane into lipid raft regions,

where it associates with co-receptor, EGFR. Eliminating the variant involved in this process would prevent downstream intracellular signalling of ERK1/2 and activation of αSMA gene expression. CD44s has previously been identified to be the CD44 variant with the highest binding affinity to HA, making it an ideal candidate for this mechanism (Bartolazzi et al. 1994).

The CD44 association with cytoskeletal proteins mediates multiple cellular functions, including directional cell migration and stress fibre formation (Hall 1998; Legg et al. 2002). ***(Figure 4.9[D])*** shows a lack of αSMA stress fibre formation in TGF-β_1-induced, myofibroblasts that were transfected with siRNA targeting CD44s. The decreased expression of CD44s prevented the incorporation and formation of αSMA into stress fibres. Moreover, cells transfected with siRNA targeting CD44s retained the spindle morphology typical of the fibroblast, suggesting differentiation was inhibited. This lack of morphological change may suggest that silencing CD44s reduced cytoskeletal/CD44 association required for differentiation.

IL-1β stimulation of keratinocytes upregulated CD44 expression and increased de-phosphorylation of a Ser-325 residue in the cytoplasmic tail region. This Ser-325 residue was identified to be directly dephosphorylated by CaMK-II in fibroblasts. The subsequent de-phosphorylation of this region is upstream of the phosphorylation of Ser-291, which increases CD44/Ezrin association and mediates CD44 cluster formation. Furthermore, inhibition of caMK-II increased CD44 cluster formation (Jokela et al. 2015). Our research has demonstrated that IL-1β stimulation increased monocyte binding, by activating the formation of a spiculated HA coat. This was dependent on CD44 forming clusters that increased HA binding affinity (Meran et al. 2013). The HA coat important for monocyte binding differs to the HA peri-cellular coat formed around myofibroblasts following TGF-β_1 stimulation. For example, the hyaldherin, tumour necrosis factor stimulating gene-6 (TSG6), is not required for the formation of IL-1β-induced HA protrusions, but is essential for forming and maintaining the

myofibroblast peri-cellular coat (Meran et al. 2013). Therefore, the formation of the monocyte-specific, HA coat commonly induced under inflammatory conditions, seems to be HA/CD44-driven by a different mechanism. This study determined that decreased CD44s expression prevented fibroblast–monocyte binding ***(Figure 4.10 [B])***. These data indicate the importance of CD44s in this process, suggesting that CD44s modulates the formation of the specific HA coat essential for monocyte binding by forming clusters, that increase HA binding affinity. Furthermore, it is known that CD44/ICAM association is essential for monocyte binding. A possible suggested mechanism for the involvement of CD44s in this process is that the binding of CD44s with HA activates downstream de-phosphorylation of the Ser-325 residue on the cytoplasmic region, by CaMK-II. In turn, the de-phosphorylation activates CD44/ezrin association which mediates cytoskeletal re-arrangement and CD44s reorganisation, resulting in CD44s forming clusters and ICAM-1 association. However, to confirm this, further research would be required.

Finally, transfection with siRNA targeting CD44s did not affect the expression of other CD44 variants investigated. These preliminary data suggest that CD44s was not mediating the expression of other CD44 variants by ICD translocation to the nucleus; and that the siRNA targeting CD44s did not target other CD44 variants. Therefore, this preliminary data suggested that of the variants identified only CD44s is involved in modulating αSMA expression and monocyte binding.

In summary, this chapter shows that silencing the mRNA expression of CD44s prevents TGF-β_1 induced αSMA expression and IL-1β-induced monocyte binding. None of the other variants had a role in this process, with the possible exception of v8. This CD44 variant was observed to have an opposite role to CD44s and decreased CD44v8 expression was associated with increased monocyte binding, suggesting a regulatory for this variant in monocyte binding. Determining the exact mechanisms involved, however, would require further research.

Chapter 5-The Role of CD147 in Fibroblast Differentiation and Monocyte Binding

5.1- Introduction

5.1.1. - CD147 Discovery and Overview

CD147 is a type-1 transmembrane glycoprotein and a member of the immunoglobulin superfamily. Also known as extracellular matrix metalloproteinase inducer (EMMPRIN) or Basigin (Bsg), CD147 was originally discovered in the plasma membrane of human LX-1 lung carcinoma cells (Biswas 1982). It was further identified in multiple species and was designated several names, including, mouse gp42 (Altruda et al. 1989), neurothelin (Schlosshauer and Herzog 1990), rat OX-47 (Fossum et al. 1991); and chicken HT7 (Seulberger et al. 1990). It was later discovered that these proteins were all the same glycoprotein with different names in various species (Seulberger et al. 1992). CD147 was firstly identified as either an antigen or its carrier, however, further research discovered that CD147 had a functional role. It was observed that a membrane-bound protein mediated increased collagenase production by fibroblasts that were co-cultured with the human LX-1 carcinoma cell line and was originally named, tumour cell derived collagenase stimulatory factor (TCSF) (Biswas 1984; Biswas and Nugent 1987). Later research discovered that TCSF expression on tumour cells increased fibroblast expression of other MMPs, including gelatinase (MMP-2) and stromolysin-1 (MMP-3) (Kataoka et al. 1993). It was renamed EMMPRIN. Later studies discovered that EMMPRIN and Bsg had identical cDNA sequences and were identical proteins (Biswas et al. 1995).

The majority of CD147 research is focused on its upregulation in tumour cells and the implications in tumour development (Gabison et al. 2005; Zheng et al. 2006). However, CD147 has a role in several other pathological diseases, including rheumatoid arthritis. In this inflammatory disease, CD147 is upregulated on the cell surface of monocytes/macrophages and induces resident fibroblasts to produce MMPs (Zhu et al. 2005). The upregulation of CD147 is also associated with pathogenic infections, including human immunodeficiency virus

(HIV) (Pushkarsky et al. 2001) and hepatitis B (Tian et al. 2010). Involvement of CD147 in disease is commonly associated with its interaction with multiple surface receptors and ligands. These include integrins, cyclophilins, caveolin-1 and monocarboxylate transporters (MCTs) (reviewed by Xiong et al. 2014). Independent from MMP production, CD147 is multifunctional and has functional roles in cell metabolism (Kirk et al. 2000), spermatogenesis (Chen et al. 2011), lymphocyte activation (Chiampanichayakul et al. 2006); and cell-cell contact (Fadool and Linser 1993).

5.1.2. - CD147 Gene and Protein Structure

CD147 is a member of the immunoglobulin superfamily (IgSF), composed of a large group of proteins involved in cell recognition, association and adhesion, which are all dependent on a putative immunoglobulin domain (Williams and Barclay 1988). It is encoded by 1797 base pairs on the CD147 gene at chromosome position 19P13.3 (Kaname et al. 1993). The 5' promotor region contains a 30bp site from -142bp to -112bp that codes for a binding site for specific protein 1 (Sp1), AP1TFII and early growth response 2 (EGR-2); all important nuclear factors involved in CD147 transcription (Liang et al. 2002). The CD147 gene encodes for a 185 amino acid extracellular region, a 24 amino acid highly-conserved, transmembrane region; and a 39 amino acid cytoplasmic domain (Fossum et al. 1991; Biswas et al. 1995). The extracellular region is composed of two Ig domains (***Figure 5.1***); and it is these domains that have similar characteristics to other members of the immunoglobulin superfamily. The transmembrane region contains mainly hydrophobic residues, with the exception of one charged glutamic acid residue, thought to increase protein-protein affinity. The translated CD147 protein is 28kDa, however, the molecular range of the protein is between 32-66kDa, due to post-translational glycosylation. There are four alternative spliced variants of CD147/Bsg identified, they are CD147/Bsg 1, 2, 3 and 4. The most recently discovered, CD147/Bsg-1 is retina specific and has an additional unglycosylated Ig domain, thought to be

associated with homophilic binding (Hanna et al. 2003). CD147/Bsg-3 and 4 have a single Ig domain. CD147/Bsg- 2 contains two Ig domains (***Figure 5.1.).*** CD147/Bsg-2 is the most characterised form of CD147, due to its ubiquitous expression and regulation of MMPs (Nabeshima et al. 2006; Belton et al. 2008). As CD147/Bsg-2 is the most studied CD147 variant, it will be the focus of this introduction. Here on, it will be referred to as CD147 in humans and BSG in murine, unless stated otherwise.

5.1.3. - CD147 Glycosylation

The crystal structure of CD147 revealed three different asparagine (Asn) sites for glycosylation within the proximal Ig domain: Asn 44 within the distal Ig domain, Asn 152 and Asn 186 (see ***Figure 5.1)*** (Yu et al. 2008). Most glycosylation studies on CD147 demonstrate that CD147 is mainly an N-linked glycosylated glycoprotein, which varies between species and cell type. The three glycosylation domains give rise to multiple glycosylated forms of CD147 that are categorised into two groups. A lower glycosylated CD147 (LG-CD147) form, that has a molecular weight of ~32kDa; and multiple higher glycosylated CD147 (HG-CD147) that have a molecular mass range between ~40-66kDa (Tang et al. 2004). It is suggested that a high mannose form of LG-CD147 glycosylated in the endoplasmic reticulum (ER), is a precursor to HG-CD147, which is modified in the Golgi apparatus (Bai et al. 2014). Once modified, HG-CD147 is translocated to the membrane.

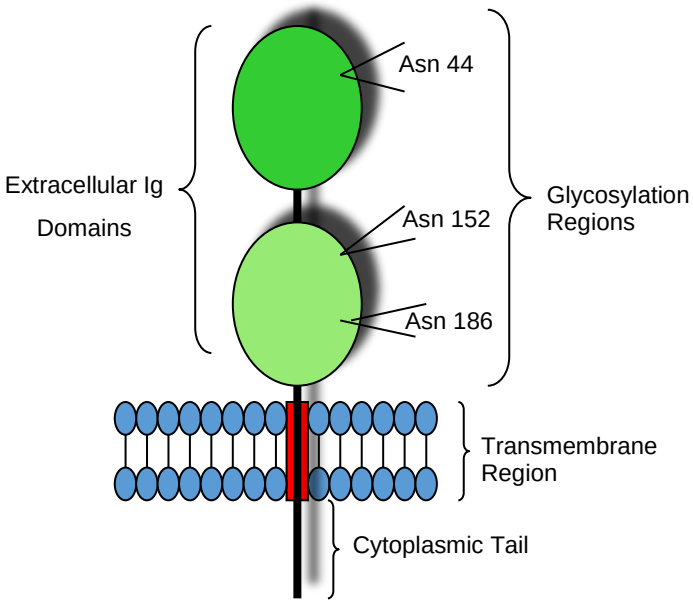

Figure 5.1 – CD147 Structure and Glycosylation

Schematic demonstrates the extracellular Ig arrangement of CD147 variant 2. The isoform contains two Ig domains with glycosylation sites at amino acid positions, Asn 44 in the distal domain and Asn152 and 186 within the proximal domain. Diagram is modified from review article (Xiong et al. 2014)

5.1.4.-CD147-Protein Interactions

CD147 also associates with integrins α3β1 and α6β1; and mediates their reorganisation and distribution around points of cellular contact (Berditchevski et al. 1997). These integrins bind to laminin, which is a major components of the basement membrane and CD147 regulates integrin/laminin associations which are fundamental to processes such as foetal development, cell adhesion and angiogenesis (reviewed by Iacono et al. 2007). The association of CD147 with integrin α6β1 has been demonstrated to upregulate hepatoma cellular invasion and metastasis, by increased MMP production and activation of intracellular signalling phosphatidylinositol 3-kinase (Pl3K), a known integrin-induced pathway (Guinebault et al. 1995; Dai et al. 2009). Similarly, CD147 association with integrin α3β1 was linked to invadapodia and metastasis in hepatoma cells and the deletion of either CD147 or inhibition of α3β1, decreased focal adhesions, MMP expression and altered cytoskeletal arrangement.

Overexpressing CD147 did not increase the overall expression of α3β1, but did increase its activity and its association with the adhesion-associated proteins, focal adhesion kinase (FAK) and paxillin (a protein that associates with FAK); and increased cellular metastatic potential (Tang et al. 2008b).

Caveolin exists as three isoforms Cav-1, -2 and -3. Cav-1 and Cav-2 are expressed in multiple cell types, whereas Cav-3 is the only isoform expressed in skeletal muscle tissue, cardiac myocytes and smooth muscle cells (Song et al. 1996; Okamoto et al. 1998). Caveolin-1 is also a major component of caveolae rafts. These are dynamic invaginated domains in the plasma membrane that often also contain multiple proteins and lipids (Parton and Simons 2007). Caveolins have multiple functions, including organising signalling receptors, cholesterol homeostasis, tumour suppression and endocytosis (reviewed by Okamoto et al. 1998; Williams and Lisanti 2004). Only Cav-1 has been documented to associate with CD147, but the research has been controversial. For example, Cav-1 negatively regulated CD147 and preventing CD147/Cav-1 association, promoted CD147 self-clustering and increased MMP induction. Further, only the lower glycosylated form of CD147 was identified to associate with Cav-1 in multiple carcinoma cell lines; and it was suggested that regulation starts in the Golgi apparatus and that the CD147-Cav 1 association prevents further glycosylation and formation of the HG-CD147 (Tang et al. 2004). Conversely, in a hepatocarcinoma cell line, it was identified that increased Cav-1 upregulated the expression of HG-CD147 and MMP-11; and that these increases upregulated tumour invasion (Jia et al. 2006). This conflicting research into Cav-1 and its interaction with CD147 suggests that the association with different glycosylated forms of CD147 molecular weights may be cell-type specific.

5.1.5. - CD147 in Disease

CD147/EMMPRIN is an MMP inducer, commonly documented to be associated with cancer progression. The upregulated MMP production mediated by CD147 degrade the surrounding ECM, to allow for cellular movement and cancer progression (Donadio et al. 2008). Much of the current research investigating the involvement of CD147 in cancer progression focuses on tumour cell expression of CD147, induction of stroma fibroblasts to express and activate MMPs (Kanekura et al. 2002; Gabison et al. 2005). In specific cancer types, CD147 induction of MMPs correlates with the intracellular signalling of protein kinases. For example, the induction of MMP-1 (collagenase) secreted by fibroblasts through the phosphorylation of tyrosine kinase p-38 was associated with high levels of CD147 expressed on lung tumour cells (Lim et al. 1998). More recently, the upregulation of CD147 expression was linked to an increased mitogen-activated protein kinase (MAPK) signalling, including extracellular signalling kinase (ERK), p38 and c-Jun N terminal kinase (JNK), in metastatic ovarian cancer. The observed increase of CD147 and MAPK signalling was determined to increase MMP-2 (Davidson et al. 2003).

Although well-researched in tumourgenesis, CD147 has also been associated with several other diseases. For example, Alzhemier's disease is a neurodegenerative disease, resulting from the formation of amyloid plagues and neurofibrillary tangles, within cortical regions of the brain. These proteins damage nerve cells and prevent cell-cell contact at synapses regions (Cummings and Cotman 1995). The multi-protein, γ-secretase complex, consisting of presenilin 1, nicastrin, anterior pharynx defective 1 (APH-1) and presenilin enhancer 2 (PEN-2), exists within cell membrane regions and cleaves membrane bound, β-amyloid precursor protein (APP). The cleavage of APP firstly by β-secretase, followed by γ-secretase, forms Aβ-peptides. These are sticky proteins units that form amyloid plaques between neurons. CD147 has been demonstrated to co-immunoprecipitate with γ-secretase and silencing CD147

increased the expression of Aβ-peptides, suggesting that CD147 has a regulatory role in the disease (Zhou et al. 2005). Furthermore, CD147 has been widely associated with inflammatory disease through its interaction with cyclophilin A (CypA), a ubiquitously expressed member of the intracellular peptidyl-prolyl *cis-trans* isomerase family. The principle function of these enzymes is to convert the *cis* and *trans* forms of proline by facilitating protein folding. However, these enzymes are also secreted extracellularly in response to inflammatory stimuli and act in a chemotactic manner, attracting leukocytes to the region. Moreover, CD147 is a known receptor for CypA and is expressed highly expressed on the membrane of leukocytes under inflammatory conditions (Yurchenko et al. 2002). In rheumatoid arthritis (RA), it has been identified that the chemotactic function of CypA and its interaction with CD147, has an essential role in collagen-induced RA in mice. Blocking CD147 expression with an anti-CD147 monoclonal antibody prevented leukocytes, such as neutrophils and T-cells, migrating in response to CypA and inhibited the inflammatory response (Damsker et al. 2009). Therefore, CD147 also has a role in inflammatory responses.

5.1.6 – CD147 in Wound Healing and Fibrosis

The overexpression of CD147 in corneal fibroblasts upregulates αSMA expression and the subsequent contractile potential of these fibroblasts. Furthermore, silencing CD147 in these cells reduced αSMA presence and the contractile phenotype, following TGF-β_1 induction (Huet et al. 2008b). Similarly, the involvement of CD147 in fibrotic progression was demonstrated in CD147/Bsg deficient mice, $Bsg^{-/-}$, that were subjected to a unilateral ureteral obstruction (UUO). Extracted tissue showed that $Bsg^{-/-}$ mice had a decreased collagen and hyaluronan deposition, αSMA expression and MMP production. Furthermore, they had a lower macrophage infiltration, compared to $Bsg^{+/+}$mice, suggesting a role for CD147 in regulating an immune response (Kato et al. 2011).

It has been well-documented that CD147 has an increased expression on immune cells in inflammatory diseases, including antigen-presenting cells and T cells (Woodhead et al. 2000); and an increased immune response is associated with fibrotic progression. However, the regulation of CD147 by IL-1β is not understood. The upregulation of IL-1β in periodontal ligaments has been demonstrated to increase mRNA expression of MMP-1 and -2, which, contributed to the inflammation and eventual detachment of periodontal ligaments. However, the increased MMP expression did not correlate with an increase in CD147 expression, leading to the assumption that CD147 had no role in the IL-1β induction of MMPs in periodontal disease (Xiang et al. 2009). Although it is understood that IL-1β stimulation facilitates fibroblast–monocyte binding, the role of CD147 is unknown. Both CD147 and IL-1β have previously been observed to become upregulated in inflammatory diseases (Kolb et al. 2001; Yang et al. 2008). However, only IL-1β has been implicated in increased monocyte binding by fibroblasts in fibrotic disease (Yang et al. 2008; Meran et al. 2013). Therefore, a further aim of this study is to investigate the effect of IL-1β stimulation on CD147 expression in fibroblasts and determine if the pro-inflammatory cytokine, IL-1β; and CD147 have synergistic roles in the IL-1β/HA/CD44/ICAM-1-dependent monocyte binding by fibroblasts.

5.2. – Chapter Aims

- Determine the expression of CD147 in fibroblasts, TGF-β_1-induced myofibroblasts and IL-1β-fibroblasts.
- Analyse the role of TGF-β_1 induction on CD147 and determine if CD147 has a role in HA/CD44/EGFR fibroblast to myofibroblast differentiation.
- Investigate the role of IL-1β on CD147 induction and determine if CD147 has a role in HA/CD44/ICAM-1-mediated, monocyte binding.

5.3. – Methods

5.3.1. – Effective Knockdown of CD147 at the mRNA and Protein Level.

To investigate the importance of CD147 in fibroblasts to myofibroblast differentiation and in monocyte binding, a siRNA targeting was used. In order to identify the sufficient knockdown of CD147 mRNA and protein expression for the use in future experiments, a timecouse of 24-144 h was used.

Preliminary assessment demonstrated that as early as 24 h following transfection with the siRNA targeting CD147, fibroblasts had a decreased CD147 mRNA expression by approximately 50%, compared to fibroblasts transfected with the scrambled control ***(Figure 5.2. [A])***. The decreased CD147 mRNA expression was maintained at all subsequent time-points. It had previously been identified and clarified again in this study that myofibroblasts are terminally differentiated following 72 h of TGF-β_1 stimulation ***(Figure 4.1[A&B])***. Similarly, IL-1β significantly increased monocyte binding following 72 h of stimulation ***(Figure 4.2. [B])***. Therefore, combining this earlier data with the data gathered here, which demonstrated the maintained knockdown of CD147 mRNA expression by the siRNA, it was decided that all experiments investigating CD147 function at the mRNA level would be carried out 72 h following transfection.

Figure 5.2 [B] shows the protein expression of CD147 over a time course of 144 h. Samples were transfected with either a siRNA targeting CD147 or a scrambled control. Total protein expression for CD147 was completely inhibited following 144 h transfection with the siRNA to CD147. Therefore, all experiments which investigated the role of CD147 protein in fibroblast differentiation and monocyte binding were carried out 144 h following transfection with the siRNA targeting CD147, as shown in ***Figure 5.2. [C]***.

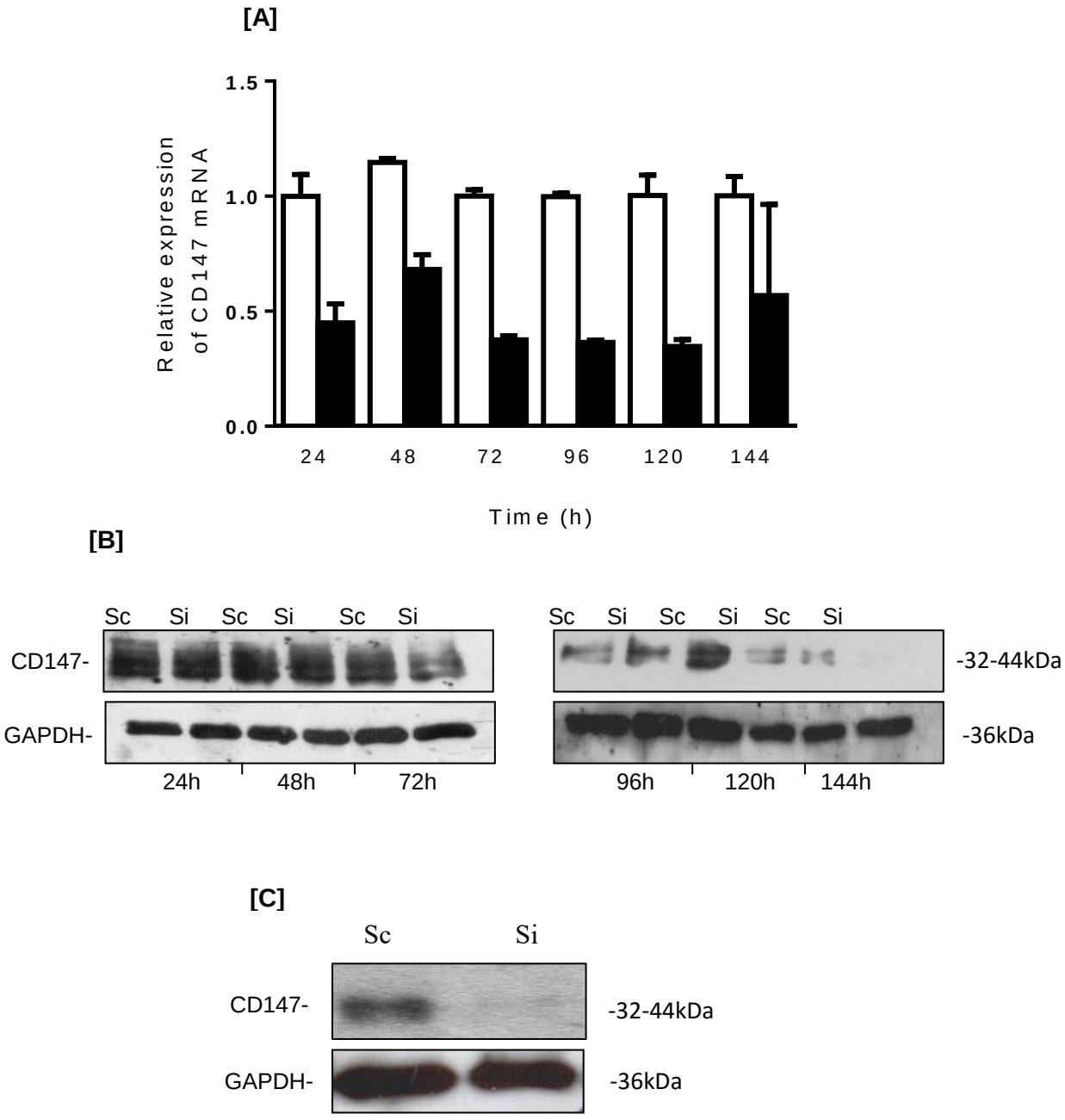

Figure 5.2. – Time Course to Determine Knockdown of CD147 at mRNA and Protein Level Using siRNA to CD147

In order to determine sufficient knockdown of CD147 at the mRNA and protein level, a siRNA to CD147 was used and its effects analysed over a time course of 144 h (***figure [A]***). Fibroblasts were grown to 50-60% confluence and growth- arrested for 24 h, prior to transfection. Fibroblasts were transfected with a siRNA targeting CD147 ***(black bars)*** or a scrambled control siRNA (***white bars).*** Fibroblasts were incubated for 6 h in the transfection medium. DMEM/F12 containing 20% v/v foetal calf serum (FCS) was added to samples, which were further incubated for 24 h. The medium was removed fresh serum-free DMEM/F12 was added. The time course was initiated at this point. Following 24h incubation and for every consecutive 24 h period, samples were extracted and analysed using qPCR .Data represents ± S.D. of a single experiment sample n=3. ***Figure [B]*** shows the effective knockdown of CD147 protein expression. Fibroblasts were transfected with a siRNA targeting CD147 ***(Si)*** or a scrambled control ***(Sc)***, as described above. ***Figure [C]*** shows the effective knockdown of CD147 following 144 h of transfection with an siRNA that targeted CD147.

5.3.2. Assessment of Experimental Conditions

Due to the extended time required for the CD147 protein expression to be silenced, an analysis of the experimental conditions was required. This was carried out to validate that cells were still metabolically active and viable. The florescent intensity of the cellular medium treated with AlamarBlue was used to analyse cellular metabolism. The experiment was carried out using a negative untransfected control, a scrambled siRNA control and a siRNA targeting CD147. To analyse all experimental conditions cells, were stimulated with TGF-β_1 or IL-1β in two separate assays ***(Figure 5.3. [A&B])***. The AlamarBlue assay was carried out 144 h following transfection, as this was the time point that CD147 protein levels were previously observed to be totally silenced ***(Figure 5.1. [B])***. Cells were stimulated with either TGF-β_1 or IL-1β stimulation 72 h after the experimental start time, they were then extracted at 144 h. Therefore, this enabled total protein to be knocked down and a stimulation time of 72 h, which had been previously identified to be the time-point of interest. Unstimulated fibroblasts transfected with siRNA to CD147 had a similar florescent intensity to untransfected fibroblasts and fibroblasts transfected with siRNA to CD147. Silencing the protein expression of CD147 had no effect on cell viability, when stimulated with TGF-β_1 or IL-1β; and florescent intensity was consistent with those observed under the control conditions. These data suggest that the experimental conditions did not have an effect on cellular viability.

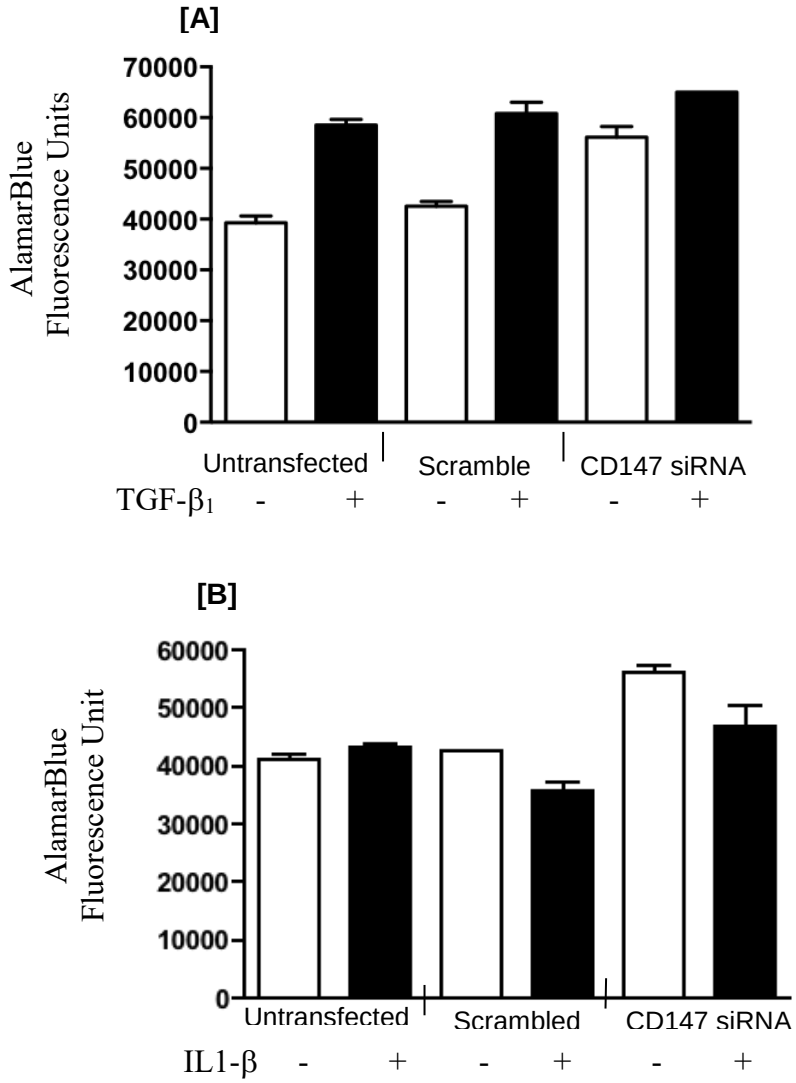

Figure 5.3. – Assessment of Experimental Conditions

Analyse of experimental conditions was carried out using an AlamarBlue assay. Fibroblasts were grown until 50-60% confluence, before being growth-arrested for 24 h. Fibroblasts were treated with transfection medium alone (untransfected cells), a scrambled control siRNA an siRNA targeting CD147. Following a 6 h incubation period, fibroblasts were treated with fresh DMEM/F12 containing 20% v/v FCS and incubated for a further 24 h. Fresh serum-free medium was added and cells were incubated for 72 h. Samples were them treated with fresh serum-free medium containing TGF-β_1 (10ng/ml) ***[A]*** or IL-1β (1ng/ml) ***[B]***. Unstimulated samples were treated with fresh serum-free DMEM/F12 alone. An AlamarBlue assay was carried out according to the manufactures protocol. Data shows the fluorescence units displayed by fibroblasts treated with medium alone (untransfected) and fibroblasts transfected with a scrambled siRNA or a siRNA targeting CD147. Samples stimulated with either TGF-β_1 or IL-1β ***(black bars)***,were compared to control samples ***(white bars)***,under all three conditions. Data represents 3 separate samples ± S.D.

5.4. – Results

5.4.1. – CD147 mRNA Expression in Fibroblasts and Myofibroblasts

Primarily, the mRNA expression of CD147 in quiescent fibroblasts and fibroblast-stimulated with either TGF-β_1 (***Figure 5.4. [A])*** or IL-1β (***Figure 5.4. [B])*** was investigated. The expression of CD147 in quiescent fibroblasts was relatively high. Stimulation with TGF-β_1 did not significantly alter the overall expression of CD147 by myofibroblasts. The effects of IL-1β on CD147 were assessed over a time course of 0-72 h. IL-1β-stimulated fibroblasts had a significant increase of CD147 expression at 72 h, compared to fibroblasts treated with serum-free medium alone (control fibroblasts). There was no difference in expression of CD147 at any of the earlier time-points, compared to control fibroblasts.

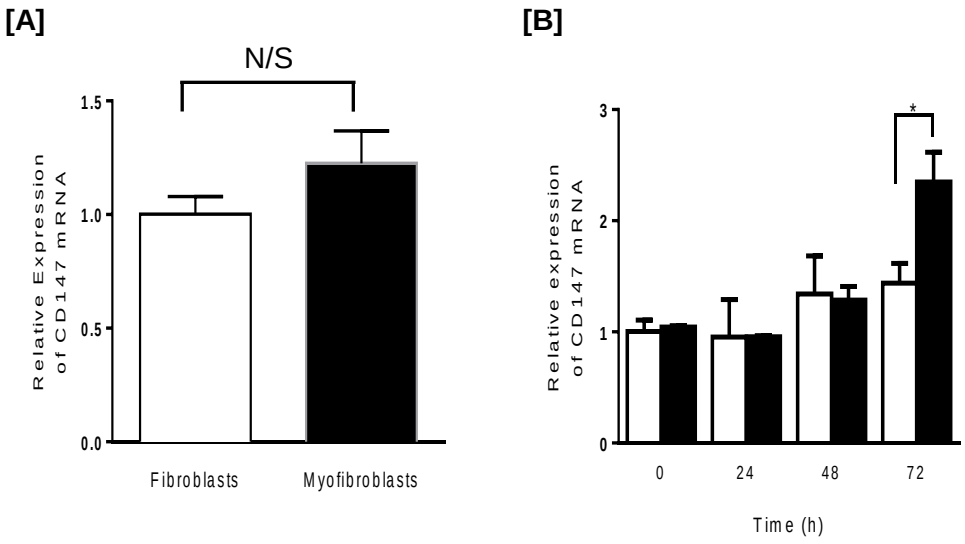

Figure 5.4. - CD147 mRNA Expression in Quiescent Fibroblasts, TGF-β_1-Induced Myofibroblasts and IL-1β-Stimulated Fibroblasts.

Figure demonstrates CD147 mRNA expression by TGF-β_1-induced myofibroblasts ***[A]*** and IL-1β-stimulated fibroblasts ***[B]***. Briefly, fibroblasts were grown to 80%. Following growth arrest, fibroblasts were treated with fresh serum-free DMEM/F12 containing TGF-β_1 (10ng/ml) ***[A]*** or IL-1β (1ng/ml) ***[B]***, for 72 h. Control samples were treated with serum free DMEM alone. Analysis was carried out using qPCR. The expression of CD147 either TGF-β_1- or IL-1β-stimulated fibroblasts ***(black bars)***, were compared to control unstimulated fibroblasts ***(white bars)***. Data is displayed as ±SEM from 3 separate experiments. Statistical analysis was carried out using one way ANOVA, followed by the unpaired student's *t* test *P>0.05, N/S (not significant).

5.4.2. - Co-localisation of CD147 With CD44

Central to TGF-β_1-induced differentiation and IL-1β-induced monocyte binding pathways, is HA association with the receptor, CD44 (Webber et al. 2009b; Meran et al. 2013; Midgley et al. 2013). An initial assessment investigated the association of CD147 with CD44 and the effects of TGF-β_1 and IL-1β stimulation were analysed. Immunoprecipitation (IP) of CD147 was used to extract CD147 and a SDS-PAGE Western blot analysis was carried out to identify CD44 association. CD147 was identified to co-localise with CD44 in control fibroblasts ***(Figure 5.5. [A&B])***. TGF-β_1 stimulation increased co-localisation of CD147/CD44 in terminally differentiated myofibroblasts ***(Figure 5.5. [A])***. However, there was no increased observed in the CD147/CD44 association in fibroblasts stimulated with IL-1β, compared to unstimulated fibroblasts ***(Figure 5.5. [B])***. The Western blot analysis was carried out using a pan-CD44 antibody that targets all CD44 variants. The detection of a single CD44 band was identified to co-precipitate with CD147 in quiescent, TGF-β_1-and IL-1β-stimulated fibroblasts. The band was observed at approximately 85-90kDa, the molecular mass range expected for the standard form of CD44 (CD44s). Therefore, these data suggest that the CD44 variant observed to co-localise with CD147 in this study is CD44s and that this co-localisation increases in TGF-β_1 induced, myofibroblasts.

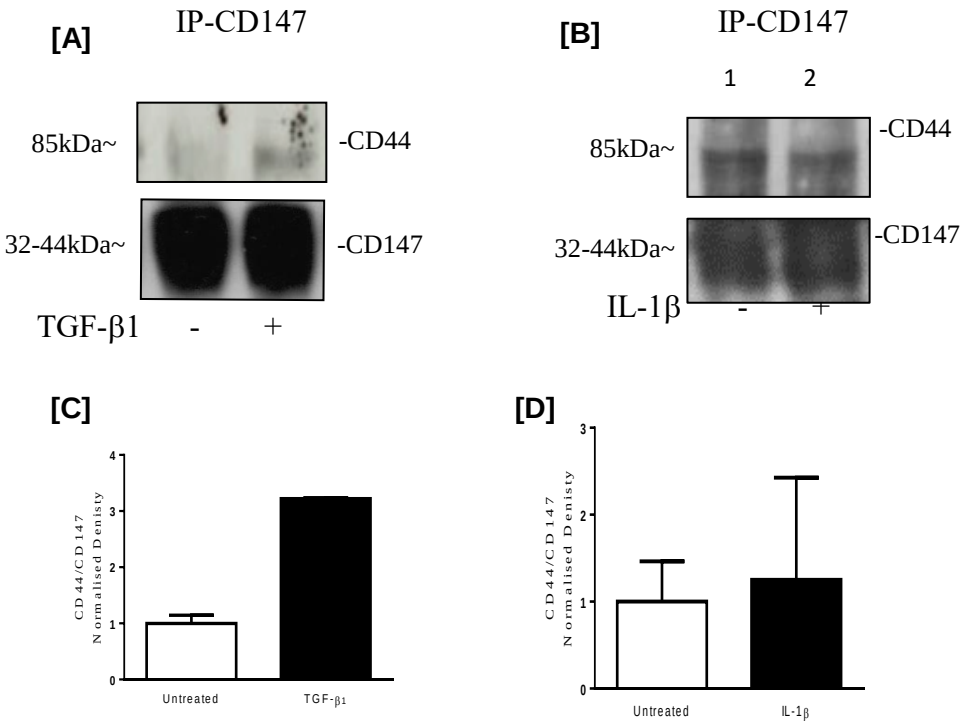

Figure 5.5. - Co-localisation of CD147/CD44 and the effects of TGF-β_1- and IL-1β-Stimulated Fibroblasts.

Images show CD147 co-localisation with CD44 in fibroblasts ***Figure [A&B], (Lane 1)***, TGF-β_1 induced, myofibroblasts ***[A] (Lane 2)*** and IL-1β-stimulated fibroblasts ***[B] (Lane 2)***. Briefly, cells were grown to 80% confluence. Following growth arrest samples were treated with serum-free DMEM/F12, containing either TGF-β_1 (10ng/ml) or IL-1β (1ng/ml). Control fibroblasts were treated with fresh serum-free medium alone. Total cell lysate was extracted and analysis was carried out using immunoprecipitation of CD147, followed by Western blot analysis for CD44 and CD147. ***Figures [C&D]*** demonstrate the densitometry analysis of co-localisation following TGF-β_1 ***[C]*** and IL-1β ***[D]***. Data represents a single experiment using two samples ± S.D.

5.4.3. –CD147 Involvement in IL-1β Mediated Monocyte Binding

CD147 was significantly upregulated in IL-1β-induced, fibroblasts (***Figure 5.4. [B])***, suggesting that CD147 may have a role in fibroblast-monocyte binding. However, it is well-established that the HA/CD44 is central to monocyte binding and IL-1β stimulation did not increase co-localisation of CD147 with CD44 in fibroblasts (***Figure5.5. [B])***. However, monocyte binding is not solely HA/CD44-dependent, it also involves the increased co-localisation of CD44 with ICAM-1, a cell adhesion molecule previously shown to be important for leukocyte binding and signalling (Walpola et al. 1995). Therefore, it may be assumed that ICAM-1 associates with CD147; and not CD44. To investigate this possibility, two separate co-IP experiments were carried out for CD147 and ICAM-1. The co-IP for ICAM-1 and Western blot analysis of CD147 determined that ICAM-1 did associate with CD147 ***(Figure 5.6. [A])***. This was confirmed by the reciprocal experiment, where a co-IP was carried out for CD147, followed by a Western blot analysis for ICAM-1 (***Figure 5.6. [B])***. There was no difference observed in the CD147/ICAM-1 co-localisation by IL-1β-stimulated fibroblasts, compared to unstimulated fibroblasts. Therefore, although CD147 mRNA expression increased in IL-1β stimulated fibroblasts (***Figure 5.4. [B])***, the lack of increased CD147/CD44 or CD147/ICAM-1 association, suggests it is unlikely to have a role in monocyte binding. A final experiment which knocked down CD147 expression was carried out, to determine if CD147 had a functional role in monocyte binding, which may be mediated through a different mechanism. Knockdown was achieved using a siRNA targeting CD147 (***Figure 5.6. [C])*** and monocyte binding was assessed using CD45 ***(Figure 5.6. [D])***. Silencing CD147 did not have any effect on IL-1β induction of fibroblast-monocyte binding. Therefore, combining all the data from ***(Figure 5.3.)***, it has been concluded that CD147 does not seem to have a role in IL-1β-induced monocyte binding, through the pre-determined HA/CD44/ICAM-1 pathway or any

other mechanism. Therefore, the effects of CD147 on monocyte binding has not been further analysed in this study.

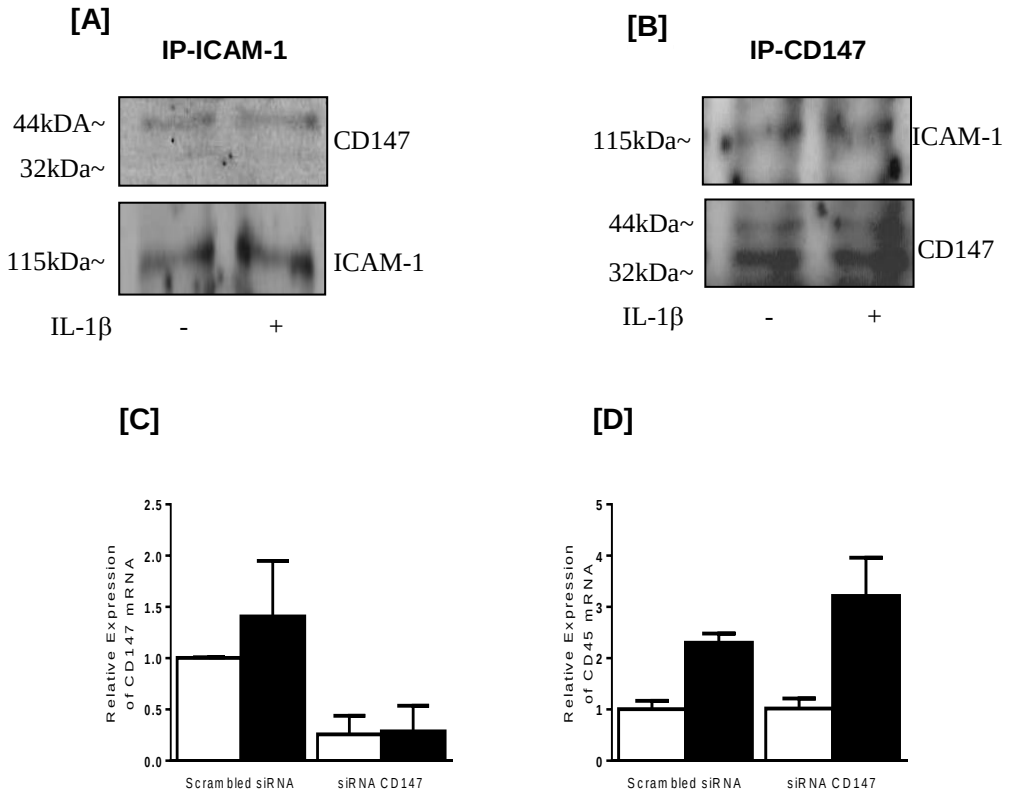

Figure 5.6. – CD147 has no Role in IL-1β/HA/CD44/ICAM-1 Fibroblast -Monocyte Binding

Fibroblasts were grown to approximately 80% confluence and growth-arrested, before being treated with fresh serum-free DMEM/F12, containing IL-1β (1ng/ml) or serum-free DMEM/F12 alone for 72 h. The protein was extracted and co-localisation was assess using immunoprecipitation and Western blot analysis. ***Figure [A]*** shows the IP of ICAM-1 followed by a Western blot analysis for CD147. ***Figure [B]*** is the reciprocal experiment, with an IP carried out for CD147 and a Western blot analysis for ICAM-1. ***Figure[C]*** shows the decreased expression of CD147 in fibroblasts following transfection with a siRNA to CD147. A scrambled siRNA was used as a control. Following transfection, fibroblasts were growth-arrested and treated with fresh medium alone (control samples) ***(White bars)*** or medium containing IL-1β (1ng/ml) ***(black bars)*** for 72 h. Fresh DMEM/F12 containing $1x10^6$/ml of U937/monocytes was added and incubated for 4 h. Cultures were carefully washed before analysis. CD147 knockdown was confirmed ***Figure 5.5[C]***, before assessment of monocyte binding by qPCR ***Figure 5.5[D].*** Data represents a single experiment 3 separate samples ±S.D.

5.4.4. – Further Evidence for CD147/CD44 Co-localisation in Myofibroblasts.

Previously, it was determined that there was an increased CD147/CD44 co-localisation in myofibroblast compared to fibroblasts ***(Figure 5.5)***. Recent research by Grass et al. (2013) implicated CD147 in breast cancer invasion, by promoting EGFR downstream activation of ERK1/2 signalling; a process dependent on HA/CD44 association. It was determined that CD147 formed a complex with CD44 and EGFR in lipid raft regions. This is similar to previous research in our laboratory that showed the importance of the CD44/EGFR association in lipid rafts and subsequent downstream activation of ERK1/2, for complete fibroblast to myofibroblast differentiation (Midgley et al. 2013).

The co-localisation of CD147/CD44 previously observed was confirmed using immunocytochemistry (ICC). ***Figure 5.7*** shows the ICC analysis used to investigate the association of CD147 (green stain) with CD44 (red stain). Both CD147 and CD44 were abundantly expressed throughout the cell membrane in fibroblasts ***[A-B]*** and myofibroblasts ***[C-D]***. Merger of the two images showed two distinct populations in fibroblasts. The first showed CD147/CD44 merging (***Figure 5.7. [C-D]***; yellow regions). The second had CD147 (green regions) alone diffusely spread throughout the membrane (***Figure 5.7. [C-D]***; white arrow). Conversely, myofibroblasts had complete CD147/CD44 co-localisation ***(Figure 5.7. [G-H])***; and separate populations were no longer observed. These data confirm co-IP results previous obtained (***Figure 5.4. [A])***; and demonstrate an increased CD147/CD44 co-localisation in myofibroblasts.

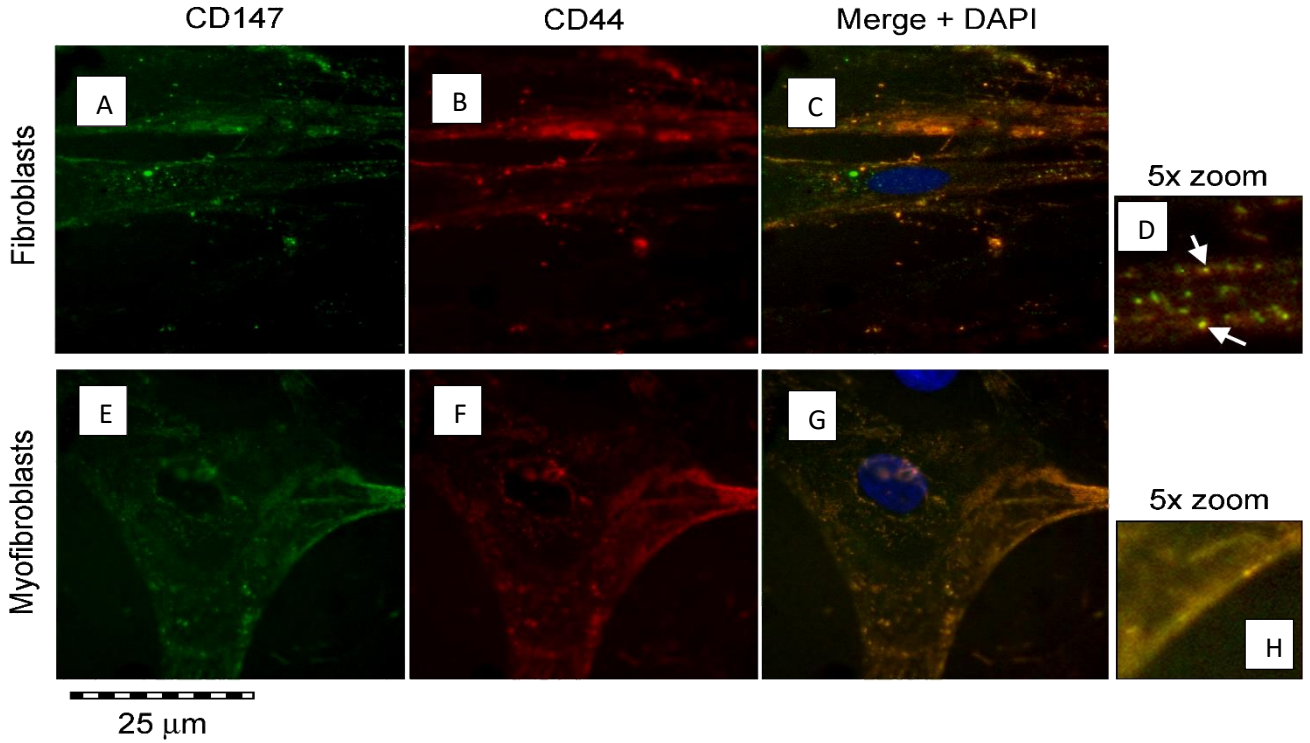

Figure 5.7. – Confirmation of CD147/CD44 Co-localisation in Myofibroblasts

Immunocytochemistry analysis, demonstrating CD147/CD44 co-localisation on the membrane of fibroblasts ***[A-D]*** and myofibroblasts ***[E-H]***. Fibroblasts were grown to approximately 50% confluence in DMEM, containing 20% v/v FCS. Following growth arrest, cells were treated with serum-free DMEM containing TGF-β_1 (10ng/ml) or fresh serum-free DMEM/F12 alone (control fibroblasts), for 72 h. Cells were fixed and analyse using immunocytochemistry. Images show ICC florescence staining of: CD147 green stain [A&E], CD44 (red stain [B&E]; and merged staining [C, D, G and H]. Original magnification x400

5.4.5. – Assessment of CD147 Association With EGFR in Myofibroblasts

Previously, it was reported that CD147 co-localised with CD44 and EGFR in TGF-β_1-stimulated, breast cancer cells. The co-localisation of these three surface receptors contributed to increased invadapodia, dependent on ERK1/2 (Toole and Slomiany 2008). Investigation of CD147/EGFR co-localisation in fibroblasts (green stain) and myofibroblasts (red stain) was carried out by ICC. Following merger of CD147 (***Figure 5.8. [A])*** with CD44 ***(Figure 5.8. [B])***, fibroblasts demonstrated total CD147/CD44 co-localisation (***Figure 5.8. [C&D]***; yellow merge). Conversely, myofibroblasts (***Figure 5.8. [D-G])*** showed no co-localisation of CD147 (green stain) (***Figure 5.8. [E])*** with EGFR (red stain) ***(Figure 5.8. [F])***; and two distinct populations were observed throughout the plasma membrane ***(Figure 5.8. [G-H])***.

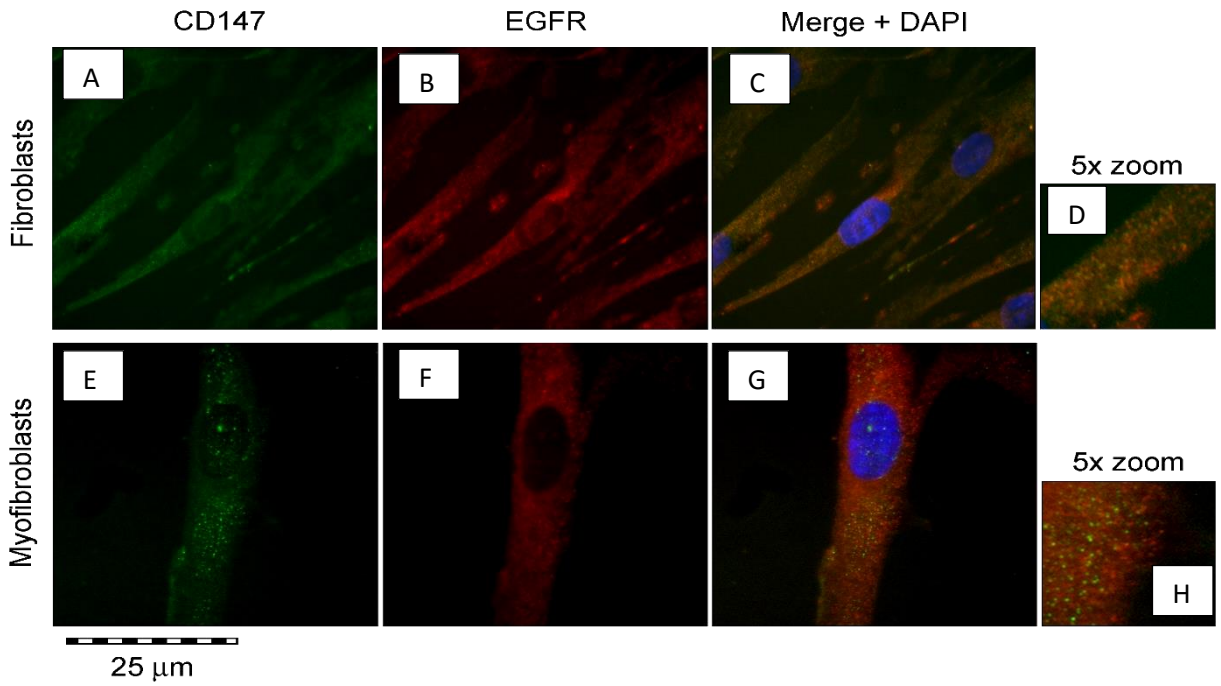

Figure 5.8. - CD147 Co-localises With EGFR in Fibroblasts, But Not Myofibroblasts

Immunocytochemistry analysis demonstrating CD147/EGFR co-localisation on the membrane of fibroblasts ***[A-D]*** and myofibroblasts ***[E-H]***. Fibroblasts were grown to approximately 50% confluence in DMEM containing 20% v/v FCS. Following growth arrest cells were treated with serum-free DMEM, containing TGF-β_1 (10ng/ml) or fresh serum-free DMEM/F12 alone (control fibroblasts), for 72 h. Cells were fixed and analyse using immunocytochemistry. Images show ICC florescence staining of: CD147 (green stain [A&E]), EGFR (red stain [B&E]); and merged staining [C, D, G and H]. Original magnification x400

5.4.6. – Expression of CD147 Glycosylated Forms in Fibroblasts and Myofibrobasts

CD147 exists in multiple glycosylated forms that mediate different functions and are variable expressed between cell types (Bai et al. 2014). Therefore, it may be speculated that a specific glycosylated form of CD147 co-localises with CD147 in myofibroblasts. Identification of the glycosylated forms could also suggest a specific functional role. Western blot analysis of fibroblasts and myofibroblasts identified two bands of a 32 and 44kDa molecular mass ***(Figure 5.9. [A])***; suggesting that a LG-CD147 (32 kDa) and a HG-CD147 (44 kDa) form of CD147 was expressed in fibroblasts and myofibroblasts. Quantification of the bands using densitometry analysis (sample density was normalised using a corresponding GAPDH control), compared the expression of each glycosylated CD147 form between fibroblasts and myofibroblasts ***(Figure 5.9. [B])***. There was no significant difference of LG-CD147 between fibroblasts and myofibroblasts, suggesting that this LG-CD147 is equally expressed in both cell types. Analysis of HG-CD147, however, showed a significantly increased expression in myofibroblasts, compared to fibroblasts. Therefore, it may be assumed from this data the higher glycosylated form of CD147 out of the two forms identified, has an increased expression in TGF-β_1-induced myofibroblasts.

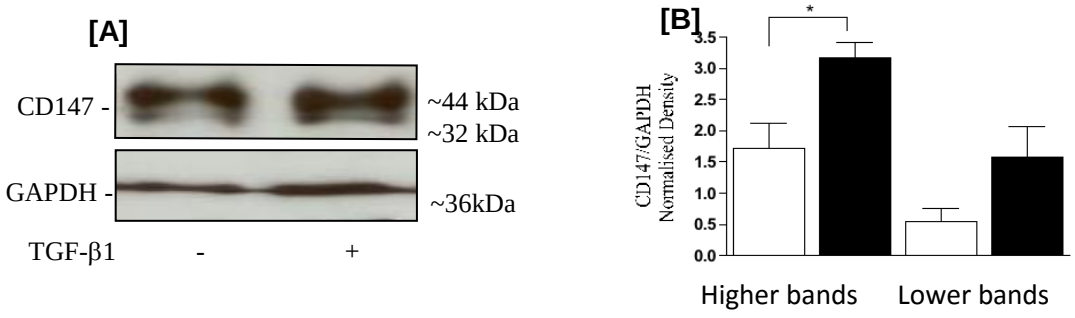

Figure 5.9. Expression of Glycosylated Forms of CD147 in Fibroblasts and Myofibroblasts

Analysis of glycosylated forms of CD147 expressed by fibroblasts and myofibroblasts. Fibroblasts were grown to approximately 80% and growth-arrested. Fresh serum-free DMEM/F12 alone (control samples) or containing TGF-β_1 (10ng/ml), was the added for 72 h. Total protein was extracted and samples were separated using SDS-PAGE and analysed by Western blot. ***Figure [A]*** shows the Western blot identification of 2 bands LG-CD147 ***(~32kDa)*** and HG-CD147 ***(~44kDa)***. ***Figure [B]*** is the densitometry analysis of CD147 bands normalised to the corresponding GAPDH control. Graph shows the density analysis of both the HG-CD147 ***(higher bands)*** and LG-CD147 ***(lower bands)*** of CD147, in both fibroblasts ***(white bars)*** and myofibroblasts ***(black bars)***. Data is displayed as ±SEM from 3 separate experiments. Statistical analysis was carried out using One way ANOVA, followed by the student's unpaired *t* test *P <0.05.

5.4.7. – CD147 Distribution Throughout the Plasma Membrane

The HA mediated co-localisation of CD44/EGFR in lipid raft regions has been demonstrated as essential for αSMA induction and terminal myofibroblast differentiation (Midgley et al. 2013). This study has identified that CD147/CD44 association is increased in myofibroblasts, compared to fibroblasts ***(Figure 5.5. and 5.7.).*** To determine the association of CD147 with lipid raft regions within the cell membrane, ICC was used to analyse CD147 distribution in the plasma membrane of fibroblasts and myofibroblasts ***(Figure 5.10. [A-H])***.

ICC analysis using cholera toxin B (CTX-B), a lipid raft marker (red stain); and CD147 (green stain), was carried out in fibroblasts ***(Figure 5.10. A-D)*** and myofibroblasts ***(Figure 5.10. E-H).*** CD147 was situated mainly in lipid raft regions in fibroblasts and merger of CD147 ***(Figure 5.10. [A])*** with *CTX-B* ***(Figure 5.10. [B])***, observed almost complete co-localisation ***(Figure 5.10. [C-D];*** yellow merge***)***. Myofibroblasts had partial CD147/CTX-B co-localisation and merger of CD147 ***(Figure 5.10. [E])*** with *CTX-B* ***(Figure 5.10. [F])***, revealed small clusters of co-localisation (white arrows) ***(Figure 5.10. [G-H]),*** compared to the complete co-localisation observed in fibroblasts. These data suggest that a population of CD147 may relocate from raft regions to non-raft regions when TGF-β_1-stimulated, to give 2 distinct populations of CD147.

One form of lipid raft that has previously been identified as important for CD44/EGFR co-localisation in myofibroblasts, are caveolae. These are abundantly expressed flask-shaped, lipid rafts, containing various lipids and caveolin (Quest et al. 2004; Tang et al. 2004). CD147 is widely accepted to associate with Cav-1 and it has been demonstrated that the association regulates CD147 functions (Tang et al. 2004). To investigate CD147 association with Cav-1 in fibroblasts and myofibroblasts, a gradient fractional analysis of the membrane was performed. Fractions 5-10 were identified as containing CAV-1 (band MW ~21kDa). Fractions 9-10 were identified as non-lipid raft regions, using early endosomal antigen 1 (EEA-

1) as a marker (band MW ~170 kDa). The position of CD147 within the membrane was assessed in fibroblasts (***Figure 5.11. [A])*** and myofibroblast ***(Figure 5.9. [B])***.

CD147 was observed to be situated in fractions 5-8 in fibroblasts, these were all Cav-1 associated regions. Fractions 5-7 were previously determined to be lipid raft regions. This suggests that the majority of CD147 is present in lipid raft regions in fibroblasts. There were two distinct populations of CD147 throughout the membrane observed in myofibroblasts. The first was detected by a single band in fraction 7 (a pre-determined raft region). Two further bands were located within fractions 9 and 10 (both pre-determined non-raft regions) ***(Figure 5.11 [B])***. These data are consistent with the previous ICC analysis in ***(Figure 5.5 [A]),*** that also identified two distinct populations of CD147; that existed in and out of lipid raft regions.

It was previously identified that there were two glycosylated forms of CD147 in fibroblasts and myofibroblasts ***(Figure 5.9 [A-B]***). Interestingly, fibroblasts and myofibroblast analysis observed a single band with a molecular mass of approximately 44kDa. This suggested that is the HG-CD147 form that associates with the plasma membrane. It was previously demonstrated that CD44 is expressed diffusely throughout the plasma membrane in fibroblasts, but is more associated with caveolae rafts in myofibroblasts. Moreover, the CD44 identified had a molecular mass between 80-95kDa, suggesting it was CD44s (Midgley et al. 2013). Previously in this study, it was suggested that it was CD44s that co-localised with CD147 ***(Figure 5.5 [A])***. Analysis of CD44s (bands 80-95kDa) in fibroblasts and myofibroblasts were consistent with previous findings and the majority of CD44s was observed to be present within caveolin regions in myofibroblasts ***(Figure 5.11 [B])***. However, there was a small proportion of CD44 in fraction 10 (a pre-determined non-raft region). Interestingly, these data observed CD147 and CD44s to be situated in the same membrane fractions, in and out of caveolae regions, in myofibroblasts.

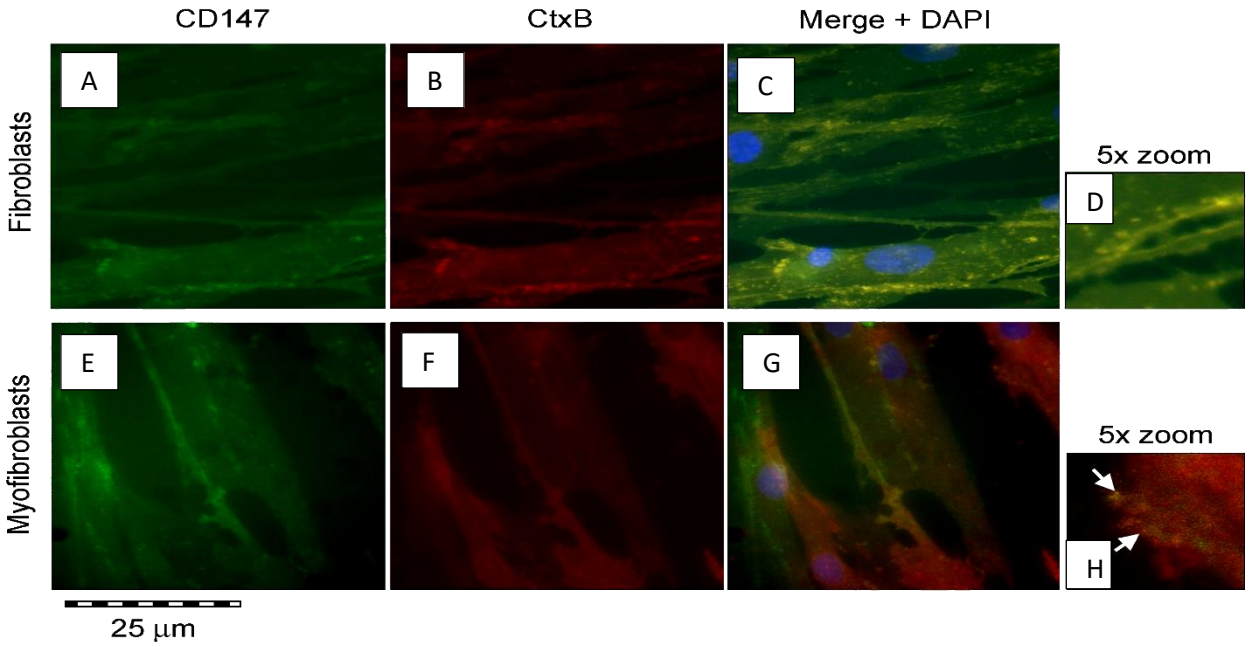

Figure 5.10 – CD147 Association With Lipid Rafts

CD147 association with lipid rafts was analysed using ICC. Fibroblasts were grown to 80% and growth-arrested. Cells were then treated with serum-free DMEM/F12, containing TGF-β_1 (10ng/ml) or serum-free DMEM/F12 alone (control fibroblasts); and incubated for 72 h. Cells were fixed and stained before analysis...Images show CD147 (green stain) and CTX-B (red stain) in fibroblasts ***[A-D]*** and myofibroblasts [E-H]. Co-localisation can be observed as yellow stain, resulting from image merger. White arrow ***[H]*** show regions of CD147/CTX co-localisation. Images are representative pictures of cell populations Magnification x 400.

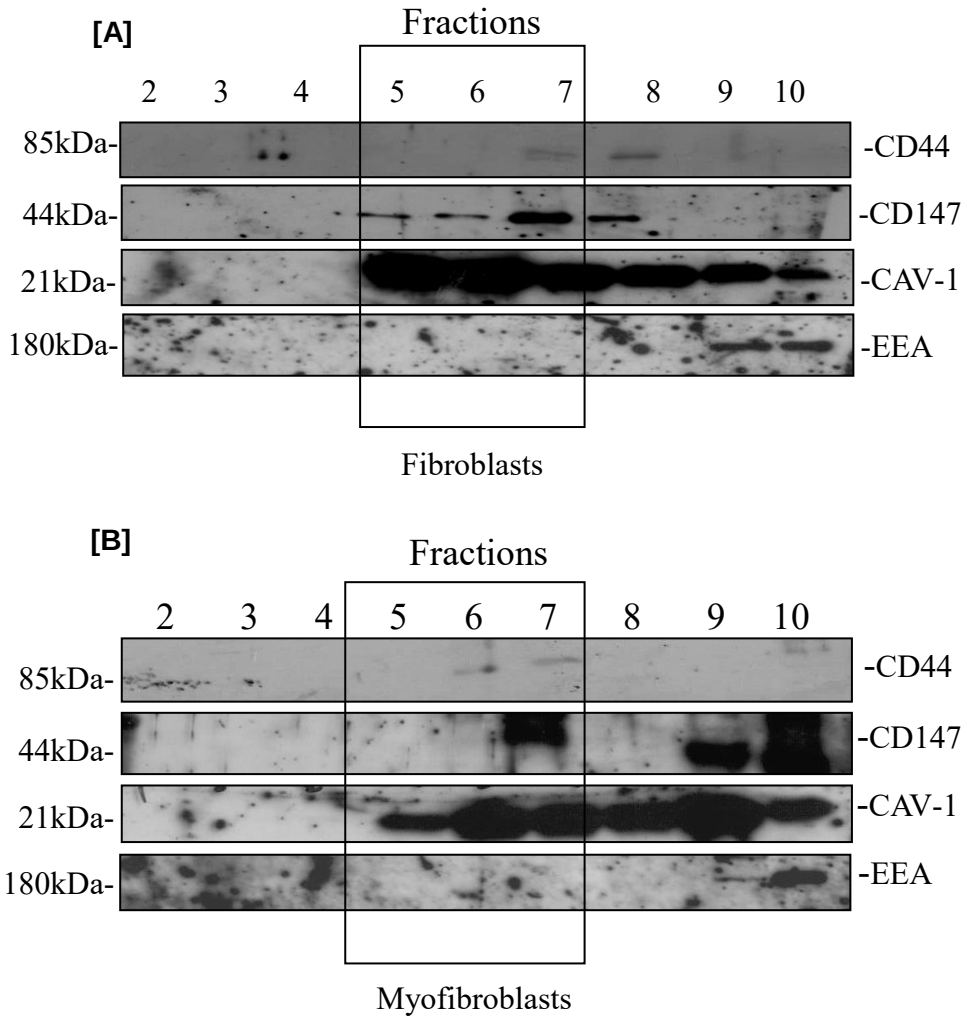

Figure 5.11 – CD147 Association with Caveolae Rafts

The caveolae raft isolation was performed using a Caveolae/Raft Isolation Kit (Sigma-Aldrich). Fibroblasts were grown to 80% confluence and growth-arrested, before being treated with in serum-free medium containing TGF-β_1 (10ng/ml) or fresh serum-free medium alone (control fibroblasts), for 72 h. Fractions were separated using SDS-PAGE. Images show Western /blot analysis for fractions 2-10 in fibroblasts ***[A]*** and myofibroblasts ***[B]***

5.4.8. - CD147 Regulation of αSMA

Previous studies demonstrated that silencing total CD44 decreased αSMA mRNA and protein expression, preventing fibroblast differentiation (Simpson et al. 2009; Midgley et al. 2013). This study has identified that CD44/CD147 co-localisation increased in myofibroblasts, suggesting that the CD147/CD44 co-localisation may also be essential for αSMA expression. Following knockdown of CD147, the mRNA and protein expression of αSMA was analysed. A scrambled siRNA was used as a control.

Silencing CD147 mRNA ***(Figure 5.12 [A])*** expression had no significant effect on myofibroblasts αSMA expression ***(Figure 5.12 [B])***, when compared to myofibroblasts transfected with the scrambled control.

Fibroblasts transfected with the siRNA to CD147 did not express large amounts of αSMA protein and had identical morphology to fibroblasts transfected with the scrambled control siRNA (***Figure5.13 [A&C])***. Myofibroblasts transfected with the scrambled siRNA formed distinct αSMA stress fibres, commonly associated with the myofibroblasts phenotype ***Figure 5.13[B]***. Interestingly, myofibroblasts that had previously been transfected with a siRNA to CD147 had an increased αSMA expression, compared to fibroblasts. However, αSMA stress fibres that are a common characteristic of myofibroblasts did not form in the usual uniform manner and αSMA was randomly situated throughout the myofibroblasts, leading to incomplete fibre formation (***Figure 5.13[D]***. Interestingly, total αSMA protein expression did not decrease following silencing of CD147 in myofibroblasts transfected with the siRNA, compared to those transfected with the scrambled siRNA ***(Figures 13 [E-F])***. These data, therefore, indicate that CD147 does not have a role in αSMA transcription or translation, but is more associated with the incorporation and polymerization of αSMA into stress fibre bundles.

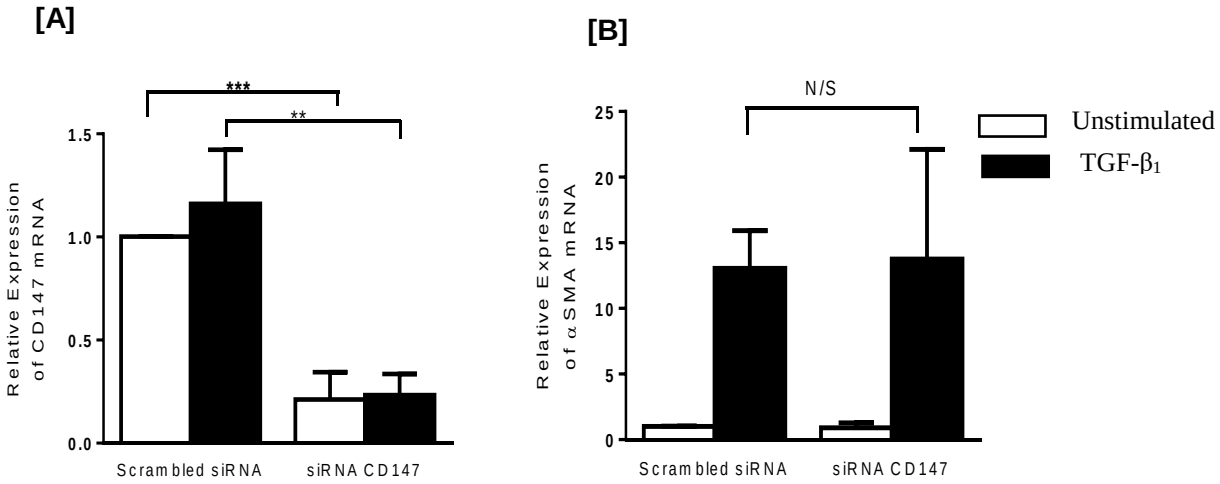

Figure 5.12. - Silencing CD147 Had no Effect on αSMA mRNA Expression

Data compares the expression of αSMA in fibroblasts ***(white bars)*** and myofibroblasts ***(black bars)***, following transfection with a siRNA targeting CD147. Control fibroblasts were transfected with a scrambled control siRNA. Following transfection, the cells were treated with serum-free DMEM/F12 (control fibroblasts) or serum-free DMEM/F12 containing TGF-β_1 (10ng/ml), for 72 h. Samples were analysed using qPCR. ***Figure [A]*** demonstrates the significant knock down of CD147 mRNA expression and ***[B]*** shows the expression of αSMA expression. Data is representative of 3 individual experiments ± SEM. Statistical analysis was carried out using the one way ANOVA, followed by the unpaired student's *t* test. **P<0.01, ***P<0.001, N/S (not significant).

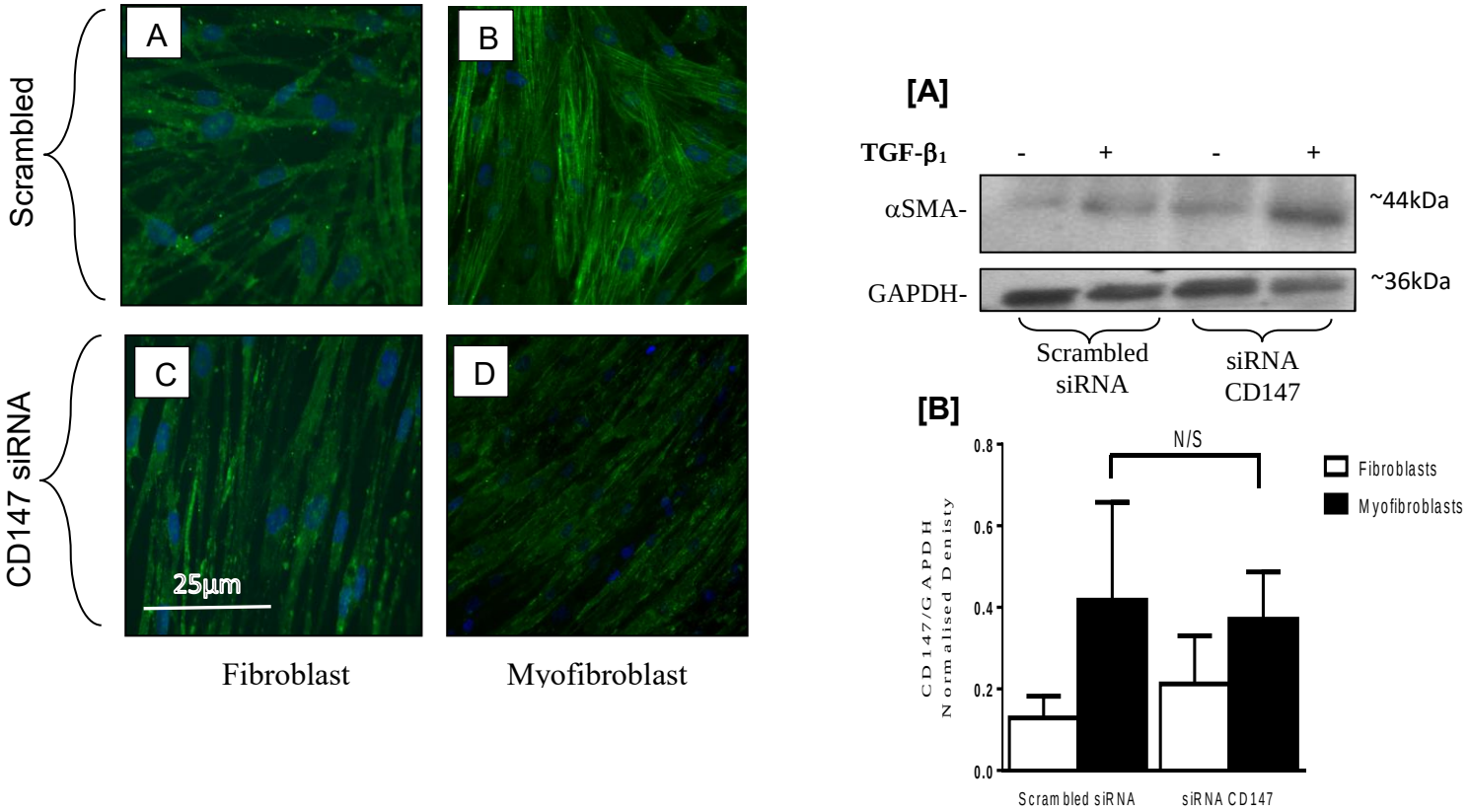

Figure 5.13 – siCD147 Prevents the Formation of αSMA Stress Fibres

To visualise αSMA stress fibres, fibroblasts were grown to 50% confluence before growth arrest. Cells were then transfected with siRNA to CD147 or a siRNA scrambled control for 72 h, before being treated with serum-free DMEM (controls) or serum-free DMEM containing TGF- β_1 (10ng/ml). Following a further 72 h incubation period, cells were fixed and analysed using ICC or extracted for Western blot analysis. A representative picture was taken of each cell population under each condition. Images show fibroblasts transfected with ***[A]*** scrambled control or ***[C]*** siRNA to CD147 and myofibroblasts transfected with ***[B]*** scrambled control and ***[D]*** siRNA to CD147. Data is representative of two individual experiments. Original magnification x 400. Figure ***[E]*** shows Western blot analysis of αSMA and GAPDH used as a loading control. Densitometry analysis was carried out normalising αSMA density to GAPDH density ***[F]***. Experiment represents three individual experiments ± SEM. N/S (not significant).

5.4.9. -CD147 Transcriptional Regulation of Differentiation Mediators

Silencing CD147 failed to prevent αSMA transcription or translation. Combining this data with previous data that identified a lack of CD147/EGFR association, suggests CD147 does not have a role in the TGF-β_1-induced pathway. To confirm this, the transcriptional regulation of another mediator known to be essential for terminal differentiation were assessed. Both TSG-6 and TGF-β1 have an increased expression, following TGF-β_1 activation (Simpson et al. 2009; Webber et al. 2009b). Following knockdown of CD147 ***(Figure 5.14. [A])***, the expression of these two mediator were assessed. There was no effect on the auto-induction of TGF-β_1 ***(Figure 5.14. [B])*** or TSG-6 mRNA expression ***(Figure 5.14. [C])*** in fibroblasts transfected with the siRNA to CD147, compared to fibroblasts transfected with a scrambled control. A further analysis examined the role of CD147 on the transcriptional regulation of EGFR. The analysis determined that CD147 did not regulate EGFR transcription ***(Figure 5.14. [D])***. These data conclude that CD147 does not seem to directly induce the TGF-β_1-dependent differentiation pathway. Therefore, the lack of stress fibre formation following CD147 knockdown and the CD147/CD44 co-localisation previously observed, suggest that CD147 may have a more indirect regulation of differentiation, by mediating the correct mechanical tension required for SMA incorporation. Therefore, the rest of this study focused on the involvement of CD147 a mechanotransduction mediator.

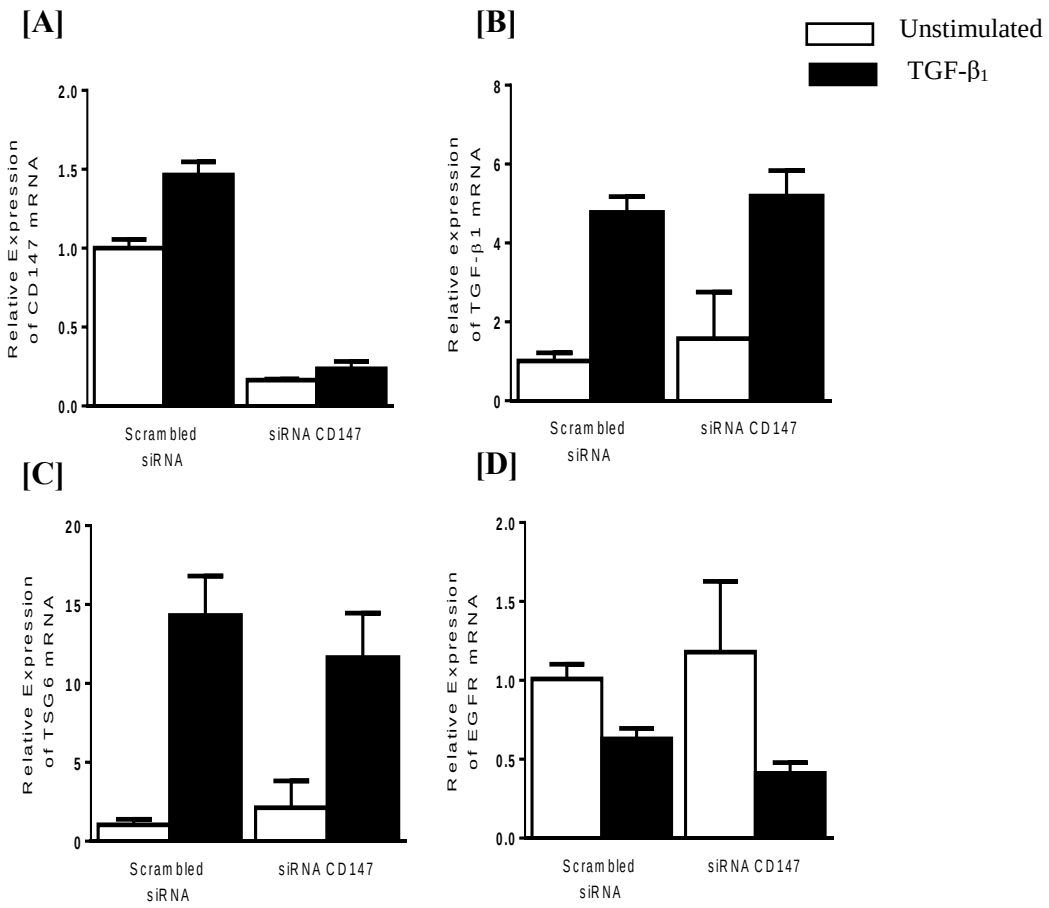

Figure 5.14. – CD147 Does Not Regulate TGF-β1-Induced Mediators

Analysis of CD147 knockdown ***[A]*** on TGF-β1-induced differentiation mediators, TGF-β1 ***[B]***, TSG-6 ***[C]*** and EGFR ***[D].*** Data compares their expression in fibroblasts ***(white bars)*** and myofibroblasts ***(black bars)***, following transfection with a siRNA targeting CD147. Control fibroblasts were transfected with a scrambled control siRNA. Following transfection the cells were treated with serum-free DMEM/F12 (control fibroblasts) or serum-free DMEM/F12, containing TGF-β1 (10ng/ml), for 72 h. Samples were analysed using qPCR. Data is representative of a single experiment consisting of 3 separate samples ± S.D.

5.4.10. - CD147 Mediation of Myofibroblast Contraction

The expression of αSMA stress fibres and is often associated with the contractile phenotype of myofibroblasts (Hinz et al. 2001). The lack of uniform stress fibre formation in myofibroblasts transfected with siRNA targeting CD147, suggested that the contractile ability of the myofibroblasts would be impaired. Using collagen gels, the effect of silencing CD147 on the contractile ability of myofibroblasts was assessed. The percentage decrease of the collage area was calculated at each time point by subtracting the total area from untreated fibroblasts at 0

h. ***Figure 5.15.*** shows the images of the contraction gels that were seeded with fibroblasts and transfected with a scrambled control siRNA ***[A-C]*** or a siRNA targeting CD147 ***[D-E]***.

Following 72 h of TGF-β_1 stimulation, there was a decrease area of ~14.5% in collagen gels transfected with the scramble control siRNA ***(Figure 5.15.[B])***. A further 18.5% decrease was observed between 72 h and 144 h of TGF-β_1 stimulation, giving a total percentage decrease of ~33% compared to unstimulated fibroblasts at 0 h ***(Figure 5.15. [C])***. Cells transfected with the siRNA targeting CD147 had a decreased gel area of ~22.5% following 72 h of TGF-β_1 stimulation ***(Figure 5.15. [E])***. A small decrease observed of 2.8% was observed between 72 h and 144 h of stimulation with TGF-β_1, indicating that contraction ability had been reduced in fibroblasts transfected with a siRNA to CD147, when compared to fibroblasts transfected with the scrambled siRNA ***Figure 5.15. [F]***. The protein expression of CD147 is not totally silenced until 144 h, following transfection with the siRNA ***(Figure 5.2 [B])***. Therefore, that contraction ability was functional at 72 h, suggests that the CD147 protein was no totally knocked down. The lack of uniform αSMA stress fibre formation in myofibroblast was also observed at 144 h, following transfection with siRNA to CD147 ***(Figure 5.13. [D]).*** It may, therefore, be assumed that the lack of contraction observed between 72 h and 144 h of TGF-β_1 stimulation, was the result of a decreased CD147 protein expression that limited αSMA stress fibres formation and functional contraction. ***Figure 5.15. [G]*** shows the percentage decrease of collagen gels seeded with fibroblasts that were transfected with either the scrambled control siRNA or a siRNA to CD147 at 72 and 144 h timepoints.

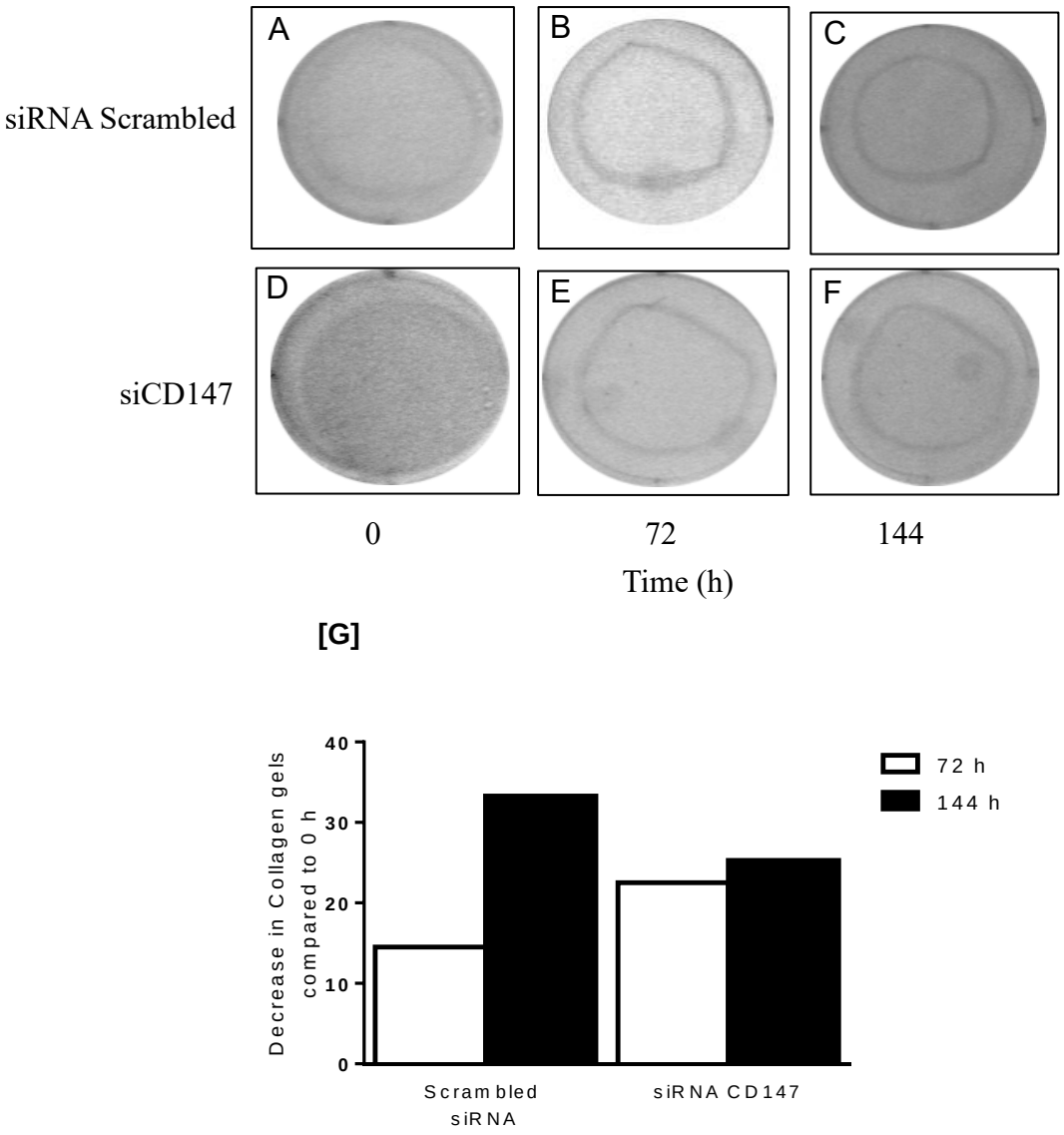

Figure 5.15. - Silencing CD147 Regulates Myofibroblast Contraction Ability

To assess the role of CD147 in the contraction ability of myofibroblasts, fibroblasts were seeded onto pre-made collagen gels and grown to 50-60% confluence. Following growth arrest, fibroblasts were transfected with a siRNA targeting CD147 or a scrambled control siRNA. Fibroblasts were further growth-arrested before being treated with serum-free DMEM/F12 alone ***(controls)*** or serum-free DMEM/F12, containing TGF- β1 (10ng/ml). Collagen gels were photographed at 0h, 72 h and 144 h, following TGF-β_1 stimulation. ***[A-C]*** show contraction gel of fibroblasts transfected with a scrambled control siRNA. ***[D-F]*** show fibroblasts transfected with a siRNA targeting CD147 ***[G]*** shows the percentage decrease at 72 h ***(black bars)*** and 144 h ***(white bars)***, compared to 0 h. Data represents a single experiment.

5.4.11. - CD147 and F-Actin Arrangement by Fibroblasts and Myofibroblasts

It is necessary for the F-actin cytoskeleton to remain intact and maintain the correct mechanical tension for αSMA subunits to become incorporated. HA/CD44 association mediates changes in the cytoskeleton arrangement and mechanical tension, through interaction with intracellular extracellular matrix (ERM) proteins, which mediates multiple cellular processes (Ponta et al. 2003). This study has shown an increased CD147/CD44 association and a distinct lack of αSMA stress fibre formation in fibroblasts, transfected with a siRNA to CD147. Therefore, it was hypothesised that silencing CD147 protein expression may alter the cytoskeletal interaction of CD44 with F-actin, resulting in a dysregulation of F-actin which prevented the effective polymerisation and incorporation of αSMA. To investigate this, F-actin arrangement was analyses in fibroblasts and myofibroblasts, following transfection with siRNA to CD147. The arrangement of F-actin fibres alters from fibroblast to myofibroblast. F-actin fibres in fibroblasts are arranged around the peripheral edge of the cell. Myofibroblast F-actin has a more cortical distribution of F-actin fibres. This can be observed in ***Figure 5.16. [A&B]***,which show the F-actin arrangement in fibroblasts ***[A]*** and myofibroblasts ***[B]***.

Fibroblasts and myofibroblasts transfected with the siRNA to CD147 (***Figure 5.16. [C-D])*** respectively, showed no difference in F-actin arrangement, compared to fibroblasts or myofibroblasts transfected with the scrambled control. The lack of disruption to the F-actin filaments suggests that silencing CD147 expression does not alter F-actin arrangement in myofibroblasts. This suggests that CD147/CD44 co-localisation is not central to CD44/F-actin association and does not contribute to the lack of αSMA incorporation into stress fibres.

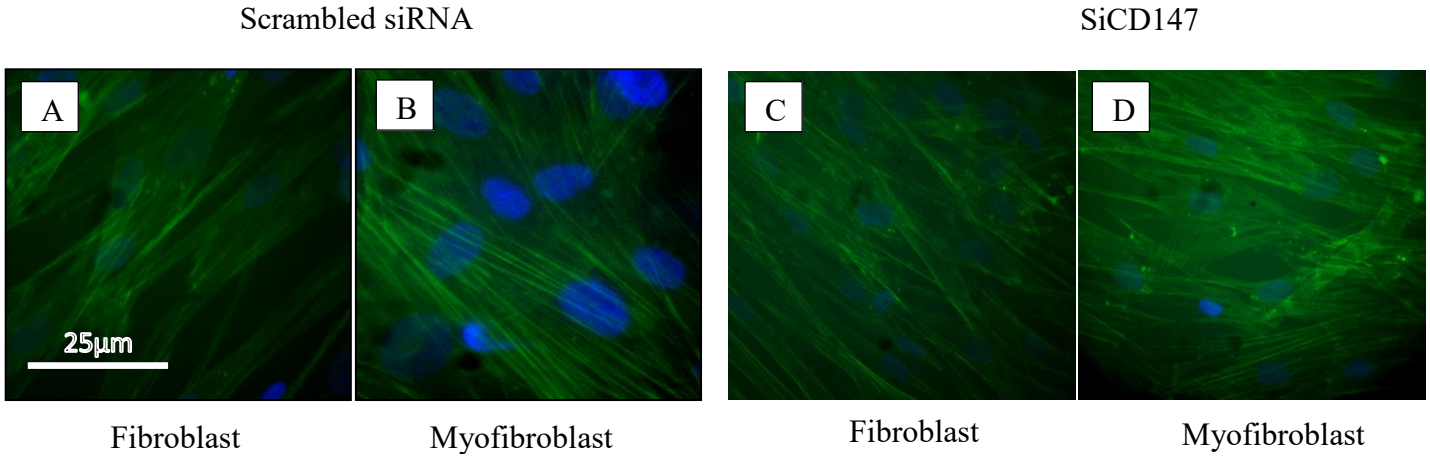

Figure 5.16. - Silencing CD147 Has no Effect on F-actin Arrangement

The effects of siRNA to CD147 on the cytoskeletal arrangement of F-actin arrangement was investigated. Fibroblasts were grown to 50% confluence in chamber and growth-arrested. Cells were transfected with siRNA to CD147 or a scrambled control siRNA. Following transfection and a further growth-arrested period, fibroblasts were treated with serum-free DMEM/F12 (controls) or serum-free DMEM/F12, containing TGF β_1 (10ng/ml), for 72 h. Cells were then fixed and analysed using ICC. Cells were visualised by florescent microscopy. A representative picture was taken of each cell populations under each condition. Images show fibroblasts transfected with ***[A]*** scrambled control or ***[C]*** siRNA to CD147 and myofibroblasts transfected with ***[B]*** scrambled control and ***[D]*** siRNA to CD147. Original magnification x 400.

5.4.12. – Investigation into CD147 Regulation of CD44s

Previously, it was identified that CD147/CD44 co-localisation increased in myofibroblasts (***Figure 5.5. [A])***. Further, the molecular weight of the CD44 at ~80-95kDa, suggested it was an increased CD147/CD44s co-localisation. It has been shown that CD44s can be cleaved within the transmembrane region, producing an intracellular domain (ICD) that regulates its own gene transcription and the gene expression of multiple other genes, including gelatinase (MMP-9) (Miletti-González et al. 2012). Moreover, MMP-9 cleaves CD44, resulting in the release of extracellular domains (ECDs) and ICDs (Chetty et al. 2012). CD147 is an inducer of MMP-9, suggesting that CD147/CD44s co-localisation upregulates MMP-9 activation and increases CD44s cleavage and elevates gene transcription from ICDs. More recently, TGF-β_1 stimulation has been shown to increase CD147 intracellular signalling of known fibrotic transcription factors, including SMAD2, co-SMAD4 and ERK1/2 (Li et al. 2015). Therefore, it could be suggested that CD44s and CD147 regulate the gene transcription of each other. To investigate this, the mRNA expression of CD147 and CD44s here analysed, following transfection with either a siRNA to CD44s or CD147 ***(Figure 5.17. [A-D])***.

Following the significant knockdown of CD147 ***(Figure 5.17. [A])*** and CD44s ***(Figure 5.17. [C])***, the expression of CD44s ***(Figure 5.17. [B])*** and CD147 ***(Figure 5.17. [D])*** was assessed. There was no effect on CD44s mRNA expression following silencing of CD147, compared to the scrambled controls. Similarly, there was no effect on CD44s expression in cells transfected with the siRNA targeting CD147. This concludes that the previously observed CD147/CD147 co-localisation is not central to mediating ICD regulation of each other.

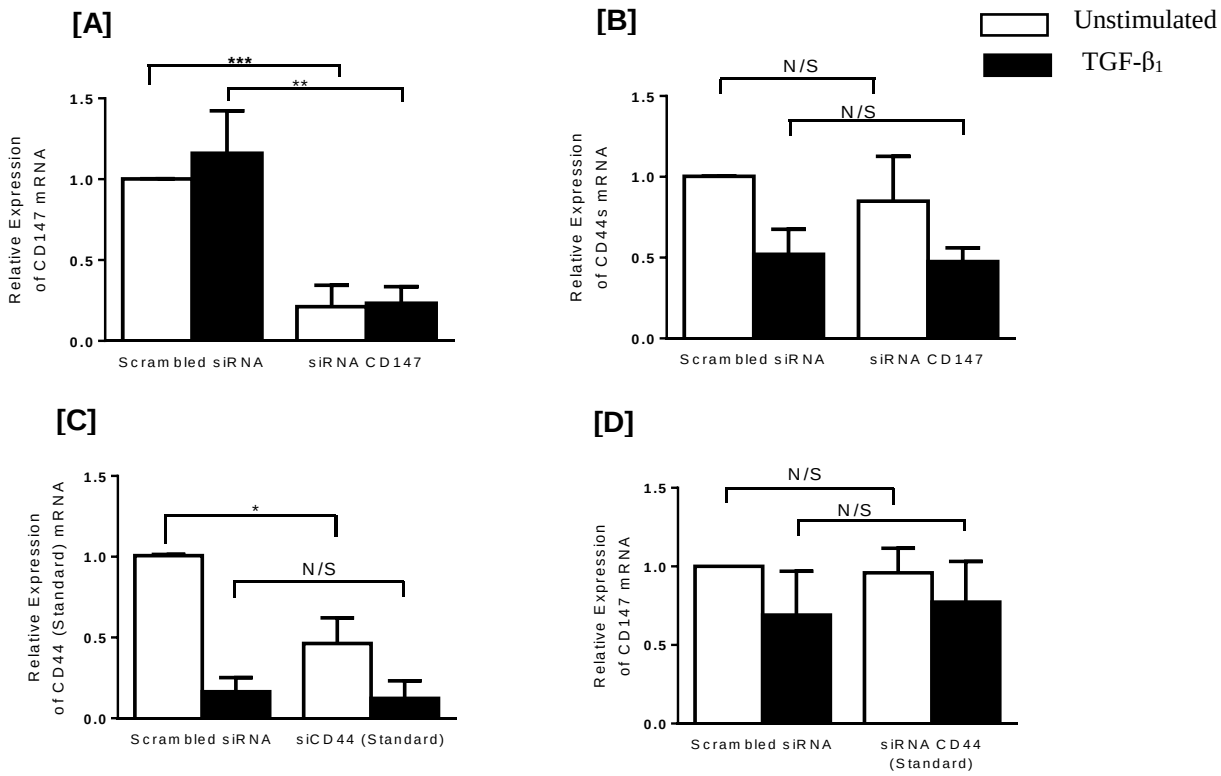

Figure 5.17. Analysis of CD147 and CD44s Gene Transcription

Fibroblasts were sub-cultured until 50-60% confluence and growth-arrested. Fibroblasts were transfected with siRNA targeting CD147 or siCD44s. A negative scrambled siRNA was used in control samples. Following a further growth arrest period, cells were treated with serum-free DMEM/F12 containing TGF-β_1 (10ng/ml) or serum free DMEM/F12 alone (control samples), for 72 h. Samples were analysed by qPCR. Figures [A&C] show the knockdown of CD147 and CD44s, respectively. Figure [D] shows the relative expression mRNA of CD44s, following transfection with siRNA to CD147. All data were comparative to scramble controls. Control fibroblasts *(white bars)* were compared to myofibroblasts *(black bars).* Data is displayed as ±SEM of three individual experiments. Statistical analysis was carried out using one way ANOVA followed by the unpaired student's *t* test. *P<0.05, **P<0.01, ***P<0.001, N/S (not significant).

5.4.13. – CD147 Regulation of TGF-β1 Induced EDA-Fibronectin Expression

Mechanical tension is an important factor regulating fibroblast to myofibroblast differentiation. A combination of supermature focal adhesion formation and increased cell-ECM and cell-cell contact increases the tensile strength of F-actin. The correct tension is essential for incorporation and polymerisation of αSMA, through its NH_2-terminal sequence, Ac-EEED (Chaponnier et al. 1995). EDA-fibronectin (EDA-FN) is essential for myofibroblast terminal differentiation, its upregulation precedes that of αSMA in proto-myofibroblasts. Lack of EDA-FN association prevents differentiation (Serini et al. 1998). Therefore, the CD147 regulation of EDA-FN was investigated.

Following significant knockdown of CD147 mRNA expression (***Figure 5.18. [A])***, the effects on EDA-FN expression were observed. Silencing CD147 did not have an effect on EDA-FN and a similar increase was observed in myofibroblasts transfected with the siRNA to CD147 that were observed in the scrambled controls (***Figure 5.18. [B])***.

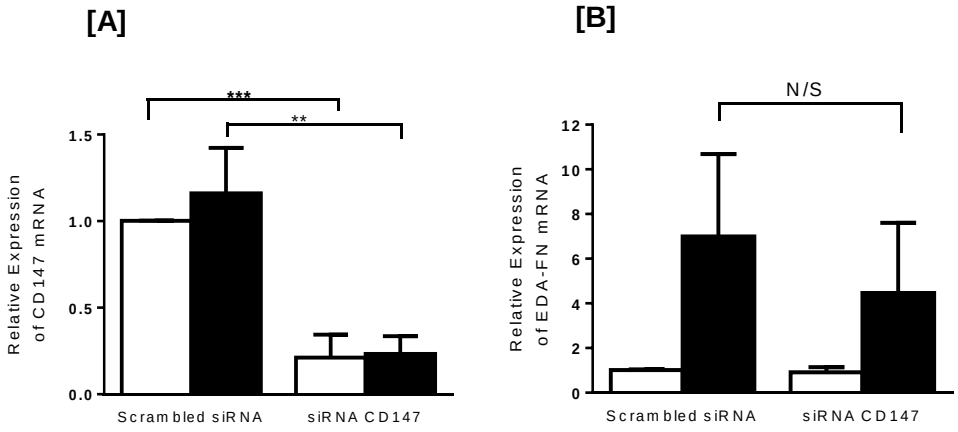

Figure 5.18. Knockdown of CD147 Does Not Affect TGF-β_1 Induction of EDA-Fibronectin by Myofibroblasts

To investigate CD147 regulation of EDA-FN, fibroblasts were grown to 50-60% confluence and growth-arrested. Cells were transfected with a siRNA targeting CD147 or a scrambled control siRNA. Following a further growth arrest period, fibroblasts were treated with serum-free DMEM, containing TGF-β_1 (10ng/ml) or serum-free DMEM/F12 alone (control samples). Samples were analysed using qPCR. ***[A]*** demonstrates the knockdown of CD147 mRNA expression in fibroblasts (white bars) and myofibroblast (black bars). [B] shows the mRNA expression of EDA-FN, following CD147 knockdown. Data is displayed as ±SEM of three individual experiments. Statistical analysis was carried out using one way ANOVA, followed by the student unpaired *t* test. **P<0.01, ***P<0.001, N/S (not significant).

5.4.14. - CD147 Co-localises with Integrin α4β7 in Myofibroblasts

The mechanical tension resulting from supermature focal adhesions is dependent on ECM-cell contact, for which EDA-FN/integrin association is essential (Hinz 2007). Recently, integrin α4β7/EDA-FN association was shown to mediated fibroblast to myofibroblast differentiation in an FAK- and ERK1/2-dependent manner (Kohan et al. 2010). CD147 is known to associate with and mediate the interactions of integrins, including their association with FAK (Tang et al. 2008b). Therefore, a CD147 association with integrin α4β7 was investigated using ICC ***(Figure 5.19 [A-F])***.

CD147 was highly expressed in fibroblasts and myofibroblast (green stain) (***Figures 5.19 [A&D]).*** Integrin α4β7 was also expressed in both fibroblasts and myofibroblasts (***Figures 5.19. [B&E].*** To identify CD147/α4β7 association, the images were merged. The merger of CD147 and integrin α4β7 in fibroblasts showed no co-localisation. This was confirmed by an Intensity Scattergram, that showed a mainly green intensity of the merged images ***(Figure 5.19. [G])***. This suggests that there is a higher expression of CD147 in fibroblasts, compared to myofibroblasts. Merger of myofibroblast images, however, did have a degree of co-localisation ***(Figure 5.19 [F])*** and the corresponding Intensity Scattergram had an equal expression of red and green intensity ***(Figure 5.19. [H])***. That CD147/α4β7 co-localised in myofibroblasts, suggests that the association may contribute to maintaining the correct tension for αSMA incorporation into F-actin fibers.

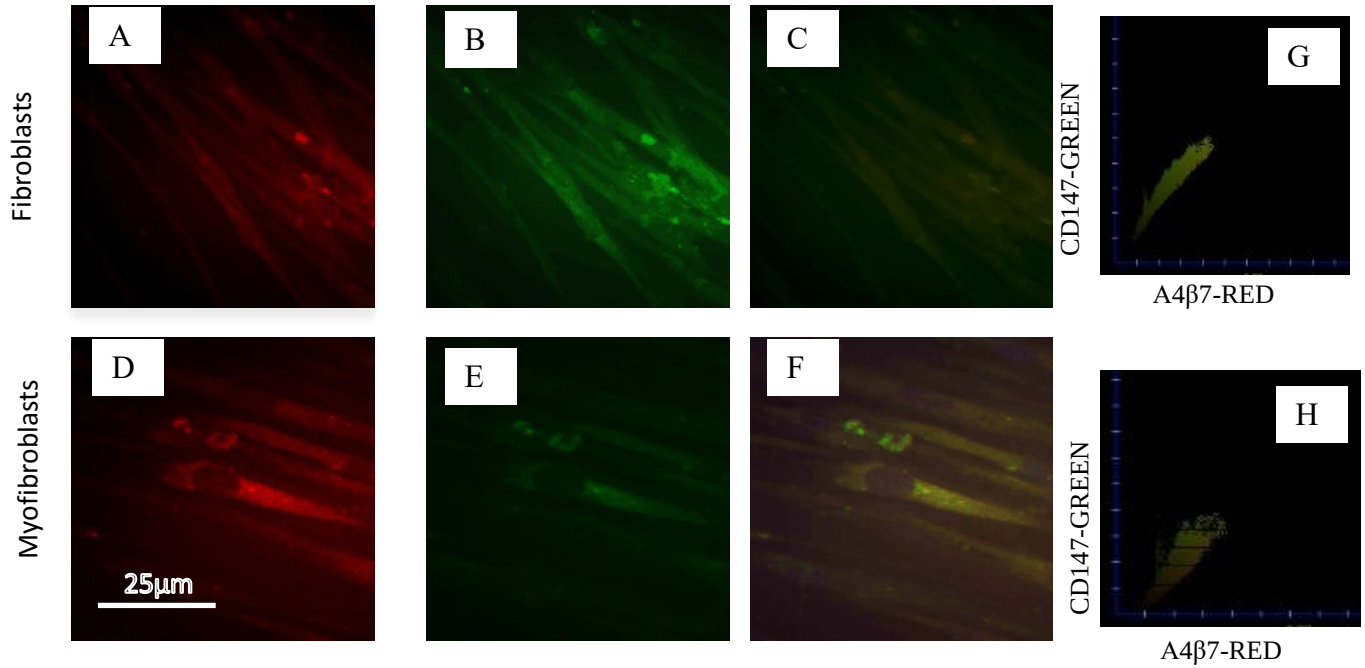

Figure 5.19. CD147 and Integrin α4β7 Co-localise in Myofibroblasts

CD147 co-localisation with integrin α4β7 was investigated using ICC. Cells were grown to 50% confluence and growth-arrested, before being treated with serum-free DMEM/F12, containing TGF-β_1 (10ng/ml) or serum-free DMEM/F12 alone (control), for 72 h. Figure ***[A-F]*** show the ICC analysis of fibroblasts ***[A-C]*** and myofibroblasts ***[D-F]*** and the analysis of CD147 ***(green stain)*** and integrin α4β7 ***(red stain).*** Intensity scatterplots were used to analyse merged images ***[C&F].*** Images are representative pictures of three individual experiments. Magnification x 400.

5.4.15. CD147 Regulates Intracellular ERK1/2 Activation

CD147, CD44 and integrin α4β7, have been identified to mediate downstream ERK1/2 following certain activation stimuli (Tolg et al. 2006; Toole and Slomiany 2008; Kohan et al. 2010; Midgley et al. 2013). Phospho-ERK1/2 activation has also been associated with mechanical tension, through HA/CD44 association with the cytoskeleton (Kawamura et al. 2003). This study has identified a decreased incorporation of αSMA into stress fibres, when CD147 expression is silenced. This may suggest that the association of CD147 with CD44 or α4β7, may regulate essential downstream signalling mediators that are important for the correct mechanical tension. Previous research in our laboratory demonstrated p-ERK1/2 to activate in a biphasic manner following TGF-β_1 stimulation, over a timecourse of 0-3 h. Therefore, these times have been used in this study.

ERK1/2 activation was investigated using Western blot of fibroblasts, transfected with a siRNA targeting CD147 or a scrambled control siRNA. Samples transfected with the scrambled control siRNA had a similar biphasic peak that was previously described (Meran et al. 2011a). There was an activation of p-ERK1/2 at 5 and 10 min, followed by a decreased p-ERK1/2 expression at 30 min. The second activation was observed at the 1 h time-point and was still present at 3 h. Silencing CD147 decreased p-ERK1/2 expression at all time-points, compared to the scrambled control, suggesting that CD147 has a regulatory role in p-ERK activation.

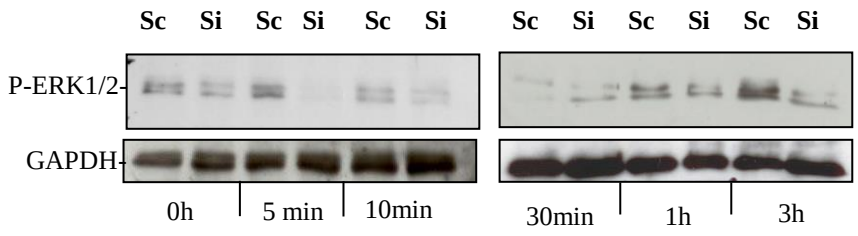

Figure 5.19. - CD147 Regulates Intracellular p-ERK1/2 Activation

Investigation of CD147 activation of p-ERK1/2. Fibroblasts were grown to 50-60% confluence and growth-arrested, before being transfected with a siRNA to CD147 or a scrambled siRNA for 144 h. Fibroblasts were stimulated with TGF-β_1 (10ng/ml), over a time course of 0-3 h. Samples were analysed using SDS-PAGE, followed by Western blot. Image shows p-ERK1/2 activation, following TGF-β_1 induction in fibroblasts transfected with a scrambled control siRNA ***(Sc)*** or a siRNA targeting CD147 ***(Si).*** Data is representative of 1 experiment.

5.5. -Discussion.

Chapters 3 and 4 identified which CD44 spliced variants were expressed by fibroblasts and determined that CD44s was the principle CD44 variant involved in TGF-β_1-induced, fibroblast differentiation and IL-1β-induced, monocyte binding. Central to both these mechanisms is CD44. This chapter investigated the association of CD44 with CD147/EMMPRIN, a MMP inducer, previously identified to induce breast cancer invasiveness through association with CD44 and EGFR in lipid rafts (Grass et al. 2013). Similarly, both CD44 and CD147 have an increased expression in prostate cancer and promote cell growth and metastasis, via intracellular ERK1/2 (Hao et al. 2012). Separately, CD44 and CD147 have been identified as mediators of fibrotic progression (Kato et al. 2011; Meran et al. 2013; Midgley et al. 2013). However, it is not known if CD147 has a role in the TGF-β_1-induced, HA/CD44/EGFR or IL-1β induction of HA/CD44/ICAM-1 pathways. This chapter investigates the role of CD147 in these two pathways.

This study identified that CD147 was highly expression in fibroblasts, however, this expression did not increase following stimulation with TGF-β_1. This suggested that TGF-β_1 did not regulate CD147 transcription in fibroblast differentiation. This is in contrast to previous reports that TGF-β_1 induced CD147 expression in corneal fibroblasts (Huet et al. 2008b). Interestingly, CD147 mRNA expression increased following IL-1β treatment. This study and previous studies have shown that fibroblast-monocyte binding is increased following IL-1β activation (Meran et al. 2013). Therefore, this suggests that the increased CD147 mRNA may be associated with monocyte binding.

CD147 and CD44 have both previously been associated with the activation of intracellular ERK1/2, which is known to be a mediator of cellular growth and survival (Roskoski Jr 2012). In prostate cancer cells, silencing the expression of either CD147 or CD44

separately, reduced invadapodia and intracellular ERK1/2 signaling (Hao et al. 2012). Further, the HA/CD44 association along with CD147 have been found to be fundamental in chemo-resistant treatments in some cancer cell lines and more recently, it has been shown that the increased growth and invasive properties of cancer cells is associated with a CD147/CD44 co-localisation (Toole and Slomiany 2008; Grass et al. 2013). This study determined that CD147/CD44 co-localised in fibroblasts. Interestingly, this association was increased in myofibroblasts, suggesting a regulatory role for TGF-β_1 in the association of these two receptors. Stimulation with IL-1β did not increase the CD147/CD44 co-localisation from that observed in quiescent fibroblasts. A pan-CD44 antibody that recognised all CD44 spliced variants determined that CD44s co-localised with CD147 preceding TGF-$\beta_1$stimulation. The CD147/CD44s co-localisation had previously been reported in pancreatic cancer. The study found that the CD147/CD44s association was observed in lipid raft regions of the plasma membrane and both receptors were required for intracellular activation for tumor growth (Li et al. 2013). Chapter 4 in this study identified CD44s as the principle CD44 variant involved in the TGF-β_1-induced, HA/CD44/EGFR and IL-1β-induced HA/CD44/ICAM-1 mechanisms. The CD147/CD44s co-localisation observed in this study suggests that CD44s associates with multiple other surface receptors in fibroblasts and myofibroblasts.

CD147/CD44 co-localisation was not effected by IL-1β stimulation. CD147 has been shown to co-localise with ICAM-1 in the U397 cell line and activation of CD147 was important for activation of ICAM-1 signaling and cell binding properties (Khunkeawla et al. 2001). This suggested that it could be CD147 association with ICAM-1 that mediates monocyte binding by fibroblasts. This study identified that CD147/ICAM-1 co-localised in fibroblasts and IL-1β stimulated fibroblasts, however, no difference in the co-localisation was observed. That CD147 co-localised with both CD44 and ICAM-1, both of which are central adhesion molecules to monocyte binding; the functional role of CD147 was investigated. Silencing CD147 had no

effect on IL-1β-induced, monocyte binding, suggesting it had no role in the IL-1β-induced HA/CD44/ICAM-1 pathway. Although CD147 failed to be associated with monocyte binding by fibroblasts, does not eliminate its involvement. For example, in a study by Khunkeawla et al. (2001), CD147 was found to be essential for homotypic aggregation in the U397 cell line. Therefore, CD147 may involve the monocytes ability to bind HA on fibroblasts and not fibroblasts ability to bind monocytes. As CD147 expression was not silenced in U397 cells, it cannot be concluded that it has no involvement, although from the results in this study, it seems it does not regulate fibroblasts ability to bind monocytes.

The increased co-localisation of CD147/CD44 following TGF-β_1 stimulation was further confirmed by ICC. Interesting, CD147 did not co-localise with EGFR, following TGF-β1 stimulation. Our previous research has shown that fibroblast to myofibroblast differentiation requires HA to move CD44 through the membrane, where it associates with EGFR in caveolin rafts (Midgley et al. 2013). As CD147 did not co-localise with EGFR it suggests that CD147 has a role in fibroblast to myofibroblast differentiation in a CD44-dependent manner. For example, CD44 and CD147 are both known to regulate MMP transcription and activation (Sun and Hemler 2001; Murray et al. 2004). Further CD44 has been documented to act as a platform for MMPs (Seiki 2002). The association of CD44 with CD147 (a known MMP inducer) may allow for a synergistic relationship, where CD44 positions the MMPs and mediates CD147 activation. MMPs are known to be ECM regulators, therefore, an increased production may result in an ECM re-arrangement that allows HA to associate with and move CD44 through the membrane to associate with EGFR in lipid raft regions. Interestingly, it has been previously observed in gland epithelium that CD44v3 is a platform for MMP-7, which activates the epidermal growth factor receptor 4 (ErbB4) (Yu et al. 2002). This may suggest that CD147 regulates the activation of MMPs positioned on the CD44, which then activate EGFR in the HA/CD44/EGFR complex. TGF-β_1 and TSG-6 are essential differentiation mediators.

Silencing CD147 had no effect on the transcription of these two mediators again suggesting that CD147 has no role in the TGF-β_1/HA/CD44/EGFR pathway.

High and low glycosylated forms of CD147 have been reported to associate with lipid rafts (Tang et al. 2004). This study found that both high and low glycosylated forms of CD147 were expressed by fibroblast and myofibroblasts. It was also determined that there was an increased expression of the HG-CD147, following TGF-β_1 stimulation. The HG-CD147 form has previously been identified to have increased expression under fibrotic conditions. For example, rats treated with the antibiotic, bleomycin (which results in a fibrotic response and fibrosis), had an increased expression of a CD147 glycosylated form of 55kDa (Barth et al. 2006). This is also in line with the observations by Tang et al. (2004), that shows that the higher glycosylated form of CD147 is an activator of MMPs. Although the pathology of fibrosis is the result of an imbalance between ECM production and degradation, some MMPs have been shown to be upregulated in fibrotic conditions. For example, the increased expression of both MMP-9 and MMP-2 has been reported to be associated with fibrotic progression. Increased MMP-9 expression has been reported to degrade the tubular basement membrane, therefore, activating epithelial cells to undergo EMT in obstructive nephrology (Liu 2006). Further, MMP-2 has also been shown to be required for tubular EMT (Cheng and Lovett 2003). Therefore, the increase expression of a higher glycosylated form of CD147 in myofibroblasts in this study may be associated with MMP activation and upregulation in fibrosis.

Fibroblasts had a total co-localisation of CD147 with lipid raft regions, however, myofibroblasts had a sub-population situated outside of raft regions. Therefore, TGF-β_1 activation re-localised CD147 to form two populations throughout the membrane. Interestingly, CD147 was identified to be situated mainly in CAV-1 regions in the membrane in fibroblasts (these regions were identified lipid raft regions known as caveolae rafts). CD147 was situated in CAV-1 regions and non-raft regions in myofibroblasts. CD44 was also present

in and out of CAV-1 regions in fibroblasts, which re-localised in myofibroblasts to become mainly situated in CAV-1 regions, this is in line with previous research. A population of CD44 was observed to be associated with non-raft regions. That both CD44 and CD147 were present in the same membrane regions suggests that the increased CD147/CD44 co-localisation, previously observed in myofibroblasts could be in or out of raft regions or both. In a study by, Tang and Hemler (2004), it was observed that overexpression of CAV-1 had a negative effect on CD147 regulation of MMP-1; and the increased presence of CAV-1 resulted in decreased CD147 self-clustering and MMP-1 induction in three different cell types. This was confirmed in a study that silenced CAV-1 protein expression and found and increased expression of MMP-1 and intracellular ERK1/2 in dermal fibroblasts (Haines et al. 2011). Therefore, the presence of a population of CD147 outside of raft regions in myofibroblasts may contribute to increased cluster formation and MMP production via its association with CD44.

Only HG-CD147 was observed in the membrane fractions. This is in line with the cell type, as fibroblasts and myofibroblasts are known for MMP induction to mediate ECM degradation and turnover. The high glycosylated form of CD147 is mainly associated with MMP production and, therefore, it would be expected in a cell that has MMP production as a specific function to express this glycosylated form of CD147 (Tang et al. 2004). It was previously observed that there were two glycosylated forms of CD147 in fibroblasts and myofibroblast total lysate. An explanation for this is that LG-CD147 form is a precursor to HG-CD147 and is only present within the Golgi; although it has previously been observed to exist on the plasma membrane, it seems this is cell-specific. For example, in lung cancer cells in a study by Huang et al. (2013), only the high molecular form of CD147 was expressed on the plasma membrane, compared to the presence of two glycosylated forms in the total cell lysate; this is in line with observation made in this study.

CD44 is well established to be a regulator of the actin cytoskeleton. Furthermore, it has been shown that the association of CD44 with the cytoskeleton is lipid raft-dependent (Oliferenko et al. 1999). Interestingly, silencing CD147 has shown to alter the cytoskeletal architecture in human hepatocellular cancer cells (Qian et al. 2008). The CD147/CD44 co-localisation and the presence of a population within lipid rafts may, therefore, indicate a regulatory role of CD44/CD147 in mediating the cytoskeleton. Myofibroblasts can be characterized by the increased expression of αSMA and its incorporation into F-actin to form αSMA stress fibers. That silencing CD147 did not have an effect on αSMA transcription or translation following TGF-β_1 activation, further suggests that it is not involved in the classical HA/CD44/EGFR induction of differentiation. Interestingly, silencing CD147 prevented αSMA incorporation into F-actin and form stress fiber formation. The incorporation of αSMA into stress fibers is highly dependent on mechanical tension. A decrease in mechanical tension limits αSMA stress fibre formation and the contractile ability of myofibroblasts (Hinz et al. 2001). Preliminary data from this study identified that following total knockdown of CD147, the contractile ability of myofibroblast was decreased. These data combined suggests that CD147 may be involved in maintaining the correct mechanical tension required for αSMA stress fibre formation.

It is well-established that CD44 regulates the movement of F-actin through the association with ERM proteins and regulates cellular migration, proliferation and differentiation, through its activation by HA (Ponta et al. 2003). Moreover, CD147 has also been associated with cytoskeletal re-arrangement by the upregulation of integrins, focal adhesion kinase (FAK) and other focal adhesion proteins, through the activation of Ras homolog gene family, member A (RhoA), which has also been associated to be downstream from CD44 (Zhao et al. 2011). Therefore, it could be assumed that the removing CD147 protein expression may prevent CD44/F-actin re-arrangement and differentiation. However, silencing

CD147 did not alter the F-actin re-arrangement and it was observed to move from peripheral regions of fibroblasts and to a more cortical arrangement in myofibroblasts.

This study found that CD44s co-localised with CD147. CD44s has previously shown to regulate its own transcription and to regulate MMP-9 expression, through cleaving and release of the ICD. Further, CD147 is well-documented to increase the expression of many MMPs as well as vascular endothelial growth factor (VEGF) and HA (Nabeshima et al. 2006). Therefore, it was thought to be important to determine if these two associated receptor regulated the transcription of each other. There was no evidence to suggest that these two receptors regulate transcription of each other.

EDA–FN is essential for fibroblast to myofibroblast differentiation and its up-regulation precedes that of αSMA and collagen in the intermediate proto-myofibroblast stage. Further, its expression is greatly upregulated under fibrotic condition. The importance of EDA-FN in fibrosis can be shown in a study carried out by Muro et al.(2008). The study showed that EDA–FN-deficient mice treated with bleomycin (a fibrotic inducer) failed to induce fibrosis, compared to wild-type mice. EDA-FN has been associated with the formation of focal adhesions, through the association with integrins and other FA proteins. Moreover, the inhibition of EDA-FN prevents supermature focal adhesions formation. These are essential for αSMA stress fibre formation in myofibroblasts and for creating the correct tensile strength for αSMA incorporation into F-actin (Dugina et al. 2001). This study showed that CD147 does not regulate transcription of EDA-FN. However, the fact that CD147 does not regulate transcription of EDA-FN, does not exclude it from regulating EDA-FN interactions with integrins.

CD147 associates with multiple integrins, which are associated with cell adhesion and are essential mediators of mechanical tension. The association of CD147 with integrin α3β1

in human hepatoma cells has been shown to be important for cell adhesion, invasion and MMP production; as well as a reduction in focal adhesion (FA) quality and defective actin cytoskeletal re-arrangement (Tang et al. 2008b). This study investigated the association of CD147 with integrin α4β7 which had previously, through its association with EDA-FN, been identified to mediate fibroblast differentiation. It was identified that CD147/ α4β7 co-localised in myofibroblasts. Through this association, CD147 may mediate integrin α4β7 interaction with EDA-FN, making it an essential mediator for obtaining the correct mechanical tension and αSMA incorporation. However, further research into this hypothesis is required.

CD147, CD44 and multiple integrins have all been identified to activate downstream p-ERK1/2. Interestingly, ERK1/2 has previously been shown to be involved in mechanotransduction signaling, cytoskeletal re-arrangement and upregulation of differentiation mediators, including HAS2, EGFR and αSMA (Kawamura et al. 2003; Shi et al. 2011; Midgley et al. 2013). This study identified that CD147 has a regulatory role in p-ERK1/2 activation and silencing CD147 expression decreased p-ERK1/2 activation. This suggests that CD147 mediates mechanotransduction in a p-ERK1/2-dependent manner, although to clarify this, further research is required.

In conclusion, this chapter has identified a possible role for CD147 in maintaining the correct mechanical tension for αSMA incorporation and terminal myofibroblast differentiation. However, more research is required to determine if the CD147/CD44 association or the CD147/α4β7 association are central to this process. This study has elucidated that CD147 is unlikely to play a role in the classical TGF-β_1-driven differentiation through the HA/CD44/EGFR pathway. Similarly, CD147 was not identified to have a role in regulating monocyte binding by fibroblasts.

Chapter 6-General Discussion

6.1 General Discussion

This thesis investigated the roles of CD44 variants and the MMP inducer, CD147, in pro-fibrotic and pro-inflammatory phenotypic changes in myofibroblast. Multiple CD44 variants were expressed in fibroblasts and it was that these existed as both single exon or multiple exons spliced, between the two common regions. Ten CD44 variants were identified preceding stimulation with transforming growth factor-β_1 (TGF-β_1) (which **decreased** expression of all the variants) and interleukin-1β (IL-1β) (which **increased** all variant expression). The standard form of CD44 (CD44s) was identified as essential for TGF-β_1-driven, fibroblast to myofibroblast differentiation ***(Figure 6.1[A])*** and the IL-1β induction of fibroblast-monocyte binding ***(Figure 6.2[B])***. The study also determined that CD147 was essential for αSMA incorporation into F-actin stress fibres in myofibroblasts, suggesting a control mechanism for the cells' contractile ability. A regulatory role for CD147 was also determined in the activation of the intracellular signalling kinase extracellular signal-regulated kinase1/2 (ERK1/2). CD147 associated with two key differentiating mediators, CD44 and the EDA-fibronectin (EDA-FN) associated integrin, α4β7, following TGF-β_1 induction. The investigation also determined that it was most probably CD44s that was co-localised with CD147, suggesting a dual role for the simplest CD44 variant in fibrotic progression.

Combining data from this study and previous research from our laboratory suggests that association of hyaluronan (HA) with CD44s is central to the TGF-β_1-mediated, HA/CD44/EGFR and the IL-1β activation of the HA/CD44/ICAM-1 pathways (***Figure 6.1[A-B]***). The peri-cellular HA arrangements resulting from these two pathways differ and are specific to their function. One suggestion for this variation in HA arrangement is the nature of the association of CD44s in the plasma membrane. The CD44/EGFR association observed in myofibroblasts requires association with CAV-1 lipid rafts (caveolae). However, the CD44s/ intracellular adhesion molecule-1 (ICAM-1) co-localisation resulting from IL-1β stimulation

happens within non-lipid raft regions (Meran et al. 2013). Downstream intracellular signalling is mediated through the association of receptors with different cell membrane components and receptor interactions. Both the TGF-β_1 and IL-1β pathways investigated in our laboratory activate downstream ERK1/2. These protein kinases have been identified to regulate multiple signalling pathways and transcription factors (Roskoski 2012). Therefore, the activation of ERK1/2 via different regions of the plasma membrane may mediate HA re-arrangements by promoting different gene transcription. For example, recently it has been identified that the hyaldherin, tumour necrosis factor-inducible gene 6 (TSG-6), is essential for myofibroblast TGF-β_1 induced, HA peri-cellular coat formation, but is not required for the formation of the HA spikes induced by IL-1β. This suggests that the protein transcription required for the HA coat assembly differs following different stimuli. A further explanation as to why the same CD44 variant can mediate different HA arrangement is the varied post-translational modifications which can effect HA interaction and signalling (Bartolazzi et al. 1996). Therefore, to examine the varied functional role of CD44s in mediating different HA arrangements requires further investigation.

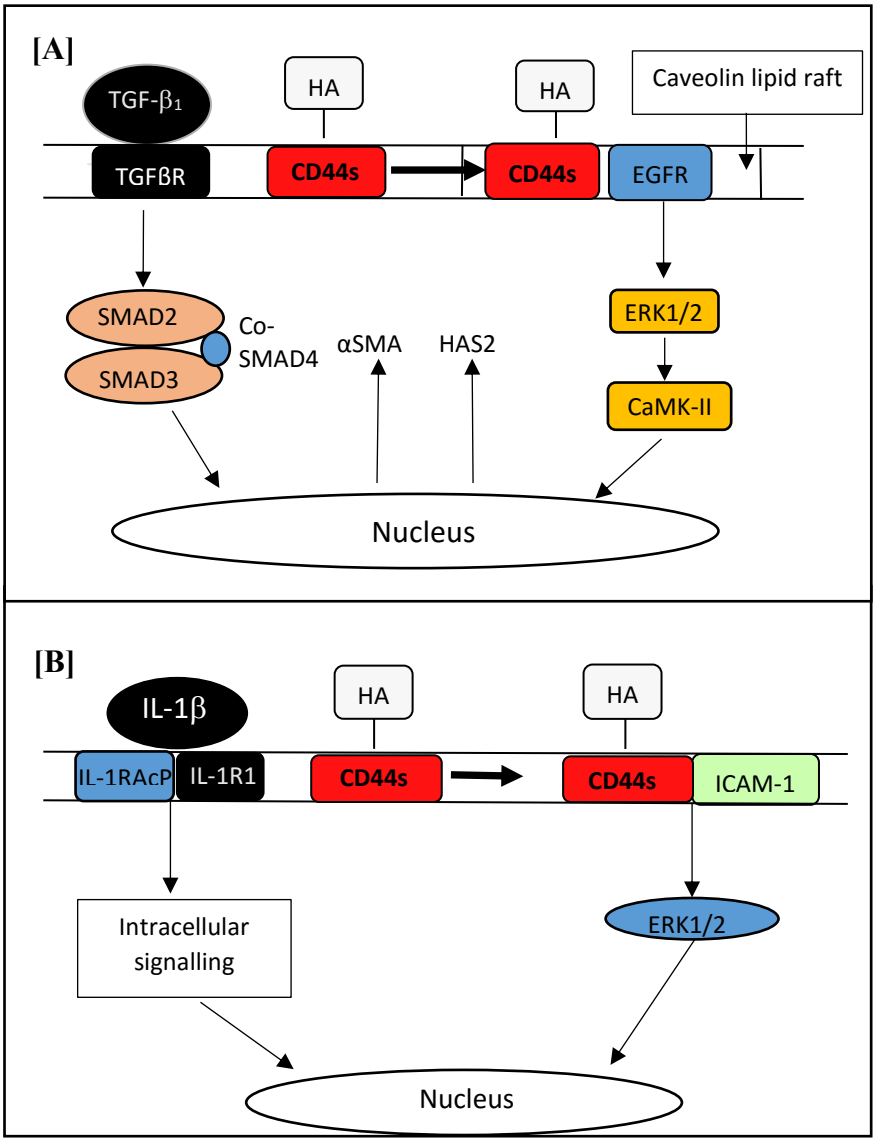

Figure 6.1. - Schematics ***[A&B]*** illustrate the role of CD44s and its re-location in TGF-β_1-induced fibroblast differentiation and IL-1β induced monocyte binding, respectively.

That none of the other CD44 spliced variants were identified to have a role in TGF-β1-induced, differentiation or IL-1β-induced, monocyte binding, does not eliminate their involvement. A recent fibrotic reversal model identified in our laboratory has shown CD44v7/8 to be essential for preventing TGF-β_1-induced, fibrosis, through its induction by the anti-fibrotic growth factor, bone morphogenic protein-7 (BMP-7) (Midgley et al. 2015). The study examined the effect of silencing CD44v7/8 expression on the ability of BMP-7 to prevent

or reverse the fibrotic response induced by TGF-β_1. It was shown that decreasing the expression of CD44v7/8 prevented the anti-fibrotic effects of BMP-7 on fibroblast differentiation and upregulated αSMA expression. Further, it was suggested that the dampened fibrotic response by BMP-7 was the result of a CD44v7/8 specific function that initiated the internalisation of HA and prevented the formation of the myofibroblast HA coat (Midgley et al. 2015). A similar response was observed in this study, which identified that a decreased expression of CD44v8 increased fibroblast-monocyte binding. This CD44 variant shares a partial exonic sequence with CD44v7/8, suggesting that the v8/exon 12 may have a functional role in the internalisation of HA.

The majority of fibroblast populations undergo differentiation to become myofibroblasts following TGF-β_1 stimulation, including lung and dermal fibroblasts (Desmoulière et al. 1993). However, TGF-β_1 stimulation of oral mucosal fibroblasts results in an anti-fibrotic phenotype that resists differentiation and a proliferative response (Stephens et al. 1996; Szpaderska et al. 2003; Meran et al. 2007; Meran et al. 2008a). Furthermore, the TGF-β1 induction of proliferation of dermal fibroblasts is CD44-dependent, however, the anti-proliferative response of oral fibroblasts is CD44 independent, resulting from a HA-deficient environment (Meran et al. 2011b). Interestingly, preliminary data analysing CD44 mRNA variant expression in oral and dermal cells undertaken in our laboratory, suggests that oral cells have a high expression of v7 (see appendix 2). This may suggest that non-scarring cells express a HA regulating CD44 variant, which contributes to the non-scarring properties. Therefore, for future investigations, it may be interesting to analyse the inhibitory effects of CD44 variant expression on HA regulation in non-scarring cell types.

Analysing the protein involvement of CD44s is restricted due to the limitations of available antibodies. Although there are specific antibodies that target variant-specific stem regions, antibodies that target CD44s, target the amino domain that is common to all variants.

Therefore, using conventional protein methods, such as immunocytochemistry (ICC) and Confocal Microscopy, to confirm CD44s co-localisation with either epidermal growth factor receptor (EGFR) or intercellular adhesion molecule-1 (ICAM-1) is not possible and conclusive results would require more advanced techniques, such as Florescence Resonance Emission Transfer (FRET).

CD147 is a major contributor to cancer invadapodia, through its ability to induce and activate matrix metalloproteinases (MMPs); and contribute to the re-arrangement of the ECM. However, it has also previously been associated with fibrotic progression (Huet et al. 2008b; Kato et al. 2011; Li et al. 2015). The current study identified that CD147 had an increased co-localisation in TGF-β_1-induced myofibroblasts, with CD44s and EDA-FN associated integrin, $\alpha4\beta7$. CD44 and EDA-FN are essential mediators of myofibroblast terminal differentiation (Serini et al. 1998; Muro et al. 2008; Webber et al. 2009b; Meran and Steadman 2011; Midgley et al. 2013). Downregulation of the CD147 mRNA expression did not affect the mRNA expression of αSMA following TGF-β_1 stimulation. However, the incorporation of αSMA into F-actin stress fibres was prevented. Further, a decreased contractile ability was observed in TGF-β_1-induced, myofibroblasts, when CD147 protein expression was completely silenced. The incorporation of αSMA into the F-actin cytoskeleton by the NH_2-terminal motif AC-EED, requires the correct mechanical tension mediated by the combination of mature focal adhesion formation, cell-cell contact, cell-ECM contact and cytoskeletal re-arrangement (Hinz et al. 2002; Clement et al. 2005). EDA-FN is central to focal adhesion formation and fundamental for the correct mechanical tension required for differentiation (Hinz et al. 2001). That CD147 was also found to co-localise with the EDA-FN-associated integrin, $\alpha4\beta7$; and CD44, suggests that CD147 has a role in mediating the required tension for αSMA incorporation.

Combining the findings of this thesis with previously published data, three possible mechanism for the function of CD147 differentiation are given below:

1) CD147 forms a complex with both CD44 and integrin α4β7, which links the ECM

Integrin α4β7 has been determined to associate with a small GTPase known as, Ras Homolog Gene Family Member A (RhoA)(Abdi et al. 2013). This signalling protein is activated when HA associates with CD44 and mediates intracellular cytoskeletal re-organisation (Bourguignon 2008). Interestingly, in a study by Kawamura et al. (2003), RhoA activation was upstream from ERK1/2 in a signalling mechanism that was determined to be CAV-1-dependent. The current study also determined that silencing CD147 prevented TGF-β_1-dependent, ERK1/2 signalling. Furthermore a sub-population of CD147 was observed in lipid raft regions that contained CAV-1 in myofibroblasts. Combining these data suggests that the intracellular activation of RhoA may depend on all three membrane proteins forming a CD44/CD147/α4β7 complex. However, to confirm this, an analysis of RhoA and ERK1/2 signalling by myofibroblast would be required, following inhibition of all the proteins separately. The association of integrin α4β7 with EDA-FN is essential to myofibroblast formation (Kohan et al. 2010). Therefore, the proposed CD44/CD147/α4β7 complex may contribute to mechanical tension by an intracellular and extracellular contractile force ***(Figure 6.3)***. However, to confirm this hypothesis a more extensive analysis into CD44/CD147/α4β7 co-localisation and their position within the plasma membrane would be required.

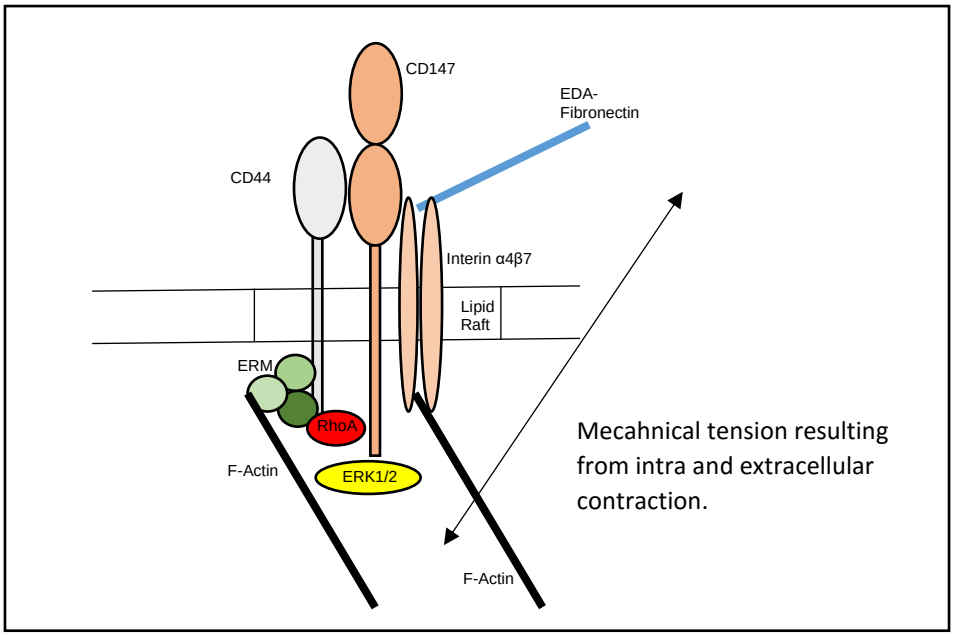

Figure 6.3 – Schematic demonstrates possible CD44/CD147/α4β7 complex formation that may contribute towards the essential mechanical tension required for αSMA incorporation into F-actin stress fibres. The signalling pathway shows the downstream activation of RhoA and ERK1/2, following TGF-β_1 activation within CAV-1 lipid raft regions.

2) CD147 mediates the correct mechanical tension for αSMA incorporation through separate association with integrin α4β7 and CD44s

A further proposal for the role of CD147 in differentiation is that it associates with integrin α4β7 and CD44 independently; and mediates two separate functional properties. CD44 is known to be essential for re-arrangement of the cytoskeleton that mediates multiple cellular functions, including differentiation, proliferation and migration (Thomas et al. 1993; Trochon et al. 1996; Meran et al. 2011b; Pham et al. 2011; Midgley et al. 2013). Furthermore, RhoA activates downstream mediator Rho-associated coiled coil containing kinase (ROCK), a serine/threonine kinase, known to be involved in actin contraction and stress fibre formation (Riento and Ridley 2003). ROCK has been shown to phosphorylate myosin light chains of non-muscle myosin II (NM-II) and cofilin, both of which are actin binding proteins that play a pivotal role in stress fibre contraction and actin polymerisation, respectively. CD147 also mediates the RhoA/ROCK pathway in cancer cell migration (Zhao et al. 2011). Members of

the Rho family have also been identified as essential for integrin signalling complexes to form and decreased Rho expression prevents downstream activation of ERK1/2 (Hotchin and Hall 1995).

Integrins are associated with cell-cell, cell-ECM and focal adhesion formation, all of which contribute to mechanotransduction signalling (Chen et al. 2004). CD147 is primarily a MMP inducer and has been identified to accumulate around regions of cell-cell contact (Ma et al. 2010). It is widely identified to be associated with cell-ECM contact, due to its remodelling properties, facilitated by MMPs (Huet et al. 2008a; Ma et al. 2010). The functional role of CD147 association with the integrin α3β1 has previously been identified as essential for cell adhesion, invasion, MMP induction and ECM remodelling; and the subsequent inhibition of α3β1 decreased these CD147 dependent responses (Dai et al. 2009). Similarly, in hepatoma cells, it was identified that FAK and paxillin, both essential downstream mediators of integrin function, were CD147-dependent (Tang et al. 2008a).

That this study determined that silencing CD147 inhibited ERK1/2 activation may suggest that ERK1/2 is downstream from CD147/CD44 signalling or CD147/α4β7 signalling. Furthermore, previous studies have shown inhibiting CD44 or α4β7 decreases ERK1/2 signalling, suggesting all are required for ERK1/2 activation (Kohan et al. 2010). Interestingly, ERK1/2 activation is also regulated through mechanical tension, therefore, the decreased ERK1/2 expression observed in this study may also result from CD147 reduction of mechanical tension from both pathways (Zou et al. 1998). ***(Figure 6.4)*** shows the hypothetical roles of CD147/CD44 and CD147/α4β7 independently in mecahnotransduction and possible signalling regulation by each complex. However, to confirm this hypothesis, further research is required.

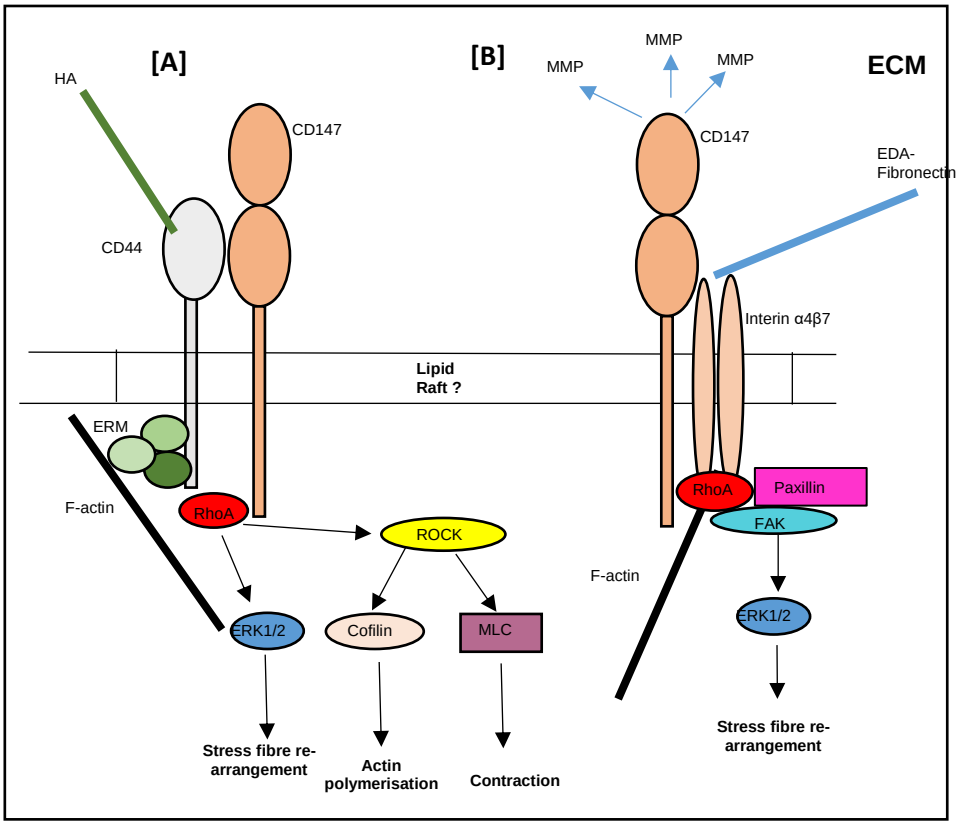

Figure 6.3 – Schematic to demonstrate hypothetical role of CD147 in mecahnotransduction signalling through mediation of two individual pathways. ***[A]*** shows a possible intracellular signalling mechanisms that may result from HA/CD44/CD147 association. ***[B]*** represents a hypothetical role for CD147 association with the EDA-FN integrin, α4β7.

3) CD147 mediates α4β7/EDA-FN and HA/CD44 association through the re-arrangement of the ECM, via MMP induction.

A final hypothesis suggests that CD147 mediates the receptor association with ECM components by induction and activation of MMPs which mediate ECM re-arrangement; facilitating receptor-ligand association. In fact, one major area of research for CD147 induction of MMPs examines the ECM re-arrangement to facilitate metastasis and invasiveness in cancer biology (Kanekura et al. 2002; Gabison et al. 2005). In multiple tumour studies, CD147 requires association with integrins for MMP activation (Tang et al. 2008b; Dai et al. 2009). Therefore, the CD147/integrin α4β7 association observed in this

study may be required for MMP induction and facilitate the EDA-FN/integrin α4β7 association. Similarly, for terminal differentiation, the association of HA/CD44 is required for intracellular signalling and cytoskeletal re-arrangement (Ponta et al. 2003). CD147 is thought to associate with CAV-1 in the membrane through its lower proximal Ig domain. Furthermore, this association is thought to promote clustering and induce MMP production (Tang and Hemler 2004). The distal Ig domain of CD147 is well-recognised as an MMP activator (Iacono et al. 2007). The current study identified a population of CD147 in CAV-1 raft regions. This may suggest that CD147 also anchors co-localised receptors within raft regions; which are commonly associated with essential intracellular signalling ***(Figure 6.4)***. Therefore, silencing CD147 in this study may have prevented, firstly, the ECM re-arrangement and secondly anchorage to the plasma membrane within raft regions; both reported to be essential for receptor ligand association and signalling (Simons and Toomre 2000; Stivarou and Patsavoudi 2015). Importantly failure of receptor ligand association and intracellular signalling would prevent the contractile response required for αSMA incorporation, as was observed in this study.

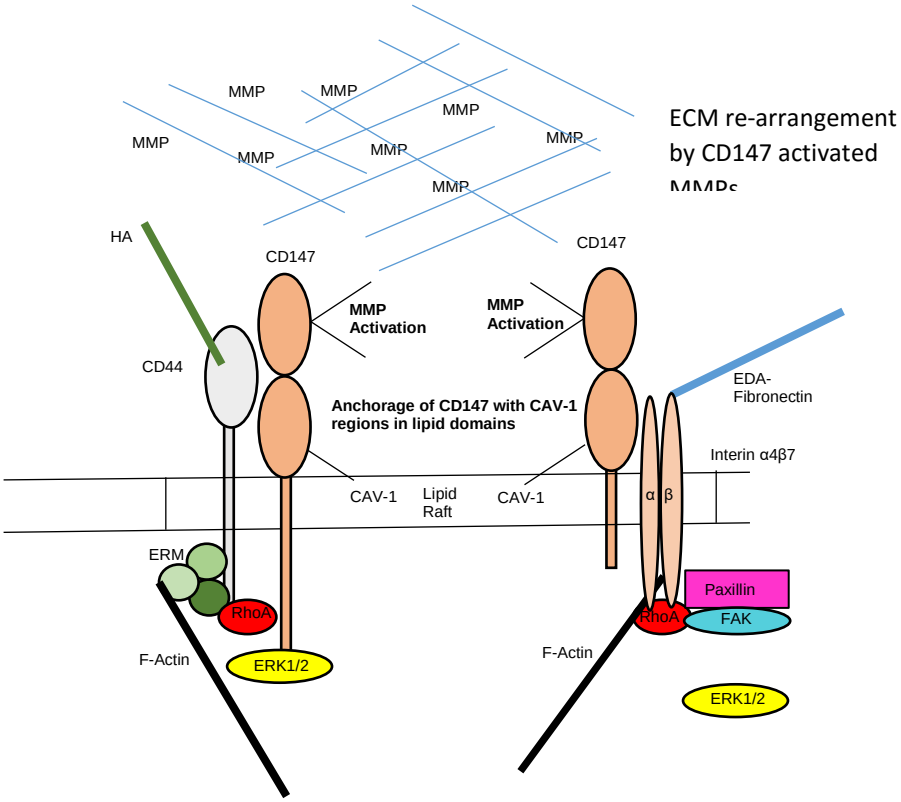

Figure 6.4. - Schematic to show a possible role for CD147 in differentiation. It is hypothesised that CD147 mediates ECM re-arrangement, via MMP induction by the distal Ig domain and anchorage to CAV-1 lipid rafts, via CD147 proximal domain.

In conclusion CD147 and CD44s have both been identified to have a role in fibroblast differentiation. However, these two abundantly expressed receptors are essential mediators for multiple cellular function and therefore, could not be used directly as a target for therapeutic treatments.

This study determined that CD147 was only important in TGF-β_1 differentiation, but was not observed to mediate the IL-1β pro-inflammatory pathway. One distinct difference between TGF-β_1 and IL-1β pathways is the association with lipid raft regions. The CD44/ICAM-1 association is independent of lipid raft regions, which may suggest that the pro-fibrotic role observed by CD147 is raft-dependent. A more detailed examination of ICAM-1 and its interaction/associations with the plasma membrane, may lead to a better understanding of cell membrane mediated signalling. This current study identified separate populations of

CD147 in and out of raft regions in myofibroblasts. Intracellular activation by CD147 has previously shown to be lipid raft-dependent, with an essential role for CAV-1 association (Tang and Hemler 2004). A further investigation to this study may benefit from sorting lipid raft and non-raft populations of CD147, with an aim to determine which population is mediating the mechanical tension demonstrated in this thesis. This may lead to identification of more specific targets that may be useful as a therapeutic treatment. Indeed, some research has targeted lipid rafts directly and found that disruption of these regions prevented activation of downstream mediators (Parpal et al. 2001; Mollinedo et al. 2010). However, for this to be a useful the treatment would need to specifically target diseased areas.

Similarly a much more specific target would be required for therapeutic treatments of fibrotic and inflammatory responses than targeting HA/CD44s association directly. CD44v7 has been shown to be highly expressed in non-differentiating, anti-fibrotic oral cells (See Appendix 2). This study also determined that CD44v8 had a pro-inflammatory response. Furthermore, our recent studies have found that BMP-7 induction of CD44v7/8 in lung fibroblast prevents and reverses fibroblast differentiation.

Future work may well identify therapeutic targets associated with the expression of these variants and their potential interactions.

References

Aarden, L. A. et al. 1980. Revised nomenclature for antigen-nonspecific t-cell proliferation and helper factors. *Molecular Immunology* 17(5), pp. 641-643.

Abdi, J. et al. 2013. Drug resistance in multiple myeloma: latest findings and new concepts on molecular mechanisms. *Oncotarget* 4(12), pp. 2186-2207.

Abe, R. et al. 2001. Peripheral Blood Fibrocytes: Differentiation Pathway and Migration to Wound Sites. *The Journal of Immunology* 166(12), pp. 7556-7562.

Afify, A. et al. 2009. Role of CD44s and CD44v6 on human breast cancer cell adhesion, migration, and invasion. *Experimental and Molecular Pathology* 86(2), pp. 95-100.

Afify, A. M. et al. 1993. Purification and characterization of human serum hyaluronidase. *Archives of Biochemistry and Biophysics* 305(2), pp. 434-441.

Akiyama, Y. et al. 2001. Hyaluronate receptors mediating glioma cell migration and proliferation. *Journal of Neuro-Oncology* 53(2), pp. 115-127.

Albeiroti, S. et al. 2015. Hyaluronan's Role in Fibrosis: A Pathogenic Factor or a Passive Player? *Biomed Research International*.

Algrain, M. et al. 1993. Ezrin contains cytoskeleton and membrane-binding domains accounting for its proposed role as a membrane-cytoskeletal linker. *Journal of Cell Biology* 120(1), pp. 129-139.

Altruda, F. et al. 1989. Cloning of cdna for a novel mouse membrane glycoprotein (gp42) - shared identity to histocompatibility antigens, immunoglobulins and neural-cell adhesion molecules. *Gene* 85(2), pp. 445-452.

Andres, J. L. et al. 1992. Binding of two growth factor families to separate domains of the proteoglycan betaglycan. *Journal of Biological Chemistry* 267(9), pp. 5927-5930.

Andres, J. L. et al. 1989. Membrane-anchored and soluble forms of betaglycan, a polymorphic proteoglycan that binds transforming growth factor-beta. *Journal of Cell Biology* 109(6), pp. 3137-3145.

Aoki, H. et al. 2006. Autocrine loop between TGF-beta(1) and IL-1 beta through Smad3- and ERK-dependent pathways in rat pancreatic stellate cells. *American Journal of Physiology-Cell Physiology* 290(4), pp. C1100-C1108.

Arend, W. P. 2002. The balance between IL-1 and IL-1Ra in disease. *Cytokine & Growth Factor Reviews* 13(4–5), pp. 323-340.

Arend, W. P. et al. 1998. Interleukin-1 receptor antagonisT: Role in Biology. *Annual Review of Immunology* 16(1), pp. 27-55.

Asano-Kato, N. et al. 2005. TGF-beta1, IL-1beta, and Th2 cytokines stimulate vascular endothelial growth factor production from conjunctival fibroblasts. *Experimental Eye Research* 80(4), pp. 555-560.

Bai, Y. et al. 2014. Importance of N-Glycosylation on CD147 for Its Biological Functions. *International Journal of Molecular Sciences* 15(4), pp. 6356-6377.

Baker, A. H. et al. 2002. Metalloproteinase inhibitors: biological actions and therapeutic opportunities. *Journal of Cell Science* 115(19), pp. 3719-3727.

Barrientos, S. et al. 2008. Growth factors and cytokines in wound healing. *Wound Repair and Regeneration* 16(5), pp. 585-601.

Barth, K. et al. 2006. Lack of evidence for caveolin-1 and CD147 interaction before and after bleomycin-induced lung injury. *Histochemistry and Cell Biology* 126(5), pp. 563-573.

Bartolazzi, A. et al. 1995. Regulation of growth acid dissemination of a human lymphoma by cd44 splice variants. *Journal of Cell Science* 108, pp. 1723-1733.

Bartolazzi, A. et al. 1996. Glycosylation of CD44 is implicated in CD44-mediated cell adhesion to hyaluronan. *The Journal of Cell Biology* 132(6), pp. 1199-1208.

Bartolazzi, A. et al. 1994. Interaction between CD44 and hyaluronate is directly implicated in the regulation of tumor-development. *Journal of Experimental Medicine* 180(1), pp. 53-66.

Bataller, R. and Brenner, D. A. 2005. Liver fibrosis. *Journal of Clinical Investigation* 115(2), pp. 209-218.

Baum, C. L. and Arpey, C. J. 2005. Normal cutaneous wound healing: Clinical correlation with cellular and molecular events. *Dermatologic Surgery* 31(6), pp. 674-686.

Beanes, S. R. et al. 2003. Skin repair and scar formation: the central role of TGF-[beta]. *Expert Reviews in Molecular Medicine* 5(08), pp. 1-22.

Beasley, J. 2012. Osteoarthritis and Rheumatoid Arthritis: Conservative Therapeutic Management. *Journal of Hand Therapy* 25(2), pp. 163-171.

Belton, R. J. et al. 2008. Basigin-2 Is a Cell Surface Receptor for Soluble Basigin Ligand. *The Journal of Biological Chemistry* 283(26), pp. 17805-17814.

Bennett, K. L. et al. 1995. CD44 isoforms containing exon V3 are responsible for the presentation of heparin-binding growth factor. *The Journal of Cell Biology* 128(4), pp. 687-698.

Berditchevski, F. et al. 1997. Generation of Monoclonal Antibodies to Integrin-associated Proteins: evidence that α3β1 complexes with EMMPRIN/BASIGIN/OX47/M6. *Journal of Biological Chemistry* 272(46), pp. 29174-29180.

Biswas, C. 1982. Tumor-cell stimulation of collagenase production by fibroblasts. *Biochemical and Biophysical Research Communications* 109(3), pp. 1026-1034.

Biswas, C. 1984. Collagenase stimulation in cocultures of human-fibroblasts and human-tumor cells. *Cancer Letters* 24(2), pp. 201-207.

Biswas, C. and Nugent, M. A. 1987. membrane association of collagenase stimulatory factor(s) from B-16 melanoma-cells. *Journal of Cellular Biochemistry* 35(3), pp. 247-258.

Biswas, C. et al. 1995. The Human Tumor Cell-derived Collagenase Stimulatory Factor (Renamed EMMPRIN) Is a Member of the Immunoglobulin Superfamily. *Cancer Research* 55(2), pp. 434-439.

Bodevin-Authelet, S. et al. 2005. Biosynthesis of Hyaluronan: DIRECTION OF CHAIN ELONGATION. *Journal of Biological Chemistry* 280(10), pp. 8813-8818.

Bommaya, G. et al. 2011. Tumour necrosis factor-stimulated gene (TSG)-6 controls epithelial-mesenchymal transition of proximal tubular epithelial cells. *International Journal of Biochemistry & Cell Biology* 43(12), pp. 1739-1746.

Booth, M. et al. 2004. Periportal fibrosis in human Schistosoma mansoni infection is associated with low IL-10, low IFN-gamma, high TNF-alpha, or low RANTES, depending on age and gender. *J Immunol* 172(2), pp. 1295-1303.

Bourguignon, L. Y. W. 2008. Hyaluronan-mediated CD44 activation of RhoGTPase signaling and cytoskeleton function promotes tumor progression. *Seminars in cancer biology* 18(4), pp. 251-259.

Bourguignon, L. Y. W. and Iida, N. 1994. New CD44 splice variants associated with human breast cancers. *Journal of Cellular Biochemistry*, pp. 241-241.

Bourguignon, L. Y. W. et al. 2004. CD44 Interaction with Na+-H+ Exchanger (NHE1) Creates Acidic Microenvironments Leading to Hyaluronidase-2 and Cathepsin B Activation and Breast Tumor Cell Invasion. *Journal of Biological Chemistry* 279(26), pp. 26991-27007.

Bourguignon, L. Y. W. et al. 1998. CD-44 isoform-cytoskeleton interaction in oncogenic signaling and tumor progression. *Frontiers in Bioscience* 3(CITED JULY 22, 1998), pp. D637-649.

Bretscher, A. et al. 2002. ERM proteins and merlin: Integrators at the cell cortex. *Nature Reviews Molecular Cell Biology* 3(8), pp. 586-599.

Brinckerhoff, C. E. and Matrisian, L. M. 2002. Matrix metalloproteinases: a tail of a frog that became a prince. *Nat Rev Mol Cell Biol* 3(3), pp. 207-214.

Brinkman, B. M. N. 2004. Splice variants as cancer biomarkers. *Clinical Biochemistry* 37(7), pp. 584-594.

Brocker, C. et al. 2010. Evolutionary divergence and functions of the human interleukin (IL) gene family. *Human Genomics* 5(1), pp. 30-55.

Burger, D. et al. 2006. Is IL-1 a good therapeutic target in the treatment of arthritis? *Best Practice & Research Clinical Rheumatology* 20(5), pp. 879-896.

Burrage, P. S. et al. 2006. Matrix metalloproteinases: Role in arthritis. *Frontiers in Bioscience* 11, pp. 529-543.

Campo, G. M. et al. 2010. Molecular size hyaluronan differently modulates toll-like receptor-4 in LPS-induced inflammation in mouse chondrocytes. *Biochimie* 92(2), pp. 204-215.

Campo, G. M. et al. 2012. Hyaluronan in part mediates IL-1beta-induced inflammation in mouse chondrocytes by up-regulating CD44 receptors. *Gene* 494(1), pp. 24-35.

Castor, C. W. et al. 1962. Characteristics of human fibroblasts cultivated in vitro from different anatomical sites. *Laboratory Investigation* 11(9), pp. 703-&.

Chaponnier, C. et al. 1995. The specific NH2-terminal sequence AC-EEED of alpha-smooth muscle actin plays a role in polymerization in-vitro and in-vivo. *Journal of Cell Biology* 130(4), pp. 887-895.

Chen, C. S. et al. 2004. Mechanotransduction at Cell-Matrix and Cell-Cell Contacts. *Annual Review of Biomedical Engineering* 6(1), pp. 275-302.

Chen, H. et al. 2011. CD147 is required for matrix metalloproteinases-2 production and germ cell migration during spermatogenesis. *Molecular Human Reproduction* 17(7), pp. 405-414.

Chen, M. and Manley, J. L. 2009. Mechanisms of alternative splicing regulation: insights from molecular and genomics approaches. *Nature Reviews Molecular Cell Biology* 10(11), pp. 741-754.

Cheng, S. and Lovett, D. H. 2003. Gelatinase A (MMP-2) Is Necessary and Sufficient for Renal Tubular Cell Epithelial-Mesenchymal Transformation. *The American Journal of Pathology* 162(6), pp. 1937-1949.

Chetty, C. et al. 2012. MMP-9 induces CD44 cleavage and CD44 mediated cell migration in glioblastoma xenograft cells. *Cellular Signalling* 24(2), pp. 549-559.

Chiampanichayakul, S. et al. 2006. CD147 contains different bioactive epitopes involving the regulation of cell adhesion and lymphocyte activation. *Immunobiology* 211(3), pp. 167-178.

Clarris, B. J. and Fraser, J. R. E. 1968. On the pericellular zone of some mammalian cells in vitro. *Experimental Cell Research* 49(1), pp. 181-193.

Clayton, A. et al. 1997. Cells isolated from the human cortical interstitium resemble myofibroblasts and bind neutrophils in an ICAM-1-dependent manner. *Journal of the American Society of Nephrology* 8(4), pp. 604-615.

Clement, S. et al. 2005. The N-terminal Ac-EEED sequence plays a role in alpha-smooth-muscle actin incorporation into stress fibers. *Journal of Cell Science* 118(7), pp. 1395-1404.

Cohen-Solal, L. et al. 1986. Proline hydroxylation of collagens synthesized at different temperatures in vivo by two poikilothermic species. *Comparative Biochemistry and Physiology Part B: Comparative Biochemistry* 83(2), pp. 483-486.

Colón, E. et al. 2009. Transfer of Inter-α-inhibitor Heavy Chains to Hyaluronan by Surface-linked Hyaluronan-TSG-6 Complexes. *Journal of Biological Chemistry* 284(4), pp. 2320-2331.

Coombe, D. R. et al. 1994. MAC-1 (CD11B/CD18) and CD45 mediate the adhesion of hematopoietic progenitor cells to stromal cell elements via recognition of stromal heparan-sulfate. *Blood* 84(3), pp. 739-752.

Craig, E. A. et al. 2009. Size-dependent regulation of Snail2 by hyaluronan: Its role in cellular invasion. *Glycobiology* 19(8), pp. 890-898.

Csoka, A. B. et al. 2001. The six hyaluronidase-like genes in the human and mouse genomes. *Matrix Biology* 20(8), pp. 499-508.

Cummings, B. J. and Cotman, C. W. 1995. Image analysis of β-amyloid load in Alzheimer's disease and relation to dementia severity. *The Lancet* 346(8989), pp. 1524-1528.

Dai, J.-y. et al. 2009. The interaction of HAb18G/CD147 with integrin alpha 6 beta 1 and its implications for the invasion potential of human hepatoma cells. *Bmc Cancer* 9.

Damsker, J. M. et al. 2009. Targeting the chemotactic function of CD147 reduces collagen-induced arthritis. *Immunology* 126(1), pp. 55-62.

Davidson, B. et al. 2003. Matrix metalloproteinases (MMP), EMMPRIN (extracellular matrix metalloproteinase inducer) and mitogen-activated protein kinases (MAPK): Co-expression in metastatic serous ovarian carcinoma. *Clinical & Experimental Metastasis* 20(7), pp. 621-631.

Day, A. J. and de la Motte, C. A. 2005. Hyaluronan cross-linking: a protective mechanism in inflammation? *Trends in Immunology* 26(12), pp. 637-643.

Day, A. J. and Prestwich, G. D. 2002. Hyaluronan-binding Proteins: Tying Up the Giant. *Journal of Biological Chemistry* 277(7), pp. 4585-4588.

Day, A. J. and Sheehan, J. K. 2001. Hyaluronan: polysaccharide chaos to protein organisation. *Current Opinion in Structural Biology* 11(5), pp. 617-622.

de la Motte, C. A. 2011. Hyaluronan in intestinal homeostasis and inflammation: implications for fibrosis. *American Journal of Physiology - Gastrointestinal and Liver Physiology* 301(6), pp. G945-G949.

de la Motte, C. A. et al. 1999. Mononuclear Leukocytes Preferentially Bind via CD44 to Hyaluronan on Human Intestinal Mucosal Smooth Muscle Cells after Virus Infection or Treatment with Poly(I·C). *Journal of Biological Chemistry* 274(43), pp. 30747-30755.

Desmouliere, A. et al. 1993. Transforming growth-factor-beta-1 induces alpha-smooth muscle actin expression in granulation-tissue myofibroblasts and in quiescent and growing cultured fibroblasts. *Journal of Cell Biology* 122(1), pp. 103-111.

Desmoulière, A. et al. 1993. Transforming growth factor-beta 1 induces alpha-smooth muscle actin expression in granulation tissue myofibroblasts and in quiescent and growing cultured fibroblasts. *The Journal of cell biology* 122(1), pp. 103-111.

Dinarello, C. A. 1988. Biology of interleukin 1. *The FASEB Journal* 2(2), pp. 108-115.

Dinarello, C. A. 1991. Interleukin-1 and interleukin-1 antagonism. *Blood* 77(8), pp. 1627-1652.

Donadio, A. C. et al. 2008. Extracellular matrix metalloproteinase inducer (EMMPRIN) and matrix metalloproteinases (MMPs) as regulators of tumor–host interaction in a spontaneous metastasis model in rats. *Histochemistry and cell biology* 130(6), pp. 1155-1164.

Dougherty, G. J. et al. 1991. Molecular-cloning of cd44r1 and cd44r2, 2 novel isoforms of the human cd44 lymphocyte homing receptor expressed by hematopoietic-cells. *Journal of Experimental Medicine* 174(1), pp. 1-5.

Driesen, R. B. et al. 2014. Reversible and irreversible differentiation of cardiac fibroblasts. *Cardiovascular Research* 101(3), pp. 411-422.

Dugina, V. et al. 2001. Focal adhesion features during myofibroblastic differentiation are controlled by intracellular and extracellular factors. *Journal of Cell Science* 114(18), pp. 3285-3296.

Eddy, A. A. 1996. Molecular insights into renal interstitial fibrosis. *Journal of the American Society of Nephrology* 7(12), pp. 2495-2508.

Enghild, J. J. et al. 1999. Organization of the Inter-α-Inhibitor Heavy Chains on the Chondroitin Sulfate Originating from Ser10 of Bikunin: Posttranslational Modification of IαI-Derived Bikunin. *Biochemistry* 38(36), pp. 11804-11813.

Eriksson, J. E. et al. 2009. Introducing intermediate filaments: from discovery to disease. *The Journal of Clinical Investigation* 119(7), pp. 1763-1771.

Evanko, S. P. et al. 1999. Formation of Hyaluronan- and Versican-Rich Pericellular Matrix Is Required for Proliferation and Migration of Vascular Smooth Muscle Cells. *Arteriosclerosis, Thrombosis, and Vascular Biology* 19(4), pp. 1004-1013.

Evans, R. A. et al. 2003a. TGF-β1-mediated fibroblast–myofibroblast terminal differentiation—the role of smad proteins. *Experimental Cell Research* 282(2), pp. 90-100.

Evans, R. A. et al. 2003b. TGF-beta 1-mediated fibroblast-myofibroblast terminal differentiation - the role of Smad proteins. *Experimental Cell Research* 282(2), pp. 90-100.

Faassen, A. E. et al. 1992. A cell-surface chondroitin sulfate proteoglycan, immunologically related to cd44, is involved in type-I collagen-mediated melanoma cell motility and invasion. *Journal of Cell Biology* 116(2), pp. 521-531.

Fadool, J. M. and Linser, P. J. 1993. 5A11 antigen is a cell recognition molecule which is involved in neuronal-glial interactions in avian neural retina. *Developmental Dynamics* 196(4), pp. 252-262.

Fantuzzi, G. and Dinarello, C. A. 1996. The inflammatory response in interleukin-1 beta-deficient mice: comparison with other cytokine-related knock-out mice. *Journal of Leukocyte Biology* 59(4), pp. 489-493.

Feng, X.-H. and Derynck, R. 1996. Ligand-independent Activation of Transforming Growth Factor (TGF) β Signaling Pathways by Heteromeric Cytoplasmic Domains of TGF-β Receptors. *Journal of Biological Chemistry* 271(22), pp. 13123-13129.

Fitzgerald, K. A. et al. 2000. Ras, Protein Kinase Cζ, and IκB Kinases 1 and 2 Are Downstream Effectors of CD44 During the Activation of NF-κB by Hyaluronic Acid Fragments in T-24 Carcinoma Cells. *The Journal of Immunology* 164(4), pp. 2053-2063.

Fonseca, I. et al. 2000. Expression of CD44 isoforms in normal salivary gland tissue: an immunohistochemical and ultrastructural study. *Histochemistry and Cell Biology* 114(6), pp. 483-488.

Fontana, R. J. et al. 2008. Relationship of serum fibrosis markers with liver fibrosis stage and collagen content in patients with advanced chronic hepatitis C. *Hepatology* 47(3), pp. 789-798.

Fossum, S. et al. 1991. The MRC-OX-47 antigen is a member of the immunoglobulin superfamily with an unusual transmembrane sequence. *European Journal of Immunology* 21(3), pp. 671-679.

Fraser, J. R. E. et al. 1997. Hyaluronan: Its nature, distribution, functions and turnover. *Journal of Internal Medicine* 242(1), pp. 27-33.

Gabbiani, G. 2003. The myofibroblast in wound healing and fibrocontractive diseases. *Journal of Pathology* 200(4), pp. 500-503.

Gabbiani, G. et al. 1971. Presence of modified fibroblasts in granulation tissue and their possible role in wound contraction. *Experientia* 27(5), pp. 549-&.

Gabison, E. E. et al. 2005. EMMPRIN/CD147, an MMP modulator in cancer, development and tissue repair. *Biochimie* 87(3), pp. 361-368.

Gallatin, W. M. et al. 1983. A cell-surface molecule involved in organ-specific homing of lymphocytes. *Nature* 304(5921), pp. 30-34.

Gan, H. et al. 2002. Activation of nuclear factor-kappaB and its relationship with cytokine gene expression in colonic mucosa of ulcerative colitis patients. *Zhonghua nei ke za zhi* 41(4), pp. 252-255.

Gao, A. C. et al. 1997. CD44 is a metastasis suppressor gene for prostatic cancer located on human chromosome 11p13. *Cancer research* 57(5), pp. 846-849.

Gary, R. and Bretscher, A. 1993. Heterotypic and homotypic associations between ezrin and moesin, 2 putative membrane cytoskeletal linking proteins. *Proceedings of the National Academy of Sciences of the United States of America* 90(22), pp. 10846-10850.

Geiger, B. et al. 2001. Transmembrane extracellular matrix-cytoskeleton crosstalk. *Nature Reviews Molecular Cell Biology* 2(11), pp. 793-805.

Gelse, K. et al. 2003. Collagens—structure, function, and biosynthesis. *Advanced Drug Delivery Reviews* 55(12), pp. 1531-1546.

Ghatak, S. et al. 2014. Overexpression of c-Met and CD44v6 Receptors Contributes to Autocrine TGF-β1 Signaling in Interstitial Lung Disease. *The Journal of Biological Chemistry* 289(11), pp. 7856-7872.

Giannandrea, M. and Parks, W. C. 2014. Diverse functions of matrix metalloproteinases during fibrosis. *Disease Models & Mechanisms* 7(2), pp. 193-203.

Gill, S. E. et al. 2010. Tissue Inhibitor of Metalloproteinases 3 Regulates Resolution of Inflammation following Acute Lung Injury. *American Journal of Pathology* 176(1), pp. 64-73.

Goldman, R. 2004. Growth factors and chronic wound healing: past, present, and future. *Advances in skin & wound care* 17(1), pp. 24-35.

Goumans, M. J. et al. 2002. Balancing the activation state of the endothelium via two distinct TGF-β type I receptors. *The EMBO journal* 21(7), pp. 1743-1753.

Granet, C. et al. 2004. Increased AP-1 and NF-kappa B activation and recruitment with the combination of the proinflammatory cytokines IL-1 beta, tumor necrosis factor alpha and IL-17 in rheumatoid synoviocytes. *Arthritis Research & Therapy* 6(3), pp. R190-R198.

Grass, G. D. et al. 2013. CD147, CD44, and the Epidermal Growth Factor Receptor (EGFR) Signaling Pathway Cooperate to Regulate Breast Epithelial Cell Invasiveness. *Journal of Biological Chemistry* 288(36), pp. 26089-26104.

Guinebault, C. et al. 1995. Integrin-dependent translocation of phosphoinositide 3-kinase to the cytoskeleton of thrombin-activated platelets involves specific interactions of p85 alpha with actin filaments and focal adhesion kinase. *The Journal of Cell Biology* 129(3), pp. 831-842.

Haines, P. et al. 2011. Caveolin-1 is a negative regulator of MMP-1 gene expression in human dermal fibroblasts via inhibition of Erk1/2/Ets1 signaling pathway. *Journal of Dermatological Science* 64(3), pp. 210-216.

Hale, L. P. et al. 1995. Expression of CD44 variants in human inflammatory synovitis. *Journal of Clinical Immunology* 15(6), pp. 300-311.

Halfon, P. et al. 2005. Accuracy of hyaluronic acid level for predicting liver fibrosis stages in patients with hepatitis C virus. *Comparative hepatology* 4, pp. 6-6.

Hall, A. 1998. Rho GTPases and the actin cytoskeleton. *Science* 279(5350), pp. 509-514.

Hanna, S. M. et al. 2003. A novel form of the membrane protein CD147 that contains an extra Ig-like domain and interacts homophilically. *BMC Biochemistry* 4, pp. 17-17.

Hao, J. et al. 2012. In Vitro and In Vivo Prostate Cancer Metastasis and Chemoresistance Can Be Modulated by Expression of either CD44 or CD147. *Plos One* 7(8).

Harada, H. and Takahashi, M. 2007. CD44-dependent Intracellular and Extracellular Catabolism of Hyaluronic Acid by Hyaluronidase-1 and -2. *Journal of Biological Chemistry* 282(8), pp. 5597-5607.

Hardingham, T. and Bayliss, M. 1990. Proteoglycans of articular-cartilage - CHANGES IN AGING AND IN JOINT DISEASE. *Seminars in Arthritis and Rheumatism* 20(3), pp. 12-33.

Hayes, G. M. et al. 2002. Identification of Sequence Motifs Responsible for the Adhesive Interaction between Exon v10-containing CD44 Isoforms. *Journal of Biological Chemistry* 277(52), pp. 50529-50534.

Haynes, B. F. et al. 1991. Measurement of an adhesion molecule as an indicator of inflammatory disease-activity - up-regulation of the receptor for hyaluronate (CD44) in rheumatoid-arthritis. *Arthritis and Rheumatism* 34(11), pp. 1434-1443.

He, Q. et al. 1992. Molecular isoforms of murine CD44 and evidence that the membrane proximal domain is not critical for hyaluronate recognition. *The Journal of Cell Biology* 119(6), pp. 1711-1719.

Heiska, L. et al. 1998. Association of ezrin with intercellular adhesion molecule-1 and -2 (ICAM-1 and ICAM-2) - Regulation by phosphatidylinositol 4,5-bisphosphate. *Journal of Biological Chemistry* 273(34), pp. 21893-21900.

Heldin, C.-H. et al. 1997. TGF-[beta] signalling from cell membrane to nucleus through SMAD proteins. *Nature* 390(6659), pp. 465-471.

Henis, Y. I. et al. 1994. The type-ii and type-iii transforming growth-factor-beta receptors form homo-oligomers. *Journal of Cell Biology* 126(1), pp. 139-154.

Hileman, R. E. et al. 1998. Glycosaminoglycan-protein interactions: definition of consensus sites in glycosaminoglycan binding proteins. *Bioessays* 20(2), pp. 156-167.

Hinz, B. 2007. Formation and function of the myofibroblast during tissue repair. *Journal of Investigative Dermatology* 127(3), pp. 526-537.

Hinz, B. et al. 2003. alpha-smooth muscle actin is crucial for focal adhesion maturation in myofibroblasts. *Molecular Biology of the Cell* 14(6), pp. 2508-2519.

Hinz, B. et al. 2002. The NH2-terminal peptide of α–smooth muscle actin inhibits force generation by the myofibroblast in vitro and in vivo. *The Journal of Cell Biology* 157(4), pp. 657-663.

Hinz, B. et al. 2001. Mechanical tension controls granulation tissue contractile activity and myofibroblast differentiation. *American Journal of Pathology* 159(3), pp. 1009-1020.

Hinz, B. et al. 2007. The Myofibroblast: One Function, Multiple Origins. *The American Journal of Pathology* 170(6), pp. 1807-1816.

Hirao, M. et al. 1996. Regulation mechanism of ERM (ezrin/radixin/moesin) protein/plasma membrane association: Possible involvement of phosphatidylinositol turnover and Rho-dependent signaling pathway. *Journal of Cell Biology* 135(1), pp. 37-51.

Horst, E. et al. 1990. Adhesion molecules in the prognosis of diffuse large-cell lymphoma - expression of a lymphocyte homing receptor (CD44), LFA-1 (CD11A/18), and ICAM-1 (CD54). *Leukemia* 4(8), pp. 595-599.

Hotchin, N. A. and Hall, A. 1995. The assembly of integrin adhesion complexes requires both extracellular matrix and intracellular rho/rac GTPases. *The Journal of cell biology* 131(6), pp. 1857-1865.

Huang, W. et al. 2013. Modulation of CD147-induced matrix metalloproteinase activity: role of CD147 N-glycosylation. *Biochemical Journal* 449(2), pp. 437-448.

Hudson, D. L. et al. 1995. CD44 is the major peanut lectin-binding glycoprotein of human epidermal-keratinocytes and plays a role in intercellular-adhesion. *Journal of Cell Science* 108, pp. 1959-1970.

Huet, E. et al. 2008a. Role of emmprin/CD147 in tissue remodeling. *Connective tissue research* 49(3-4), pp. 175-179.

Huet, E. et al. 2008b. Extracellular matrix metalloproteinase inducer/CD147 promotes myofibroblast differentiation by inducing α-smooth muscle actin expression and collagen gel contraction: implications in tissue remodeling. *The FASEB Journal* 22(4), pp. 1144-1154.

Iacono, K. T. et al. 2007. CD147 immunoglobulin superfamily receptor function and role in pathology. *Experimental and Molecular Pathology* 83(3), pp. 283-295.

Ibrahim, E. M. et al. 2006. Upregulation of CD44 expression by interleukins 1, 4, and 13, transforming growth factor-beta 1, estrogen, and progestogen in human cervical adenocarcinoma cell lines. *International Journal of Gynecological Cancer* 16(4), pp. 1631-1642.

Iczkowski, K. A. et al. 2003. Prostate cancer overexpresses CD44 variants 7-9 at the messenger RNA and protein level. *Anticancer Research* 23(4), pp. 3129-3140.

Ignotz, R. A. and Massague, J. 1986. Transforming growth factor-beta stimulates the expression of fibronectin and collagen and their incorporation into the extracellular matrix. *Journal of Biological Chemistry* 261(9), pp. 4337-4345.

Iida, N. and Bourguignon, L. Y. W. 1997. Coexpression of CD44 variant (v10/ex14) and CD44S in human mammary epithelial cells promotes tumorigenesis. *Journal of Cellular Physiology* 171(2), pp. 152-160.

Itano, N. 2008. Simple primary structure, complex turnover regulation and multiple roles of hyaluronan. *Journal of Biochemistry* 144(2), pp. 131-137.

Itano, N. et al. 1999. Three Isoforms of Mammalian Hyaluronan Synthases Have Distinct Enzymatic Properties. *Journal of Biological Chemistry* 274(35), pp. 25085-25092.

Ito, T. et al. 2004. Hyaluronan and proximal tubular cell migration. *Kidney International* 65(3), pp. 823-833.

Iwano, M. et al. 2002. Evidence that fibroblasts derive from epithelium during tissue fibrosis. *Journal of Clinical Investigation* 110(3), pp. 341-350.

Jalkanen, S. and Jalkanen, M. 1992. Lymphocyte CD44 binds the cooh-terminal heparin-binding domain of fibronectin. *Journal of Cell Biology* 116(3), pp. 817-825.

Jalkanen, S. T. et al. 1986. A lymphoid-cell surface glycoprotein involved in endothelial-cell recognition and lymphocyte homing in man. *European Journal of Immunology* 16(10), pp. 1195-1202.

Janis, J. E. and Harrison, B. 2014. Wound Healing: Part I. Basic Science. *Plastic and Reconstructive Surgery* 133(2), pp. 199E-207E.

Jenkins, R. H. et al. 2004. Myofibroblastic differentiation leads to hyaluronan accumulation through reduced hyaluronan turnover. *Journal of Biological Chemistry* 279(40), pp. 41453-41460.

Jia, L. et al. 2006. Caveolin-1 up-regulates CD147 glycosylation and the invasive capability of murine hepatocarcinoma cell lines. *The International Journal of Biochemistry & Cell Biology* 38(9), pp. 1584-1593.

Jiang, D. H. et al. 2011. Hyaluronan as an Immune Regulator in Human Diseases. *Physiological Reviews* 91(1), pp. 221-264.

Jokela, T. et al. 2015. Interleukin-1-induced Reduction of CD44 Ser-325 Phosphorylation in Human Epidermal Keratinocytes Promotes CD44 Homomeric Complexes, Binding to Ezrin, and Extended, Monocyte-adhesive Hyaluronan Coats. *Journal of Biological Chemistry* 290(19), pp. 12379-12393.

Jurica, M. S. and Moore, M. J. 2003. Pre-mRNA splicing: Awash in a sea of proteins. *Molecular Cell* 12(1), pp. 5-14.

Kaname, T. et al. 1993. Mapping basigin (bsg), a member of the immunoglobulin superfamily, to 19p13.3. *Cytogenetics and Cell Genetics* 64(3-4), pp. 195-197.

Kanekura, T. et al. 2002. Basigin (CD147) is expressed on melanoma cells and induces tumor cell invasion by stimulating production of matrix metalloproteinases by fibroblasts. *International Journal of Cancer* 99(4), pp. 520-528.

Kasper, M. et al. 1995. Distinct expression patterns of cd44 isoforms during human lung development and in pulmonary fibrosis. *American Journal of Respiratory Cell and Molecular Biology* 13(6), pp. 648-656.

Kassiri, Z. et al. 2009. Loss of TIMP3 Enhances Interstitial Nephritis and Fibrosis. *Journal of the American Society of Nephrology* 20(6), pp. 1223-1235.

Kataoka, H. et al. 1993. tumor cell-derived collagenase-stimulatory factor increases expression of interstitial collagenase, stromelysin, and 72-kda gelatinase. *Cancer Research* 53(13), pp. 3154-3158.

Kato, N. et al. 2011. Basigin/CD147 Promotes Renal Fibrosis after Unilateral Ureteral Obstruction. *American Journal of Pathology* 178(2), pp. 572-579.

Kawamura, S. et al. 2003. Initiation and Transduction of Stretch-induced RhoA and Rac1 Activation through Caveolae: cytoskeletal regulation of erk translocation. *Journal of Biological Chemistry* 278(33), pp. 31111-31117.

Khunkeawla, P. et al. 2001. Engagement of CD147 molecule-induced cell aggregation through the activation of protein kinases and reorganization of the cytoskeleton. *Immunobiology* 203(4), pp. 659-669.

Kim, K. K. et al. 2006. Alveolar epithelial cell mesenchymal transition develops in vivo during pulmonary fibrosis and is regulated by the extracellular matrix. *Proceedings of the National Academy of Sciences* 103(35), pp. 13180-13185.

Kirk, P. et al. 2000. CD147 is tightly associated with lactate transporters MCT1 and MCT4 and facilitates their cell surface expression. *Embo Journal* 19(15), pp. 3896-3904.

Kjellen, L. and Lindahl, U. 1991. Proteoglycans - structures and interactions. *Annual Review of Biochemistry* 60, pp. 443-475.

Kohan, M. et al. 2010. EDA-containing cellular fibronectin induces fibroblast differentiation through binding to α4β7 integrin receptor and MAPK/Erk 1/2-dependent signaling. *The FASEB Journal* 24(11), pp. 4503-4512.

Kolb, M. et al. 2001. Transient expression of IL-1 beta induces acute lung injury and chronic repair leading to pulmonary fibrosis. *Journal of Clinical Investigation* 107(12), pp. 1529-1536.

Konstan, M. W. et al. 2010. Trends in the Use of Routine Therapies in Cystic Fibrosis: 1995–2005. *Pediatric pulmonology* 45(12), pp. 1167-1172.

Koprich, J. B. et al. 2008. Neuroinflammation mediated by IL-1 beta increases susceptibility of dopamine neurons to degeneration in an animal model of Parkinson's disease. *Journal of Neuroinflammation* 5.

Kosaki, R. et al. 1999. Overproduction of hyaluronan by expression of the hyaluronan synthase Has2 enhances anchorage-independent growth and tumorigenicity. *Cancer Research* 59(5), pp. 1141-1145.

Kouvidi, K. et al. 2011. Role of Receptor for Hyaluronic Acid-mediated Motility (RHAMM) in Low Molecular Weight Hyaluronan (LMWHA)-mediated Fibrosarcoma Cell Adhesion. *Journal of Biological Chemistry* 286(44), pp. 38509-38520.

Krumm, B. et al. 2014. Structural biology of the IL-1 superfamily: Key cytokines in the regulation of immune and inflammatory responses. *Protein Science* 23(5), pp. 526-538.

Lachmandas, E. et al. 2015. The Effect of Hyperglycaemia on In Vitro Cytokine Production and Macrophage Infection with Mycobacterium tuberculosis. *PLoS ONE* 10(2), p. e0117941.

Lang, K. et al. 1987. Catalysis of protein folding by prolyl isomerase. *Nature* 329(6136), pp. 268-270.

Laskin, D. L. et al. 2011. Macrophages and Tissue Injury: Agents of Defense or Destruction? *Annual review of pharmacology and toxicology* 51, pp. 267-288.

Lau, W. M. et al. 2014. CD44v8-10 Is a Cancer-Specific Marker for Gastric Cancer Stem Cells. *Cancer Research* 74(9), pp. 2630-2641.

Lawrence, D. A. 1996. Transforming growth factor-beta: A general review. *European Cytokine Network* 7(3), pp. 363-374.

Lech, M. and Anders, H.-J. 2013. Macrophages and fibrosis: How resident and infiltrating mononuclear phagocytes orchestrate all phases of tissue injury and repair. *Biochimica et Biophysica Acta (BBA) - Molecular Basis of Disease* 1832(7), pp. 989-997.

Ledebur, H. C. and Parks, T. P. 1995. Transcriptional Regulation of the Intercellular Adhesion Molecule-1 Gene by Inflammatory Cytokines in Human Endothelial Cells: Essential roles of a variant nf-κb site and p65 homodimers. *Journal of Biological Chemistry* 270(2), pp. 933-943.

Lee, C. G. et al. 2001. Interleukin-13 Induces Tissue Fibrosis by Selectively Stimulating and Activating Transforming Growth Factor β1. *The Journal of Experimental Medicine* 194(6), pp. 809-822.

Legg, J. W. et al. 2002. A novel PKC-regulated mechanism controls CD44-ezrin association and directional cell motility. *Nature Cell Biology* 4(6), pp. 399-407.

Lesley, J. et al. 1995. Variant cell-lines selected for alterations in the function of the hyaluronan receptor cd44 show differences in glycosylation. *Journal of Experimental Medicine* 182(2), pp. 431-437.

Li, H.-Y. et al. 2015. Activation of TGF-β1-CD147 positive feedback loop in hepatic stellate cells promotes liver fibrosis. *Scientific Reports* 5, p. 16552.

Li, J. et al. 2007. Pathophysiology of acute wound healing. *Clinics in Dermatology* 25(1), pp. 9-18.

Li, L. et al. 2013. HAb18G/CD147 Promotes pSTAT3-Mediated Pancreatic Cancer Development via CD44s. *Clinical Cancer Research* 19(24), pp. 6703-6715.

Liacini, A. et al. 2002. Inhibition of interleukin-1-stimulated MAP kinases, activating protein-1 (AP-1) and nuclear factor kappa B (NF-κB) transcription factors down-regulates matrix metalloproteinase gene expression in articular chondrocytes. *Matrix Biology* 21(3), pp. 251-262.

Liang, J. et al. 2011. The Role of Hyaluronan and Hyaluronan Binding Proteins in Human Asthma. *The Journal of allergy and clinical immunology* 128(2), pp. 403-411.e403.

Liang, L. et al. 2002. Characterization of the promoter of human extracellular matrix metalloproteinase inducer (EMMPRIN). *Gene* 282(1-2), pp. 75-86.

Lim, M. et al. 1998. Tumor-derived EMMPRIN (extracellular matrix metalloproteinase inducer) stimulates collagenase transcription through MAPK p38. *Febs Letters* 441(1), pp. 88-92.

Liu, D. C. and Sy, M. S. 1997. Phorbol myristate acetate stimulates the dimerization of CD44 involving a cysteine in the transmembrane domain. *Journal of Immunology* 159(6), pp. 2702-2711.

Liu, Y. 0000. Renal fibrosis: New insights into the pathogenesis and therapeutics. *Kidney Int* 69(2), pp. 213-217.

Liu, Y. H. 2006. Renal fibrosis: New insights into the pathogenesis and therapeutics. *Kidney International* 69(2), pp. 213-217.

Lokeshwar, V. B. et al. 1994. Ankyrin-binding domain of CD44(GP85) is required for the expression of hyaluronic acid-mediated adhesion function. *Journal of Cell Biology* 126(4), pp. 1099-1109.

Ma, X.-K. et al. 2010. HAb18G/CD147 cell-cell contacts confer resistance of a HEK293 subpopulation to anoikis in an E-cadherin-dependent manner. *BMC Cell Biology* 11(1), pp. 1-13.

Martin, P. and Leibovich, S. J. Inflammatory cells during wound repair: the good, the bad and the ugly. *Trends in Cell Biology* 15(11), pp. 599-607.

Martin, P. and Leibovich, S. J. 2005. Inflammatory cells during wound, repair: the good, the bad and the ugly. *Trends in Cell Biology* 15(11), pp. 599-607.

Matsui, T. et al. 1998. Rho-Kinase Phosphorylates COOH-terminal Threonines of Ezrin/Radixin/Moesin (ERM) Proteins and Regulates Their Head-to-Tail Association. *The Journal of Cell Biology* 140(3), pp. 647-657.

Mayeda, A. et al. 1993. Modulation of exon skipping and inclusion by heterogeneous nuclear ribonucleoprotein-a1 and premessenger rna splicing factor SF2/ASF. *Molecular and Cellular Biology* 13(5), pp. 2993-3001.

McAnulty, R. J. 2007. Fibroblasts and myofibroblasts: Their source, function and role in disease. *The International Journal of Biochemistry & Cell Biology* 39(4), pp. 666-671.

McKeown-Longo, P. J. and Mosher, D. F. 1983. Binding of plasma fibronectin to cell layers of human skin fibroblasts. *The Journal of Cell Biology* 97(2), pp. 466-472.

McKeownlongo, P. J. and Mosher, D. F. 1985. INTERACTION OF THE 70,000-MOL-WT AMINO-TERMINAL FRAGMENT OF FIBRONECTIN WITH THE MATRIX-ASSEMBLY RECEPTOR OF FIBROBLASTS. *Journal of Cell Biology* 100(2), pp. 364-374.

Meirelles, L. D. S. et al. 2006. Mesenchymal stem cells reside in virtually all post-natal organs and tissues. *Journal of Cell Science* 119(11), pp. 2204-2213.

Meran, S. et al. 2011a. Hyaluronan Facilitates Transforming Growth Factor-beta 1-dependent Proliferation via CD44 and Epidermal Growth Factor Receptor Interaction. *Journal of Biological Chemistry* 286(20), pp. 17618-17630.

Meran, S. et al. 2011b. Hyaluronan Facilitates Transforming Growth Factor-β1-dependent Proliferation via CD44 and Epidermal Growth Factor Receptor Interaction. *Journal of Biological Chemistry* 286(20), pp. 17618-17630.

Meran, S. et al. 2013. Interleukin-1 beta Induces Hyaluronan and CD44-Dependent Cell Protrusions That Facilitate Fibroblast-Monocyte Binding. *American Journal of Pathology* 182(6), pp. 2223-2240.

Meran, S. and Steadman, R. 2011. Fibroblasts and myofibroblasts in renal fibrosis. *International Journal of Experimental Pathology* 92(3), pp. 158-167.

Meran, S. et al. 2008a. Hyaluronan facilitates TGF beta 1 mediated myofibroblastic differentiation. *Wound Repair and Regeneration* 16(2), pp. A12-A12.

Meran, S. et al. 2007. Involvement of hyaluronan in regulation of fibroblast phenotype. *Journal of Biological Chemistry* 282(35), pp. 25687-25697.

Meran, S. et al. 2008b. Hyaluronan facilitates transforming growth factor-beta(1)-mediated fibroblast proliferation. *Journal of Biological Chemistry* 283(10), pp. 6530-6545.

Meyer, K. and Palmer, J. W. 1934. The polysaccharide of the vitreous humor. *Journal of Biological Chemistry* 107(3), pp. 629-634.

Midgley, A. C. et al. 2015. Hyaluronan Regulates Bone Morphogenetic Protein-7-dependent Prevention and Reversal of Myofibroblast Phenotype. *Journal of Biological Chemistry* 290(18), pp. 11218-11234.

Midgley, A. C. et al. 2013. Transforming Growth Factor-beta 1 (TGF-beta 1)-stimulated Fibroblast to Myofibroblast Differentiation Is Mediated by Hyaluronan (HA)-facilitated Epidermal Growth Factor Receptor (EGFR) and CD44 Co-localization in Lipid Rafts. *Journal of Biological Chemistry* 288(21), pp. 14824-14838.

Miletti-González, K. E. et al. 2012. Identification of Function for CD44 Intracytoplasmic Domain (CD44-ICD): modulation of matrix metalloproteinase 9 (MMP-9) transcription via novel promoter response element. *Journal of Biological Chemistry* 287(23), pp. 18995-19007.

Mirza, R. E. et al. 2013. Blocking Interleukin-1β Induces a Healing-Associated Wound Macrophage Phenotype and Improves Healing in Type 2 Diabetes. *Diabetes* 62(7), pp. 2579-2587.

Mollinedo, F. et al. 2010. Lipid raft-targeted therapy in multiple myeloma. *Oncogene* 29(26), pp. 3748-3757.

Morrison, H. et al. 2001. The NF2 tumor suppressor gene product, merlin, mediates contact inhibition of growth through interactions with CD44. *Genes & Development* 15(8), pp. 968-980.

Muro, A. F. et al. 2008. An essential role for fibronectin extra type III domain A in pulmonary fibrosis. *American Journal of Respiratory and Critical Care Medicine* 177(6), pp. 638-645.

Murray, D. et al. 2004. Increased invasion and expression of MMP-9 in human colorectal cell lines by a CD44-dependent mechanism. *Anticancer Research* 24(2A), pp. 489-494.

Nabeshima, K. et al. 2006. Emmprin (basigin/CD147): Matrix metalloproteinase modulator and multifunctional cell recognition molecule that plays a critical role in cancer progression. *Pathology International* 56(7), pp. 359-367.

Nagano, O. and Saya, H. 2004. Mechanism and biological significance of CD44 cleavage. *Cancer Science* 95(12), pp. 930-935.

Nakamura, K. et al. 2004. High, but not low, molecular weight hyaluronan prevents T-cell-mediated liver injury by reducing proinflammatory cytokines in mice. *Journal of Gastroenterology* 39(4), pp. 346-354.

Naor, D. et al. 2009. Involvement of CD44, a Molecule with a Thousand Faces, in Cancer Dissemination. *Hyaluronan in Cancer Biology, 1st Edition*, pp. 127-146.

Narmada, B. C. et al. 2013. HGF regulates the activation of TGF-β1 in rat hepatocytes and hepatic stellate cells. *Journal of Cellular Physiology* 228(2), pp. 393-401.

Neame, S. J. et al. 1995. CD44 exhibits a cell-type dependent interaction with triton x-100 insoluble, lipid rich, plasma-membrane domains. *Journal of Cell Science* 108, pp. 3127-3135.

Nedvetzki, S. et al. 2004. RHAMM, a receptor for hyaluronan-mediated motility, compensates for CD44 in inflamed CD44-knockout mice: A different interpretation of redundancy. *Proceedings of the National Academy of Sciences of the United States of America* 101(52), pp. 18081-18086.

Ng, T. et al. 2001. Ezrin is a downstream effector of trafficking PKC-integrin complexes involved in the control of cell motility. *Embo Journal* 20(11), pp. 2723-2741.

Oertli, B. et al. 1998. Mechanisms of Hyaluronan-Induced Up-Regulation of ICAM-1 and VCAM-1 Expression by Murine Kidney Tubular Epithelial Cells: Hyaluronan Triggers Cell Adhesion Molecule Expression Through a Mechanism Involving Activation of Nuclear Factor-κB and Activating Protein-1. *The Journal of Immunology* 161(7), pp. 3431-3437.

Okamoto, I. et al. 2001. Proteolytic release of CD44 intracellular domain and its role in the CD44 signaling pathway. *The Journal of Cell Biology* 155(5), pp. 755-762.

Okamoto, T. et al. 1998. Caveolins, a Family of Scaffolding Proteins for Organizing "Preassembled Signaling Complexes" at the Plasma Membrane. *Journal of Biological Chemistry* 273(10), pp. 5419-5422.

Oliferenko, S. et al. 1999. Analysis of CD44-Containing Lipid Rafts: Recruitment of Annexin II and Stabilization by the Actin Cytoskeleton. *The Journal of Cell Biology* 146(4), pp. 843-854.

Onozuka, I. et al. 2011. Cholestatic liver fibrosis and toxin-induced fibrosis are exacerbated in matrix metalloproteinase-2 deficient mice. *Biochemical and Biophysical Research Communications* 406(1), pp. 134-140.

Ouhtit, A. et al. 2007. In vivo evidence for the role of CD44s in promoting breast cancer metastasis to the liver. *American Journal of Pathology* 171(6), pp. 2033-2039.

Parish, C. R. 2006. The role of heparan sulphate in inflammation. *Nature Reviews Immunology* 6(9), pp. 633-643.

Parpal, S. et al. 2001. Cholesterol Depletion Disrupts Caveolae and Insulin Receptor Signaling for Metabolic Control via Insulin Receptor Substrate-1, but Not for Mitogen-activated Protein Kinase Control. *Journal of Biological Chemistry* 276(13), pp. 9670-9678.

Parton, R. G. and Simons, K. 2007. The multiple faces of caveolae. *Nature Reviews Molecular Cell Biology* 8(3), pp. 185-194.

Peach, R. J. et al. 1993. Identification of hyaluronic acid binding sites in the extracellular domain of CD44. *The Journal of Cell Biology* 122(1), pp. 257-264.

Peck, D. and Isacke, C. M. 1998. Hyaluronan-dependent cell migration can be blocked by a CD44 cytoplasmic domain peptide containing a phosphoserine at position 325. *Journal of Cell Science* 111, pp. 1595-1601.

Perschl, A. et al. 1995. Transmembrane domain of cd44 is required for its detergent insolubility in fibroblasts. *Journal of Cell Science* 108, pp. 1033-1041.

Pham, P. V. et al. 2011. Differentiation of breast cancer stem cells by knockdown of CD44: promising differentiation therapy. *Journal of Translational Medicine* 9(1), pp. 1-13.

Pierce, G. F. et al. 1992. Platelet-derived growth-factor (bb homodimer), transforming growth factor-beta-1, and basic fibroblast growth-factor in dermal wound-healing - neovessel and matrix formation and cessation of repair. *American Journal of Pathology* 140(6), pp. 1375-1388.

Pietromonaco, S. F. et al. 1998. Protein Kinase C-θ Phosphorylation of Moesin in the Actin-binding Sequence. *Journal of Biological Chemistry* 273(13), pp. 7594-7603.

Ponta, H. et al. 2003. CD44: From adhesion molecules to signalling regulators. *Nat Rev Mol Cell Biol* 4(1), pp. 33-45.

Prockop, D. J. et al. 1998. Procollagen N-proteinase and procollagen C-proteinase. Two unusual metalloproteinases that are essential for procollagen processing probably have important roles in development and cell signaling. *Matrix Biology* 16(7), pp. 399-408.

Pushkarsky, T. et al. 2001. CD147 facilitates HIV-1 infection by interacting with virus-associated cyclophilin A. *Proceedings of the National Academy of Sciences of the United States of America* 98(11), pp. 6360-6365.

Qian, A.-R. et al. 2008. Downregulation of CD147 expression alters cytoskeleton architecture and inhibits gelatinase production and SAPK pathway in human hepatocellular carcinoma cells. *Journal of Experimental & Clinical Cancer Research : CR* 27(1), pp. 50-50.

Quest, A. F. G. et al. 2004. Caveolins, caveolae, and lipid rafts in cellular transport, signaling, and disease. *Biochemistry and Cell Biology-Biochimie Et Biologie Cellulaire* 82(1), pp. 129-144.

Ra, H.-J. and Parks, W. C. 2007. Control of matrix metalloproteinase catalytic activity. *Matrix Biology* 26(8), pp. 587-596.

Rai, S. K. et al. 2001. Candidate tumor suppressor HYAL2 is a glycosylphosphatidylinositol (GPI)-anchored cell-surface receptor for jaagsiekte sheep retrovirus, the envelope protein of which mediates oncogenic transformation. *Proceedings of the National Academy of Sciences* 98(8), pp. 4443-4448.

Rampanelli, E. et al. 2014. Opposite role of CD44-standard and CD44-variant-3 in tubular injury and development of renal fibrosis during chronic obstructive nephropathy. *Kidney International* 86(3), pp. 558-569.

Repesh, L. A. et al. 1982. Fibronectin involvement in granulation-tissue and wound-healing in rabbits. *Journal of Histochemistry & Cytochemistry* 30(4), pp. 351-358.

Riento, K. and Ridley, A. J. 2003. ROCKs: multifunctional kinases in cell behaviour. *Nat Rev Mol Cell Biol* 4(6), pp. 446-456.

Robertson, I. B. et al. 2015. Latent TGF-beta-binding proteins. *Matrix biology : journal of the International Society for Matrix Biology* 47, pp. 44-53.

Rosenberg, W. M. C. et al. 1995a. Increased expression of CD44v6 and CD44v3 in ulcerative colitis but not colonic Crohn's disease. *The Lancet* 345(8959), pp. 1205-1209.

Rosenberg, W. M. C. et al. 1995b. Increased expression of cd44v6 and cd44v3 in ulcerative-colitis but not colonic crohns-disease. *Lancet* 345(8959), pp. 1205-1209.

Rosenberg, W. M. C. et al. 2004. Serum markers detect the presence of liver fibrosis: a cohort study. *Gastroenterology* 127(6), pp. 1704-1713.

Roskoski Jr, R. 2012. ERK1/2 MAP kinases: Structure, function, and regulation. *Pharmacological Research* 66(2), pp. 105-143.

Roskoski, R., Jr. 2012. ERK1/2 MAP kinases: Structure, function, and regulation. *Pharmacological Research* 66(2), pp. 105-143.

Rouschop, K. M. A. et al. 2004. CD44 Deficiency Increases Tubular Damage But Reduces Renal Fibrosis in Obstructive Nephropathy. *Journal of the American Society of Nephrology* 15(3), pp. 674-686.

Ruffell, B. et al. 2011. Differential Use of Chondroitin Sulfate to Regulate Hyaluronan Binding by Receptor CD44 in Inflammatory and Interleukin 4-activated Macrophages. *The Journal of Biological Chemistry* 286(22), pp. 19179-19190.

Salemi, S. et al. 2003. Detection of interleukin 1 beta (IL-1 beta), IL-6, and tumor necrosis factor-alpha in skin of patients with fibromyalgia. *Journal of Rheumatology* 30(1), pp. 146-150.

Sandbo, N. and Dulin, N. 2011. The actin cytoskeleton in myofibroblast differentiation: Ultrastructure defining form and driving function. *Translational Research* 158(4), pp. 181-196.

Schlosshauer, B. and Herzog, K. H. 1990. Neurothelin - an inducible cell-surface glycoprotein of blood-brain-barrier specific endothelial-cells and distinct neurons. *Journal of Cell Biology* 110(4), pp. 1261-1274.

Seiki, M. 2002. The cell surface: the stage for matrix metalloproteinase regulation of migration. *Current Opinion in Cell Biology* 14(5), pp. 624-632.

Selbi, W. et al. 2004. BMP-7 Modulates Hyaluronan-Mediated Proximal Tubular Cell-Monocyte Interaction. *Journal of the American Society of Nephrology* 15(5), pp. 1199-1211.

Selbi, W. et al. 2006. Characterization of hyaluronan cable structure and function in renal proximal tubular epithelial cells. *Kidney International* 70(7), pp. 1287-1295.

Seoane, J. 2006. Escaping from the TGFβ anti-proliferative control. *Carcinogenesis* 27(11), pp. 2148-2156.

Serini, G. et al. 1998. The fibronectin domain ED-A is crucial for myofibroblastic phenotype induction by transforming growth factor-beta 1. *Journal of Cell Biology* 142(3), pp. 873-881.

Serini, G. and Gabbiani, G. 1999. Mechanisms of myofibroblast activity and phenotypic modulation. *Experimental Cell Research* 250(2), pp. 273-283.

Seulberger, H. et al. 1990. The inducible blood-brain-barrier specific molecule ht7 is a novel immunoglobulin-like cell-surface glycoprotein. *Embo Journal* 9(7), pp. 2151-2158.

Seulberger, H. et al. 1992. HT7, NEUROTHELIN, BASIGIN, GP42 AND OX-47 - many names for one developmentally regulated immunoglobulin-like surface glycoprotein on blood-brain-barrier endothelium, epithelial tissue barriers and neurons. *Neuroscience Letters* 140(1), pp. 93-97.

Sherman, L. S. et al. 2015. Hyaluronan Synthesis, Catabolism, and Signaling in Neurodegenerative Diseases. *International journal of cell biology* 2015, pp. 368584-368584.

Shi, Y. et al. 2011. Continuous cyclic mechanical tension inhibited Runx2 expression in mesenchymal stem cells through RhoA-ERK1/2 pathway. *Journal of cellular physiology* 226(8), pp. 2159-2169.

Simons, K. and Toomre, D. 2000. Lipid rafts and signal transduction. *Nat Rev Mol Cell Biol* 1(1), pp. 31-39.

Simpson, R. M. L. et al. 2009. Age-Related Changes in Pericellular Hyaluronan Organization Leads to Impaired Dermal Fibroblast to Myofibroblast Differentiation. *The American Journal of Pathology* 175(5), pp. 1915-1928.

Simpson, R. M. L. et al. 2010. Aging Fibroblasts Resist Phenotypic Maturation Because of Impaired Hyaluronan-Dependent CD44/Epidermal Growth Factor Receptor Signaling. *American Journal of Pathology* 176(3), pp. 1215-1228.

Singh, P. et al. 2010. Assembly of Fibronectin Extracellular Matrix. *Annual Review of Cell and Developmental Biology, Vol 26* 26, pp. 397-419.

Smith, T. J. et al. 1989. Hormonal-regulation of hyaluronate synthesis in cultured human-fibroblasts - evidence for differences between retroocular and dermal fibroblasts. *Journal of Clinical Endocrinology & Metabolism* 69(5), pp. 1019-1023.

Song, K. S. et al. 1996. Expression of caveolin-3 in skeletal, cardiac, and smooth muscle cells - Caveolin-3 is a component of the sarcolemma and co-fractionates with dystrophin and dystrophin-associated glycoproteins. *Journal of Biological Chemistry* 271(25), pp. 15160-15165.

Spicer, A. P. and McDonald, J. A. 1998. Characterization and Molecular Evolution of a Vertebrate Hyaluronan Synthase Gene Family. *Journal of Biological Chemistry* 273(4), pp. 1923-1932.

Stamenkovic, I. et al. 1991. The hematopoietic and epithelial forms of cd44 are distinct polypeptides with different adhesion potentials for hyaluronate-bearing cells. *Embo Journal* 10(2), pp. 343-348.

Steed, D. L. 1997. The role of growth factors in wound healing. *Surgical Clinics of North America* 77(3), pp. 575-586.

Stephens, P. et al. 1996. A Comparison of the Ability of Intra-oral and Extra-oral Fibroblasts to Stimulate Extracellular Matrix Reorganization in a Model of Wound Contraction. *Journal of Dental Research* 75(6), pp. 1358-1364.

Stivarou, T. and Patsavoudi, E. 2015. Extracellular Molecules Involved in Cancer Cell Invasion. *Cancers* 7(1), pp. 238-265.

Streuli, C. H. et al. 1993. Extracellular-matrix regulates expression of the tgf-beta-1 gene. *Journal of Cell Biology* 120(1), pp. 253-260.

Stridh, S. et al. 2012. Renal interstitial hyaluronan: functional aspects during normal and pathological conditions. *American Journal of Physiology - Regulatory, Integrative and Comparative Physiology* 302(11), pp. R1235-R1249.

Stylianou, E. and Saklatvala, J. 1998. Interleukin-1. *The International Journal of Biochemistry & Cell Biology* 30(10), pp. 1075-1079.

Sullivan, D. E. et al. 2005. Tumor Necrosis Factor-α Induces Transforming Growth Factor-β1 Expression in Lung Fibroblasts Through the Extracellular Signal–Regulated Kinase Pathway. *American Journal of Respiratory Cell and Molecular Biology* 32(4), pp. 342-349.

Sun, H. B. et al. 2008. Coordinate regulation of IL-1 beta and MMP-13 in rat tendons following subrupture fatigue damage. *Clinical Orthopaedics and Related Research* 466(7), pp. 1555-1561.

Sun, J. and Hemler, M. E. 2001. Regulation of MMP-1 and MMP-2 Production through CD147/Extracellular Matrix Metalloproteinase Inducer Interactions. *Cancer Research* 61(5), pp. 2276-2281.

Swann, D. A. et al. 1974. Role of hyaluronic acid in joint lubrication. *Annals of the Rheumatic Diseases* 33(4), pp. 318-326.

Szpaderska, A. M. et al. 2003. Differential Injury Responses in Oral Mucosal and Cutaneous Wounds. *Journal of Dental Research* 82(8), pp. 621-626.

Tak, P. P. and Firestein, G. S. 2001. NF-κB: a key role in inflammatory diseases. *Journal of Clinical Investigation* 107(1), pp. 7-11.

Tang, J. et al. 2008a. Overexpression of HAb18G/CD147 promotes invasion and metastasis via alpha3beta1 integrin mediated FAK-paxillin and FAK-PI3K-Ca2+ pathways. *Cell Mol Life Sci* 65.

Tang, J. et al. 2008b. Overexpression of HAb18G/CD147 promotes invasion and metastasis via alpha 3 beta 1 integrin mediated FAK-paxillin and FAK-PI3K-Ca(2+) pathways. *Cellular and Molecular Life Sciences* 65(18), pp. 2933-2942.

Tang, W. et al. 2004. Links between CD147 Function, Glycosylation, and Caveolin-1. *Molecular Biology of the Cell* 15(9), pp. 4043-4050.

Tang, W. and Hemler, M. E. 2004. Caveolin-1 Regulates Matrix Metalloproteinases-1 Induction and CD147/EMMPRIN Cell Surface Clustering. *Journal of Biological Chemistry* 279(12), pp. 11112-11118.

Termeer, C. et al. 2002. Oligosaccharides of Hyaluronan Activate Dendritic Cells via Toll-like Receptor 4. *The Journal of Experimental Medicine* 195(1), pp. 99-111.

Terpe, H. J. et al. 1994. CD44 variant isoforms are preferentially expressed in basal epithelia of nonmalignant human fetal and adult tissues. *Histochemistry* 101(2), pp. 79-89.

Thomas, L. et al. 1993. Migration of human melanoma cells on hyaluronate is related to CD44 expression. *Journal of Investigative Dermatology* 100(2), pp. 115-120.

Thornberry, N. A. et al. 1992. A novel heterodimeric cysteine protease is required for interleukin-1[beta]processing in monocytes. *Nature* 356(6372), pp. 768-774.

Tian, X. et al. 2010. Hepatitis B Virus (HBV) Surface Antigen Interacts with and Promotes Cyclophilin A Secretion: Possible Link to Pathogenesis of HBV Infection. *Journal of Virology* 84(7), pp. 3373-3381.

Tolg, C. et al. 2006. Rhamm−/− fibroblasts are defective in CD44-mediated ERK1, 2 motogenic signaling, leading to defective skin wound repair. *The Journal of cell biology* 175(6), pp. 1017-1028.

Tolg, C. et al. 2012. A RHAMM Mimetic Peptide Blocks Hyaluronan Signaling and Reduces Inflammation and Fibrogenesis in Excisional Skin Wounds. *The American Journal of Pathology* 181(4), pp. 1250-1270.

Tomasek, J. J. et al. 2002a. Myofibroblasts and mechano-regulation of connective tissue remodelling. *Nature Reviews Molecular Cell Biology* 3(5), pp. 349-363.

Tomasek, J. J. et al. 2002b. Myofibroblasts and mechano-regulation of connective tissue remodelling. *Nat Rev Mol Cell Biol* 3(5), pp. 349-363.

Toole, B. P. and Slomiany, M. G. 2008. Hyaluronan, CD44 and Emmprin: Partners in cancer cell chemoresistance. *Drug Resistance Updates* 11(3), pp. 110-121.

Tremmel, M. et al. 2009. A CD44v6 peptide reveals a role of CD44 in VEGFR-2 signaling and angiogenesis. *Blood* 114(25), pp. 5236-5244.

Trochon, V. et al. 1996. Evidence of involvement of CD44 in endothelial cell proliferation, migration and angiogenesis in vitro. *International journal of cancer* 66(5), pp. 664-668.

Tsukita, S. et al. 1994. ERM family members as molecular linkers between the cell-surface glycoprotein cd44 and actin-based cytoskeletons. *Journal of Cell Biology* 126(2), pp. 391-401.

Urb, M. and Sheppard, D. C. 2012. The Role of Mast Cells in the Defence against Pathogens. *PLoS Pathogens* 8(4), p. e1002619.

Urbich, C. et al. 2002. Shear Stress–Induced Endothelial Cell Migration Involves Integrin Signaling Via the Fibronectin Receptor Subunits α5 and β1. *Arteriosclerosis, Thrombosis, and Vascular Biology* 22(1), pp. 69-75.

Usui, T. et al. 1998. Extracellular matrix production regulation by TGF-beta in corneal endothelial cells. *Investigative Ophthalmology & Visual Science* 39(11), pp. 1981-1989.

van der Velden, V. H. J. et al. 1998. Interleukin-1 beta and interferon-gamma differentially regulate release of monocyte chemotactic protein-1 and interleukin-8 by human bronchial epithelial cells. *European Cytokine Network* 9(3), pp. 269-277.

Varga, J. et al. 1987. Transforming growth factor β (TGFβ) causes a persistent increase in steady-state amounts of type I and type III collagen and fibronectin mRNAs in normal human dermal fibroblasts. *Biochemical Journal* 247(3), pp. 597-604.

Vaughan, M. B. et al. 2000. Transforming Growth Factor-β1 Promotes the Morphological and Functional Differentiation of the Myofibroblast. *Experimental Cell Research* 257(1), pp. 180-189.

Veeraraghavan, S. et al. 2001. Lung fibrosis: new classifications and therapy. *Current Opinion in Rheumatology* 13(6), pp. 500-504.

Walpola, P. L. et al. 1995. Expression of ICAM-1 and VCAM-1 and Monocyte Adherence in Arteries Exposed to Altered Shear Stress. *Arteriosclerosis, Thrombosis, and Vascular Biology* 15(1), pp. 2-10.

Wang, S. J. and Bourguignon, L. W. 2006. HYaluronan and the interaction between cd44 and epidermal growth factor receptor in oncogenic signaling and chemotherapy resistance in head and neck cancer. *Archives of Otolaryngology–Head & Neck Surgery* 132(7), pp. 771-778.

Wang, S. J. et al. 2007. Association of CD44 v3-containing isoforms with tumor cell growth, migration, matrix metalloproteinase expression, and lymph node metastasis in head and neck cancer. *Head and Neck-Journal for the Sciences and Specialties of the Head and Neck* 29(6), pp. 550-558.

Wayner, E. A. and Carter, W. G. 1987. Identification of multiple cell-adhesion receptors for collagen and fibronectin in human fibrosarcoma cells possessing unique alpha-subunits and common beta-subunits. *Journal of Cell Biology* 105(4), pp. 1873-1884.

Webber, J. et al. 2009a. Modulation of TGF beta 1-Dependent Myofibroblast Differentiation by Hyaluronan. *American Journal of Pathology* 175(1), pp. 148-160.

Webber, J. et al. 2009b. Maintenance of the myofibroblastic phenotype: a role for Hyaluronan. *International Journal of Experimental Pathology* 90(2), pp. A95-A95.

Webber, J. et al. 2009c. Hyaluronan Orchestrates Transforming Growth Factor-beta 1-dependent Maintenance of Myofibroblast Phenotype. *Journal of Biological Chemistry* 284(14), pp. 9083-9092.

Weigel, P. H. and DeAngelis, P. L. 2007. Hyaluronan Synthases: A Decade-plus of Novel Glycosyltransferases. *Journal of Biological Chemistry* 282(51), pp. 36777-36781.

Weissmann, B. and Meyer, K. 1954. the structure of hyalobiuronic acid and of hyaluronic acid from umbilical cord. *Journal of the American Chemical Society* 76(7), pp. 1753-1757.

Wesche, H. et al. 1997. The Interleukin-1 Receptor Accessory Protein (IL-1RAcP) Is Essential for IL-1-induced Activation of Interleukin-1 Receptor-associated Kinase (IRAK) and Stress-activated Protein Kinases (SAP Kinases). *Journal of Biological Chemistry* 272(12), pp. 7727-7731.

Wielenga, V. J. M. et al. 2000. Expression of c-Met and heparan-sulfate proteoglycan forms of CD44 in colorectal cancer. *American Journal of Pathology* 157(5), pp. 1563-1573.

Wight, T. N. et al. 1992. The role of proteoglycans in cell adhesion, migration and proliferation. *Current Opinion in Cell Biology* 4(5), pp. 793-801.

Wilgus, T. A. et al. 2013. Neutrophils and Wound Repair: Positive Actions and Negative Reactions. *Advances in Wound Care* 2(7), pp. 379-388.

Williams, A. F. and Barclay, A. N. 1988. The Immunoglobulin Superfamily—Domains for Cell Surface Recognition. *Annual Review of Immunology* 6(1), pp. 381-405.

Williams, T. M. and Lisanti, M. P. 2004. The caveolin proteins. *Genome Biology* 5(3).

Wittig, B. M. et al. 2000. Abrogation of Experimental Colitis Correlates with Increased Apoptosis in Mice Deficient for Cd44 Variant Exon 7 (Cd44v7). *The Journal of Experimental Medicine* 191(12), pp. 2053-2064.

Wolny, P. M. et al. 2010. Analysis of CD44-Hyaluronan Interactions in an Artificial Membrane System: insights into the distinct binding properties of high and low molecular weight hyaluronan. *Journal of Biological Chemistry* 285(39), pp. 30170-30180.

Woodhead, V. E. et al. 2000. Novel molecular mechanisms of dendritic cell-induced T cell activation. *Int Immunol* 12(7), pp. 1051-1061.

Wu, K. K. et al. 1988. Endothelial cell function in hemostasis and thrombosis. *Advances in experimental medicine and biology* 242, pp. 127-133.

Wynn, T. A. 2004. Fibrotic disease and the T(H)1/T(H)2 paradigm. *Nature Reviews Immunology* 4(8), pp. 583-594.

Wynn, T. A. 2008. Cellular and molecular mechanisms of fibrosis. *The Journal of pathology* 214(2), pp. 199-210.

Wynn, T. A. et al. 1995. An IL-12-based vaccination method for preventing fibrosis induced by schistosome infection. *Nature* 376(6541), pp. 594-596.

Xiang, J. et al. 2009. Expression of matrix metalloproteinase-1, matrix metalloproteinase-2 and extracellular metalloproteinase inducer in human periodontal ligament cells stimulated with interleukin-1beta. *Journal of Periodontal Research* 44(6), pp. 784-793.

Xie, L. et al. 2004. Activation of the Erk Pathway Is Required for TGF-β1-Induced EMT In Vitro. *Neoplasia* 6(5), pp. 603-610.

Xiong, L. et al. 2014. The Biological Function and Clinical Utilization of CD147 in Human Diseases: A Review of the Current Scientific Literature. *International Journal of Molecular Sciences* 15(10), pp. 17411-17441.

Xu, Y. B. et al. 1998. The crystal structure of bikunin from the inter-alpha-inhibitor complex: A serine protease inhibitor with two Kunitz domains. *Journal of Molecular Biology* 276(5), pp. 955-966.

Xue, J. et al. 2015. Alternatively activated macrophages promote pancreatic fibrosis in chronic pancreatitis. *Nature communications* 6, pp. 7158-7158.

Yamaguchi, Y. et al. 1990. negative regulation of transforming growth-factor-beta by the proteoglycan decorin. *Nature* 346(6281), pp. 281-284.

Yamashita, C. M. et al. 2011. Matrix Metalloproteinase 3 Is a Mediator of Pulmonary Fibrosis. *American Journal of Pathology* 179(4), pp. 1733-1745.

Yang, Y. et al. 2008. Cyclophilin A up-regulates MMP-9 expression and adhesion of monocytes/macrophages via CD147 signalling pathway in rheumatoid arthritis. *Rheumatology* 47(9), pp. 1299-1310.

Yonemura, S. et al. 1998. Ezrin/radixin/moesin (ERM) proteins bind to a positively charged amino acid cluster in the juxta-membrane cytoplasmic domain of CD44, CD43, and ICAM-2. *Journal of Cell Biology* 140(4), pp. 885-895.

Yoshiji, H. et al. 2000. Tissue inhibitor of metalloproteinases-1 promotes liver fibrosis development in a transgenic mouse model. *Hepatology* 32(6), pp. 1248-1254.

Young, A. et al. 2007. Mortality in rheumatoid arthritis. Increased in the early course of disease, in ischaemic heart disease and in pulmonary fibrosis. *Rheumatology* 46(2), pp. 350-357.

Yu, J. et al. 2009. The anti-inflammatory effect of celecoxib does not prevent liver fibrosis in bile duct-ligated rats. *Liver Int* 29(1), pp. 25-36.

Yu, Q. and Stamenkovic, I. 2000. Cell surface-localized matrix metalloproteinase-9 proteolytically activates TGF-beta and promotes tumor invasion and angiogenesis. *Genes & Development* 14(2), pp. 163-176.

Yu, W.-H. et al. 2002. CD44 anchors the assembly of matrilysin/MMP-7 with heparin-binding epidermal growth factor precursor and ErbB4 and regulates female reproductive organ remodeling. *Genes & Development* 16(3), pp. 307-323.

Yu, X.-L. et al. 2008. Crystal Structure of HAb18G/CD147: implications for immunoglobulin superfamily homophilic adhesion. *Journal of Biological Chemistry* 283(26), pp. 18056-18065.

Yurchenko, V. et al. 2002. Active Site Residues of Cyclophilin A Are Crucial for Its Signaling Activity via CD147. *Journal of Biological Chemistry* 277(25), pp. 22959-22965.

Zavadil, J. and Böttinger, E. P. 2005. TGF-β and epithelial-to-mesenchymal transitions. *Oncogene* 24(37), pp. 5764-5774.

Zeisberg, M. et al. 2001. Renal Fibrosis: Collagen Composition and Assembly Regulates Epithelial-Mesenchymal Transdifferentiation. *The American Journal of Pathology* 159(4), pp. 1313-1321.

Zeisberg, M. et al. 2003. BMP-7 counteracts TGF-[beta]1-induced epithelial-to-mesenchymal transition and reverses chronic renal injury. *Nat Med* 9(7), pp. 964-968.

Zen, K. et al. 2008. CD44v4 Is a Major E-Selectin Ligand that Mediates Breast Cancer Cell Transendothelial Migration. *PLoS ONE* 3(3), p. e1826.

Zhang, K. et al. 1994. Myofibroblasts and their role in lung collagen gene-expression during pulmonary fibrosis - a combined immunohistochemical and in-situ hybridization study. *American Journal of Pathology* 145(1), pp. 114-125.

Zhang, W. et al. 2010. Monomeric type I and type III transforming growth factor-beta receptors and their dimerization revealed by single- molecule imaging. *Cell Research* 20(11), pp. 1216-1223.

Zhang, X. L. et al. 2004. Renal proximal tubular epithelial cell transforming growth factor-β1 generation and monocyte binding. *American Journal of Pathology* 165(3), pp. 763-773.

Zhao, P. et al. 2011. HAb18G/CD147 promotes cell motility by regulating annexin II-activated RhoA and Rac1 signaling pathways in hepatocellular carcinoma cells. *Hepatology* 54(6), pp. 2012-2024.

Zheng, H. C. et al. 2006. Upregulated EMMPRIN//CD147 might contribute to growth and angiogenesis of gastric carcinoma: a good marker for local invasion and prognosis. *Br J Cancer* 95(10), pp. 1371-1378.

Zhou, S. X. et al. 2005. CD147 is a regulatory subunit of the gamma-secretase complex in Alzheimer's disease amyloid beta-peptide production. *Proceedings of the National Academy of Sciences of the United States of America* 102(21), pp. 7499-7504.

Zhu, P. et al. 2005. Expression of CD147 on monocytes/macrophages in rheumatoid arthritis: its potential role in monocyte accumulation and matrix metalloproteinase production. *Arthritis Research & Therapy* 7(5), pp. R1023-R1033.

Zou, Y. et al. 1998. Signal transduction in arteriosclerosis: mechanical stress-activated MAP kinases in vascular smooth muscle cells (review). *International journal of molecular medicine* 1(5), pp. 827-861.

Appendix 1 - CD44v6-10 sequence

CD44v6 -Forward primer

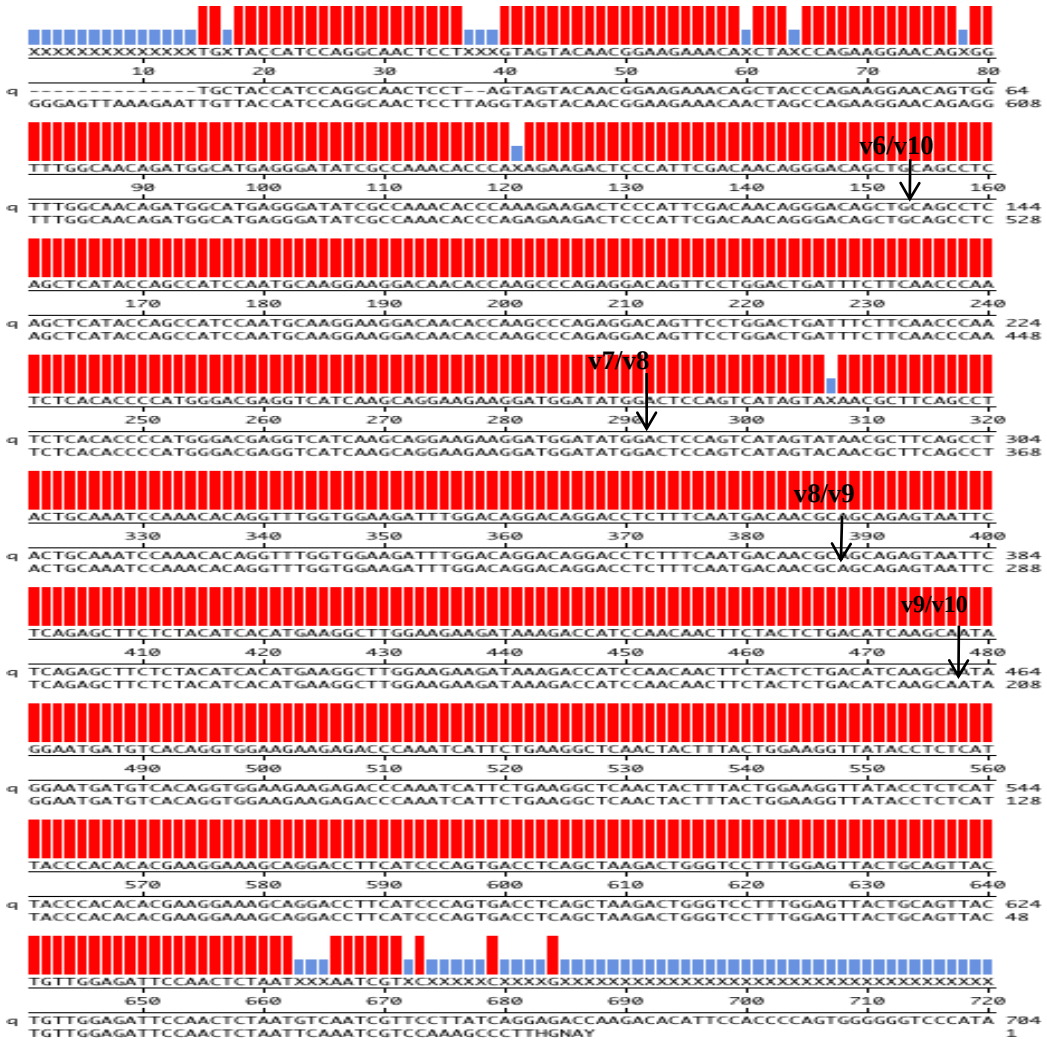

Consensus sequence is shown on the top row. The reference sequence is shown on the second row. The sequence for CD44v6-10 is shown on the bottom row. Exon-exon boundaries are indicated with arrows and annotations.

Appendix 2- Comparison of CD44 Variant expression in Dermal and Oral Fibroblasts

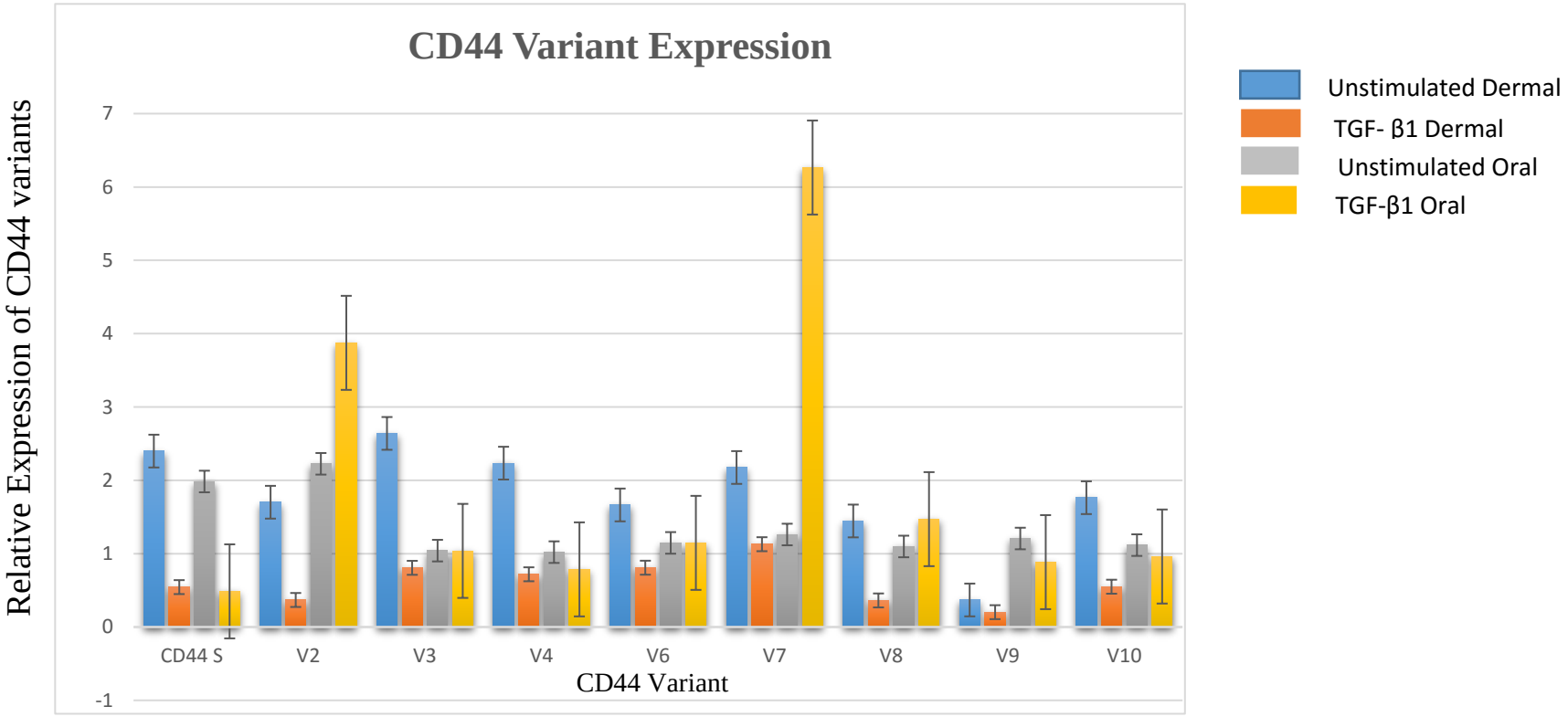

Data demonstrates CD44 variant expression by unstimulated dermal and oral fibroblast and TGF-β1 induced fibroblasts. Data shows independent experiments with each CD44 variant being relative to its Dermal fibroblast control. Analysis was carried out by Sian Gardiner under my supervision.